SYMMETRY-OUT ASYMMETRY-IN: THE ROLE OF DMRT2

RAQUEL DE AMARO LOURENÇO

Dissertation presented to obtain the PhD degree in Biology
at the Instituto de Tecnologia Química e Biológica
da Universidade Nova de Lisboa

Oeiras, Janeiro 2011

SYMMETRY-OUT ASYMMETRY-IN: THE ROLE OF DMRT2

RAQUEL DE AMARO LOURENÇO

SUPERVISOR:
LEONOR SAÚDE, PhD

Dissertation presented to obtain the PhD degree in Biology
at the Instituto de Tecnologia Química e Biológica
da Universidade Nova de Lisboa

Oeiras, Janeiro 2011

Apoio financeiro da Fundação para a Ciência e a Tecnologia e do FSE no
âmbito do Quadro Comunitário de Apoio, BD nº SFRH/BD/24861/2005

FCT Fundação para a Ciência e a Tecnologia
MINISTÉRIO DA CIÊNCIA, TECNOLOGIA E ENSINO SUPERIOR

Acknowledgements

Durante estes últimos anos tive a sorte e o privilégio de trabalhar com pessoas que em muito contribuíram para a minha formação. Em primeiro lugar quero agradecer à minha orientadora, obrigada Leonor por me ter aceite no grupo e supervisionar o meu PhD. Por tudo o que me ensinou e por todo o apoio e incentivo que me deu ao longo dos anos. Não podia ter tido melhor chefe!

Agradeço ao Instituto Gulbenkian de Ciência e ao Instituto de Medicina Molecular por me terem acolhido durante a realização do meu doutoramento. À Fundação para a Ciência e Tecnologia agradeço o apoio financeiro essencial à realização deste trabalho (Apoio financeiro da FCT e do FSE no âmbito do Quadro Comunitário de Apoio, SFRH/BD/24861/2005).

A todo o grupo que fez com que o ambiente de trabalho fosse simplesmente óptimo, desde o tempo em que nos chamávamos SD até agora em que somos UDEV. O vosso apoio foi fundamental: Rita, a tua inteligência é inspiradora, obrigada por todos os ensinamentos, pela ajuda preciosa na construção do transgénico e por todas as boleias até casa; Susana L., gostei de poder trabalhar contigo num mesmo projecto, obrigada pelas discussões e por todo o incentivo para enfrentar a próxima etapa; Susana P., a minha companheira de secretária, já viste o espaço que vais ganhar?! Obrigada pelo apoio em momentos mais difíceis; Raquel M. e Sofia, foi bom ter-vos como colegas de doutoramento, boa sorte para a vossa fase final! João, chegaste em último mas ainda partilhaste a tua boa disposição e conhecimentos, boa sorte no Canadá! Andreia, Patrícia e Ana Margarida, a vossa ajuda no laboratório fez muitas vezes a diferença. Ainda um grande obrigado aos grupos UMO e UBD por todas as discussões científicas e por contribuírem também para um ambiente de trabalho estimulante.

Agradeço ao Moises Mallo a à Ana Tavares por terem feito parte do meu comité de tese quando realizei parte do trabalho no IGC.

Um grande obrigado ao Miguel G. por me ensinar a técnica de Western blot, pelos ensinamentos e incentivo.

A todos os serviços técnicos do IGC e do IMM que tanto contribuíram para a realização deste trabalho. Às Unidade de Imagiologia do IMM e IGC. Às equipes dos biotérios de ambos os institutos, em especial ao Yuri Weber e à Alina Costa por toda ajuda no biotério do IMM. À equipe da Zebrafish Facility do IMM, obrigada à Lara e ao Fábio por todo o trabalho em manter as diversas linhas de peixes, pelo número infindável de caixas de cruzamentos que tiveram de organizar e por serem sempre prestáveis para tudo.

A todos os amigos pela companhia durante estes anos. Marta, obrigada pelos cafés e por me tornares "tia", um dia o Lourenço ainda ouve as nossas histórias. Ana Raquel, as tuas gargalhadas continuam contagiantes, como gosto de ouvir as histórias que vais contando, qualquer dia vejo um filme sobre a tua vida! Obrigada pelas longas conversas. À Tânia, pelos desabafos sobre tudo e mais alguma coisa e pelas guaridas, tu és a próxima, boa sorte! À Susana e à Lena, sempre boas companhias. Fred e Susana, longas conversas que tão bem me fizeram, boa sorte para os dois. Ao Pedro e aos seus discursos tão loucos e hilariantes, tu vais longe!

Sílvia, obrigada por todo o apoio, foi muito importante. Cristina, em breve faço-te uma visita! Rita, quase que te tive como vizinha, mas não é por isso que não vamos continuar as nossas longas conversas. Marta, obrigada por toda a confiança que transmites. Filipa, que mulher de força, és uma inspiração! Obrigada por me animares mesmo estando tu tão longe. Boa sorte para tudo sei que vais dar a volta por cima. Ao trio maravilha, sempre presente! Obrigada às três por todo o apoio e por todos os momentos disparatados que tão bem me fizeram em muitos fins de dia, pode ser que um dia o nosso livrinho seja publicado! Mariana, obrigada por todas as conversas, companhia em tantos espectáculos e por disponibilizares sempre o "tanque", o veiculo maravilha! Elsa, vizinha da outra e desta margem,

obrigada pela confiança, pelo ombro amigo e bons conselhos que tens dado, és extraordinária! Catarina, a força do norte que tanto apoio também me deu, obrigada por tudo! Terei sempre um cantinho para quando as três me visitarem, prometo escolher bons restaurantes para os nossos jantares! Lara, desde os tempos do IGC que estás presente. Nem sei por onde começar a agradecer todo o apoio que me tens dado, por cada palavra de força e por de certa forma teres ajudado a mudar a minha vida, sabes bem disso. Obrigada também ao Nuno, pela boa disposição e obras de arte!

A toda a minha família. Ao meu irmão, por todo o incentivo, conhecimento e ajuda gráfica na tese. Aos meus pais, obrigado por todo o apoio incondicional, sem vocês não estava onde estou.

E ao Gonçalo, "I'm new here, will you show me around?".

TABLE OF CONTENTS

Summary

It may come as a surprise that vertebrates are not entirely bilaterally symmetric. In fact, at the internal level they are asymmetric with the organs acquiring a biased disposition along the left-right (LR) axis. Problems in the establishment of both symmetric and asymmetric features may give rise to several human developmental disorders. Thus, it is very important to study in more detail how LR embryonic development is initiated and maintained. The built of the axial skeleton and its associated skeletal muscles is dependent on somite formation and differentiation. The somites are formed as pairs and are bilaterally symmetric between both sides of the LR axis. Interestingly, it has been suggested that asymmetric somite formation may account for problems at the level of the axial skeleton. At the same time that the somites are being formed, asymmetric signals are being transferred only to the left side of the axis being responsible to set up the correct asymmetric internal organs distribution. In fact, an incorrect transfer of information leads to serious problems in organ situs. It has become clear that several mechanisms are necessary to initiate the LR asymmetry pathway however, something that only recently has been acknowledge is that symmetry is not a default state and there are in fact mechanisms responsible for promoting it. It is not completely understood how, but there are indications that there is a crosstalk between the mechanisms necessary to regulate symmetry vs. asymmetry. Surprisingly, a zebrafish transcription factor named Dmrt2a/Terra, a gene that belongs to a family mainly associated with sex determination, as been shown to play a role in regulating these two contradictory features. Not only is it necessary for bilateral symmetric somite formation but also for the correct establishment of asymmetry in the left side of the axis. Given this, it is extremely important to study the signalling cascade where it operates and to identify its downstream targets.

In this thesis the main objective was to improve our knowledge about the role of Dmrt2 during the establishment of a symmetric and asymmetric body structure, and address its level of conservation in zebrafish and mouse.

Chapter I consists in a general introduction of the process of symmetric somite formation, establishment and regulation of the LR asymmetry pathway and how they need to be tightly regulated so that imposed asymmetries do not influence symmetric body features. It also addresses the clinical implications of vertebral malformations and LR patterning disturbance. Chapter II describes the work involved in studying the degree of conservation of Dmrt2 function during embryonic development. Different phyla, such as arthropods, nematodes and vertebrates, present a different number of *dmrt* orthologue genes suggesting that during evolution gene duplication and/or loss as occurred. In vertebrates, Dmrt2 is present in humans, mouse, fish and chick. Since zebrafish Dmrt2a/Terra has been described to regulate symmetric somite formation and LR asymmetry pathway, and given the fact that mouse Dmrt2 had previously been described to be involved in somite differentiation, we addressed the degree of Dmrt2 conservation during zebrafish and mouse development regarding the regulation of symmetry vs. asymmetry. Contrary to its homologue in zebrafish, we show that mouse Dmrt2 is not required to regulate these two opposite pathways, indicating that its function was not evolutionarily conserved. Mouse *dmrt2* and zebrafish *dmrt2a/terra* are expressed in the anterior region of the presomitic mesoderm (PSM) and somites however, while *dmrt2a/terra* is also expressed in the Kupffer's vesicle (KV), *dmrt2* is absent from the mouse node. We suggest that Dmrt2 is regulating somite differentiation at the level of the PSM and somites, and that symmetric somite formation and LR asymmetry pathway are being regulated at the level of the zebrafish KV where *dmrt2a/terra* is expressed. Since we do not know how Dmrt2a/Terra is regulating these two processes, Chapter III and IV describes the initiation of two different approaches with the aim of finding its target genes. We discuss the potential of performing a ChIP-on-chip and a microarray assay techniques and the tool that we were able to generate. The ChIP-on-chip combines chromatin immunoprecipitation with microarray technology and would allow us to investigate *in vivo* interactions between Dmrt2a/Terra and the DNA sequences to which it binds to. It relies on using a specific antibody against Dmrt2a/

Terra however, since it was not successfully obtained we decided to undergo to a microarray approach. To be able to compare changes in the expression levels of Dmrt2a/Terra target genes we would have used two different conditions where Dmrt2a/Terra would be downregulated, through morpholino injection, and upregulation. To overexpress it in a specific developmental time period, we constructed an inducible transgenic zebrafish line where Dmrt2a/Terra is under the control of a heat-shock promoter. With this tool built, we are now able to proceed with a controlled microarray experiment that will allow us to identify Dmrt2a/Terra direct targets during zebrafish embryonic development.

Different developmental processes have been shown to share the same molecular player and the Notch signalling pathway is no exception. Not only it drives the expression of oscillating genes that constitute the segmentation clock, associated with vertebrate somite formation, but it is also necessary to regulate the LR asymmetry cascade. Given the fact that this role during LR patterning is less understood during zebrafish embryonic development, in Chapter V we address at what level Notch is having an impact in the LR pathway. We show that it is through the ligand DeltaD that Notch is regulating cilia length and consequently the correct transfer of information only to the left side of the axis. Interestingly, Notch is the first signalling pathway shown to be able to decrease or increase cilia length, either when it is downregulated or upregulated. With the regulation of cilia length being associated with several human ciliopathies, understanding how Notch signalling modulates this regulation is thus of great importance for the search for other regulatory players.

Finally, Chapter VI consists in a general discussion that integrates the results obtained during the course of the work with the information that is currently accepted in the field regarding the protection of symmetric somite formation from the influence of asymmetric signals.

Resumo

O facto de os vertebrados não serem totalmente bilateralmente simétricos pode à primeira vista parecer surpreendente mas de facto, ao nível interno, os órgãos apresentam uma disposição assimétrica. Problemas no estabelecimento de características simétricas e assimétricas durante o desenvolvimento estão por vezes associadas a várias doenças em humanos. Desta forma, é extremamente importante estudar em maior detalhe como o desenvolvimento embrionário, em termos de simetria e assimetria esquerda-direita, é estabelecido e mantido. A formação do esqueleto axial e dos seus músculos esqueléticos associados depende da formação e diferenciação de estruturas chamadas sómitos, os quais são formados aos pares e são bilateralmente simétricos entre os dois lados do eixo esquerdo-direito. A correcta regulação da sua formação é muito importante, tendo sido sugerido que uma formação assimétrica dos sómitos possa ser responsável por problemas ao nível do esqueleto axial. Ao mesmo tempo que os sómitos são formados, sinais assimétricos são transferidos apenas para o lado esquerdo do eixo sendo responsáveis pela correcta distribuição dos órgãos internos. Uma incorrecta transferência desta informação induz graves problemas no posicionamento dos órgãos. Tem-se tornado cada vez mais claro que vários mecanismos são necessários para iniciar a via de sinalização responsável pela assimetria esquerda-direita contudo, apenas recentemente foi reconhecida a existência de mecanismos responsáveis por promover simetria durante o desenvolvimento. Apesar de ainda não se compreender totalmente como, várias têm sido as indicações de que é necessário que os mecanismos que regulam simetria vs assimetria interactuem. Surpreendentemente, um factor de transcrição chamado Dmrt2a/Terra presente no peixe zebra, pertencente a uma família maioritariamente associada à determinação sexual, foi demonstrado ter um papel na regulação destas duas características contraditórias. Não só é necessário para a formação simétrica dos sómitos, como também regula o correcto estabelecimento da assimetria no lado esquerdo do eixo. Desta forma, é extremamente importante estudar a cascata sinalizadora onde Dmrt2a/Terra opera e identificar os genes que regula.

O principal objectivo nesta tese foi aprofundar o conhecimento relativamente ao papel do Dmrt2 durante o estabelecimento de estruturas simétricas e assimétricas, bem como abordar o nível de conservação destas funções nos mamíferos. O Capitulo I consiste numa introdução geral ao processo da formação simétrica dos sómitos, estabelecimento e regulação da assimetria esquerda-direita e em como estes dois processos necessitam de ser altamente regulados de modo a que assimetrias impostas durante o desenvolvimento não influenciem a formação de características simétricas. São também abordadas as implicações clínicas de malformações ao nível da coluna vertebral e vértebras e de perturbações ao nível do estabelecimento da assimetria esquerda-direita. No Capitulo II é descrito o trabalho relativo ao estudo do grau de conservação da função do gene *dmrt2* durante o desenvolvimento embrionário. Filos diferentes, como o dos artrópodes, nemátodes e vertebrados, apresentam um número variável de genes ortólogos do *dmrt2*, sugerindo que durante a evolução duplicações ou perda de genes possam ter ocorrido. Nos vertebrados, o gene Dmrt2 encontra-se presente em humanos, ratinhos, peixes e galinhas. Uma vez que no peixe zebra o *dmrt2a/terra* foi demonstrado regular a formação simétrica dos sómitos e a cascata genética responsável por regular a assimetria esquerda-direita, e uma vez que o *dmrt2* em ratinho foi demonstrado estar envolvido na regulação da diferenciação dos sómitos, abordámos o grau de conservação do *dmrt2* durante o desenvolvimento embrionário do peixe zebra e ratinho relativamente à regulação da simetria vs assimetria. Ao contrário do seu homólogo no peixe zebra, o *dmrt2* no ratinho não é necessário para regular estes dois processos, indicando que a sua função não foi evolutivamente conservada. O *dmrt2* no ratinho e o *dmrt2a/terra* no peixe zebra são expressos na região anterior da mesoderme presomítica (MPS) e sómitos contudo, enquanto o *dmrt2a/terra* é também expresso na vesícula de Kupffer, o *dmrt2* não é expresso no nó do ratinho. Sugerimos então que o Dmrt2 regula a diferenciação dos sómitos ao nível da MPS e sómitos, e que a formação simétrica dos sómitos e a cascata genética que regula a assimetria esquerda-direita são reguladas ao nível da vesícula de Kupffer no peixe zebra,

onde o *dmrt2a/terra* é expresso. Uma vez que não sabemos como o Dmrt2a/Terra regula estes dois processos, nos Capítulos III e IV é descrita a iniciação de duas abordagens diferentes com o intuito de descobrir quais os genes que regula. Discutimos o potencial de desenvolver as técnicas de "ChIP-o-chip" e "microarray" e ainda um transgene indutível que desenvolvemos. A técnica do "ChIP-o-chip" combina imuno-precipitação de cromatina com a tecnologia de "microarray" e permitiria investigar interacções *in vivo* entre o Dmrt2a/Terra e as sequências de DNA genómico às quais se liga. O seu sucesso depende do uso de um anticorpo específico contra o Dmrt2a/Terra contudo, como este não foi obtido com sucesso decidimos avançar para o uso da tecnologia de microarray. De modo a podermos comparar alterações nos níveis de expressão dos genes que o Dmrt2a/Terra regula, usaríamos duas condições diferentes em que a expressão do Dmrt2a/Terra seria inibida, através da injecção de um morpholino específico, e também aumentada ectopicamente. De modo a ser sobre-expresso num período específico do desenvolvimento embrionário, construímos uma linha transgénica de peixe zebra em que a expressão do Dmrt2a/Terra se encontra sob o controle de um promotor indutível pelo calor. Com este transgénico construído, podemos agora avançar para um microarray bastante controlado que nos permitirá identificar os genes alvo directos do Dmrt2a/Terra durante o desenvolvimento embrionário do peixe zebra.

Diferentes processos durante o desenvolvimento têm sido demonstrados partilhar as mesmas vias moleculares sinalizadoras, sendo que a via de sinalização Notch não é excepção. Não só controla a expressão de genes oscilatórios que constituem o relógio da segmentação, associado com a formação dos sómitos, como é também necessário para regular a cascata genética da assimetria esquerda-direita. Uma vez que este papel durante a modulação da assimetria esquerda-direita durante o desenvolvimento embrionário do peixe zebra não era completamente compreendido, no Capítulo V abordamos a que nível a via Notch controla a lateralidade. Mostramos que é através do ligando DeltaD que o Notch regula o comprimento dos cílios e, como consequência, a correcta transferência de informação apenas para o lado es-

querdo do eixo. Surpreendentemente, a via de sinalização Notch é a primeira a ser demonstrada capaz de diminuir ou aumentar o tamanho dos cílios, uma vez inibida ou sobre-expressa, respectivamente. Uma vez que a regulação do tamanho dos cílios se encontra associada a várias ciliopatias em humanos, compreender como a via de sinalização Notch modula esta regulação é de extrema importância na procura de outras vias/genes reguladores.

Por fim, o Capítulo VI consiste numa discussão geral que integra os resultados obtidos durante o desenvolvimento deste trabalho com a informação que é actualmente aceite na área, relativamente à protecção da formação simétrica dos sómitos da influência de sinais assimétricos.

Abbreviations

AP Anterior-posterior
bHLH Basic-helix-loop-helix
cDNA Complementary DNA
CFP Cyan Fluorescent protein
CHD Congenital heart disease
ChIP Chromatin immunoprecipitation
Cyc Cyclops
Cyp26a1 Cytochrome p450 26a1
DDC Duplication-degeneration-complementation
DFC's Dorsal forerunner cells
Dll3 Delta-like 3
DM Doublesex and Mab-3
DMRT Doublesex and Mab-3 Related Transcription Factor
Dsx Doublesex
DV Dorso-ventral
Dvl Dishevelled
E Embryonic day
EGF-CFC Epidermal Growth Factor-like - *Cripto*, *Frl-1,* and *Cryptic*
FGF Fibroblast growth factor
Fsi Frequent situs inversus
GAGs Glycosaminoglycans
GJC Gap junction communication
GRP Gastrocoel roof plate
GST Glutathione-S-Transferase
H^+/K^+ ATPase Hydrogen-potassium adenosine triphosphatase
Hsp Heat-shock protein
Iv Inversus viscerum
KV Kupffer's vesicle
Lfng Lunatic fringe
LPM Lateral plate mesoderm
LR Left-right
Lrd Left-right dynein
ML Medio-lateral
MO Morpholino
MRF Myogenic regulatory factor
mRNA Messenger RNA
Ntl No tail
Oep One-eye pinhead
PAPC Paraxial protocadherin
PCD Primary cilia dyskinesia
PCP Planar cell polarity
PCR Polymerase chain reaction
PNC Posterior notochord
PSM Presomitic mesoderm
RA Retinoic acid
Raldh2 Retinaldehyde dehydrogenase 2
RAR Retinoic acid receptor
Rbp-jk Recombination signal-binding protein1 for j-kappa
RNA Ribonucleic acid
RXR Retinoid X receptor
Shh Sonic hedgehog
Su(H) Suppressor of Hairless
Sur Schmalspur
TGF-β Transforming growth factor beta
Vang Van gogh
WT Wild-type

Index of Figures

CHAPTER V

Notch signalling regulates left-right asymmetry through ciliary length control

CHAPTER I

Introduction

The introduction was partially published in
Lourenço, R. and Saúde, L. (2010).
Symmetry OUT, Asymmetry IN.
Symmetry **2**, 1033-1054.

I.1. What needs to happen in order to produce a symmetric body plan?

I.1.1. The bilateral symmetry of somitogenesis

The bilateral symmetric appearance of the vertebrate body plan is largely due to the symmetric organization of the skeleton and its associated muscles. The origin of this symmetry can be traced back to early developmental stages when the somites, embryonic structures that will differentiate into the axial skeleton (vertebrae, intervertebral discs and ribs) and skeletal muscles, are being formed. Each new pair of somites is progressively laid down from the rostral region of the presomitic mesoderm (PSM) in a bilateral symmetric way on both sides of the axial structures *i.e*. neural tube and notochord. Somite formation is coupled with the constant supply of new somite precursors cells that are added into the caudal region of the PSM coming from a progenitor zone located in the tailbud. The long lasting fascination about the somites comes from the observation that these embryonic structures are produced in species-specific regular intervals in space and time. Every 4-5 hours a new pair of somites is formed in the human embryo, every 120 minutes in the mouse, every 90 minutes in the chick and every 30 minutes in the zebrafish (Dequéant and Pourquié, 2008).

I.1.2. The segmentation clock sets the periodicity of somite formation

The "clock and wavefront" model proposed by Cooke and Zeeman in 1976 provides an explanation for the precise temporal and spatial segmental pattern established in the vertebrate body plan. It postulates the existence of an internal clock that sets the time when PSM cells are competent to form a somite and a wavefront of differentiation that moves posteriorly along the PSM and sets the position where the next pair of somites will form, *i.e.* the determination front. With these two components, both temporal and spatial patterns can be established in the PSM. Only when PSM cells are located anterior to the determination front, a transition from an immature to a mature state can occur and a new somite will form in response to the clock cycle.

The molecular evidence for the existence of a segmentation clock came with the discovery of the first cyclic gene, the avian basic-helix-loop-helix (bHLH) transcription factor *hairy1.* The chick *hairy1* gene shows a dynamic and reiterated expression pattern in the PSM with the exact same periodicity of somite formation (Palmeirim et al., 1997). These *hairy1* messenger RNA (mRNA) oscillations occur autonomously in PSM cells and because they are synchronized with adjacent cells, describe a wave of expression starting at the posterior PSM and moving towards the anterior PSM, where it slows down and eventually stops, concomitant with somite formation (Figure 1.1). Therefore, PSM cells undergo several periodic oscillations of *hairy1* gene expression before they incorporate into the next somite (Palmeirim et al., 1997).

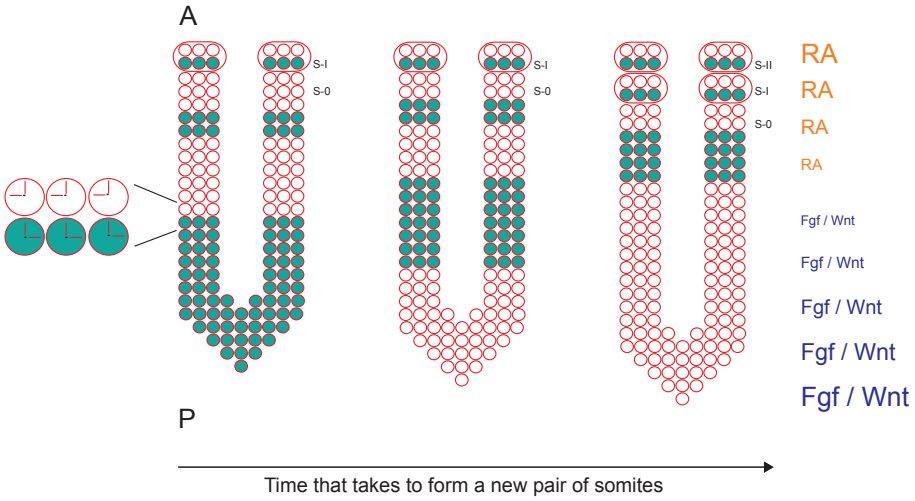

Figure 1.1. The formation of a new pair of somites is under the control of a molecular clock and a wavefront of differentiation. mRNA oscillations of cyclic genes are detected in PSM cells (blue dots) and since they are synchronized with neighboring cells, describe a wave of expression that starts at the posterior region of the PSM and moves towards the anterior region of the PSM. Here, the wave of expression slows down and stabilizes in the formed somite (S-I). Somite formation is also under the control of a wavefront of differentiation defined by a Fgf/Wnt signalling gradient in the posterior region of the PSM, which is counteracted by a RA gradient in the anterior region of the PSM. Anterior (A) is up, posterior is down (P). S-0 is the new forming somite.

Soon after this discovery, a number of *Hairy-Enhancer of Split*-related genes, named *hes* in mice and *her* in zebrafish, were identified and shown to produce the same type of oscillating behavior at the level of the PSM (Dequéant and Pourquié, 2008). These genes are primary targets of the Notch signaling pathway and encode transcriptional regulators of the bHLH class that mainly work as repressors (Kageyama et al., 2007). This suggested that the oscillatory behavior of the cyclic genes could be due to feedback inhibition. Indeed the first indication that this was the case came from a pioneering study performed in cell culture. It was shown that not only the mRNA but also the Hes1 protein levels oscillate with the same periodicity as somite formation. These oscillations are generated by a mechanism of negative feedback, where the Hes1 protein periodically represses its own transcription (Hirata et al., 2002). It has been shown that negative feedback loops also underlie the oscillatory expression of a number of cyclic genes in the mouse, zebrafish and chick PSM (Oates et al., 2002; Holley et al., 2002; Dale et al., 2003; Bessho et al., 2003; Hirata et al., 2004; Sieger et al., 2003; Brend and Holley, 2009 A). A mathematical model based essentially on experimental data of zebrafish *her* genes clearly shows that sustained oscillations can indeed be generated by a negative feedback loop, if transcriptional and translational time delays are taken into account and if the lifetimes of cyclic mRNAs and proteins are short (Lewis, 2003).

The fact that the *Hairy-Enhancer of Split*-related genes are targets of Notch signaling suggested that this pathway is a fundamental component of the segmentation clock. Indeed, the analysis of mouse and zebrafish mutants for several components of the Notch pathway revealed that cyclic gene expression and somite boundary formation were disrupted to varying degrees. Nevertheless, the anterior somites developed normally and only the posterior ones were affected in the Notch mutants (Conlon et al., 1995; Huppert et al., 2005; van Eeden et al., 1996). These findings showed that Notch signaling is not entirely necessary for somite formation but instead suggested that its failure leads to a gradual perturbation in somite segmentation.

Furthermore, a closer look at the expression of the Notch ligand *deltaC*, one of the oscillatory genes in zebrafish, in Notch signaling mutants revealed that individual PSM cells still expressed *deltaC* in a cyclic manner but the levels varied quite a lot between neighboring cells. This led to the idea that the main function of Notch signaling is to coordinate oscillations between individual cells and to keep them synchronized and not so much to drive the oscillations (Figure 1.2). Therefore, it was proposed that in zebrafish Notch mutants, PSM cells begin oscillations in synchrony forming normal anterior somites but after a few cycles gradually loose their synchrony forming abnormal somite boundaries (Jiang et al., 2000).

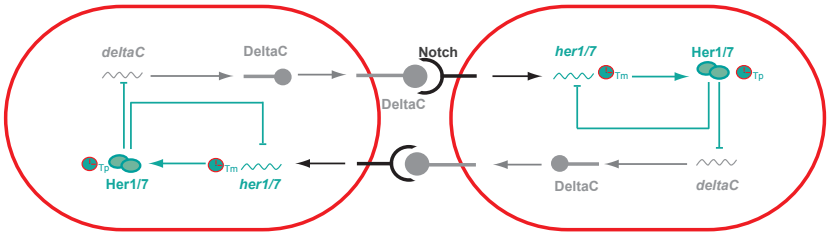

Figure 1.2. Synchronized oscillations between adjacent cells in zebrafish presomitic mesoderm. Activation of Notch, upon interaction with DeltaC, activates the expression ***her*** genes. ***her*** genes encode transcriptional repressors that have the ability to inhibit their own expression generating negative feedback loops that are then responsible for the PSM intracellular oscillations. Importantly, the period of these oscillations are dependent on both transcriptional (Tm) and translational delays (Tp). Her proteins will not only inhibit their own expression, but also inhibit the expression of ***deltaC*** that for this reason is also expressed in an oscillatory manner. DeltaC in one cell will then activate Notch signalling in the neighbouring cell and as a consequence generates intracellular oscillations. Thus, oscillations between adjacent cells are synchronized with one another since they are coupled via Notch signalling.

A model put forward by Lewis (2003) proposed a way by which DeltaC synchronizes oscillations between neighboring cells (Figure 1.2). It postulates that the intracellular negative feedback oscillations of *her1/her7* genes are coupled to an intercellular oscillator involving Delta ligands. In fact, Her1/Her7 negatively regulate *deltaC,* influencing Notch activity in the neigh-

boring cells and finally their own intracellular oscillations. This Delta/Notch mediated coupling mechanism results in synchronization between adjacent cells (Lewis, 2003; Oates et al., 2002; Giudicelli et al., 2007; Jülich et al., 2005; Ozbudak and Lewis, 2008).

Several studies performed in zebrafish clearly demonstrated that DeltaC maintains synchronized oscillations in PSM cells. Mosaic embryos were generated by transplantation of prospective PSM cells taken from an embryo with impaired expression of the oscillatory *her* genes into the prospective PSM region of a wild-type embryo. In these mosaics, the transplanted cells caused an abnormal segmentation behavior in their neighbors but failed to cause segmentation defects if in addition they did not express *deltaC* (Horikawa et al., 2006). The same type of conclusion was reached from a high-resolution in situ hybridization analysis that allowed the visualization of the distinct sub-cellular localizations of the cyclic mRNAs corresponding to their different phases of oscillations in PSM cells. In contrast to a wild-type PSM, in the absence of DeltaC, completely different mRNA localizations could be observed in PSM cells located next to each other (Mara et al., 2007). Further support that Notch signaling serves to maintain synchrony in the PSM but is not necessary for oscillations of individual cells comes from studies where the γ-secretase inhibitor DAPT was used to block Notch signaling in a time controlled manner (Ozbudak and Lewis, 2008; Riedel-Kruse et al., 2007). In these reports, it was shown that there is a delay between the time of DAPT treatment and the disruption of somite boundaries and a delay between DAPT wash and the recovery of normal somite boundaries. Altogether, these results argue, at least in zebrafish, against the idea that Notch signaling is the oscillation generator and favors the idea that its main function is to synchronize oscillations within the PSM cells. Recently, a detailed sub-cellular mRNA localization study, revealed that besides its role in the synchronization of oscillations in posterior PSM, Notch signaling through DeltaD is necessary to initiate non-oscillating expression of the cyclic genes and to start the oscillations in PSM progenitors located in the tail bud (Mara et al., 2007).

In contrast to what happens in zebrafish, it was recently shown that elimination of all Notch activity abolishes cyclic gene expression and somite formation in mouse PSM (Ferjentsik et al., 2009). This finding is not incompatible with the possibility presented by others of Notch being a clock synchronizer during mouse somitogenesis (Aulehla and Pourquié, 2008; Feller et al., 2008) since it could integrate both functions. Although a clear demonstration that this pathway synchronizes the oscillations of PSM cells in amniotes is still missing, this could still be a possibility since perturbation of cell-cell interactions upon PSM cell dissociation in chick and mouse leads to irregular desynchronized oscillations (Maroto et al., 2005; Masamizu et al., 2006).

The different roles that Notch signaling seems to play during mouse and zebrafish somitogenesis could be due to different degrees of complexity of the segmentation clock mechanism in these two species. A mouse transcriptome study has shown that a large number of genes are in fact oscillating in the mouse PSM. Many of these genes belong not only to the Notch pathway as expected but also to the Wnt and *Fibroblast growth factors (FGF)* pathways. In addition, this study also revealed that while the Notch and FGF pathway genes oscillate in synchrony, they are in anti-phase with the oscillations of the Wnt pathway genes. This points to a possible cross-talk between them in a way that Wnt pathway may be coupled to Notch and FGF through mutual inhibition, so that all are integrated in one molecular clock (Dequéant et al., 2006). In zebrafish there is no evidence for the existence of Wnt or FGF-based cyclic genes (Dequéant and Pourquié, 2008).

I.1.3. The wavefront sets the position of somite formation

According to the original clock and wavefront model, the regular spacing of somites is also under the control of a wavefront that sets the position where the next somite boundary is going to be formed. Indeed there are several lines of evidence that show that this position is defined by a threshold of FGF and Wnt signaling along the PSM (Dubrulle et al., 2001; Aulehla et al.,

2003) (Figure 1.1). While under the influence of FGF/Wnt signaling, the PSM cells are maintained in an immature state and are prevented from starting the genetic program of somite formation.

The posterior-to-anterior gradient of *fgf8* mRNA in the PSM of several vertebrate embryos was the first one to be described (Dubrulle et al., 2001; Sawada et al., 2001; Dubrulle and Pourquié, 2004). This gradient is generated via a decay mechanism from a pool of transcripts produced by progenitor PSM cells (Dubrulle and Pourquié, 2004). According to the clock and wavefront model (Cooke and Zeeman, 1976), displacing the position of the determination front by altering the extent of the *fgf8* gradient results in the shift of the somite boundary position (Dubrulle et al., 2001). It is thought that this gradient is translated into a protein gradient, which is then converted into a MAPK/ERK activity gradient along the PSM (Sawada et al., 2001; Dubrulle and Pourquié, 2004; Delfini et al., 2005).

Parallel to the *fgf* gradient there is also a posterior-to-anterior gradient of Wnt signaling along the PSM. The expression of *wnt3a* in the posterior PSM (Aulehla et al., 2003) could be responsible for the nuclear β-*catenin* gradient reaching from the tailbud to the determination front (Aulehla et al., 2008) and for the graded expression of the Wnt target *axin2* (Aulehla et al., 2003).

It has been proposed that the determination front established by the *fgf* and *wnt* gradients is opposed by an anterior-to-posterior gradient of retinoic acid (RA) (Diez del Corral et al., 2003; Moreno and Kintner, 2004) (Figure 1.1). RA is the oxidized version of vitamin A. It is synthesized in the anterior PSM and somite region by the enzyme retinaldehyde dehydrogenase 2 (Raldh2), and degraded in the posterior PSM by the enzyme cytochrome p450 26a1 (Cyp26a1) (Swindell et al., 1999). RA in the anterior PSM has been shown to control somite boundary positioning by attenuating Fgf8 in that region. These mutually inhibitory gradients control somite differentiation by defining the determination front in a growing tissue (Diez del Corral et al., 2003).

I.1.4. Somites epithelialization

The maturation of the anterior PSM involves changes in cellular organization that ultimately lead to tissue epithelialization. This process is dependent on extracellular matrix proteins, such as fibronectin, with their presence in the PSM being essential for morphological somite formation (Georges-Labouesse et al., 1996; Rifes et al., 2007). Cadherins, such as the paraxial protocadherin (PAPC), have also been shown to regulate this process. PAPC is a cell adhesion molecule that is restricted to their anterior region of the last formed somite pair and the three next to be formed, being important to maintain somite cohesivity (Yamamoto et al., 1998; Kim et al., 2000; Johnson et al., 2001). In addition, somites are compartmentalized structures and the determination of their anterior-posterior (AP) polarity is actually established in the anterior PSM prior to the appearance of segmental borders. *mesp* genes encode bHLH transcription factors and are involved in the initial definition of the segments. They act downstream of the Notch signalling and are expressed in the anterior halves of the presumptive and forming somites, having a role in the acquisition of their anterior identity (Saga et al., 1997; Sawada et al., 2000; Durbin et al., 2000; Buchberger et al., 1998).

Somites also become dorso-ventral (DV) and medio-lateral (ML) patterned with distinct compartments subsequently giving rise to distinct cell lineages (reviewed in Brent and Tabin 2002; reviewed in Kalcheim and Ben-Yair 2005; reviewed in Andrade et al., 2007). Their ventral portion will undergo an epithelial to mesenchymal transition originating the sclerotome that will give rise to the vertebral column and ribs (Figure 1.3A,B). The formation of the sclerotome is induced by signals from the axial structures (notochord and floorplate) being mediated in part by Sonic hedgehog (Shh). Cells from the dorsal epithelial somite compartment form the dermomyotome (Figure 1.3A,B). This compartment is sub-divided into two domains, the medial and lateral, which are induced by Wnt signals coming from the dorsal neural tube and surface ectoderm, respectively (reviewed in Brent and Tabin 2002; reviewed in Kalcheim and Ben-Yair

2005; reviewed in Andrade et al., 2007). Cells from the dermomyotome delaminate from the edges and migrate underneath to form the myotome, which contains the skeletal muscle precursors (Figure 1.3C). The myotome is a transient structure where myogenesis is initiated by the activation of the bHLH myogenic regulatory factors (MRFs) *myf5* and *myoD*. Their activation depends on ventral midline Shh signalling and is maintained by dorsal neural tube and surface ectoderm Wnt signaling. In addition to muscle defects, mutants for some of these genes also present rib malformations. Since they are not expressed in the sclerotome, these results suggest that dermomyotome cells influence sclerotomal development through a non-cell autonomous pathway (reviewed in Kalcheim and Ben-Yair, 2005). Myotome formation involves two sequential steps: first, cells from the dorsomedial edge of the dermomyotome move underneath and form the epaxial myotome, which will elongate bi-directionally and differentiate into the musculature of the back and intercostals muscles; in a second phase the central dermomyotome cells de-epithelialize and form the dorsal dermis of the trunk, while cells from the ventrolateral edge of the dermomyotome migrate to different regions depending on the axial level at which they are located (Figure 1.3C). At the limb bud level they migrate into the lateral plate mesoderm (LPM) and form the limb muscles, while at the thoracic level they move underneath the dermomyotome to form the hypaxial myotome that will give rise to the abdominal muscles (Figure 1.3D). The myotome is delimited by a laminin rich basement membrane, an extracellular matrix structure that separates myotome from sclerotome (reviewed in Brent and Tabin, 2002). Despite morphologically alike, the most rostral somites give rise to non-segmented structures contributing to the bones of the base of the skull (Huang et al., 2000).

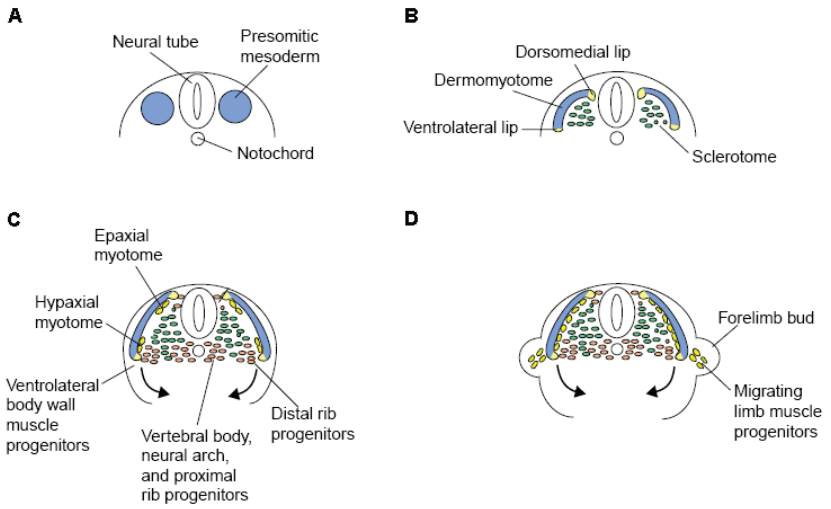

Figure 1.3. Somite differentiation. (A-B) Somites first differentiate into the dermomyotome, which will give rise to the dermis and skeletal muscle precursors, and to the sclerotome that will give rise to the vertebral column and ribs. (C) Cells from the dorsomedial edge of the dermomyotome delaminate to form the epaxial myotome, which differentiates into the musculature of the back and intercostals muscles, while cells from the dermomyotome ventrolateral edge delaminate to form the hypaxial myotome, which will give rise to the abdominal muscles. (D) At the limb bud level, cells from the ventrolateral edge of the dermomyotome migrate to the lateral plate mesoderm and form the limb muscles. *Adapted from Brent and Tabin, 2002*.

I.2. Is the body plan all about symmetry?

When looking at the exterior of a vertebrate body, one could say that it is fully bilaterally symmetric. Nonetheless, this external symmetry encloses unexpected surprises, since the internal organs acquire an asymmetric disposition with respect to the left-right (LR) axis. On the left side of the vertebrate body we can find the heart, stomach, spleen and the part of the lung with fewer lobes, while on the right side we have the liver, gall bladder and the part of the lung with more lobes (Figure 1.4). This normal distribution of the internal organs is referred to as *situs solitus* and is largely conserved among a population of a given species. Nevertheless, deviations from the norm can

arise in single individuals and will result in laterality defects: *situs inversus* corresponds to a situation where the position of the internal organs is completely reverted as a mirror-image; left or right isomerism is a situation where bilateral symmetry is not broken and two left or two right sides will form; *situs ambiguus* or heterotaxia that corresponds to some organs being well oriented and others reversed (Fliegauf et al., 2007).

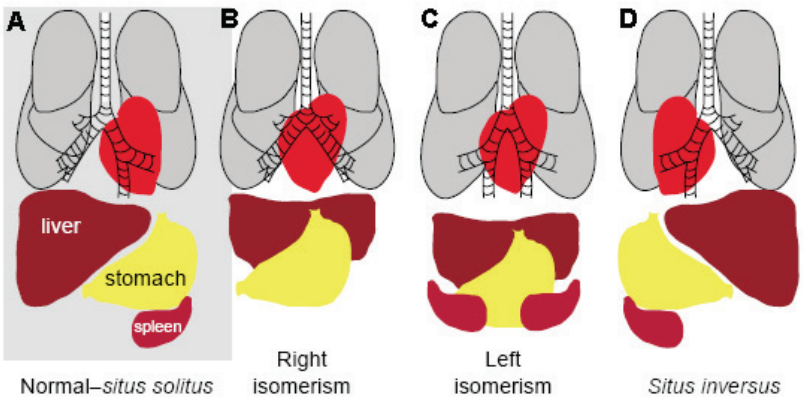

Figure 1.4. Internal organ asymmetric organization. (A) Normal distribution of the internal organs referred to as ***situs solitus***. Heart, stomach, spleen and the part of the lung with fewer lobes are found on the left side of the vertebrate body, while on the right side we have the liver and the part of the lung with more lobes. Cases with laterality defects may correspond to: (B) right isomerism, two right sides are formed; (C) left isomerism, two left sides are formed; (D) ***situs inversus***, the position of the internal organs is completely reverted as a mirror-image. *Adapted from McGrath and Brueckner, 2003*.

Well before visible morphological asymmetries can be observed in the vertebrate embryo, a conserved cascade of asymmetrically expressed genes, called the Nodal cascade is activated at the onset of gastrulation. Genes belonging to this cascade are the transforming growth factor beta (TGF-β) family members, *nodal*, *lefty1*, *lefty2* and the homeobox transcription factor, *pitx2*. It is though that an excess of Nodal activity on the left side of the node will be transferred to the left LPM and in this location Nodal exerts a positive feedback on itself. Consequently, the expression of *nodal* is amplified in the left LPM. At the same time, nodal activates its negative regula-

tors, the *lefty* genes. *Lefty1* in the midline prevents *nodal* activation on the right LPM, while *lefty2* restricts the domain of *nodal* expression on the left LPM. Here, Nodal induces *pitx2* expression. Pitx2 will promote LR asymmetry of the internal organs, through a mechanism not yet fully understood (Hamada, 2008) (Figure 1.5C).

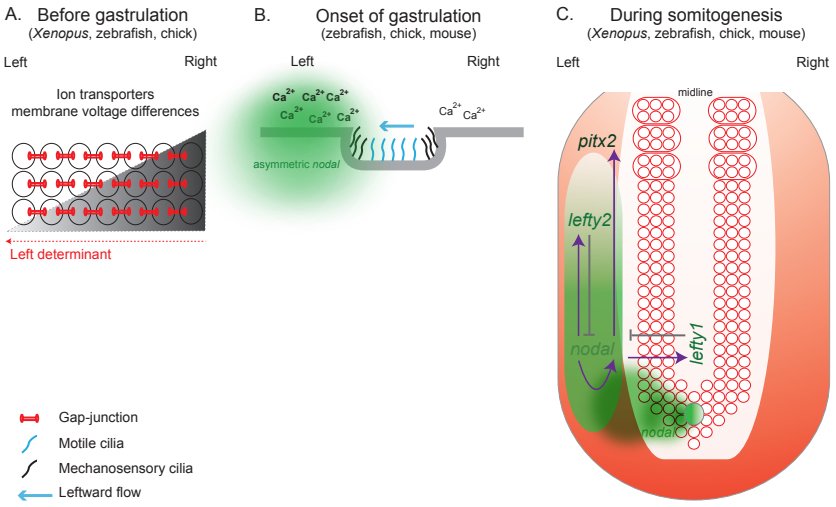

Figure 1.5. Set of events that might culminate with the establishment of the left-right patterning in different vertebrates. A) Prior to gastrulation in *Xenopus*, zebrafish and chick, ion transporters asymmetrically distributed in the embryo generate differences in membrane voltage potential between the left and right side. It is thought that this asymmetric membrane polarization promotes the accumulation of LR determinants through directional transport involving gap-junction channels. B) In mouse, it is though that mechanosensory cilia present in the node epithelia sense the leftward fluid flow created by motile cilia and as a consequence trigger an asymmetric Ca^{2+} release which will induce an asymmetric ***nodal*** expression around the node. This Ca^{2+} accumulation on the left side has also been described in zebrafish and chick although its relation with cilia-driven flow has not been established. C) A conserved Nodal cascade is activated at the onset of gastrulation in ***Xenopus***, zebrafish, chick and mouse. ***nodal*** is asymmetrically transferred from the node to the left LPM. There, it induces its own expression through a positive feedback loop and also the expression of its own inhibitors, ***lefty1*** and ***lefty2***. ***Lefty1*** is expressed in the midline and prevents ***nodal*** spreading to the right LPM, while ***lefty2*** is expressed in the left LPM restricting Nodal expression on the left side.

Although the Nodal cascade is conserved among vertebrates, the mechanism that induces *nodal* in the node in the first place shows differences between vertebrates. In mouse and chick, Notch signaling activates *nodal* in the node region (Collignon et al., 1996; Raya et al., 2004). Mouse mutants for the *notch1/notch2* receptors and for the *recombination signal-binding protein1 for j-kappa* (*rbp-jk*), the primary transcriptional mediator of Notch signaling, show absence of *nodal* expression around the node and LPM but do not interfere with the expression of its inhibitor *cerl2* (Krebs et al., 2003; Raya et al., 2003; Takeuchi et al., 2007). In zebrafish, Notch signaling activates the Nodal negative regulator *charon* around the Kupffer's vesicle (KV), a fluid-filled sac that lies between the tailbud and the yolk and is considered the node homologous LR organ. After blocking Notch signaling with DAPT, *charon* expression is either reduced or absent while *nodal* expression in the KV region is not affected (Gourronc et al., 2007). Nevertheless, the involvement of Notch in establishing the LR axis is thus conserved among vertebrates. In addition to Notch signaling, Fgf8 also regulates *nodal* asymmetric expression in the mouse and chick node. In the mouse, Fgf8 acts as a positive *nodal* regulator and therefore is a left determinant. In the chick, *fgf8* is asymmetrically expressed on the right side of the node where it represses *nodal,* thereby acting as a right determinant (Meyers and Martin, 1999). The role of Fgf8 in controlling expression at the KV has not been determined, although *fgf8* mutants show LR defects (Albertson and Yelick, 2005). Also Wnt signaling, namely Wnt3a, indirectly regulates *nodal* expression in the mouse node indirectly through Dll1 (Nakaya et al., 2005). In the chick, *wnt8c* is asymmetrically expressed on the right side of the node but functions as a left determinant controlling the expression of *nodal* (Rodríguez-Esteban et al., 2001).

The fact that Nodal is able to act over long distances suggests that it may travel from the node to the left LPM (Yamamoto et al., 2003; Norris et al., 2002; Saijoh et al., 2000). In fact, it has been shown that Nodal signal travels from the node to the left LPM via interaction with sulfated glycosaminoglycans (GAGs), specifically localized to the basement membrane between the node and the LPM (Oki et al., 2007). In its route from the node to the

LPM, Nodal will cross the PSM region. One question that arises is why is the PSM non-responsive to Nodal? An explanation comes from previous reports were it was shown that the zebrafish *cryptic* and *one-eye pinhead* (*oep*), membrane attached proteins members of the Epidermal Growth Factor-like - *Cripto*, *Frl-1,* and *Cryptic* (EGF-CFC) family, are necessary for the activation of Nodal in the left LPM. These proteins are extracellular cofactors for Nodal signalling and are expressed only in the LPM and not in the node and PSM (Shen et al., 1997; Zhang et al., 1998; Gritsman et al., 1999). Moreover, Cryptic is not required for the initiation of *nodal* expression in the node being only necessary for *nodal* expression in the left LPM (Gaio et al., 1999; Oki et al., 2007). Either in the absence of *cryptic* or *oep*, no asymmetric expression of *nodal*, *lefty2/antivin* and *pitx2* is observed in the LPM (Gaio et al., 1999; Yan et al., 1999). These results indicate that Nodal travels from the node to the left LPM through GAGs, and that *cryptic* and *oep* are required for its activation in the LPM (Gaio et al., 1999; Yan et al., 1999; Oki et al., 2007).

Interestingly, Nodal signalling is not only involved in regulating positional asymmetries of the internal organs but also controls brain asymmetries. Important insights regarding the genetic of brain asymmetries come from studies in zebrafish (reviewed in Concha and Wilson, 2001). In addition of being expressed in the LPM, several genes from the Nodal pathway are also expressed in the zebrafish brain prior to the development of asymmetries in the same region – *cyclops* (*cyc*), a *nodal*-related gene, *lefty1* and *pitx2* are expressed in the left diencephalon, while *oep* and *schmalspur* (*sur*), an orthologue of *foxH1* necessary to maintain expression of *nodal* genes, are bilaterally expressed (Concha et al., 2000; Liang et al., 2000; reviewed in Concha and Wilson, 2001). Also, *spaw* (*nodal*-related gene) in the left LPM was shown to regulate diencephalic asymmetric gene expression, implying that Nodal signaling within LPM influences laterality in the diencephalon (Long et al., 2003). These results suggested a role for Nodal signalling in the establishment of brain asymmetries, characterized by an enlarged left habenula and a parapineal organ situated to the left side of the brain. In fact,

Nodal was shown to initiate asymmetry in habenular neurogenesis that will indirectly bias parapineal migration toward the left, which will then maintain the left-sided habenula identity (Concha et al., 2003; Roussigné et al., 2009). Interestingly, in zebrafish with *situs inversus* not only at the viscera level but also in the CNS, such as in the *frequent situs inversus* (*fsi*) mutant zebrafish, not all behaviors were reversed. This implies that behavior lateralization cannot be explained by a switch in the brain anatomical lateralization and that another level of regulation exists (Barth et al., 2005).

I.2.1. How can cilia break symmetry?

Apart from of the signaling pathways that might activate *nodal* in the node region and the subsequent signaling cascade, it is important to understand the event that turns *nodal* expression asymmetric on the left side of the node. In other words, how is the initial embryonic symmetry broken in the node region? A clue to start to solve this question came from the observation that Kartagener's syndrome patients have ultrastructural defects in Dynein, a component of the ciliary motion motor (Afzelius, 1976; Afzelius, 1985). This particular defect was readily associated with the chronic respiratory infections and male infertility observed in these patients as a result of lack of cilia/flagella motility within the respiratory epithelium and sperm. However, the connection with *situs inversus* was only established later. It turned out that *left-right dynein* (*lrd*) is expressed in the mouse node (Supp et al., 1997), that node cells possess monocilia (Sulik et al., 1994) and that the *inversus viscerum* (*iv*) mutant mouse that shows a clear randomized laterality phenotype has a mutation in *lrd* (Singh et al., 1991; Schreiner et al., 1993; Lowe et al., 1996). Most importantly it was shown that these node cilia, microtubule-based organelles involved in signal transduction, rotate in a clockwise manner and due to their posteriorly tilted position on each cell create a leftward extracellular fluid flow that induces left-side specific gene expression (Nonaka et al., 1998; Nonaka et al., 2005) (Figure 1.5B). The reversed laterality obtained when an artificial rightward flow is imposed on the mouse node is consistent with the idea

that a directional fluid flow provides the asymmetry cue that determines laterality (Nonaka et al., 2002). Moreover, using the same experimental setup, it was possible to rescue the laterality phenotype of the *iv* mouse mutant, in which no flow is observed by simply exposing their nodes to a strong leftward fluid flow (Nonaka et al., 2002; Okada et al., 1999). In addition, in mouse mutants for the cellular motor proteins *kif3a*$^{-/-}$ and *kif3b*$^{-/-}$ no cilia are formed, resulting in an altered leftward flow and consequently perturbed LR asymmetry (Nonaka et al., 1998; Okada et al., 1999; Takeda et al., 1999). Given these results, nodal fluid flow was suggested to be a key factor in establishing LR asymmetry, with ciliary beating clearly being important in its generation.

How the flow is interpreted and then converted into LR asymmetric gene expression is still unknown. Nevertheless, two models have been proposed to date. One model states that a morphogen might be transported as a consequence of the leftward fluid flow created by motile *lrd*-containing cilia. The resulting asymmetric morphogen distribution would initiate downstream molecular events that then establish LR asymmetries in the LPM (Nonaka et al., 1998). More recently, vesicular particles containing Shh and RA were shown to form in the node stimulated by FGF and are transported to the left edge of the node where they fragment and release their contents (Tanaka et al., 2005). An alternative model mentions the existence of two different subpopulations of cilia in the node. In addition to the motile *lrd*-containing cilia, there are also immotile mechanosensory cilia that lack dynein arms and containing the polycystin-2 (PKD) calcium activated channel (McGrath et al., 2003; Tabin and Vogan, 2003). It has been proposed that immotile mechanosensory cilia sense the fluid flow pressure on the left side of the node and trigger an asymmetric intracellular Ca^{2+} flux that then breaks LR symmetry by inducing asymmetric *nodal* expression (McGrath et al., 2003) (Figure 1.5B). These two models are not mutually exclusive and it is possible that both mechanosensors and morphogens are involved in setting up the asymmetric pathway.

I.2.2. Cilia distribution in the laterality organ

Although, first described in mouse, the directional flow produced by motile cilia in the node is not exclusive to murine embryos. In fact a directional type of flow is generated in node-equivalent structures in a wide range of vertebrates. In zebrafish and medaka, the motile cilia inside the KV produce a counterclockwise fluid flow. The rabbit posterior notochord (PNC) and *Xenopus* gastrocoel roof plate (GRP) also have motile cilia, which have been shown to create a leftward fluid flow (Essner et al., 2005; Okada et al., 2005; Hojo et al., 2007; Schweickert et al., 2007; Basu and Brueckner, 2008). As for the chick, it is clear that ciliated cells are present in the Hensen's node. However it has been proposed that the distance between single monocilia is too long to create a directional flow thus compromising their role in LR determination (Essner et al., 2002; Männer, 2001). Instead, it seems that asymmetry in the node is promoted by outside tissues (Pagán-Westphal and Tabin, 1998), most likely through asymmetric cell rearrangements that generate a leftward movement of cells around the node (Gros et al., 2009; Cui et al., 2009).

This unidirectional flow produced by cilia movement determines/maintains the left sidedness of the axis. Importantly, it has been shown that the unidirectional flow depends on the posteriorly tilted position of cilia on the surface of the node cells. This tilted position allows cilia to generate a weak stroke when moving in their rightward direction and passing close to the cell surface, and generate a stronger stroke when moving towards the left and passing further away from the cell surface. This asymmetric stroke is then responsible for generating the unidirectional flow towards the left. If cilia were in a perpendicular position to the node surface, then this rotational movement would create a vortex that would lead to a circular flow instead of a linear one (Nonaka et al., 2005; Okada et al., 2005). More recently, it has been shown that cilia localization in the posterior part of the cell is also important for the cilia posterior tilt orientation (Figure 1.6). Several studies have shown that the planar cell polarity (PCP) pathway, an evolutionarily conserved mechanism involved in regulating polarized cellular orientation and migration, is necessary for cilia posterior displacement within the node cells. Mice lacking *dishevelled* (*dvl*) genes, cytoplasmic

PCP core proteins, were shown not to be able to place the basal bodies (from which cilia elongate) in the posterior region of the node cells and were unable to generate a unidirectional leftward flow (Hashimoto and Hamada, 2010) (Figure 1.6B). Also, in mouse conditional mutants for both *vangl1* and *vangl2* (encode PCP transmembrane proteins homologues of the *Drosophila* gene *van gogh* (*vang*)), the basal bodies do not acquire a posterior localization within the cells and consequently cilia also do not acquire a posterior localization nor a posterior tilt orientation (Figure 1.6B). Further, the unidirectional leftward flow is compromised, left side specific genes become randomized and internal organs acquire laterality problems (Song et al., 2010). It was also shown in zebrafish and *Xenopus* that the PCP gene *vangl2* is also regulating the posterior position and tilt of cilia in the KV and gastrocoel roof plate, respectively (Borovina et al., 2010; Antic et al., 2010). Given this, the PCP mediated polarity in ciliated cells is clearly a conserved approach in mouse, zebrafish and *Xenopus*.

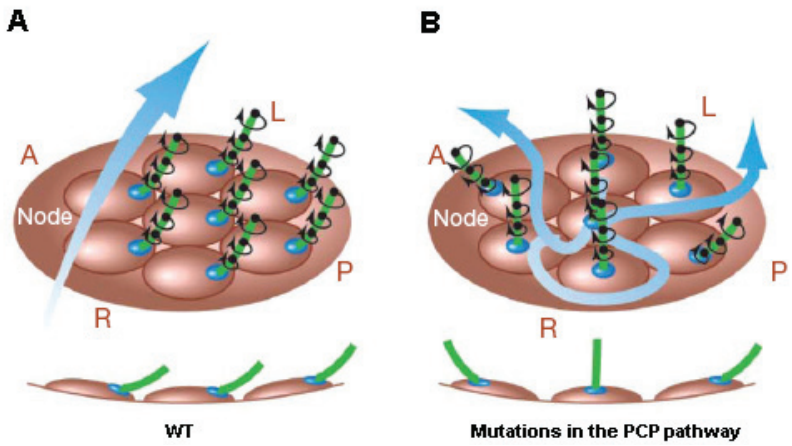

Figure 1.6. Cilia distribution, tilt and flow generation. (A) In a WT situation, cilia are localized in the posterior part of the node cells. This localization is important for their posterior tilt orientation necessary for the induction of a leftward extracellular fluid flow, required to regulate left-right asymmetry pathway. (B) PCP pathway is required for the correct positioning and orientation of cilia in the cells. In PCP pathway mutants, the basal bodies do not acquire a posterior localization within the cells and consequently cilia also do not acquire a posterior localization nor a posterior tilt orientation. Given this, cilia are unable to generate a unidirectional leftward flow. *Adapted from Song et al., 2010.*

I.2.3. More than cilia: other players in the scene

Although it is clear that monocilia play a fundamental role in LR patterning, several lines of evidence suggest that earlier LR asymmetries already exist prior to the directional fluid flow generated by ciliary motion, at least in amphibians, chick and fish.

In *Xenopus*, an asymmetrically localized ion flux is set up through a hydrogen-potassium adenosine triphosphatase (H^+/K^+ ATPase) transporter (pumps H^+ out of the cell in exchange for K^+). In fact, *H^+/K^+ ATPase* maternal mRNA is already asymmetrically localized on the right-hand side of the embryo during the first two cell divisions. In addition, it was shown that inhibition of this pump results in randomization of left side specific genes and organ heterotaxia (Levin et al., 2002). It has been suggested that asymmetric ion flux might be responsible for directing the positioning of a LR determinant to the left side through gap junction communication channels (GJC) since inhibition of these channels induces heterotaxia in *Xenopus* (Levin et al., 2002; Levin and Mercola, 1998). Generation of LR voltage differences that control laterality also seem to be important in the chicken embryo. In fact, a differential H^+/K^+ ATPase activity across Hensen's node results in left side asymmetric ion flux, which creates a differential membrane potential between the left and right sides of the primitive streak. Asymmetric ion flux has also been suggested to direct LR determinants through GJC in chick, since GJC inhibition also leads to LR patterning problems (Levin et al., 2002; Levin and Mercola, 1998). H^+/K^+ ATPase activity results in extracellular Ca^{2+} accumulation on the left side of Hensen´s node, a possible candidate for being a LR determinant molecule to pass through the GJC. In fact, Ca^{2+} accumulation was shown to induce an asymmetric activation of Notch on the left side of the node that then translates this differential activity into asymmetric *nodal* expression. Perturbing this early asymmetric ion flux, will lead to randomized gene expression and organ heterotaxia (Raya et al., 2004). In zebrafish it has been shown that the early activity of the H^+/K^+ ATPase pump determines the LR axis without affecting cilia or KV fluid flow (Kawakami et al., 2005). More recently, the function of another proton pump, the H^+-

V-ATPase, was shown to be important to establish LR asymmetries in *Xenopus*, fish and chick and in the case of zebrafish clearly impacts on cilia size/number within the KV (Adams et al., 2006). In zebrafish another pump, the sodium-potassium ATPase (Na,K-ATPase) alpha2, modulates the levels of intracellular Ca^{2+} already in the cells that are going to give rise to the KV, the dorsal forerunner cells (DFC's). In turn, these Ca^{2+} levels regulate cilia motility in the KV and consequently the cilia-driven leftward fluid flow (Shu et al., 2007). Propagation of the intracellular asymmetric Ca^{2+} flux is regulated by inositol polyphosphates, which in turn are candidates for the LR determinant that passes through GJC and influence LR determination (Sarmah et al., 2005). Consistent with this idea, Connexin43.4 (Cx43.4), a protein of the GJC channel, is required for the LR patterning through the development of a functional KV with normal cilia (Hatler et al., 2009).

Another possible candidate for the LR determinant is the neurotransmitter serotonin, which has been demonstrated to regulate LR patterning in *Xenopus* and chick before the appearance of cilia. Maternal serotonin has a rightward gradient localization during cleavage stages and its localization requires the set up of an asymmetric voltage gradient created by the H^+/K^+ ATPase coupled with GJC channels (Fukumoto et al., 2005 A; Fukumoto et al., 2005 B).

Although the fluid flow generated by cilia seems to be the first symmetry-breaking event in mouse, it may not be the initial event in other organisms where it is more likely to serve as an amplification mechanism of the LR decision made earlier in development. In zebrafish, *Xenopus* and chick, different mechanisms seem to act prior to the leftward flow initiation, such as asymmetric localization of ion channels and asymmetric function of gap junctions (Figure 1.5A). So far, no ion transporters have been described to be involved in LR establishment in mammals, however an unidentified symmetry breaking event may occur earlier in mouse development like in other vertebrate embryos. Interestingly, a recent report states that manipulation of initial cleavages in the mouse embryo leads to a reverted direction of fetal axial rotation, although the heart and gut

laterality was not affected (Gardner, 2010). This finding sets the ground for the possibility that in mammals LR embryonic patterning may be set during the cleavage stages similarly to what has been described in snails, where manipulation of the first cleavages resulted in reverted shell coiling and visceral situs inversus (Kuroda et al., 2009). Thus, there is still specullation about the timing and regulatory mechanisms of the symmetry breaking between the various species.

I.3. How are symmetric tissues protected from LR asymmetric signals?

The formation of a perfect vertebrate body plan involves the establishment of LR asymmetries in the LPM to position the internal organs. In addition, it is also crucial that bilateral symmetry is maintained in the PSM ensuring the symmetric formation of the somites and consequently of the axial skeleton and skeletal muscles. Besides sharing the same signaling pathways as discussed above, somitogenesis and LR patterning take place at around the same time during development in nearby embryonic regions. Therefore, the asymmetric signals that originate in the node have to be able to influence the LPM without affecting the bilateral symmetry of somite formation in the juxtaposed PSM. In fact, several lines of evidence show that bilateral symmetry is not a default state but instead has to be actively maintained through a mechanism that protects this territory from the LR asymmetric signals.

I.3.1. Retinoic acid buffers the PSM from the influence of LR signals

RA binds to heterodimers of retinoic acid receptor (RAR) and retinoid X receptor (RXR) and activates transcription of RA-responsive genes upon binding to specific DNA sequences known as retinoic acid response elements (RAREs) (Niederreither and Dollé, 2008). RA has been implicated in the control of bilateral symmetry in vertebrates, acting as a buffer that prevents LR signals to reach the PSM and influence somitogenesis (Figure 1.7A).

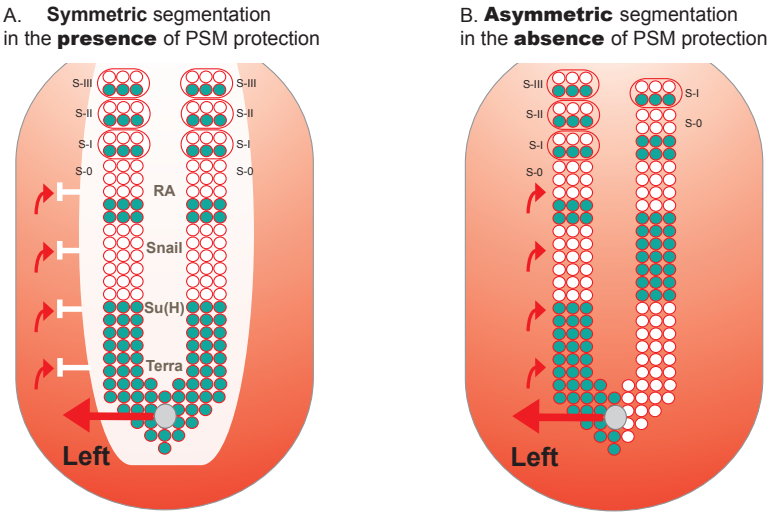

Figure 1.7. Protection of PSM segmentation from LR asymmetric patterning cues. A) PSM is protected from LR signals that come from the node and are implicated in left-right patterning (red arrows). This protection consists of a "shield" (white) which so far has been shown to be composed by RA, Snail, Su(H) and Terra. In its presence, cyclic gene expression (blue) and somite formation are symmetric between the left and right sides. B) In the absence of this protection, cyclic gene expression becomes desynchronised between both sides. Consequently, somite formation proceeds in an asymmetric way, with the left side exhibiting more somites than the right (this biased asymmetry towards the right side is seen in mouse and fish embryos, while in chick asymmetries are biased to the left side).

When the function of the RA producing enzyme *raldh2* is abolished either by a null mutation in the mouse or by morpholino (MO)-knockdown in zebrafish embryos, somite formation is delayed with a bias on the right side as assayed by the expression of *uncx4.1*, a marker of the posterior half of the mature somite (Kawakami et al., 2005; Vermot et al., 2005) (Figure 1.7B). In the *neckless* mutant, that carries a missense mutation in *raldh2*, the same phenotype is observed (Kawakami et al., 2005). Interestingly, the somitogenesis delay on the right side observed in the *raldh2* mutants and morphants only happens in a specific time window, between 8-15 somite stage in mouse and 6-13 somite stage in zebrafish. This period corresponds to the time point at which the LR information is being transferred from the

node/KV to the LPM. This phenotype in not caused by a defect in LR patterning in general, since no laterality defects are observed in the absence of *raldh2* in mouse and zebrafish (Kawakami et al., 2005; Vermot et al., 2005; Sirbu and Duester, 2006). In addition, epistatic experiments by crossing the *raldh2* with *lrd* mouse mutants lead to randomized somite defects instead of the right biased defects seen in *raldh2* single mutants (Vermot and Pourquié, 2005). This particular experiment shows that RA acts to counteract LR signals.

The right biased somite defects seen in the absence of *raldh2* can be explained by the LR desynchronization of the segmentation clock (Kawakami et al., 2005; Vermot et al., 2005) (Figure 1.7B). In these embryos, the expression of the cyclic genes *hes7* and *lfng* (in mouse), *deltaC*, *her1* and *her7* (in zebrafish) are out of phase between the left and right sides. Also consistent with the somite phenotype is the anterior displacement of the wavefront seen by the anterior expansion of *fgf8* on the right side of the PSM. Once again these LR desynchronization defects are only detected within a small time window that correlates with asymmetric somite formation (Kawakami et al., 2005; Vermot et al., 2005).

When *raldh2* was inhibited with disulphiram in chick embryos, again a delay in somite formation was observed and this effect was restricted to a specific time window. But in contrast to mouse and zebrafish now fewer somites formed on the left side of the axis (Vermot and Pourquié, 2005). The segmentation clock is in different phases between the left and the right side of PSM, as seen by the asymmetric expression of *lfng*. However in contrast to mouse and zebrafish, *fgf8* is not expanded anteriorly in an asymmetric manner in disulphiram-treated chick embryos (Vermot and Pourquié, 2005).

Thus, RA presents a conserved function, which is vital to protect symmetric somite formation by counteracting the effect of LR cues that are being transferred from the node into the LPM during a specific period of time (Figure 1.7A). After this discovery the next question that arises is what are the LR cues that RA is counteracting and where and when is this action being performed? Due to the fact that *radlh2* is expressed in the PSM it is rea-

sonable to predict that RA is performing its function in this mesodermal tissue. However, using a retinoic-acid response element (RARE)-LacZ-reporter transgene it was shown that RA signaling in mouse embryos is present not only in somites and anterior PSM, but it also extends to the adjacent neural plate and the node ectoderm (Sirbu and Duester, 2006). In the node ectoderm, RA antagonizes *fgf8* that is expressed nearby in the epiblast (primitive ectoderm). In *raldh2* mutants already at early somite stages there is an expansion of *fgf8* expression from the epiblast into the neural plate and node ectoderm. At later stages, these embryos show a right shift of *fgf8* expression in the anterior PSM, suggesting that the expansion of *fgf8* into the node ectoderm may be increasing its own levels in the adjacent PSM shifting it more anteriorly (Sirbu and Duester, 2006). These authors suggest that RA is ensuring bilateral somite formation not at the level of the PSM but at the level of the node ectoderm, where it controls the limits of *fgf8*.

Recently, an independent study using the same (RARE)-LacZ-reporter transgene showed however that the levels of RA signaling in the mouse PSM are higher on the right side (Vilhais-Neto et al., 2010). In addition, these authors show that this asymmetric RA signaling results from the function of a complex consisting of Nr2f2a and a novel RA signaling component called Rere. While *rere* is ubiquitously expressed, *nr2f2a* is asymmetrically expressed on the right PSM. In mice mutant for *Rere*, there is a lack of LR synchronization of the cyclic genes and of the *fgf8* anterior limit in the PSM, leading to a somitogenesis defect similar to the one described for *raldh2* mutants. This asymmetric RA signaling seems to be important to control the LR determination function of Fgf8 in the PSM. Interestingly, *nr2f2*a expression in the mouse is asymmetric on the right, while in the chick it is asymmetric on the left side of the PSM. This provides an explanation for the different bias in the somite formation defects observed in the absence of RA signaling in these two vertebrates (Vermot and Pourquié, 2005; Vilhais-Neto et al., 2010) and might be linked with the fact that Fgf8 is a left determinant in the mouse while in the chick it is a right determinant (Meyers and Martin, 1999; Boettger et al., 1999).

Fgf8 does not seem to be the only LR cue corrected by RA signaling. In both chick and mouse embryos, *snail1* is transiently asymmetrically expressed in the right LPM and plays a role in organ lateralization (Isaac et al., 1997; Sefton et al., 1998). Furthermore, it was shown that the period of asymmetric *snail1* expression in the LPM coincides with the time window during which RA is necessary to protect the PSM from asymmetric signals (Morales et al., 2007). Indeed, in the chick it was shown that in the absence of RA signaling, *snail1* expression is not affected in the LPM but starts to be asymmetrically expressed in the right anterior PSM. This asymmetric PSM expression of *snail1* results in asymmetric expression of the cyclic genes *snail2* and *lfng* and later leads to asynchronous somitogenesis (Morales et al., 2007). Whether or not the asymmetric somite formation seen in the absence of RA signaling in the mouse (Vermot and Pourquié, 2005) is due to a misregulation of *snail1* expression in the PSM is still unknown. However, in mice mutants for *Rere,* there is no sign of an asymmetric *snail1* expression in the PSM (Vilhais-Neto et al., 2010).

RA signaling has emerged as a conserved keeper of bilateral somite formation. Perturbations of RA function lead to a biased somitogenesis defect in a specific time window that correlates with the timing of LR cues establishment (Kawakami et al., 2005; Vermot and Pourquié, 2005; Vilhais-Neto et al., 2010). In the same studies, it was shown that RA perturbation does not result in LR defects in the LPM since the expression of *spaw* and *pitx2* in the LPM is normal. However, the somite laterality defects are linked to the LR pathway. In fact, the bias in somite defects is lost when RA signaling is perturbed along with randomization of the LR asymmetric cues upon *lrd* inactivation (Kawakami et al., 2005; Vermot and Pourquié, 2005; Vilhais-Neto et al., 2010).

I.3.2. Bridge between LR patterning and somitogenesis

Direct links between LR patterning and somitogenesis were revealed in studies in zebrafish. The transcription factor Suppressor of Hairless (Su(H)), belongs to a complex that mediates Notch signaling (Fior and Henrique, 2009).

The downregulation of any of the two Su(H) paralog genes in zebrafish leads to randomization of LR markers in the LPM and to an unbiased asymmetric somite formation. In the *su(H)* morphants, the RA degrading enzyme *cyp26a1* is misregulated in the tailbud. Since *cyp26a1* knockdown can also lead to asymmetric cycling gene expression, this suggests that Su(H) is required to regulate RA in the tailbud that will in turn regulate symmetric cycling gene expression in the PSM (Echeverri and Oates, 2007) (Figure 1.7A,B).

We have shown that Dmrt2a/Terra, a zinc finger-like transcription factor belonging to the DMRT family, regulates the body plan along the LR axis in zebrafish. In Dmrt2a/Terra morphants, the LR asymmetry pathway is also affected, with the expression of left side LPM markers being randomized and consequently affecting the positioning of the heart. On the other hand, dynamic cyclic expression of *deltaC*, *her1* and *her7* becomes desynchronized between the left and right sides of the PSM in a specific time window, leading to an unbiased somite number. Therefore, Dmrt2a/Terra has a dual role, it ensures the correct flow of LR asymmetry information to the LPM and in combination with RA signaling ensures the maintenance of symmetry in the PSM (Saúde et al., 2005) (Figure 1.7A,B). In the mouse, the knockout of *dmrt2* strongly affected somite differentiation leading to severe rib and vertebral malformations (Seo et al., 2006). It would be interesting to know whether it also regulates synchronization of the clock genes and if it has an impact on heart laterality.

Even more striking is the observation that the simple disruption of the LR determination pathway results in asymmetric somite formation in zebrafish. Downregulation of the H^+/K^+-ATPase activity, with omeoprazole from 1-cell to bud stages only, results in randomization of LR markers in the LPM and in an unbiased asymmetric somite formation between the left and right sides of the PSM (Kawakami et al., 2005). Also when Notch signaling is perturbed, with the γ-secretase inhibitor DAPT from bud to early somitogenesis stages, there is a randomization of LR markers in the LPM and an unbiased asymmetric somite formation. Once again the somitic defects are only detected in a specific time window from 6 to 13-somite stage, corresponding

to the moment when LR information is being transferred from the KV to the LPM cascade (Kawakami et al., 2005).

At this moment, there is no evidence for the existence of a LR desynchronization phenotype in somite formation upon perturbation of early LR asymmetric information in mouse laterality mutants. Since the bilateral somite phenotype can only be detected in a specific time window, there is still the possibility that it was not noticed over the extensive organ laterality analysis.

I.4. Human developmental disorders related to the LR axis

The set up of the axial skeleton is dependent on somite formation and differentiation. After epithelialization from the anterior region of the PSM, each somite undergoes a dorsal-ventral compartmentalization so that the ventral region, enclosing the sclerotome, is different from the dorsal region, the dermomyotome. This subdivision is important for later patterning events, with the sclerotome differentiating into the axial skeleton and ribs, and the dermomyotome giving rise to the dermis of the back and skeletal muscles (Andrade et al., 2007). A diverse number of human conditions associated with vertebral malformations arise as a consequence of mutations in important somitogenesis-related genes. Mutations in Notch ligand *delta-like 3* (*dll3*) (Bulman et al., 2000), *mesp2* (Whittock et al., 2004) and *lunatic fringe* (*lfng*) (Sparrow et al., 2006) are associated with the spondylocostal dysostosis syndrome. This condition exhibits vertebral column malformations from rib fusions to kypho-scoliosis (abnormal curvature of the spine). This phenotype is reminiscent of what happens in mouse mutants, highlighting the importance of mouse models in the search for the genes associated with human disorders (Gruneberg, 1961; Saga et al., 1997; Zhang and Gridley, 1998). Mutations in other genes of the Notch pathway can also lead to vertebral malformations. Mutations in two Notch pathway ligands, *jag1* and *notch2*, are associated with the Alagille syndrome which has been shown to present, among other symptoms, abnormal vertebrae formation

which are "butterfly shaped" (McDaniell et al., 2006). Fgf signalling has also been implicated in disorders associated with skeletal development. A mutation in *fgfr2* results in fused cervical vertebrae, known as the Apert syndrome (Kreiborg et al., 1992). A minor perturbation in segmentation can lead to severe clinical consequences. Thus the identification of molecules that can reduce vertebral patterning disorders will subsequently help in their prevention.

LR asymmetric cues are important to position the internal organs in a normal configuration termed *situs solitus*. When LR patterning is disturbed by a series of events, as previously discussed, abnormal laterality phenotypes appear namely *situs inversus* and *situs ambiguus*. The morbidity and mortality associated with laterality defects is mainly due to congenital heart disease (CHD) (Ramsdell, 2005) Human patients with *situs inversus* have 3% incidence of CHD compared with normal *situs solitus* humans that show a 0.08% incidence (Lurie et al., 1995; Nugent et al., 1994; Sternick et al., 2004). In *situs ambiguus* patients the incidence of CHD is greater than 90% (Nugent et al., 1994). The cardiac defects in these patients include atrial and ventricular septal defects, transposition of great arteries, double outlet right ventricle, anomalous venous return and aortic arch anomalies (Bowers et al., 1996). The clinical observations together with a number of molecular evidence from animal models are helping to understand the ethiology of CHD. It is becoming clear that heart diseases may result from abnormal looping and remodeling of the primitive heart tube into a multi-chambered organ as a consequence of LR patterning defects.

In addition, human laterality defects might be associated with primary cilia dyskinesia (PCD) or Kartagener syndrome. In PCD patients, approximately 50% display *situs inversus* while the other individuals show normal organ *situs* and only a very low percentage show *situs ambiguus* (Afzelius, 1976; Kartagener and Stucki, 1962). Once again, clinical data together with experimental results from animal models provided a biological explanation for this association, revealing that cilia are indeed early players in LR patterning.

It should be noticed that laterality defects in humans are often associated with abnormal vertebrae and scoliosis (Debrus et al., 1997). The genetic etiology of these conditions is unknown, however we speculate that they may relate to the recently uncovered molecular link between LR patterning and bilateral synchronization of the segmentation clock.

Morphological asymmetries are subtle in the brain. However, functional asymmetries are more obvious, with most people having the left hemisphere specialized for language, right-handedness preference and right ear advantage for verbal stimulus (Toga and Thompson, 2003). Interestingly, signals that establish brain functional laterality seem to be different from those that determine anatomical laterality. This lack of correlation was reported in a study where individuals with *situs inversus* have indeed reversed anatomic asymmetries of the cerebral hemispheres but, 95% of them still have language lateralized to the left cerebral hemisphere and right-handed preference. Thus, there seem to be different mechanisms responsible for brain anatomical asymmetry and functional lateralization of language (Kennedy et al., 1999). In another study, from a group of individuals with PCD only 15,2% were left-handed (normal rates in normal situs individuals). Again, the fact that there is not reversion of right-handedness indicates that brain normal lateralization is still present in *situs inversus* individuals and in this way dissociated form organs asymmetries (McManus et al., 2004). The same dissociation was also shown in a study where patients with *situs inversus* not only presented right-handedness but also REA, just like the control group (Tanaka et al., 1999). Thus, this lack of association of language lateralization, handedness and REA with organ situs suggests that ciliary function in the node, apart from being responsible for regulating body *situs*, does not seem to be the mechanism responsible for functional brain asymmetry, implying that an independent mechanism must exist. Although the understanding of the genetic mechanisms that establish visceral asymmetries has increased in recent years, very little is known about the development of brain anatomy asymmetry and how it relates to brain functional lateralization.

I.5. Conclusions

To design the vertebrate body plan it is fundamental to create asymmetry between the left and the right side of the lateral plate mesoderm, in order to correctly position the internal organs. Also, it is crucial to maintain symmetry between the left and the right side of the PSM to ensure the perfect allocation of symmetric body structures such as the axial skeleton, skeletal muscles and peripheral nerves. Although different strategies were shown to initiate the LR asymmetry in the vertebrate embryo (Levin et al., 2005), only recently the existence of mechanisms that promote symmetry have been described in several organisms (Vermot et al., 2005; Vermot and Pourquié, 2005; Kawakami et al., 2005; Saúde et al., 2005). Therefore, symmetry is no longer perceived as a default embryonic state but rather as a developmental process involving an active molecular mechanism. Although the mechanism that bridges LR patterning and bilateral synchronization of the segmentation clock is not understood, the new studies here reviewed point to the idea that a correct flow of LR signals is necessary for bilateral somite formation.

The purpose of this work was to increase the knowledge regarding the role of Dmrt2 during embryonic development. The aim was:
– to analyze the degree of conservation of Dmrt2 function during vertebrate embryonic development. Since it has already been shown to be required to regulate both symmetric somite formation and LR asymmetry pathway during zebrafish development, we analyzed the phenotype of mice carrying the *dmrt2* null mutation and compared it to the characterized phenotype in zebrafish;
– to identify the zebrafish Dmrt2a/Terra downstream targets and in this way better understand how it is regulating embryonic LR development. We initiated a ChIP-on-chip approach and also created the tools required to perform a microarray experiment;
– to address the impact of the Notch signalling in the establishment of LR

asymmetry. The Notch pathway was already associated with the regulation of the LR asymmetry cascade in several vertebrates however, the level at which it is required to regulate this process during zebrafish development has not been well characterized. We addressed its impact in cilia length and movement and consequently in the LR asymmetry cascade.

CHAPTER II

Left-right function of *dmrt2* genes is not conserved between zebrafish and mouse

The work presented here was published in **Lourenço, R., Lopes, S. S. and Saúde, L.** (2010). Left-Right Function of dmrt2 Genes Is Not Conserved between Zebrafish and Mouse. *PLoS One* **5(12)**, e14438.

RL, SL and LS conceived the experiments and analyzed the data. RL performed the mouse experiments and SL the zebrafish experiments. RL and LS wrote the manuscript.

Abstract

Members of the Dmrt family, generally associated with sex determination, were shown to be involved in several other functions during embryonic development. Dmrt2 has been studied in the context of zebrafish development where, due to a duplication event, two paralog genes *dmrt2a* and *dmrt2b* are present. Both zebrafish *dmrt2a/terra* and *dmrt2b* are important to regulate left-right patterning in the lateral plate mesoderm. In addition, *dmrt2a/terra* is necessary for symmetric somite formation while *dmrt2b* regulates somite differentiation impacting on slow muscle development. One *dmrt2* gene is also expressed in the mouse embryo, where it is necessary for somite differentiation but with an impact on axial skeleton development. However, nothing was known about its role during left-right patterning in the lateral plate mesoderm or in the symmetric synchronization of somite formation. Using a *dmrt2* mutant mouse line, we show that this gene is not involved in symmetric somite formation and does not regulate the laterality pathway that controls left-right asymmetric organ positioning. We reveal that *dmrt2a/terra* is present in the zebrafish laterality organ, the Kupffer's vesicle, while its homologue is excluded from the mouse equivalent structure, the node. On the basis of evolutionary sub-functionalization and neo-functionalization theories we discuss this absence of functional conservation. Our results show that the role of *dmrt2* gene is not conserved during zebrafish and mouse embryonic development.

Introduction

The organization of the axial skeleton and skeletal muscles is bilaterally symmetric. In contrast, vertebrates are also characterized by stereotypic LR asymmetries in the distribution of the internal organs such as the heart and stomach on the left, and the liver on the right (Lourenço and Saúde, 2010).

The axial skeleton and skeletal muscles are derived from embryonic structures called the somites. The epithelialization of a new pair of somites occurs in a bilateral symmetric manner from the anterior-most region of the mesenchymal PSM (Dequéant and Pourquié, 2008). This process is tightly regulated in space and time, with a new pair of somites of approximately the same size being formed with a regular species-specific time period (Dequéant and Pourquié, 2008).

The "clock and wavefront" model (Cooke and Zeeman, 1976) postulates the existence of two independent phenomena accounting for periodic somite formation. The clock is evident in the PSM as periodic oscillations in gene expression of the so-called cyclic genes. These genes show a dynamic and reiterated expression in PSM cells with the same periodicity of somite formation (Dequéant and Pourquié, 2008). Although the list of cycling genes is increasing, the conserved ones across species include mainly Notch targets, namely the bHLH (basic-helix-loop-helix) transcription repressors, the *hes* genes in the mouse and the *her* genes in zebrafish. More recently, a large scale transcriptome analysis revealed that the segmentation clock mechanism shows different degrees of complexity between mouse and zebrafish. In the mouse, many of the cyclic genes belong not only to the Notch pathway but also to the Wnt and FGF pathways (Dequéant et al., 2006). In zebrafish there is no evidence for the existence of cyclic genes of the Wnt or FGF pathways (Dequéant and Pourquié, 2008). In addition to the presence of a molecular clock, the PSM cells are under the influence of a wavefront of differentitaion. This wavefront is determined by gradients of Fgf and Wnt signalling coming from the posterior region of the embryo and fading towards the anterior portion of the PSM. While under the influence of Fgf/Wnt signalling, the PSM cells are maintained in an immature state and are prevented from starting the genetic program of somite formation (Dubrulle et al., 2001; Aulehla et al., 2003). Soon after being formed the somites differentiate into the dermomyotome, which segregates into the dermal layer of the skin and skeletal muscles, and into the sclerotome that forms the vertebral column (Andrade et al., 2007).

At the same time somites are being formed, LR asymmetric information is establishing laterality in the nearby LPM, culminating with the asymmetric positioning of internal organs. Before there are any signs of asymmetric organ localization in the vertebrate embryo, a conserved cascade of asymmetrically expressed genes is activated around the node in the mouse and around the KV, the functionally equivalent fish organ. An excess of Nodal activity on the left side of the node/KV is transferred to the left LPM and in this location Nodal exerts a positive feedback on itself. As a consequence, the expression of nodal is amplified in the left LPM. Nodal also activates its negative regulators, the lefty genes. Lefty1 in the midline prevents *nodal* activation on the right LPM, while Lefty2 restricts the domain of *nodal* expression on the left LPM. The strong *nodal* expression on the left LPM induces *pitx2* expression that in turn activates morphogenetic proteins required for LR asymmetry of the internal organs (Tabin, 2006). Even though this Nodal cascade is conserved, the mechanism that induces nodal in the node/KV is different between vertebrates. Notch signaling activates *nodal* in the murine node region, while in zebrafish it activates the Nodal negative regulator *charon* around the KV (Raya et al., 2003; Krebs et al., 2003; Takeuchi et al., 2007; Gourronc et al., 2007). In addition to Notch signaling, Fgf8 and Wnt3a regulate *nodal* expression in the mouse node (Meyers and Martin, 1999; Nakaya et al., 2005). The role of Fgf and Wnt signaling in controlling *nodal* expression at the KV has not been determined.

Somitogenesis and LR patterning share the same signalling pathways that occur at overlapping developmental time windows and in nearby embryonic tissues. For this reason, the asymmetric signals from the node have to be able to reach the LPM without affecting the bilateral symmetry of somite formation in the adjacent PSM. In fact, several lines of evidence show that bilateral symmetry is not a default state but instead has to be actively maintained through a mechanism that protects this territory from the LR asymmetric signals (Brend and Holley, 2009 B).

RA has emerged as a conserved keeper of bilateral somite formation by buffering the PSM from the influence of LR cues (Kawakami et al., 2005;

Vermot et al., 2005; Vermot and Pourquié, 2005; Vilhais-Neto et al., 2010). Several lines of evidence show that Fgf8 and Snail1 are the LR cues that are being antagonized by RA signaling in the PSM (Vermot et al., 2005; Vilhais-Neto et al., 2010; Sirbu and Duester, 2006; Isaac et al., 1997; Morales et al., 2007). In zebrafish, another key player regulating development along the LR axis is the zinc-finger like transcription factor Dmrt2a/Terra, that belongs to the Dmrt family. We have previously shown that in zebrafish when Dmrt2a/Terra function is blocked, the expression of the cycling genes becomes desynchronized between the left and right sides and as a consequence somite formation is no longer symmetric. In addition, the positioning of the internal organs is compromised as a result of a randomization of left side LPM markers (Saúde et al., 2005).

On the other hand, the mouse *dmrt2* null mutants have severe somite differentiation defects but nothing was known regarding a possible role of Dmrt2 in regulating symmetric somite formation and establishing the LR asymmetry pathway (Seo et al., 2006).

Here we report that *dmrt2* homozygous mouse mutants do not show LR desynchronization of somite formation and do not have LR defects regarding internal organs positioning. We show that *dmrt2a/terra* is expressed in the zebrafish KV in agreement with its function in LR development. In contrast, we did not detect *dmrt2* expression in the mouse node, consistent with its non-conserved function during the process of LR axis determination in this vertebrate.

Materials and methods

Zebrafish line

AB wild-type zebrafish were crossed and embryos collected and kept at 28°C until the appropriate stage (Kimmel et al., 1995).

Mice breeding and genotyping

Mice carrying the *dmrt2* null mutation where previously described (Seo et al., 2006) and obtained from David Zarkower´s laboratory. Dmrt2 heterozygous mice were maintained on a C57BL/6 genetic background. DNA was extracted from the tail tip of adult mice and genotyped by polymerase chain reaction (PCR) using Dmrt2 specific primers. Dmrt2 WT forward primer 5'-CTGGACCCGAGTACAGTTCC-3', Dmrt2 WT reverse primer 5'-AATGGTGCGTTCAACTCAGG-3', Dmrt2 mutant forward primer 5'- TGCGGAGGGCTGGATCTTAAGGAG-3' and Dmrt2 mutant reverse primer 5'-AGGGGGTGGGGATTTGACACCATC-3', which resulted in a 830 bp band and a 270 bp band for the WT and mutant alleles, respectively. Dmrt2 heterozygous mice were crossed and embryos collected at specific stages (8.0-9.0 dpc). Mutant embryos were identified by PCR on DNA isolated from the yolk sacs using the same primers as for the adult mice genotyping.

Cloning of mouse and zebrafish *dmrt2a/terra* and *dmrt2b* genes

Mouse *dmrt2* complementary DNA (cDNA) (IMAGE: 1248080) was used to synthesize an antisense RNA probe, linearized with EcoRI and transcribed with T3. Total RNA was extracted from appropriate staged zebrafish embryos using TRIzol (Invitrogen) and cDNA was synthesized with MMLV-Reverse Transcriptase kit (Promega). *dmrt2a/terra* full length sequence was amplified by PCR with the following primer set: *dmrt2a/terra* forward primer 5'-ATGACGGATCTGTCCGGCACG-3' and *dmrt2a/terra* reverse primer 5'-AGCAAGAAGCCTTACTGAGATTTCCG-3'. *dmrt2b* was amplified by PCR with the following primer set: *dmrt2b* forward primer 5'-TTTCTTCCCGCTGTCAGACC-3' and *dmrt2b* reverse primer 5'-TTATCTCATGAGCAGTGCCTCG-3'. The *dmrt2a/terra* amplified DNA fragment was cloned in the pCS2+ vector and *dmrt2b* in the pGEM-T easy vector. To synthesize the antisense *dmrt2a/terra* and *dmrt2b* RNA probes, plasmids were linearized with ApaI and SpeI and transcribed with SP6 and T7, respectively.

Whole-mount *in situ* hybridization

Mouse embryos were analyzed by whole-mount in situ hybridization (WISH) as previously described (Kanzler et al., 1998) using the digoxigenin (DIG) labeled antisense RNA probes for *dmrt2*, *hes7*, *lfng*, *axin2*, *sprouty2*, *nodal* and *pitx2*. Zebrafish embryos were analyzed by WISH as previously described (Thisse and Thisse, 2008) using the digoxigenin (DIG) labeled antisense RNA probes for dmrt2a/*terra* and *dmrt2b*. Embryos were photographed with a LEICA Z6 APO stereoscope coupled to a LEICA DFC490 camera.

Results

II.1. The murine Dmrt2 is not required for bilateral synchronization of somite formation

The process of somite formation is under the control of a molecular clock, revealed by the dynamic expression of the cyclic genes. This expression pattern is subdivided into three consecutive phases that are reiterated with the formation of each somite pair (Dequéant and Pourquié, 2008). Importantly, the expression pattern of the cyclic genes on the left side of the PSM is always in phase with the one present on the right side.

In zebrafish, the expression of the cyclic genes *deltaC*, *her1* and *her7* becomes out of phase between the left and right sides of the PSM when *dmrt2a*/*terra* is knocked-down (Saúde et al., 2005). This eventually leads to the formation of an extra somite on either the left or the right side of the embryonic axis. Hence, it was proposed that Dmrt2a/Terra maintains the symmetry of somite formation possibly by protecting the PSM from the influence of LR asymmetric cues. This protection is only needed in a specific developmental time window that corresponds to the timing of transfer of LR information to the LPM (Saúde et al., 2005). In the mouse, it was shown that Dmrt2 is required for somite differentiation with severe implications on axial skeleton development (Seo et al., 2006). However, its potential role in synchronizing the molecular clock that underlies somite formation was not evaluated in murine embryos.

In order to investigate the effect of abolishing Dmrt2 function in the mouse molecular clock, we analyzed the expression of cyclic genes of the Notch, Wnt and Fgf pathways in the context of *dmrt2* null mutants (Seo et al., 2006). Embryos from *dmrt2* heterozygous crosses were collected between 8 to 15-somite stages, the developmental window that corresponds to the time when the PSM needs to be protected from LR signals (Vermot et al., 2005). These embryos were genotyped by PCR and analyzed by whole-mount *in situ* hybridization to reveal the expression of the Notch pathway cyclic genes *hes7* and *lfng*, the Wnt pathway cyclic gene *axin2* and the Fgf pathway cyclic gene *sprouty2* (Aulehla et al., 2003; Bessho et al., 2001; Forsberg et al., 1998; Minowada et al., 1999). Similarly to their wild-type and heterozygous siblings, in *dmrt2* homozygous mutants the dynamic expression of *hes7* (n=8) (Fig. 2.1A-E) and *lnfg* (n=14) (Fig. 2.1F-J) was not affected and normal phases of cyclic gene expression were observed. In addition, in all embryos analyzed, cyclic gene expression was in the same phase and therefore bilaterally symmetric on the left and right PSM's (Fig. 2.1A-J). When analyzing the expression of *axin2* and *sprouty2,* the same results were observed (Fig. 2.1K-P). The expression of *axin2* (n=3) (Fig. 2.1K-M) and *sprouty2* (n=3) (Fig. 2.1N-P) in wild-type, heterozygous and *dmrt2* homozygous mutant embryos was not affected and normal phases of cyclic gene expression were bilaterally symmetric in the PSM. In clear contrast to its role in zebrafish, Dmrt2 is not necessary to maintain bilateral symmetry of cyclic gene expression and therefore is dispensable for symmetric somite formation in the mouse embryo.

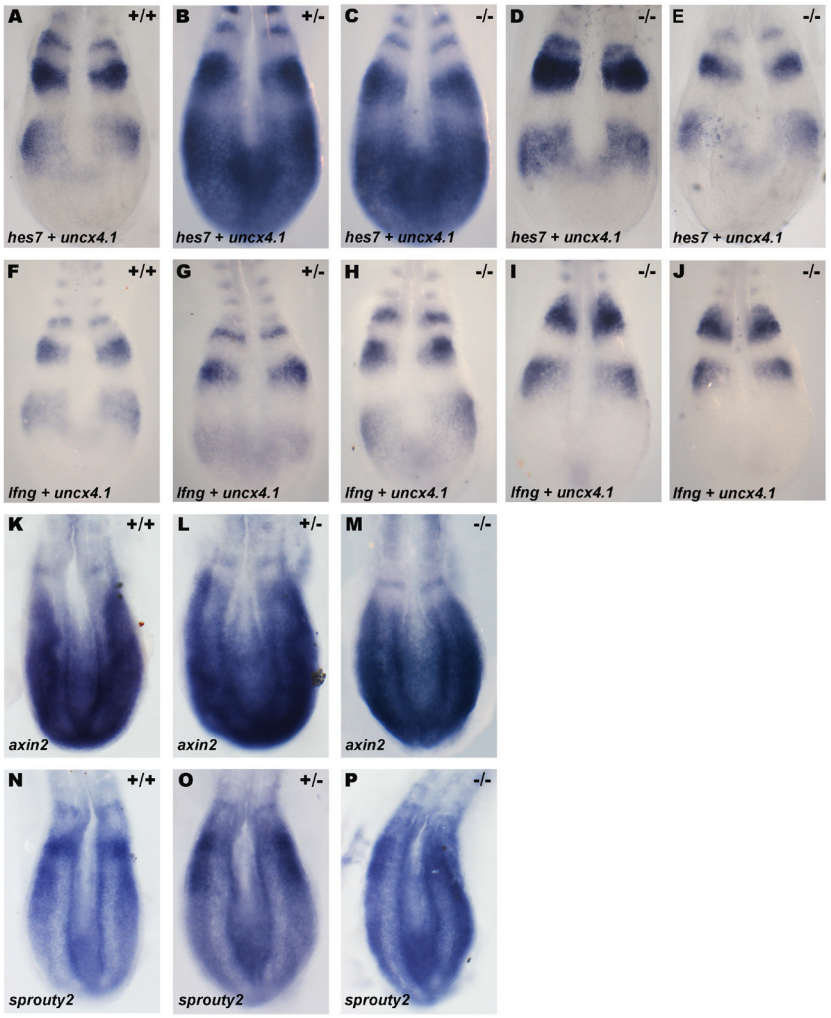

Figure 2.1. Dmrt2 is not required for symmetric somite formation in the mouse embryo. (A-P) Expression pattern of the cyclic genes ***hes7*** (A-E), ***lfng*** (F-J), ***axin2*** (K-M) and ***sprouty2*** (N-P) in E8.5 mouse embryos. (A-J) Embryos were also hybridized with the somite marker ***uncx4.1***. (A, F, K, N) WT, (B, G, L, O) heterozygous and (C-E, H-J, M, P) ***dmrt2*** homozygous mutant embryos show the same phase of ***hes1***, ***hes7***, ***axin2*** and ***sprouty2*** cyclic expression in the PSM. All views are dorsal with anterior to the top.

II.2. Mouse left-right LPM patterning is independent of Dmrt2 function

The distribution of the internal organs is controlled by a conserved LR patterning cascade of information that starts early in development in the node/KV region and is then transferred asymmetrically to the LPM.

In zebrafish, Dmrt2a/Terra is necessary for the establishment of LR asymmetries. In the absence of Dmrt2a/Terra, the transfer of the *nodal*-related gene *spaw*, from the KV region to the left LPM, is randomized instead of being consistently transferred to the left LPM. In addition, the expression of the *spaw* downstream target, *pitx2,* is also randomized in the LPM. Concomitant with this randomization of left-side specific genes, heart positioning is also misplaced (Saúde et al., 2005).

To further evaluate the putative role of Dmrt2 in LR asymmetry patterning in mouse development, we studied the expression of left-sided specific markers in *dmrt2* null mutants (Seo et al., 2006). Embryos from *dmrt2* heterozygous crosses were collected between E8.0 and E8.5, genotyped and processed by whole-mount *in situ* hybridization to reveal the expression of the left LPM genes *nodal* and *pitx2* (Collignon et al., 1996 Yoshioka et al., 1998). At embryonic day 8.0 (E8.0), *nodal* expression was stronger on the left side of the node and restricted to the left LPM in both *dmrt2*$^{-/-}$ mutants (n=8) and their siblings (Fig. 2.2A-C). At E8.5, in both *dmrt2* mutants (n=9) and their sibling embryos, *pitx2* was expressed on the left side of the LPM (Fig. 2.2D-F). This analysis reveals that Dmrt2 is not important to establish LPM laterality in the mouse embryo.

We next examined the laterality of the internal organs in newborn *dmrt2* mutants. Similarly to their siblings, *dmrt2* mutant mice (n=16) showed normal internal organ organization (Fig. 2.2G-L). The left lung had only one lobule, the right lung four lobules and the stomach and heart were always on the left side of the body cavities (Fig. 2.2I, L). This data on organ localization is in agreement with the normal expression pattern of early LR markers and indicates that the role of Dmrt2 in establishing LR asymmetries is not conserved between zebrafish and mouse.

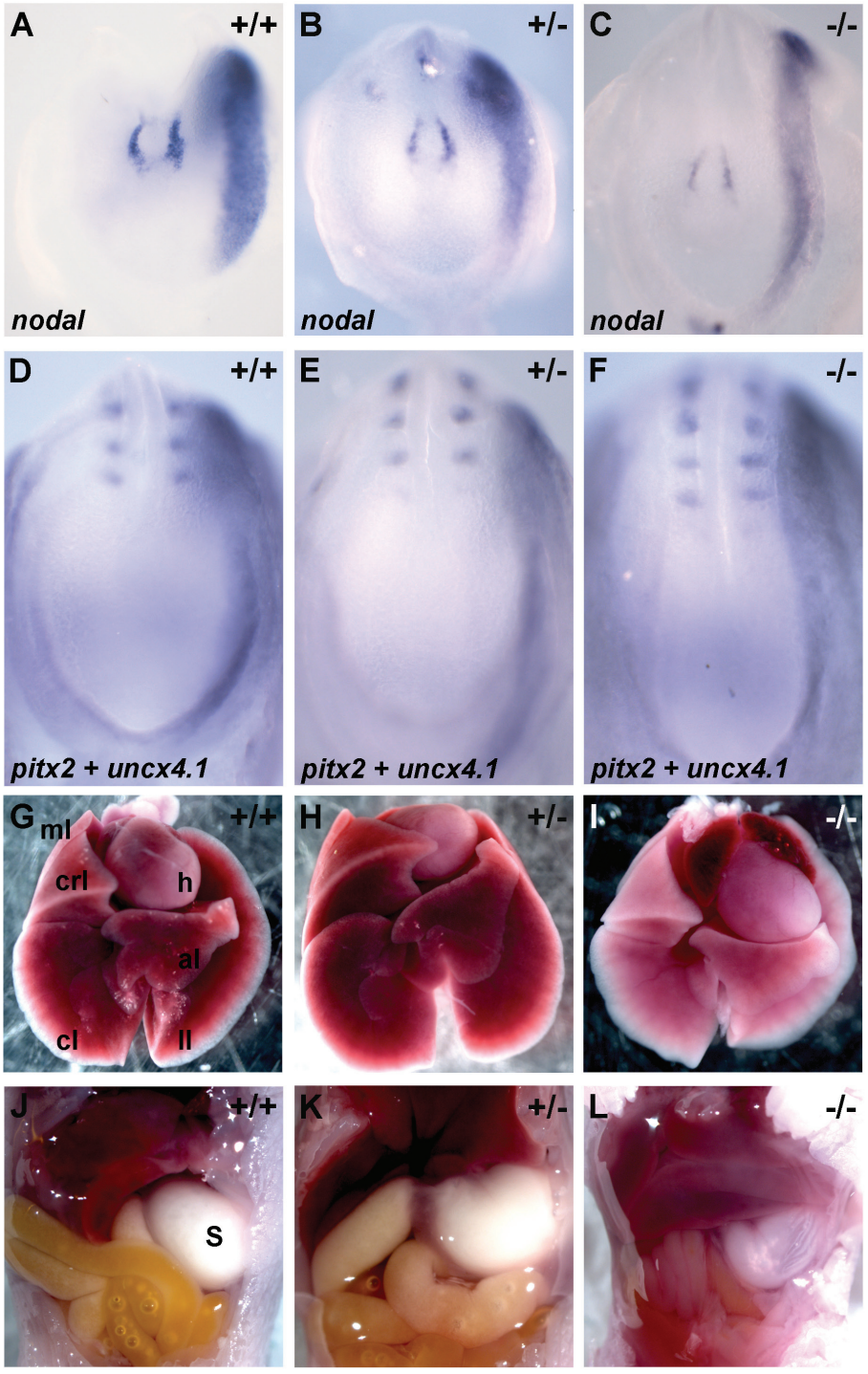
A
+/+
nodal
B
+/-
nodal
C
-/-
nodal
D
+/+
pitx2 + uncx4.1
E
+/-
pitx2 + uncx4.1
F
-/-
pitx2 + uncx4.1
G
ml
crl
h
al
cl
ll
+/+
H
+/-
I
-/-
J
+/+
S
K
+/-
L
-/-

Figure 2.2. Dmrt2 is not required for the left-right LPM patterning in the mouse embryo. (A-F) Embryos between E8.0 and E8.5 processed by whole mount *in situ* hybridization with *nodal* (A-C) and *pitx2* (D-F) probes, respectively. (A-C) *nodal* expression is restricted to the left side of the node and left LPM in (A) WT, (B) heterozygous and (C) *dmrt2* homozygous mutant embryos. (D-F) *pitx2* expression is also restricted to the left LPM in (D) WT, (E) heterozygous and (F) *dmrt2* homozygous mutant embryos. (G-L) Localization of the internal organs in newborn mice. (G) In WT, (H) heterozygous and (I) *dmrt2* homozygous mutants the heart always bend to the left, the left lung always has one lobe (ll) and the right lung has four lobes (ml, crl, cl, al). (J-L) Concomitant with the normal situs of the heart and lungs, the stomach is also always placed on the correct left side of the axis. ml (middle lobe); crl (cranial lobe); cl (caudal lobe); al (accessory lobe); ll (left lobe); h (heart); s (stomach). All views are ventral with anterior to the top.

II.3. *dmrt2a/terra* is expressed in the zebrafish Kupffer's vesicle but its homologous gene is absent from the mouse node

Our data clearly shows that the role of Dmrt2a/Terra in synchronizing somite formation and establishing LR asymmetries in the LPM, previously described in zebrafish (Saúde et al., 2005), is not conserved in the mouse. We reasoned that this non-conserved role could be due to a differential pattern of expression in these two vertebrates.

We confirmed that zebrafish *dmrt2a/terra* and its mouse homologue are expressed in the anterior region of the PSM and somites in both vertebrates (Fig. 2.3A-F) (Seo et al., 2006; Meng et al., 1999). In addition, we could detect *dmrt2a/terra* transcripts in the zebrafish KV from the 3-somite stage until the 10-somite stage (Fig. 2.3D-F). However, we could not find any expression of *dmrt2* in the mouse node from 1- somite stage to 7-somite stage, which is the equivalent laterality organ of zebrafish KV (Fig. 2.3A-C). The differential expression in the laterality organs of zebrafish and mouse may explain the different role that this transcription factor plays in controlling LR laterality and symmetric somite formation in these two vertebrates.

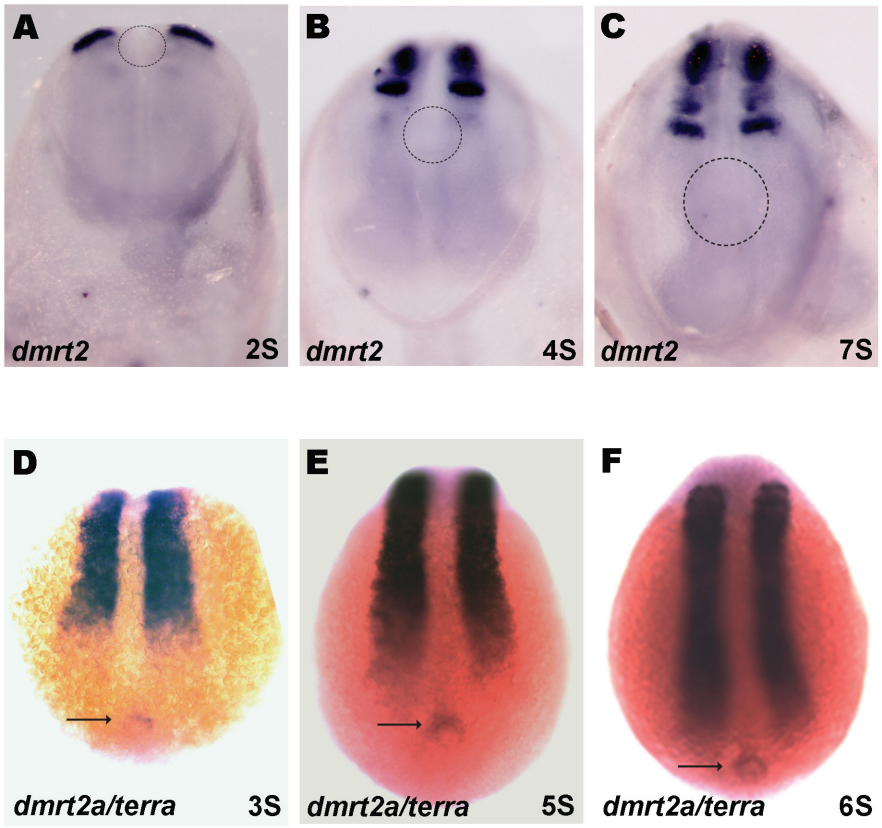

Figure 2.3. *dmrt2/terra* is expressed in the zebrafish kupfer´s vesicle. (A-F) Whole mount ***in situ*** hybridization confirming the ***dmrt2*** conserved expression pattern in the anterior PSM and somites in mice (A-C) and zebrafish (D-F) embryos. Despite not being expressed in the mouse node (dashed circle) (A-C), ***dmrt2a/terra*** is present in the zebrafish equivalent structure, the KV (arrow) (D-F). (A-C) Ventral views of mice embryos with anterior to the top. (D-F) Dorsal views of zebrafish embryos with anterior to the top. S, somite stage.

Discussion

The *dmrt* genes belong to a large family of transcription factors. These genes are present in several metazoan phyla (arthropods, nematodes and vertebrates) and show low sequence conservation outside the common DM domain, even within species (Volff et al., 2003). The number of *dmrt* orthologue genes varies in different phyla, suggesting multiple instances of independent gene duplication and/or loss throughout evolution. In the vertebrate lineage alone the number of dmrt genes varies widely: eight genes (*dmrt1-8*) in human and mouse, five genes (*dmrt1-5*) in fish, two genes (*dmrt1* and *dmrt4*) in Xenopus and three genes (*dmrt1-3*) in chick (Volff et al., 2003; Hong et al., 2007).

Despite being mainly expressed in developing gonads and associated with sex differentiation, not all the vertebrate *dmrt* genes are associated exclusively with this function. So far, from the eight known *dmrt* genes, five of them have already been implicated in other developmental processes other than sex differentiation. *dmrt* genes have been detected in the central nervous system (*dmrt3* in mouse, chick and medaka; *dmrt4* in mouse, *Xenopus*, medaka and platyfish; *dmrt5* in mouse, platyfish and zebrafish; *dmrt6* in mouse), nasal placodes (*dmrt3* in mouse and chick; *dmrt4* in *Xenopus* and platyfish; *dmrt5* in platyfish) and in the somites (*dmrt2* in mouse, chick and fish; *dmrt3* in chick) (Hong et al., 2007). It is clear that Dmrt family members present a wide variation in gene number and their expression pattern suggests distinct functions. The possible variation at the level of gene function implies that during evolution paralog genes may have been subjected to either a sub-functionalization, with the functions of the ancestral gene being segregated into a set of paralog genes, or a neo-functionalization, with one of the paralog genes acquiring a new function. A careful functional analysis should be done to fully understand the extension of the role of these genes. Additional studies on Dmrt genes from ancestor organisms would give insight on the origin and evolution of these genes.

The first *dmrt* gene suggested to have a role unrelated to sexual development was *dmrt2*. It was detected in zebrafish and mouse PSM and

somites and was reported to be absent from gonadal tissues (Seo et al., 2006; Meng et al., 1999; Kim et al., 2003). Indeed, male and female homozygous mouse mutant embryos are obtained with the same frequency (Seo et al., 2006). Functional studies in zebrafish showed that Dmrt2a/Terra protects the bilateral symmetric somite formation from the influence of LR cues. Without Dmrt2a/Terra the expression of the cycling genes in the PSM becomes desynchronized and consequently somite formation is no longer synchronized between the left and right sides of the zebrafish axis (Saúde et al., 2005). In addition, Dmrt2a/Terra was shown to establish asymmetry in the LPM, being necessary to restrict left-specific genes in the left LPM and having an impact in the localization of the heart on the left side (Saúde et al., 2005). In the mouse, these early Dmrt2 roles were not analyzed and only a later function in somite differentiation was reported (Seo et al., 2006).

To investigate the degree of functional conservation of *dmrt2* in mice, we started by characterizing the expression of the PSM Notch-related cycling genes *her7* and *lfgn*. This analysis was restricted to a specific developmental time window, 6-13 somites, which corresponds to the period when LR information is being transferred from the node to the left LPM - the time when PSM must be protected from the influence of these signals. The cyclic expression pattern of *her7* and *lfgn* in *dmrt2* null mutants showed no differences between the left and right sides of the PSM and consequently somite formation proceeded in a bilateral symmetric way. In contrast to the zebrafish, where all the cyclic genes identified so far belong to the Notch pathway, in the mouse several PSM cyclic genes are Wnt and Fgf pathway components. Among those are *axin2* and *sprouty2,* which are negative feedback inhibitors of the Wnt and Fgf pathway, respectively (Dequéant et al., 2006). Similarly to what happens with the Notch cyclic genes, no desynchronization of *axin2* and *sprouty2* expression was observed between the left and the right PSM in *dmrt2* null mutants. This is in agreement with the idea supported by experimental data and computational modeling that suggest that oscillations in the Notch, Wnt and Fgf pathways are coupled and integrated in one molecular clock (Dequéant et al., 2006; Goldbeter

and Pourquié, 2008). These results reflect a lack of conservation of the role of Dmrt2 during mouse development in what concerns LR synchronization of somite formation. Regarding a possible conservation of Dmrt2 function in establishing the LR asymmetry pathway, we looked at the expression of left-specific genes. In mice embryos mutant for *dmrt2* the expression of *spaw* and *pitx2* was restricted to the left LPM and consistently we observed a correct LR disposition of all the internal organs. Once again, these results indicate that mouse Dmrt2 does not play a role in the establishment of the LR asymmetric cascade.

During evolution the process of gene duplication is one key driving force for gene functional innovation. The evolutionary significance of gene duplication is explained by the duplication-degeneration-complementation (DDC) model, which states that the probability of a duplicate gene to be preserved increases with the occurrence of degenerative mutations in its regulatory region (Force et al., 1999). Since genes may have several functions that are controlled by different regulatory regions, when a specific subset of the gene function is subjected to a degenerative mutation, it may lose this given function and gain a new one. This leads to the emergence of different gene family members that become expressed in different tissues and/or developmental stages, thus allowing gene preservation during evolution (Force et al., 1999).

Teleost fish underwent a genome duplication that occurred during the evolution of ray-finned fish. Recently, it was reported that, due to this genome duplication event, zebrafish *dmrt2a/terra* has a paralog gene named *dmrt2b* (Liu et al., 2009). Contrary to *dmrt2a/terra*, that is present in all vertebrates, *dmrt2b* duplication only exists in the fish genome (zebrafish, tilapia, takifugu, tetraodon, medaka and stickleback), probably due to the fish lineage specific genome duplication (Zhou et al., 2008). In clear contrast to *dmrt2a/terra*, the fish-specific duplicated *dmrt2b* contributes to Hedgehog pathway (Liu et al., 2009). Due to this new function of *dmrt2b,* these two genes are not redundant and therefore one does not compensate for the loss of the other (Liu et al., 2009). The fact that *dmrt2b* allows an effec-

tive response to Hedgehog signaling explains the impact on somite differentiation in particular on slow muscle development (Liu et al., 2009). Since Shh regulates the establishment of LR asymmetries in zebrafish (Schilling et al., 1999) through its role in the midline, it is most likely that the LPM LR phenotype seen in *dmrt2b* morphants results from an impaired Hedgehog signaling at this level. This possibility is reinforced by the fact that we could not detect any *dmrt2b* expression in the zebrafish KV (data not shown). In addition, the fact that *dmrt2b* morphants lack desynchronizations of cyclic gene expression in the PSM (Liu et al., 2009) also suggests that the LR phenotype in these embryos arises from a different source when compared to *dmrt2a* LR phenotype.

We show here that *dmrt2a/terra* is expressed in the zebrafish KV, which is consistent with its role in LPM LR asymmetry establishment. In addition, we have previously shown that *dmrt2/terra* is asymmetrically expressed on the left side of Hensen's node in chick embryos (Saúde et al., 2005). Although no functional studies were performed, this expression pattern is highly suggestive of a LR patterning function of *dmrt2/terra* during chick development. In contrast to the fish and chick, we show here that *dmrt2* is not expressed in the mouse node, which is in agreement with the absence of a LR phenotype in *dmrt2* mutant mice.

Given the fact that zebrafish *dmrt2a/terra* is expressed in the KV and its homologue in chick Hensen's node, we propose that its expression and consequently its function in LR patterning was lost in the mouse lineage. This difference in function observed in mouse could arise: 1) from mutations occurring in the dmrt2 enhancer responsible for the node expression. To test this hypothesis, it would be interesting to combine bioinformatics and transgenics production to identify the zebrafish KV dmrt2 enhancer and show that it is indeed absent from the mouse genomic sequence; 2) from the loss in the mouse of a protein(s) necessary to activate specifically the node enhancer. In this situation, a bioinformatics analysis would reveal that the node enhancer will be present in the mouse genomic sequence and a new search for putative binding sites for known regulators could then be performed.

In contrast to the differential *dmrt2* expression in the KV/node reported in fish, chick and mouse, the expression at the level of the PSM and somites is conserved across all vertebrates studied so far (Saúde et al., 2005; Seo et al., 2006; Liu et al., 2009). In mouse, Dmrt2 is required for somite differentiation, in particular for patterning the axial skeleton (Seo et al., 2006). In the absence of *dmrt2*, extracellular matrix components levels in the dermomyotome are downregulated leading to disrupted differentiation of the myotome. Furthermore, signaling between myotome and the sclerotome is compromised culminating with rib and vertebral malformations and postnatal death due to respiratory problems (Seo et al., 2006). Therefore, the expression of *dmrt2* in the anterior PSM and somites correlates with its function in somite differentiation, a role already well described in mouse but still to be addressed in chick and zebrafish (Seo et al., 2006). In zebrafish, *dmrt2a/terra* is necessary for bilateral somite formation due to its ability to synchronize the segmentation clock between the left and right PSM (Saúde et al., 2005). Since LR synchronized cycling gene expression starts already in the posterior PSM, the desynchronization observed in the absence of *dmrt2a/terra* is not easily explained by its expression in the anterior PSM and somites. We propose that *dmrt2a/terra* is synchronizing the clock in the posterior most part of the PSM, through its function in the KV. In the developing zebrafish embryo, the KV is placed in close contact with the most posterior part of the PSM and therefore makes it an ideal location to protect the PSM from the asymmetric signals that emerge from this organ. Again, since *dmrt2* expression in the mouse is absent from the node, no desynchronizations of cyclic gene expression are observed in the *dmrt2* mutants.

While some *dmrt* ortholog genes show a conservation of their function in different vertebrates, some may have divergent functions. Here we report one of such cases illustrated by the mouse ortholog of the zebrafish *dmrt2*.

CHAPTER III

Searching for downstream targets of Dmrt2a/Terra: a ChIP-on-chip approach

Abstract

Dmrt genes are transcription factors that belong to a family mainly associated with sex determination. Nevertheless, they have started to be associated with other developmental processes. We focus our study in Dmrt2a/Terra, which as been shown to be necessary for zebrafish bilateral symmetric somite formation and correct transfer of asymmetric information to the left side of the axis. Given this interesting role during embryonic development and to better understand the genetic pathway where it is operating, it is of great importance to perform a search for its downstream target genes. We decided to pursue with a ChIP-on-chip approach which would allow us to determine *in vivo* direct associations of Dmrt2a/Terra with its specific target genes in a genome wide approach. This technique relies on the use of a specific antibody against Dmrt2a/Terra, which was not successfully obtained. We further discuss the implication of this technique and the use of other strategies that could have been used to overcome this limitation.

Introduction

Dmrt genes encode a large family of transcription factors. This family is related to the *Drosophila doublesex* (*dsx*) and *C. elegans mab-3* genes that contain a zinc finger-like DNA binding motif, known as DM domain (Dsx and Mab-3), outside of which there is little sequence similarity between phyla. While Dsx has a single DM domain, Mab-3 has two DM domains (Raymond et al., 1998; Volff et al., 2003; Hong et al., 2007). This domain contains an amino-terminal zinc binding site and a carboxy-terminal domain that acts like a recognition tail mediating high-affinity DNA binding. Unlike the classical zinc finger DNA binding domains, the DM domain interacts with the DNA via its minor groove rather than the major groove, which by being wider allows bases to be more accessible for transcription factors binding. It was suggested that upon DNA binding, the C-terminal tail is able to widen the miner groove without bending the DNA (Zhu et al., 2000).

The *dmrt* genes were first studied in the context of invertebrate sex determination, where both male and female *Drosophila* Dsx isoforms and *C. elegans* Mab-3 regulate similar aspects of sexual development such as yolk protein synthesis, peripheral nervous system (sex-specific neurons development) and copulatory structures differentiation (Shen and Hodgkin, 1988; Burtis and Baker, 1989; Taylor and Truman 1992; Coschigano and Wensink, 1993; Yi and Zarkower, 1999). Despite being conserved in vertebrates, some *dmrt* genes are also expressed in tissues other than the gonads. Although functional studies have not been reported for all of them, their expression analysis shows that some of these genes are detected in structures such as the central nervous system, nasal placodes and somites, suggesting an involvement in other processes rather than sexual development during vertebrate development (Hong et al., 2007). However, how they are mediating transcription during the regulation of these processes and what is the identity of their downstream targets is still poorly known.

dmrt2 is such an example of a *dmrt* gene that, besides being expressed in adult and embryonic testis, has been detected in non-gonadal tissues of several vertebrates such as kidney, skeletal muscle, and thymus in humans; PSM and somites in mouse, zebrafish and chick; Hensen's node, eye and otic vesicle in chick and KV in zebrafish (Ottolenghi et al., 2000; Meng et al., 1999; Kim et al., 2003; Saúde et al., 2005; Seo et al., 2006; Lourenço et al., 2010). Dmrt2 was the first *dmrt* gene described to play with a role during embryonic development outside the context of sex determination (Hong et al., 2007). Consistent with its expression pattern, zebrafish Dmrt2a/Terra has been shown to link bilateral symmetric somite formation to the LR asymmetry pathway (Saúde et al., 2005). This role is not conserved during mouse development where it only seems to be necessary for somite differentiation, suggesting that its activity has not been conserved during evolution (Seo et al., 2006; Lourenço et al., 2010). Due to a whole genome fish specific duplication, a second *dmrt2* gene named *dmrt2b* arose (Zhou et al., 2008; Liu et al., 2009). Its function diverges from the role of *dmrt2a/terra* since it is not

necessary for symmetric somite formation, being necessary to regulate somite differentiation at the level of slow muscle development. Despite this divergence, both *dmrt2a*/*terra* and *dmrt2b* are important to regulate LR patterning in the left LPM (Liu et al., 2009).

To understand how differential gene expression is regulated during embryonic development, and go from the gene to the signaling pathway where it operates, it is essential to study transcription factors and search for their targets. A powerful technique, called chromatin immunoprecipitation (ChIP), has been used to map the position of transcription factors, post-translational modified histones or other DNA binding proteins in a variety of cell types and species. The combination of the ChIP with a DNA microarray (DNA chip) (ChIP-on-chip) has enable to determine *in vivo* direct associations of a particular protein with specific DNA regions in a genome wide approach (Blais and Dynlacht, 2005). This technique, widely used in yeast, *Drosophila* and mammalian cells, has also been adapted for zebrafish embryos in the identification of specific DNA sequences associated with acetylated histones and transcription factors. Since most transcription factors in various models have undetermined DNA binding specificities and unknown regulatory functions, this approach leads to a better understanding of transcription regulation by allowing an unbiased analysis of transcription factors binding sites (Havis et al., 2006; Wardle et al., 2006).

At the moment we still do not know how Dmrt2a/Terra is regulating transcription, to which genes does it bind to and how does it regulates them. The identification of its target genes is of great importance to better understand its regulatory pathway and a good approach would be to perform a ChIP-on-chip assay using the zebrafish as a model. Once we start to identify these molecular players, the mechanism of Dmrt2a/Terra mode of action that ensures symmetry during somitogenesis and regulates correct asymmetry of the organs inside the vertebrate embryo will be better understood.

Results

To perform the ChIP-on-chip assay, that would allow the identification of direct targets of the zebrafish Dmrt2a/Terra transcription factor, we need to have a specific Dmrt2a/Terra antibody. The quality and specificity of this antibody is very important for the success of the ChIP-on-chip assay. The main advantage of having a specific antibody is that only DNA sequences that directly bind to the Dmrt2a/Terra protein will be identified. Given the fact that such a zebrafish Dmrt2a/Terra specific antibody was not available, two polyclonal antibodies (69 and 70) were produced by Eurogentec from specific synthesized peptides H2N-CILKRPALSLNRKSQ-COOH and AcNH-QQTLNDKNPDTNRPYC-CONH2, respectively. To test the efficiency of these antibodies, we performed a Western Blot assay with protein extracts collected from appropriately staged zebrafish embryos. Protein samples were extracted from wild-type (WT) dome stage embryos, when *dmrt2a/terra* was thought to be absent; from WT 15 to 20- somite stage embryos, when *dmrt2a/terra* is expressed in somites and anterior region of the PSM; and from 15 to 20-somite stage embryos overexpressing *dmrt2a/terra* mRNA upon ectopic expression at the 1-cell stage (Zhou et al., 2008; Meng et al., 1999; Saúde et al., 2005). Taking into account that zebrafish Dmrt2a/Terra protein weights 56 kilodaltons (KDa) our results indicate that both antibodies are recognizing this protein (Fig. 3.1A,B) (Meng et al., 1999). The analysis of the lanes corresponding to protein extracts from dome stage embryos seems to indicate that Dmrt2a/Terra is already being expressed at this developmental stage. Nevertheless, levels are lower when compared with the lanes corresponding to protein extracts from 15 to 20-somite stage embryos (Fig. 3.1A,B). We can also state that Dmrt2a/Terra overexpression is working, since protein levels are increased in the lanes that correspond to protein extracts from embryos injected with *dmrt2a/terra* mRNA when comparing with WT protein extracts (Fig. 3.1A,B). Despite the fact that antibodies are recognizing Dmrt2a/Terra, we could detect unspecific bands in the Western Blot. Since both antibodies were recognizing other sequences other than

Dmrt2a/Terra, an affinity purification of the serum was performed. After having the purified antibodies we repeated the Western Blot assay. The results showed that the purified antibodies were still not specific enough for the ChIP-on-chip assay since they were still recognizing proteins other than Dmrt2a/Terra (data not shown).

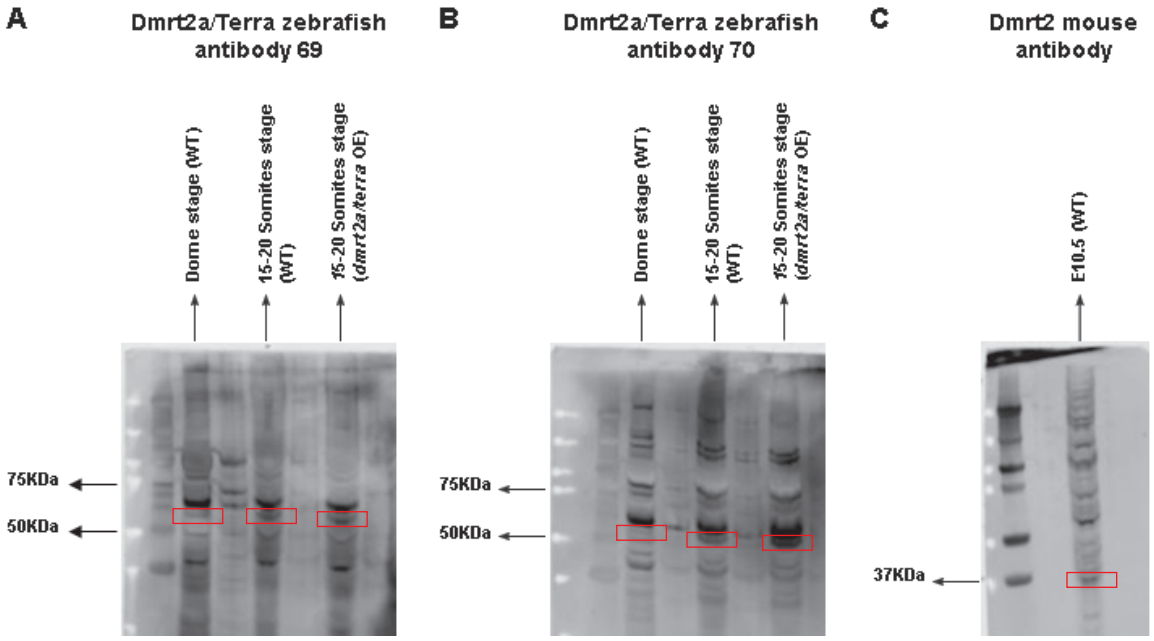

Figure 3.1. Zebrafish and mouse Dmrt2 polyclonal antibodies specificity. (A, B) Two zebrafish polyclonal antibodies were tested in a Western Blot assay using protein samples extracted from zebrafish WT embryos in dome stage and 15- to 20-somite stage and from 15- to 20-somite stage embryos overexpressing ***dmrt2a/terra*** mRNA. Both antibodies are recognizing Dmrt2a/Terra protein which weights 56 KDa however, their specificity in not very high since other proteins are being recognized other than Dmrt2a/Terra. (C) A mouse polyclonal antibody against Dmrt2 was also tested in a Western Blot assay using a protein sample extracted from mouse WT embryos in E10.5 developmental stage. This antibody is recognizing the 37 KDa Dmrt2 protein nevertheless, it is also not specific enough being recognizing several other proteins. KDa, kilodaltons.

During the course of this work, a polyclonal antibody against the mouse Dmrt2 (zebrafish Dmrt2a/Terra homolog) started to be commercially available. To address if this mouse polyclonal antibody could specifically rec-

ognize the zebrafish Dmrt2a/Terra protein we tested it in a Western Blot assay. First, its specificity was tested in mouse protein extracts collected from embryos with E10.5 stage of development, when Dmrt2 is expressed in somites and anterior region of the PSM. Taking into account that the mouse Dmrt2 protein weights 37 KDa we can say that this antibody is recognizing our protein of interest (Fig. 3.1C). However, it is not specific enough since it also recognizes several other proteins. Despite these results, we also tested it in a Western Blot using protein samples extracted from zebrafish embryos. Again, the antibody is recognizing several other proteins (data not shown) meaning that its specificity is not good enough, being discarded the hypothesis of using it in the ChIP-on-chip assay.

Discussion

Dmrt2 is a transcription factor that plays several roles in the context of embryonic development. Dmrt2 is expressed in the PSM and somites of zebrafish, mouse and chicken embryos, being also present in the chick Hensen's node and zebrafish KV (Meng et al., 1999; Saúde et al., 2005; Lourenço et al., 2010). We have previously shown that it regulates the body plan along the LR axis in zebrafish, not only by regulating the LR asymmetry pathway but also by ensuring the maintenance of symmetry in the PSM (Saúde et al., 2005). Finding the *in vivo* Dmrt2a/Terra targets and determine how their expression is regulated will certainly have great implications in the understanding of how symmetric and asymmetric embryonic development is regulated. Our approach was to perform a ChIP-on-chip assay and in this way obtain a large-scale profile of the unknown target genes of this transcription factor, a technique that has already been successfully performed in zebrafish (Wardle et al., 2006).

The ChIP consists in isolating from a mixture of crosslinked DNA/protein complexes the chromatin fragments that are bound to the transcription factor of interest. This requires the use of a specific antibody, i.e. immunoglobulin present in the serum of individuals that have been immunized with antigens

(peptides or proteins) to which it has a high affinity. Since no antibody against zebrafish Dmrt2a/Terra was available, we ordered polyclonal antibodies produced from two specific synthesized peptides. Their sequences were selected taking into account their composition, since specific amino-acids have higher probabilities to stimulate the immune system to produce antibodies that will bind to them. Their ability to promote specific structural features and surface exposure within the protein is thus highly important. Also, the length of the peptides should not be too long since they may adopt non-native structures that then lead to the production of antibodies that do not recognize the native protein. On the other hand, the peptides should not be too short to avoid insufficient epitope diversity, thereby leading to a production of antibodies that have lower opportunities to recognize the Dmrt2a/Terra protein. Given this, the optimal peptide length should be between 12 and 25 amino-acids. Another consideration to take into account is if the antibody to be used should be polyclonal or monoclonal. We chose to produce a polyclonal antibody, by immunization of rabbits with the synthesized antigens, given the fact that they are produced from different cells and are in this way able to recognize different epitopes of the same peptide. This diversity increases the probability of recognizing the protein, since small changes in the epitopes may occur during chemical treatments of the extracts, such as protein denaturation. On the other hand, monoclonal antibodies which are produced from a single cell line can only recognize one epitope of the protein. Although being efficient for binding a specific protein in a mixture of related proteins they are more vulnerable to a possible loss of the protein epitope through chemical treatments, since only one copy of the same antibody is produced. Finally, the reason for choosing to produce the antibody from peptides is that peptide antigens are of easy access and antibodies are easily affinity purified against them. Despite all this, and after testing both Dmrt2a/Terra polyclonal antibodies (69 and 70) in Western Blot assays, we concluded that neither of them was specific enough to be used in the Chip-on-chip assay, since they were recognizing other proteins either than Dmrt2a/Terra. The same was true for the commercial Dmrt2 mouse antibody.

Since the success of the ChIP assay dependents on the quality of the antibody to be used and given the fact that the produced antibodies were not specific enough, other strategies to overcome this limitation could have been taken. Instead of producing an antibody against Dmrt2a/Terra synthesized peptides, we could have purified the Dmrt2a/Terra protein and produce an antibody against it. Using proteins as antigens gives the advantage of having a high number of linear epitopes and a higher probability of producing an antibody that is useful in a high range of applications. Nevertheless, they may have homology with unwanted family member proteins. The purification of the Dmrt2a/Terra protein could have been done using the Glutathione-S-Transferase (GST) fusion-protein affinity tag to produce a Dmrt2a/Terra recombinant protein. This protein would have been expressed in bacteria and affinity purified from the lysate. The purification consists in binding and eluting the protein from a glutathione resin that selectively binds the GST-tagged protein, allowing it to be separated from all the other proteins present in the extract. Since affinity tags have the potential to interfere with their fused protein activity, the tag is normally removed through the use of site-specific proteases (Terpe, 2003). The recombinant purified protein would then be used as an antigen for antibody production in rabbits. An advantage of using GST as a tag relies with the fact that being an N-terminal tag it increases the yield of recombinant protein production by providing an efficient translation initiation. On the other hand, the use of GST holds the disadvantage of not being a good solubility-enhancing tag and in some cases the GST fusion protein is only partly soluble in the bacterial lysate under non-denaturing conditions (Terpe, 2003; Waugh, 2005). In an alternative approach, we could have used small peptide tags, fused with Dmrt2a/Terra and select the DNA/protein complexes using a commercial available antibody against the tag. There are several tags that could have been used, such as HA and Myc that do not interfere with the fused protein and have already been applied in zebrafish ChIP assays (Terpe, 2003; Havis et al., 2006). A fusion construct would have been generated and expressed in zebrafish embryos by RNA injection at the

one-cell stage. The major drawback of this approach is that Dmrt2a/Terra would have been ectopically overexpressed and this could not reflect the endogenous normal protein levels, which might interfere with the dynamic regulatory properties of the protein.

In the case of having been able to obtain a specific Dmrt2a/Terra antibody we would have performed a ChIP-on-chip assay.

For the ChIP, zebrafish embryos would have been fixed in formaldehyde so that Dmrt2a/Terra and its associated DNA targets would be crosslinked. Embryos would be selected at the 3 to 5-somite stage, when it is thought that L-R asymmetry is being established and when we predict that the symmetry pathway is being activated (Saúde et al., 2005). After harvesting the chromatin from the cells of these embryos we would have performed an immunoprecipitation of the protein sample using our Dmrt2a/Terra antibody, this way DNA sequences crosslinked to the Dmrt2a/Terra protein would co-precipitate as part of the chromatin complex. As a control, we would use chromatin fragments that were not subjected to immunoprecipitation (input sample).

To identify the Dmrt2a/Terra target genes selected in the immunoprecipitation we would have performed a ChIP-on-chip, an unbiased and genome wide approach that combines the ChIP technique with microarray analysis (Wardle et al., 2006). The microarray technology represents a powerful tool that enables to analyze the expression of many genes in different developmental contexts. A microarray consists in a membrane that contains a large number of DNA nucleotides samples, representing regions of the genome, that are arranged in a regular pattern so that the location of each spot in the array corresponds to a particular gene sequence (Blais and Dynlacht, 2005). The chromatin fragments present in the specific antibody ChIP sample would be labeled with a fluorescent molecule such as Cy5. The chromatin fragments present in the input control sample would be labeled with a fluorescent molecule such as Cy3. Both fragments would be hybridized with a zebrafish genomic tiling microarray. During hybridization,

complementary sequences from the array and labeled fragments would bind together and would be detected with a laser technology that excites the fluorescent tags, a microscope and a camera that create a digital image of the array. The ratio between the intensity of the two fluorescent molecules is calculated for each microarray spot. It allows determining the levels at what certain genes are expressed, whether a particular gene is either more or less expressed under a specific circumstance and test the regions to which a protein of interest possibly binds to. For instance, if a certain gene is downregulated or overexpressed, in a given condition and comparing with the control, then less or more sample will hybridize to the spot where that gene is represented and the fluorescence intensity will be lower or higher, respectively. By comparing the expression of thousands of genes at once allows to better understand how they interact (Blais and Dynlacht, 2005).

There are different arrays depending on what they analyze and the type of DNA used: gene expression profile arrays, determine the level at which a given gene is expressed during specific developmental stages or in response to specific developmental conditions and uses cDNA of known genes as targets; comparative genomic hybridization, used to determine genomic gains and losses using large pieces of genomic DNA as targets; detection of mutations in a gene sequence using genes with small genetic changes (Mockler et al., 2005). For this study we would have performed a gene expression microarray. Traditional whole-genome expression microarrays, designed for this purpose, use few probes that rely on prior genome annotation and are this way biased for known and predicted genes, not addressing other locations to which transcription factors might bind. To overcome this limitation and target the genome in an unbiased way, including yet unidentified genes, whole-genome tiling microarrays have been designed. They include oligonucleotide probes with a relatively short length that partially overlap the genomic sequence or do not overlap and are spaced in regular intervals through the genome (Mockler et al., 2005). Given this, a tiling array would have been chosen to perform the ChIP-on-chip assay.

Selected putative targets from the microarray hybridization would then be classified into functional categories and gene families and validated. Several approaches could have been adopted to validate the selected targets: standard PCR's, where specific primers are designed for the specific promoter DNA sequences of the selected targets; mRNA *in situ* hybridization, where genes are cloned, antisense mRNA probes generated and their expression pattern determined in time (stage) and place (tissue); mRNA *in situ* hybridization of the selected genes in the contexts of Dmrt2a/Terra downregulation, using the previously designed antisense MO oligonucleotide against the translation initiation site to specifically abolish its function, and Dmrt2a/Terra overexpression, injecting *dmrt2a/terra* mRNA at 1 cell stage embryos, in order to check their expression pattern levels in those contexts (Saúde et al., 2005). Genes that would either be downregulated or upregulated in these two contexts would be considered Dmrt2a/Terra direct targets. Its role as an activator or repressor would be deduced based on whether target gene expression was enhanced or reduced.

For a further functional analysis, the selected genes would have been cloned into appropriate expression vectors, transcribed into mRNA and overexpressed. The complementary assay would also need to be performed, with the synthesis and injection of antisense MO oligonucleotides that specifically induce their loss-of-function. In the context of our study, the phenotype of these embryos would be analyzed with molecular markers for the early L-R asymmetry pathway and markers to check the bilateral synchronization of somite formation.

Transcription factors are required in several functions within the cell such as transcription, replication and DNA repair, this way determining the regulatory task of a specific cell. In response to a stimulus, transcription factors may act at the transcriptional level, interacting with the cis-regulatory DNA sequences present either in the promoter region of the gene(s) that they specifically regulate, in enhancers located further away from the promoter region or in an intron. Each gene of the network is thus controlled by these

sequences that determine which transcription factors affect the expression of that particular gene. Some transcription factors act as activators, binding to enhancer sites and activating gene expression, while others bind to silencer sites and repress the synthesis of the corresponding RNA. These interactions may also be direct or indirect. Direct interactions consist in the connection between the target gene and its sole transcriptional regulator (protein-DNA interaction). Indirect interactions occur when a gene is regulated by a group of factors (protein-protein interactions), meaning that the transcription factor forms a dimer with a transcription coregulator protein that will either enhance the rate of gene transcription (coactivator) or decreases it (corepressors), making the DNA more or less accessible to being transcribed. Nevertheless, coordination of gene expression is regulated at many different levels and can also rely on post-transcriptional regulatory networks. It can occur through protein-mRNA or RNA-RNA interactions, with RNA binding proteins and microRNAs interacting with cis-regulatory RNA sequences and this way inhibiting translation or degrade the mRNA (Reviewed in Walhout, 2006).

Relatively little is known about how Dmrt proteins regulate gene transcription, other than that they select similar DNA binding sites. While *C. elegans* Mab-3 binds to its targets as a homodimer, *Drosophila* Dsx and some vertebrate Dmrt proteins bind as heterodimers. In mouse, Dmrt1 is in fact co-expressed with Dmrt3 and Dmrt5, having been shown to heterodimerize with both of them when binding to its targets (Murphy et al., 2007). After binding, these transcription factors seem to regulate gene expression in different ways. The *Drosophila* Dsx^{M} isoform acts like a transcription repressor of the yolk protein genes while the Dsx^{F} isoform acts as a transcription activator (Coschigano and Wensink 1993). In *C. elegans* Mab-3 has been shown to promote proneural proteins expression, acting as a repressor and antagonizing the activation of a neurogenesis repressor, and to repress yolk protein gene transcription (Yi and Zarkower, 1999; Ross et al., 2005). In vertebrates less is known about their regulatory activity. In the context of mouse testis development, Dmrt1 direct target genes have recently been

identified (1,439 genes) by performing ChIP-on-chip in mouse testis at post-natal day 9 (Murphy et al., 2010). This was performed in the context of two conditional Dmrt1 deletions, one in germ cells and another in Sertoli cells, where *dmrt1* is expressed. The identified target genes, many known to be involved in several aspects of testicular development, such as Sertoli cell differentiation, cell-cycle control, tight-junction dynamics, germ cell differentiation and pluripotency, are either activated or repressed by Dmrt1, that is this way the first Dmrt transcription factor shown to be bifunctional. Most genes had the same response to Dmrt1 deletions in both cell types nevertheless, in some cases gene regulation was cell type specific. It was shown that it can regulate its own expression by binding its own promoter and that there is cross-regulation among genes of this family since Dmrt1 was shown to regulate Dmrt3, Dmrt4, Dmrt5, Dmrt7, Dmrt8.1 and Dmrt8.2 (Murphy et al., 2010). In medaka Dmrt1 is duplicated, with Dmrt1bY (regulator of male development) being able to regulate its own expression and its transcription being regulated by Dmrt1a (Herpin et al., 2010).

To further study the role of Dmrt2a/Terra during zebrafish embryonic development it is crucial to perform a Chip-on-chip assay which will allow searching for its direct downstream targets at specific developmental stages and this way constructing the pathway in which it is operating.

Materials and methods

Zebrafish maintenance

Wild-type zebrafish (*Danio rerio*) with the AB genetic background were maintained at 28ºC on a 14 hour light/ 10 hour dark cycle. Embryos were collected and kept at 28ºC in embryo medium until the appropriate stage (Kimmel et al., 1995).

Polyclonal antibodies production

Polyclonal antibodies were produced from specific synthesized peptides, specific for the zebrafish Dmrt2a/Terra protein. Regions of the protein most

likely to be accessible on the surface of the full length Dmrt2a/Terra protein were identified and two immunogenic peptides were selected given their amino acid sequence (H2N-CILKRPALSLNRKSQ-COOH and AcNH-QQTLND-KNPDTNRPYC-CONH2) (performed by Eurogentec, EGT Group). The selected immunogenic peptides were synthesized and used to co-immunize rabbits eliciting an immune response that culminates with the production of specific antibodies (performed by Eurogentec, EGT Group). A co-immunization of the animal hosts was performed with the two peptides and the blood serum from each animal was finally recovered, each containing one antibody. The serum was purified by an affinity purification assay using the peptides against which the antibodies were raised (performed by Eurogentec, EGT Group). A commercially polyclonal antibody against the mouse Dmrt2 was also bought (AVIVA SYSTEMS BIOLOGY).

Western blotting

To test the antibodies specificity, protein samples were extracted from zebrafish embryos in different stages and in different developmental contexts. These samples were then processed in a western blotting assay.

– Embryos dechorionation and deyolking

Embryos were collected in the appropriate developmental stages and their chorion removed in batches of 100 embryos through enzymatic digestion. For this, embryos were placed in a Petri dish with 2mg/ml of pronase in 0,3x Danieau solution (heat at 37°C). The amount of time in this solution is stage dependent, younger embryos require a shorter exposure to pronase. Has soon as the chorion starts to lose consistency, embryos were rinsed several times in Danieau solution to remove the enzyme. During the washes embryos are expelled from the chorion and when necessary they can easily be removed with forceps. Up to 100 embryos were transferred to an eppendorf, the Danieau solution removed and 200µl of a deyolking buffer (55mM NaCl; 1,8mM KCl; 1,25mM NaHCO3), a low osmolarity buffer, was added to facilitate dissolving the yolk which contains proteins that may interfere with

the detection of the target protein. Embryos were gently pipetted with a narrow tip. The tubes were shacked for 5 minutes at 1100 rpm to dissolve the yolk and cells were pelleted at 300 g for 30 seconds. The supernatant was discarded and 200µl of wash buffer (110mM NaCl; 3,5mM KCl; 2,7mM CaCl2; 10mM Tris-Cl pH8.5) was added. The tubes were shacked for 2 min at 1100 rpm and cells pelleted as before. This step was repeated twice in order to reduce the amount of yolk proteins. The supernatant was discarded and protein samples stored at -80°C.

– Sample preparation

The protein samples were thawed and 200 µl (2 µl per embryo) of 2x sample loading buffer (3x sample loading buffer: 1M Tris-HCl pH6,8; 20% SDS; Glycerol 100%; B-mercaptoethanol 1,6ml; Bromophenol Blue 0,006g; to 10ml) was added to the tube. The mixture was homogenized with a pipette and boiled for 5 minutes at 100°C (proteins denaturation). Tubes were centrifuge 1-2 minutes at full speed to remove insoluble particles, the supernatant transferred to a new eppendorf and the pellet discarded. The sample was immediately loaded on a gel.

– Protein sample separation by electrophoresis

Protein samples were loaded on a precast polyacrylamide gel (NUPAGE 4-12% Bis-Tris gel). The combs were removed and the wells washed with 1X MES/SDS running buffer (20x Mes/SDS buffer: 1M MES; 1M Tris Base; 60,3 mM SDS; 20,5 mM EDTA free acid; ultrapure water to 1L; 1x buffer should have pH7.3). The gel was placed in the electrophoresis tank, the upper chamber filled with running buffer (to check for leaks) followed by the filling of the lower chamber. The molecular weight marker and samples were loaded on the wells and the gel submitted to 200V untill the dye molecule (migration front) reached the bottom of the gel (30 minutes to an 1 hour).

– Transfer of proteins onto a membrane

The Hybond-P PVDF (Polyvinylidene Fluoride) membrane was cut to the ap-

propriate size of the gel and soaked in methanol for 10 seconds, washed in distilled water for 5 minutes and equilibrated in the transfer buffer for 10 min (10x transfer buffer: 30,3 g Trizma-base; 144 g glycine; store at 4ºC; to 1x transfer buffer add methanol to a final volume of 20%). Forceps should be used when touching the membrane since fingers will interfere with the efficiency of the transfer creating dirty blots. The blotting pads (sponges) and 6 pieces of filter paper were also presoak in transfer buffer. The gel was removed from the cassette and equilibrated in 1x transfer buffer for 10-20 minutes. The electroblotting cassette is then assembled (blotting pad, 3 filter papers, gel, membrane, 3 filter papers, blotting pad) and placed between the electrodes in the blotting unit (to avoid bubbles formation between the gel and membrane a pipette can be carefully rolled over). The membrane side of the cassette was placed close to the positively charged electrode so that proteins were transferred out of the gel, away from the negatively charged electrode and into the membrane. The chamber was then filled with transfer buffer until the gel/membrane was covered. The outer chamber was filled with transfer buffer or deionized water so that heat is dissipated during the transfer. The transfer was performed at 30V for 1H with cooling. Following the transfer, the membrane was removed from the blotting cassette and the orientation of the gel marked on the membrane. This was then washed in TBST (10x TBS (Tris buffered saline): 24,2 g Trizma-base; 80 g NaCl; 800 ml with ultra pure water and pH 7,6 with pure HCl; fill to 1 L. TBST (TBS-Tween): 10x TBS; 0,05% Tween). To determine if proteins migrated uniformly the membrane was placed in a recipient with Ponceau Red (2% Ponceau S; 30% Trichloroacetic acid; 30% Sulfosalicylic acid; dilute the stock 1:10). It was left agitating for 5 minutes and when the protein bands started to be well-defined the membrane was washed with water followed by a TBST wash.

– Blocking the membrane

To block non-specific background binding of the antibodies to the membrane, it was incubated in blocking solution (5% dried milk/TBST) for 1H

with agitation. Membranes may be left in the blocking solution o/n at 4ºC. The blocking solution was removed and the membrane washed in TBST for 10 min with agitation.

– Incubation with primary antibody

The antibody was diluted in 1% dried milk/TBST (1:50; 1:250; 1:500; 1:1000) (dilution must be optimized according to the results since too much antibody will result in non-specific bands). This solution was added to the membrane and left for 1H at RT or o/n at 4ºC, always with agitation to enable an homogenous covering of the membrane and this way prevent uneven binding. After, the membrane was washed five times with TBST to remove the unbound antibody.

– Incubation with secondary antibody

The secondary antibody, conjugated with horseradish peroxidase (HRP), was diluted 1:5000 in 1% dried milk/TBST. The solution was added to the membrane and left there for 1H at RT with agitation. To remove the unbound antibody, the membrane was washed four times with TBST, 10 min each wash.

– Development

The excess of TBST was removed from the membrane with a piece of paper and then covered with the detection reagent (commercial kit: 5 ml of detection solution 1 and 5 ml of detection solution 2) during 1 min. A piece of plastic was placed in an X-ray film cassette and the membrane placed over the plastic with the protein side up. The excess of detection reagent was drained and the membrane covered with plastic. In the dark camera, the cassette was opened and an x-ray film placed over the membrane. The film was exposed during the necessary amount of time (may go from 1 minute to several hours), removed from the cassette and placed in a container with developing solution until the bands start to appear. Next, it was placed in a different container filled with water and finally in a container with the fixation solution.

CHAPTER IV

Microarray approach for the search of Dmrt2a/ Terra targets

Abstract

Zebrafish Dmrt2a/Terra was previously shown to be necessary to regulate two main embryonic developmental processes. When knocked down, cycling gene expression becomes bilaterally desynchronized between both sides of the axis, leading to asymmetric somite formation, and the LR asymmetric information is no longer transferred only to the left lateral plate mesoderm, becoming randomized and leading to a misplacement of asymmetric internal organs. Because the effect of its overexpression had not been previously addressed, we injected *dmrt2a/terra* mRNA at the one-cell stage and surprisingly, we observed that the phenotype was the same as when knocking down Dmrt2a/Terra. Since we were not able to pursue with a ChIP-on-chip approach for the search of Dmrt2a/Terra target genes, and given the LR phenotypes obtained when downregulating/overexpressing *dmrt2a/terra*, we decided to create the tolls necessary to perform a controlled microarray assay. A microarray allows to compare the expression of Dmrt2a/Terra target genes in two different conditions, when downregulated and upregulated. For a time controlled gene upregulation we generated an inducible transgenic zebrafish line where *dmrt2a/terra* is under the control of a heat-shock promoter. We were able to generate the tools necessary to perform a controlled microarray assay and therefore search for Dmrt2a/Terra target genes.

Introduction

The formation of the metazoan body plan is the outcome of several developmental processes regulated both in space and time by many cellular processes. From the several interactions between cell constituents, one of the major challenges in biology is to know how and when transcription factors regulate their downstream targets in the control of the structure and function of a living cell (Walhout, 2006). To better understand the role of a given transcription factor in the signalling cascade where it operates

and search for possible downstream targets, knockdown and transgenesis techniques are valuable tolls. The zebrafish (*Danio rerio*) has emerged as a good model to study vertebrate embryonic development allowing for genome manipulation through the use of these powerful genetic techniques. In addition, it presents other advantages that relay with the fact that it can produce a large number of offspring, its external development allows close observation of embryonic development and it has a short generation period (Kimmel, 1989; Grunwald and Eisen, 2002).

In zebrafish, insertional mutagenesis, which can rapidly lead to the identification of mutated genes, and reverse genetic approaches to investigate the functions of specific genes like TILLING and Zinc-Finger Nucleases-mediated mutagenesis are being carried out successfully (Wienholds et al., 2003; Durai et al., 2005). Another technique to effectively and easily block translation, and therefore the function of a specific gene, is also available as zebrafish embryos can be easily microinjected with antisense MO oligonucleotides (Heasman, 2002). In addition, overexpression or misexpression of a gene of interest is a fast assay in zebrafish. A simple injection of synthetic mRNA or DNA of the wt gene or a constitutively active form is instrumental to investigate its gain-of-function phenotype. Another advantage of working with zebrafish is the possibility of inserting foreign DNA into its genome and in this way generate transgenic lines. Recently, the Tol2 transposable element has been used as an important genetic tool to perform zebrafish transgenic manipulation. Tol2 transposons are transposable elements found in vertebrate genomes and consist of sequences that move from one genomic locus to another one. Transposon vectors enclosing a gene of interest, instead of the transposase gene, are catalyzed by the transposase enzyme which excises the gene from the plasmid and integrates it into the host genome (Kwan et al., 07). The Tol2 transposon from the medaka fish has emerged as an effective system to generate a high rate of stable transgenesis being capable of integration in the zebrafish genome through transposition, with the insertion being transmitted to the next generation through the germ lineage (Kawakami et al., 2000). The possibil-

ity to produce an inducible transgenic, where the gene of interest can be expressed in a timely controlled manner, is a great advantage to study gene function. The possibility to control the timing of induction of a given gene allows the identification of direct targets and to dissect early and later functions. Given this, heat-shock inducible transgenic lines, where transcription of the gene of interest is under the control of the heat-shock protein (Hsp) promoter, have been used successfully in zebrafish.

We have previously shown that the zinc finger-like transcription factor Dmrt2a/Terra is important during zebrafish embryonic development, being not only necessary to maintain symmetry in the PSM but also fundamental to maintain LR asymmetry in the LPM (Saúde et al., 2005). In Dmrt2a/Terra depleted embryos, the expression of the cycling genes *deltaC*, *her1* and *her7* becomes desynchronized between both sides of the axis, concomitant with the formation of an extra somite either one the left or right side. At the same time, the expression of left side specific genes, such as *spaw* and *pitx2*, became randomized and no longer restricted solely to the left LPM (Saúde et al., 2005).

Since nothing is known regarding Dmrt2a/Terra mode of action, a microarray approach would allow us to uncover its downstream targets. A powerful and controlled microarray experiment would be to compare changes in the expression levels of thousands of genes between a situation where *dmrt2a/terra* is downregulated and upregulated. The downregulation of *dmrt2a/terra* can be generated by using the already characterized MO. However, the appropriate tool to allow a controlled overexpression namely the generation of an inducible *dmrt2a/terra* transgenic was not available nor was the overexpression phenotype characterized. We first addressed the impact of overexpressing *dmrt2a/terra* in zebrafish embryos. The obtained phenotype was the same as when performing Dmrt2a/Terra knockdown, LR problems both at the level of the PSM and LPM were observed. We then constructed a transgenic line where Dmrt2a/Terra expression is under the control of a heat-shock promoter. In this way we will be able to find direct targets and to uncover when it might be regulating both processes.

Results

IV.1. Dmrt2a/Terra overexpression and somite formation

Somite formation is not only periodic but also bilaterally synchronous. Development between both sides of the axis is tightly coordinated and each pair of somites is formed at the same time. The process of somite formation is linked with cyclic waves of gene expression that are bilaterally symmetric between both sides of the PSM. We had previously shown that in zebrafish Dmrt2a/Terra is important to coordinate symmetric somite formation during a specific developmental time window, from the 8- to 12-somite stage. In the context of Dmrt2a/Terra downregulation, upon injection of a specific MO, the cycling genes *deltaC*, *her1* and *her7* still exhibit a cyclic expression pattern however, they become out of phase between the left and right side of the axis (Saúde et al., 2005). In order to characterize the *dmrt2a/terra* overexpression phenotype, *dmrt2a/terra* capped RNA was injected at the one-cell stage WT embryos. These embryos were then analyzed by *in situ* hybridization for the expression of several genes that belong to the signalling pathways that participate in the process of somitogenesis.

We first accessed the effect of *dmrt2a/terra* overexpression in the cycling genes pattern of expression between the 8- to 12-somite stage. In control embryos, the expression of *deltaC* was symmetric in 100% of the cases (n=15), *her1* in 100% (n=10) and *her7* in 95% (n=45) (Fig. 4.1A,E,I). Surprisingly, the phenotype in the context of *dmrt2a/terra* overexpression is similar to the one we described when Dmrt2a/Terra is knockdown. Cycling gene expression becomes desynchronized, with *deltaC* being asymmetric in 26% of the embryos (n=42), *her1* in 13% (n=31) and *her7* in 38% (n=58) (Fig. 4.1B,C,F,G,J-L). Also, like in the Dmrt2a/Terra knockdown situation, these asymmetries are restricted to a specific temporal window and from the 12 somite stage onwards, embryos are able to recover. Nevertheless, despite ceasing to be symmetrically expressed, these genes continue to exhibit an oscillatory expression pattern and different phases of their cycles are observed. When analysing the expression of *deltaC* and *her1*, we could also see that in some cases both genes cycle

in phase between both sides of the PSM however, somite boundaries are not well defined and stripes are fused together (Fig. 4.1D,H).

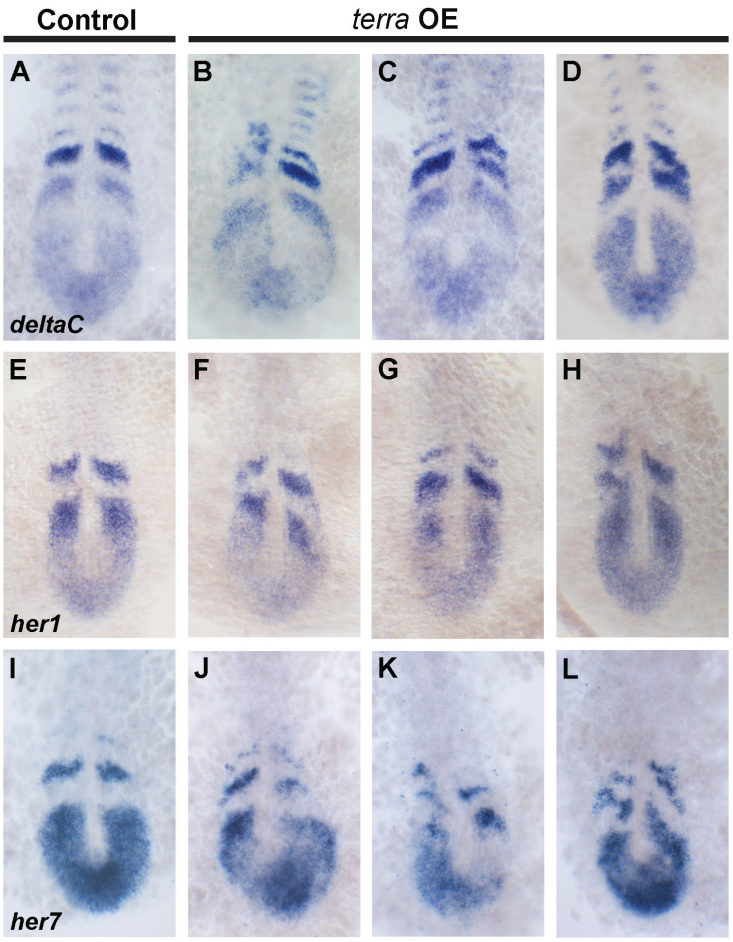

Figure 4.1. Dmrt2a/Terra overexpression leads to desynchronization of the somite clock. (A-L) Expression pattern of the cyclic genes ***deltaC*** (A-D), ***her1*** (E-H) and ***her7*** (I-L) in 8- to 12-somite stage zebrafish embryos. (A, E, I) WT embryos show a synchronized cyclic expression of these genes in the PSM. (B-D, F-H, J-L) ***dmrt2a/terra***-mRNA injected embryos. (B, C, F, G, J-L) Cyclic gene expression becomes desynchronized between both sides of the PSM. (D, H) In some cases ***deltaC*** and ***her1*** cycle in phase but boundaries are fused together. PSM, presomitic mesoderm. All panels show a dorsal view of flatmount embryos with anterior to the top.

Since the oscillations of the segmentation clock are regulating the timing of the somitogenesis, we decided to test if the observed desynchronizations of the cycling genes lead to problems in somite formation. To address if somites are affected before or after their formation, we used two markers that are involved in the initial definition of the segments by establishing their AP polarity at the level of the PSM and thus labelling the prospective somites. *mespb* is restricted to the anterior region of two or three presumptive somites, while *papc* is expressed in the anterior region of the last formed somite pair and three prospective somites (Sawada et al., 2000; Yamamoto et al., 1998). While in control embryos *mespb* is symmetrically expressed in presumptive somites in 100% (n=22) of the cases, in the context of *dmrt2a/terra* overexpression 55% (n=27) still exhibit a symmetric expression however, there is also a lack of coordination between both sides of the PSM and its expression becomes asymmetrically shifted to the right side in 19% (n=27) of the embryos and to the left side in 26% (n=27) (Fig. 4.2A-D). Regarding the expression of *papc*, while it is symmetric in 100% (n=20) of control embryos, it also becomes desynchronized in embryos overexpressing *dmrt2a/terra*, with one side of the axis being in clear advance when compared with the other. While in 63% (n=24) of the embryos there was no shift in the anterior boundary of the *papc* expression, in 15% (n=24) it was shifted anteriorly on the left side, while in 22% (n=24) it was shifted anteriorly on the right side (Fig. 4.2F-H).

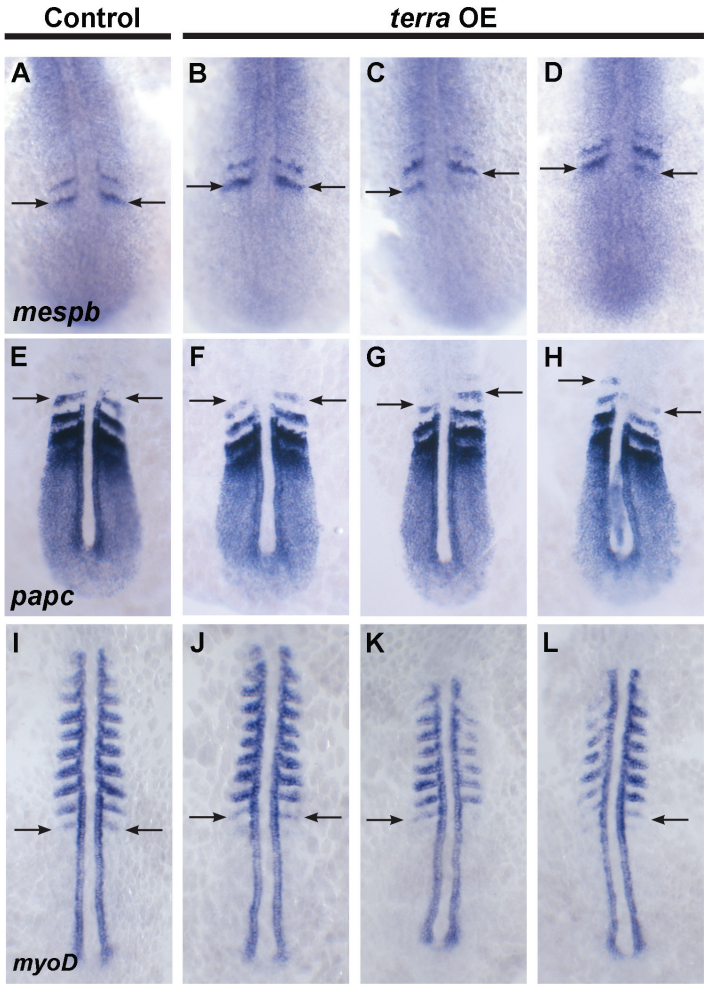

Figure 4.2. Asymmetric somite development in Dmrt2a/Terra overexpression embryos. (A-D) Expression pattern of ***mespb***, (E-H) ***papc*** and (I-L) ***myoD*** in 8- to 12-somite stage zebrafish embryos. (A, E) WT embryos show a symmetric expression pattern of ***mespb*** and ***papc*** in already formed and prospective somites, and (I) ***myoD*** labelling an equal number of formed somites between both sides of the axis. (B-D, F-H, J-L) ***dmrt2a/terra***-mRNA injected embryos. (B, F) ***mespb*** and ***papc*** are symmetrically expressed in some injected embryos however, in some cases there is a lack of coordination between the left and right sides of the PSM and their expression becomes (C, G) shifted to the right side or (D, H) shifted to the left. (J) ***myoD*** labels an equal number of somites between both side of the axis in some injected embryos, in others it reveals that one extra somite is being formed either (K) on the left or (L) on the right sides. PSM, presomitic mesoderm. Arrows show the levels at which forming and formed somites are being placed. All panels show a dorsal view of flatmount embryos with anterior to the top.

Additionally, to verify if as a consequence of prospective somites being misaligned there are also LR problems at the level of the formed somites, we used the muscle differentiation marker *myoD*. It is expressed in the adaxial cells that flank the notochord and posterior somite compartment in 100% (n=16) of WT embryos (Fig. 4.2I). However, in the context of *dmrt2a/terra* overexpression while 73% (n=33) of the embryos presented a symmetric somite formation, the rest had an uneven number of somites being formed between both sides of the axis (Fig. 4.2J-L). There was no bias in any direction, with 15% (n=33) of the embryos presenting more somites on the left and 12% (n=33) with more somites on the right (Fig. 4.2K-L).

The fact that one extra somite is being formed in one of the sides of the axis suggests that there is an acceleration or delay of the determination front regression in one of the sides of the PSM. The position of somite boundary formation is controlled by a determination front, which consists in opposite gradients of Fgf8 and RA. To understand the somite desynchronization phenotype, we analysed the caudal-to-rostral gradient of Fgf8 in the posterior PSM. In control embryos ranging from 8- to 12- somite stage, *fgf8* expression domain was symmetric in 100% of the cases (n=15) (Fig. 4.3A). However, while in 75% (n=34) of the injected embryos *fgf8* expression was symmetric, in the remaining embryos it was anteriorly expanded (Fig. 4.3B-D). This expansion was either seen on the right anterior PSM, in 14% (n=34) of the embryos, or on the left anterior PSM, in 11% (n=34) (Fig. 4.3C,D).

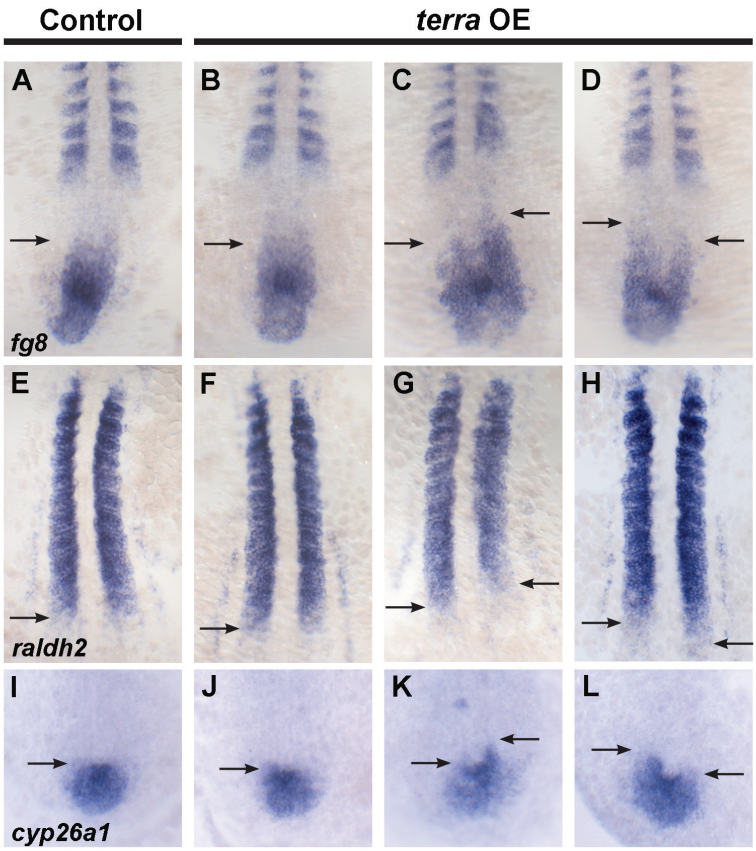

Figure 4.3. Dmrt2a/Terra overexpression induces a desynchronization of the wavefront of differentiation. Zebrafish embryos in 8- to 12-somite stage were hybridized with probes for (A-D) ***fgf8***, (E-H) ***raldh2*** and (I-L) ***cyp26a1***. (A, E, I) WT embryos show a symmetric expression pattern of ***fgf8*** in the posterior PSM, ***raldh2*** in the anterior PSM and ***cyp26a1*** in the tailbud region. (B-D, F-H, J-L) ***dmrt2a/terra***-mRNA injected embryos. Some of the injected embryos present a symmetric expression pattern of (B) ***fgf8***, (F) ***raldh2*** and (J) ***cyp26a1*** nevertheless, in some cases their expression becomes anteriorly or posteriorly expanded only in one side of the axis. ***fgf8*** becomes anteriorly shifted either (C) in the right or (D) left side of the PSM. ***raldh2*** and ***cyp26a1*** reveal a complementary expression domain with ***raldh2*** being posteriorly shifted either (G) in the left or (H) right side of the PSM and ***cyp26a1*** becoming anteriorly shifted either (K) on the right or (L) left side of the tailbud. PSM, presomitic mesoderm. Arrows indicate the level of gene expression along the left and right sides of the PSM. All panels show a dorsal view of flatmount embryos with anterior to the top.

RA counteracts Fgf8 in the anterior region of the PSM, this way regulating somite boundary positioning (Diez del Corral et al., 2003). In addition, it has been implicated in buffering the asymmetric LR information to reach the PSM, so that somite formation can proceed symmetrically (Kawakami et al., 2005; Vermot et al., 2005; Vermot and Pourquié, 2005). RA reduction leads to asymmetries in the expression of the cycling genes in zebrafish, chicken and mouse embryos, just like when we reduce/overexpress *dmrt2a/terra* in zebrafish. Therefore we went to see if RA could be acting downstream of Dmrt2a/Terra in the maintenance of symmetry during somite formation. For that, we examined the expression of the two enzymes responsible for creating the RA gradient. *raldh2* that is responsible for RA synthesis in the anterior PSM, and *cyp26a1* that degrades it in the tailbud region. When overexpressing *dmrt2a/terra*, neither *raldh2* or *cyp26a1* levels of expression were perturbed, concomitant with previous results showing that *dmrt2a/terra* downregulation was also not affecting RA gradient of expression (Fig. 4.3E-L and data not shown). Despite showing normal levels of expression, *raldh2* progressed synchronously in 82% (n=34) of the embryos, more posteriorly on the left PSM in 9% (n=34) and more posteriorly on the right PSM in 9% (n=34), comparing with the control embryos showing 100% (n=11) of symmetric *raldh2* expression pattern (Fig. 4.3E-H). In *dmrt2a/terra* overexpressing embryos the expression of *cyp26a1* in the tail bud was symmetric in 83% (n=30) but also progressed more anteriorly on the right side in 7% (n=30) and more posteriorly on the left in 10% (n=30) of the embryos, phenotype never observed in 100% (n=15) the control embryos (Fig. 4.3I-L).

IV.2. Dmrt2a/Terra overexpression and LPM left-right patterning

A conserved LR patterning cascade is responsible for regulating internal organs asymmetries in vertebrates. Incorrect transfer of information from the node into the left LPM culminates with misplaced organ(s) disposition, which implies several levels of severity in their correct functioning (Peeters and Devriendt, 2006). We had previously shown that Dmrt2a/Terra is also necessary to establish laterality within the left LPM, regulating *spaw* and *pitx2* expression in that region. When downregulating Dmrt2a/Terra, their

expression becomes randomized and as a consequence the heart not always loops to the left side and its position becomes misplaced (Saúde et al., 2005). To investigate the impact of *dmrt2a/terra* overexpression in the LR pathway we evaluated the expression of *spaw*. While in 94% (n=123) of the WT embryos *spaw* was always restricted to the left LPM, in injected embryos its expression became randomized (Fig. 4.4A-D). It became restricted to the left LPM in only 57% of the embryos (n=112), bilaterally expressed in 35% (n=112) and on the right in 8% (n=112) (Fig. 4.4B-D).

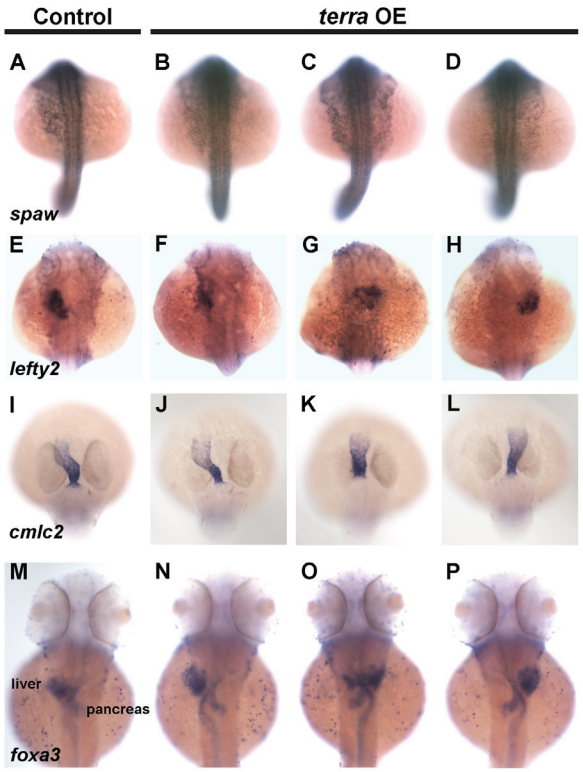

Figure 4.4. Randomization of left-sided gene expression and internal organ localization in the context of Dmrt2a/Terra overexpression. Zebrafish embryos were analyzed between 16- to 18- somite stage for ***spaw*** expression, 25 hpf for ***lefty2***, 32 hpf for ***cmlc2*** and 52hpf for ***foxa3***. (A, E) WT embryos show asymmetric gene expression with ***spaw*** and ***lefty2*** being restricted to the left side of the axis. (I, M) Internal organs asymmetric localization in WT embryos with ***cmlc2*** labelling the heart looping to the left side and ***foxa3*** labelling the gut and showing that the liver is on the left. (B-D, F-H, J-L, N-P)

Embryos injected with ***dmrt2a/terra***-mRNA. ***spaw*** expression becomes randomized (B) still being restricted to the left LPM in some embryos, (C) expressed in both side of the LPM or (D) restricted to the right side. Internal organ laterality is also affected. ***lefty2*** expression labels the heart field and also becomes randomized being restricted (F) to the left, (G) bilaterally expressed or (H) restricted to the right side. In agreement, ***cmlc2*** expression that labels the heart looping is also randomized either (J) looping to the left, (K) presenting no looping or (L) looping to the right. ***foxa3*** shows that the liver position also becomes affected in the context of dmrt2a/terra overexpression. (N) It did not always form in the left side, (O) also staying in the middle of the axis or (P) being formed on the right side. hpf, hours post fertilization. LPM, lateral plate mesoderm. All views are dorsal with anterior to the top.

To further evaluate its role in the LR asymmetry pathway we also examined the internal organs laterality. To access if *spaw* randomization also correlates with an incorrect internal organ distribution we looked at *lefty2* expression, a marker of the heart field. In WT embryos *lefty2* is restricted to the left side in 94% of the cases (n=32) and to the right in 6% (n=32) (Fig. 4.4E). In *dmrt2a/terra* overexpressing embryos, *lefty2* is in the left side in 74% of the cases (n=45), bilaterally expressed in 13% (n=45) and restricted to the right also in 13% (n=45) of the embryos (Fig. 4.4F-H). Randomized *lefty2* expression unveils future problems in the direction of the heart looping, which we confirmed by looking at the expression of *cmlc2*. In control embryos the heart loops to the left side in 98% (n=49) of the cases, while in embryos overexpressing *dmrt2a/terra* it becomes randomized, in 85% of the embryos (n=131) it loops to the left, in 9% (n=131) it stays in the middle and in 6% (n=131) of the embryos it loops to the right side (Fig. 4.4I-L). We also looked at the liver position in this context. It loops to the left in 95% (n=119) of WT the embryos, stays in the middle in 1% (n=119) and loops to the right in 4% (n=119) (Fig. 4.4M). In the context of *dmrt2a/terra* overexpression, 68% (n=173) of the embryos have the liver looping to the left, 22% (n=173) in the middle and 10% (n=173) looping to the right (Fig. 4.4N-P). These results indicate that when *dmrt2a/terra* is overexpressed, LR patterning is disturbed not only at the level of gene expression but also at the level of internal organ localization.

To evaluate the integrity of the midline structures, proposed to function as

a barrier that does not allow the diffusion of asymmetric signals from one side of the axis to the other, we accessed the expression of midline markers in embryos overexpressing *dmrt2a/terra* (Schilling et al., 1999). The notochord and floorplate marker *shh* is present in the midline of 100% (n=20) of control embryos and in 100% of the injected embryos (n=25) (Fig. 4.5A-C). We also looked at the expression of *no tail*, a notochord marker, which is expressed along the midline in 100% (n= 21) of control embryos and also in 100% (n=22) of the injected embryos (Fig. 4.5D-F). Since both markers display a continuous staining along the midline, these results indicate that the integrity of the midline in its anterior to posterior region was not compromised and that the obtained LR patterning phenotype when *dmrt2a/terra* is overexpressed is not a consequence of midline malformation.

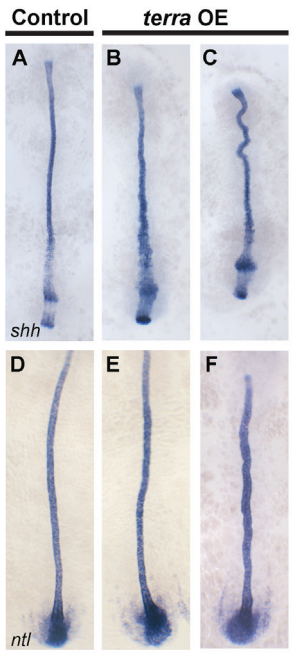

Figure 4.5. Midline structure is intact in the context of Dmrt2a/Terra overexpression. Zebrafish embryos were hybridized with probes for (A-C) ***shh*** and (D-F) ***no tail***. (A, D) WT embryos show a continuous expression of (D) ***shh*** and (F) ***ntl*** along the midline. (B-C, E-F) Embryos overexpressing ***dmrt2a/terra*** also show an intact midline structure in its anterior posterior region with a continuous staining of (B-C) ***shh*** and (E-F) ***ntl*** along the midline. All panels show a dorsal view of flatmount embryos with anterior to the top.

IV.3. Construction of an inducible transgenic zebrafish line

Dmrt2a/Terra is a DM domain transcription factor so far shown to be involved in the regulation of symmetric somite formation and LR patterning in the LPM. Nevertheless, it is not known how it regulates these two processes. To better understand its mode of action, a microarray assay would have allowed us to perform a search for its downstream targets, through the comparison of gene expression levels in different developmental contexts, such as gene downregulation and overexpression. In order to create the tools necessary to perform Dmrt2a/Terra overexpression during a specific developmental time window, we used a Tol2 transposon system as a genetic tool to create a transgenic zebrafish line where Dmrt2a/Terra is under the control of a hsp70. With this tool we will be able to induce its overexpression not at the one-cell stage, but later in development when it starts to be expressed, allowing us to increase the probability of uncover only its direct targets.

We tagged Dmrt2a/Terra with either an HA or Venus tag, to be able to perform affinity purification assays, and cloned them in the pCS2+ expression vector. Both tags were fused to either the N-terminus or C-terminus of the gene since the impact of this fusion on Dmrt2a/Terra function was not known. To check for that, the four different constructs were injected into zebrafish embryos at one-cell stage and the impact on the establishment of laterality in the left LPM was analysed by looking at the expression of spaw. In WT embryos *spaw* expression was restricted to the left LPM in 80% (n=102) of the cases, bilateral in 16% (n=102) and on the right in 4% (n=102) of the embryos (Fig. 4.6A). When injecting the constructs, *spaw* expression became randomized: HA-Dmrt2a/Terra 40% (n=68) on the left, 48% (n=68) bilateral and 12% (n=68) on the right; Dmrt2a/Terra-HA 64% (n=64) on the left, 27% (n=64) bilateral and 9% (n=64) on the right; Venus-Dmrt2a/Terra 53% (n=109) on the left, 33% (n=109) bilateral and 14% (n=109) on the right; Dmrt2a/Terra-Venus 67% (n=27) on the left, 29% (n=27) bilateral and 4% (n=27) on the right (Fig. 4.6A). All constructs gave a LR phenotype in the LPM however, at this time we choose to pursue only with Venus as a tag.

When comparing with the phenotype obtained when injecting dmrt2a/terra mRNA with no tag (*spaw* is in the left LPM in 57% (n=112), bilateral in 35% (n=112) and right in 8% (n=112) of the embryos), the injection of Venus-Dmrt2a/Terra construct gave the most similar percentages of spaw randomization, reason why we chose this construct to pursue with the transgenic.

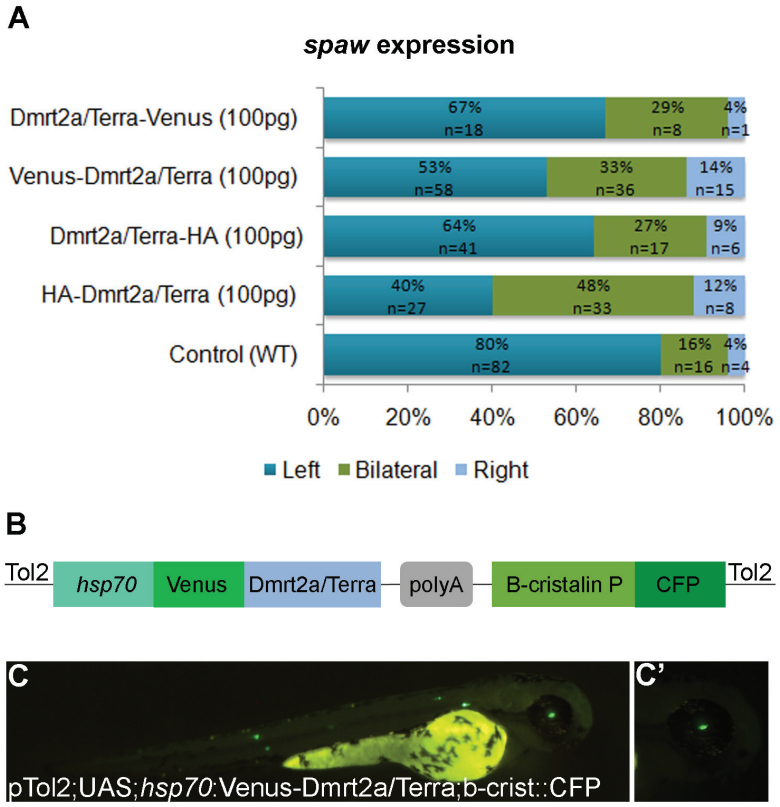

Figure 4.6. Transgenic approach. (A) Analyze of *spaw* expression in several embryos injected with the four different constructs created: HA-Dmrt2a/Terra, Dmrt2a/Terra-HA, Venus-Dmrt2a/Terra and Dmrt2a/Terra-Venus. Comparing with the expression in the control non-injected WT embryos, ***spaw*** becomes randomized in embryos injected with all the constructs. (B) Schematic representation of the transgenic construct. Venus-Dmrt2a/Terra was cloned in a Tol2 plasmid containing a heat-shock promoter and an eye lens marker. (C) 72 hpf larvae showing green eye lens, indicative that the transgenic construct was integrated in its genome. (C') Amplification of the zebrafish larvae eye lens. LPM, lateral plate mesoderm. hpf, hours post fertilization. Lateral view with anterior to the right.

Venus-Dmrt2a/Terra fusion was then cloned in the Tol2 vector under the control of an hsp70 promoter. This construct also carriers a B-cristalin promoter that labels the eye lens and is fused with CFP (Cyan Fluorescent protein), used has a marker to select the founder transgenic embryos that integrated the construct in their genome after injection (Fig. 4.6B). Because the Tol2 element lacks the transposase coding sequence it is necessary to provide exogenous transposase activity by injecting its mRNA, which is responsible for the transposition process to occur, excision from the plasmid and reintegration in the genome. After coinjecting the plasmid DNA with a capped Tol2 transposase mRNA into 1 cell stage embryos, founders exhibiting green eyes at three days pos-fertilization were selected and grown (Fig. 4.6C). The frequency of obtaining a founder fish was high, 30-50%. When reaching the age of 2-3 months, founders were crossed with WT zebrafish and the ones that could transmit the insertion to the F1 progeny were identified. The F1 generation was selected for their green eyes and grown. To test is the transgenic is working, when reaching the 2-3 months of age these F1 zebrafish were crossed with WT zebrafish and a heat-shock was given to the embryos when reaching the 3 somites stage, time when *dmrt2a/terra* starts to be expressed. Preliminary results seem to indicate that the transgenic gives a similar phenotype to when we overexpress *dmrt2a/terra* at the 1 cell stage. Although we have only looked at the phenotype at the level of the PSM, we can clearly state that symmetry is lost, with the cycling gene *deltaC* presenting a desynchronized cyclic expression pattern in the PSM region (Fig. 4.7).

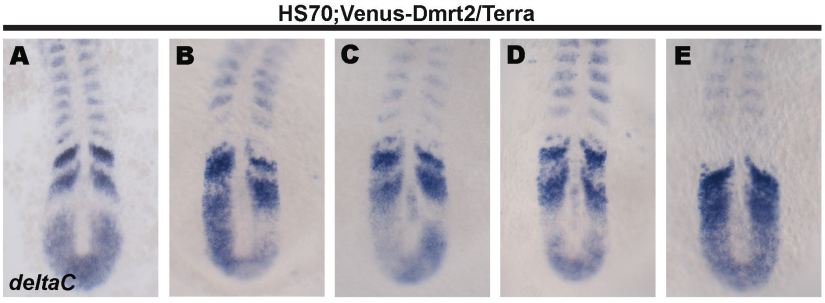

Figure 4.7. Dmrt2a/Terra heat-shock in transgenic embryos leads to desynchronization of *deltaC* cyclic expression. A HS70:Venus-Dmrt2a/Terra transgenic zebrafish from the F1 generation was crossed with a WT and a heat-shock was given to embryos when reaching the 3-somite stage. (A) While synchronized expression of ***deltaC*** was observed in some cases, (B-C) different phases of the cycle where also observed in either side of the PSM and somite boundaries were not well defined. (D) In some embryos the cycle of expression is in phase between both sides of the PSM but somite boundaries are also not well defined. Finally, in other cases (E) ***deltaC*** seems to stop its oscillations being expressed all over the PSM. PSM, presomitic mesoderm.

Discussion

Considerable advances have been made in understanding how symmetric vs. asymmetric development is regulated and, although once seen as independent, the pathways responsible for regulating these processes are now known to interact. A key component of this regulation is the Dmrt2a/Terra transcription factor. In a previous study we showed that in the context of Dmrt2a/Terra knockdown two distinct phenotypes are observed – asymmetric somite formation and randomization of left side specific information within the LPM (Saúde et al., 2005). Since nothing is known regarding the Dmrt2a/Terra regulatory pathway, our aim was to search for its downstream targets using a ChIP-on-chip approach (see Chapter III). Unfortunately, we were unable to pursue with the assay due to the lack of a specific antibody against Dmrt2a/Terra and therefore decided to follow a different approach.

The ability to rapidly discover and analyze the expression profile of thousands of genes in a single experiment and in response to different physiological conditions, such as gene knockdown, overexpression and clinical conditions, can be achieved through the microarray-based assay technology (Schena et al., 1998; Ton et al., 2002). The basic principle of this technology is that thousands of oligonucleotides spots are immobilized in a filter array, which is then hybridized with two labeled RNA samples (test and reference samples) and evaluated for differences in genes expression profile (Schena et al., 1998). Using this approach, downstream target genes of the Dmrt2a/

Terra could have been discovered. To be able to test how genes expression profile would change in response to Dmrt2a/Terra knockdown we could inject a MO against this gene. At the same time, it would be useful to induce the opposite physiological condition and upregulate *dmrt2a/terra* RNA levels. Several transgenesis methods have been developed to express particular genes of interest in the zebrafish genome such as – injection of plasmid DNA in fertilized eggs; infection with retroviral vectors; injection of constructs flanked by two *I-SceI* recognition sites and three different transposon vectors (Tc3, Sleeping-Beauty and Tol2). From these methods, the Tol2 transposon has been shown to have a higher integration in the zebrafish genome (rate of germline transmission of 30-50%) (Davidson et al., 2003; Kawakami et al., 2004; Amsterdam and Becker, 2005). The generation of expression constructs relies on the multisite Gateway system, which consists in site-specific recombination based cloning and subcloning into Tol2 based destination vectors, which have the Tol2 transposon ends necessary for transposition into the host genome (Magnani et al, 2006; Kwan et al, 2007).

A transgenic line where we would have Dmrt2a/Terra under the control of a heat-shock responsive promoter, would allow us to induce its overexpression in a specific developmental stage, namely when the gene starts to be expressed, and also to look at the immediate response in gene expression. Given this, we first characterized *dmrt2a/terra* overexpression at the one cell stage so that we could analyse if there was a LR phenotype and decide if we could pursue with the construction of a transgenic zebrafish line. Surprisingly, embryos overexpressing *dmrt2a/terra* exhibited a similar phenotype to when Dmrt2a/Terra was knockdown. Somite formation became bilaterally asymmetric and asymmetric information was not correctly transferred from the KV into the left LPM, culminating with organs becoming misplaced. These results indicate that it is not the absence or presence of Dmrt2a/Terra that regulates these two processes. Instead, a precise regulation of its levels is what is fundamental to ensure correct symmetric and asymmetric features during zebrafish embryonic development. With the

overexpression assay giving a LR phenotype, we then used the Tol2 element to integrate a *hsp70*:Venus-Dmrt2a/Terra construct throughout the zebrafish genome. We have already observed that, after applying a heat-shock at the 3-somites stage in these transgenic embryos, the expression of *deltaC* becomes desynchronized, similar to what happens when injecting *dmrt2a/terra* mRNA at the one cell stage. Thus, this transgenic is now a good tool to be used in the microarray assay that will allow us to learn more about the genetic pathway where Dmrt2a/Terra is operating and understand better how it is regulating the correct symmetric and asymmetric traits during embryonic development.

During the characterization of *dmrt2a/terra* overexpression regarding the regulation of somite formation, we observed that in addition to the asymmetric progression of the cycling genes oscillations between both sides of the PSM, one of the sides was also either delaying the regression of the determination front or speeding it. This shift of the determination front on its own is sufficient to induce somite boundary misplacement. Previous work in chick embryos has shown that altering the Fgf8 gradient in one side of the PSM, through Fgf8 bead implantation, does indeed lead to an anterior shift of the determination front (Dubrulle et al., 2001). This desynchronization of the determination front is then responsible for an anterior shift of the position of somite boundaries. Since there is a delay of the PSM cells to begin their segmental determination, an asymmetric expression of the cyclic genes is also observed. Nevertheless, the shift of the determination front was only associated with a shift in the somite boundary position and not with the formation of an extra boundary, with somites forming at the same time only with a smaller size (Dubrulle et al., 2001). Despite this, our results show that in the context of *dmrt2a/terra* overexpression not only there is a shift of the determination front and a desynchronization of the cycling genes but an extra somite is also formed. Given this, the shift of the determination front that we observed isn't sufficient to explain the extra somite formation. This phenotype seems to be associated with either an ac-

celeration or delay of the pace of the clock that as a consequence induces an extra somite formation and a shift of the determination front. Also, these desynchronizations are in fact seen before somites are formed, since prospective somite markers at the level of the anterior PSM, such as *mespb* and *papc*, are already desynchronized between both sides of the axis.

Since Dmrt2a/Terra has a complex expression pattern, in the sense that it is expressed in several structures – KV, anterior region of the PSM and also in the somites – addressing where it is operating to regulate LR symmetry vs. asymmetry is not so straightforward (Meng et al., 1999; Lourenço et al., 2010). Taking into account that it's in the KV that LR signals are established/maintained, that the KV is formed in the posterior region of the PSM and that the segmentation clock oscillations are already initiated in cells in the posterior tailbud region (Mara et al., 2007), we propose that the role of Dmrt2a/Terra in regulating bilateral symmetric somite formation is done in the KV. There, it may be necessary to protect the PSM cells from the influence of the LR signalling cascade, allowing them to initiate/maintain the segmentation clock oscillation in a bilaterally symmetric way. We could also argue that it could be regulating symmetric somite formation at the level of the anterior PSM, where it is also expressed. In fact, Notch signalling in the PSM has been shown to be necessary to maintain synchrony within that region since in zebrafish mutants for several Notch pathway components, cells begin their oscillations in synchrony but after a few cycles they become progressively desynchronized forming abnormal somite boundaries (Jiang et al., 2000). Nevertheless, Dmrt2a/Terra expression in anterior PSM and somites is possible linked with a role in somite differentiation, like it has already been described to be necessary in mouse (Seo et al., 2006). In addition, its role in regulating LR asymmetry pathway in the LPM can also be explained by its presence in the KV, where it is possibly regulating the transfer of LR signals from the KV to the left LPM (Saúde at al., 2005; Lourenço et al., 2010). A good approach to test if Dmrt2a/Terra is regulating both processes at the level of the KV would be to injecting a MO against it at the mid blastula transition stage (MBS), when only the precursors of the KV, the DFC's, are targeted (Amack and Yost, 2004).

Materials and methods

Zebrafish lines

AB and TU wild-type zebrafish were crossed and embryos collected and kept at 28ºC until the appropriate stage (Kimmel et al., 1995).

Cloning of *terra*

Total RNA was extracted from appropriate staged zebrafish embryos using TRIzol (Invitrogen) and cDNA synthesized with MMLV-Reverse Transcriptase kit (Promega). Zebrafish *dmrt2a/terra* full length sequence was amplified by PCR with the following primer set: *dmrt2a/terra*-F 5'-ATGACGGATCTGTCC-GGCACG-3' and *dmrt2a/terra*-R 5'-AGCAAGAAGCCTTACTGAGATTTCCG-3'. The amplified DNA fragment was then cloned in the pCS2+ expression vector into the NotI site.

terra overexpression

pCS2+ plasmid containing *dmrt2a/terra* full length sequence was linearized with BamHI and capped sense mRNA synthesized with the mMESSAGE mMACHINE SP6 kit (Ambion). *dmrt2a/terra* sense mRNA (30pg) was injected into 1- to 2-cell stage WT zebrafish embryos.

Whole-mount in situ hybridization

Zebrafish embryos were analyzed by whole-mount in situ hybridization (WISH) as previously described (Thisse and Thisse, 2008). Digoxigenin (DIG) labeled antisense RNA probes were synthesized from DNA templates of *deltaC* (Jiang et al., 2000), *her1* (Holley et al., 2000), *her7* (Oates and Ho, 2002), *mespb* (Sawada et al., 2000), *papc* (Yamamoto et al., 1998), *myoD* (Weinberg et al., 1996), *fgf8* (Reifers et al., 1998), *cyp26a1* (Dobbs-McAuliffe et al., 2004), *spaw* (Hashimoto et al., 2004), *pitx2* (Essner et al., 2005), *lefty2* (Bisgrove et al., 2005), *cmlc2* (Yelon et al., 1999), *shh* (Essner et al., 2005) and *ntl* (Amack and Yost, 2004). Embryos were photographed with a LEICA Z6 APO stereoscope coupled to a LEICA DFC490 camera.

Generation of Dmrt2a/Terra HA and Venus constructs

To amplify the HA-Dmrt2a/Terra template the following set of Polymerase chain reactions (PCR's) were done. Dmrt2a/Terra was amplified by adding an HA sequence to its N-terminal region and a StuI restriction site to the C-terminal region with the following primer set: Dmrt2a/Terra-HA-F 5'-CCAGACTACGCTTCCCTTATGACGGATCTGTCCGGCACGGAG-3' and Dmrt2a/Terra-StuI-R 5'-AGGGGAAAACTGAGATTTCCGATTTAAAGAAAGCGC-3'. An EcoRI restriction site was then added to the N-terminal region of the PCR product with the primer HA-EcoRI-F 5'-CCGGAATTCATGGCTTCATATCCTTACGATGTTCCAGACTACGCTTCCCTT-3'. This product was then amplified in a final PCR with the primer set: HA-EcoRI-F and Dmrt2a/Terra-StuI-R.

To obtain the Dmrt2a/Terra-HA template Dmrt2a/Terra sequence was amplified by adding an EcoRI restriction site to its N-terminal region and HA sequence to the C-terminal region with the following primer set: Dmrt2a/Terra-EcoRI-F 5'-CCGGAATTCATGACGGATCTGTCCGGCACGGAG-3' and Dmrt2a/Terra-HA-R 5'-ATCGTAAGGATATGAAGCCATCTGAGATTTCCGATTTAAAGAAAGCGC-3'. A StuI restriction site was then added to the C-terminal region of the PCR product by PCR with the HA-StuI-R primer 5'-AGGGGAAAATCAAAGGGAAGCGTAGTCTGGAACATCGTAAGGATATGAAGCCAT-3'. This product was then amplified in a final PCR with the primer set: Dmrt2a/Terra-EcoRI-F and HA-StuI-R.

To obtain the Venus-Dmrt2a/Terra template an EcoRI restriction site was first added to the N-terminal region of Venus sequence (cloned in the pKS plasmid) by PCR with the following primer set: Venus-EcoRI-F 5'-CCGGAATTCATGGTGAGCAAGGGCGAGGAGCTGTTC-3' and Venus-R 5'-GTACAGCTCGTCCATGCCGAGAGT-3'. In parallel, Dmrt2a/Terra sequence was amplified by adding the end of Venus sequence to its N-terminal region and a StuI restriction site to its C-terminal region with the following primer set: Dmrt2a/Terra-Venus-F 5'-GGCATGGACGAGCTGTACATGACGGATCTGTCCGGCACG-3' and Dmrt2a/Terra-StuI-R 5'-AGGCCTTTTTTACTGAGATTTCCGATTTAAAGAAAGCGC-3'. The PCR products were then used in a

PCR ligation to obtain a Venus-EcoRI-Dmrt2a/Terra-StuI template. The template was further amplified in a final PCR using Venus-EcoRI-F and Dmrt2a/Terra-StuI-R primers.

To obtain the Dmrt2a/Terra-Venus template a StuI restriction site was added to the C-terminal region of Venus sequence using the following primer set: Venus-F 5'-ATGGTGAGCAAGGGCGAGGAGCTGTTC-3' and Venus-StuI-R 5'-AGGCCTTTTTTACTTGTACAGCTCGTCCATGCCGAG-3'. In parallel, Dmrt2a/Terra sequence was amplified by adding an EcoRI restriction site to its N-terminal region and the begging of Venus sequence to its C-terminal region with the following primer set: Dmrt2a/Terra-EcoRI-F 5'-CCGGAATTCATGACGGATCTGTCCGGCACG-3' and Dmrt2a/Terra-Venus-R 5'-CTCGCCCTTGCTCACCATCTGAGATTTCCGATTTAAAGAAAGCGC-3'. The PCR products were then used in a PCR ligation to obtain a Dmrt2a/Terra-EcoRI-Venus-StuI template. The template was further amplified in a final PCR using Dmrt2a/Terra-EcoRI-F and Venus-StuI-R primers.

Each amplified fragment (HA-Dmrt2a/Terra; Dmrt2a/Terra-HA; Venus-Dmrt2a/Terra; Dmrt2a/Terra-Venus) was further cloned in the pCS2+ plasmid, previously digested with EcoRI and StuI restriction enzymes.

Cloning of pTol2;*hsp70*:Venus-Dmrt2a/Terra to produce a transgenic zebrafish line

The selected construct for the transgenesis approach was the Venus-Dmrt2a/Terra, being amplified from the pCS2+ vector using the following primer set: Venus-ClaI-Kosak-F 5'-CCATCGATGGCCACCATGGTGAGCAAGGGCGAGGAGCTGTTC-3' and Dmrt2a/Terra-StuI-R 5'-AGGGGAAAACTGAGATTTCCGATTTAAAGAAAGCGC-3'. The PCR product was cloned in pGEM plasmid and positive clones further sequenced. The Tol2 destination vector containing a *hs70* promoter (pTol2;UAS;*hsp70*:2xHA;b-crist::CFP kindly provided by Julian Lewis) was digested with ClaI and StuI in order to remove the 2xHA sequence. A selected Venus-Dmrt2a/Terra construct was also digested with ClaI and StuI and inserted in the Tol2 vector, downstream of the *hs70* promoter.

Plasmids injection

Each generated constructs HA-Dmrt2a/Terra, Dmrt2a/Terra-HA, Venus-Dmrt2a/Terra and Dmrt2a/Terra-Venus were injected in zebrafish embryos at the one cell stage at the concentration of 100pg. The pTol2;UAS;*hsp70*:Venus-Dmrt2a/Terra;b-crist::CFP construct was coinjected with the transposase mRNA, 30 pg of plasmid with 25 pg of mRNA in embryos at the one cell stage. Three days after the injection, embryos that had positively integrated the plasmid were selected for their green eye lens.

CHAPTER V

Notch signalling regulates left-right asymmetry through ciliary length control

The work presented here was published in **Lopes, S. S., Lourenço, R., Pacheco, L., Moreno, N., Kreiling, J. and Saúde, L.** (2010). Notch signalling regulates left-right asymmetry through ciliary length control. *Development* **137(21)**, 3625-32.

SL and LS conceived the experiments and wrote the manuscript. RL performed injections, *in-situ* hybridizations, embryos scoring and photography.

Abstract

The importance of cilia in embryonic development and adult physiology is emphasized by human ciliopathies. Despite its relevance, molecular signalling pathways behind cilia formation are poorly understood. We show that Notch signalling is a key pathway for cilia length control. In *deltaD* zebrafish mutants, cilia length is reduced in the Kupffer´s vesicle and can be rescued by the ciliogenic factor *foxj1a*. Conversely, cilia length increases when Notch signalling is hyperactivated. Short cilia found in *deltaD* mutants reduce the fluid flow velocity inside the Kupffer´s vesicle, thus compromising the asymmetric expression of the flow sensor *charon.* Notch signalling brings together ciliary length control and fluid flow hydrodynamics with transcriptional activation of laterality genes. In addition, our *deltaD* mutant analysis discloses an uncoupling between gut and heart laterality.

Introduction

Internal body LR asymmetry is a common trait among vertebrates. In contrast to the symmetric external body plan, the heart, digestive organs and parts of the brain display highly conserved asymmetric orientations that are essential for their correct functions. When the normal asymmetric distribution of the internal organs is compromised, human laterality disorders arise such as heterotaxy and *situs inversus* (Fliegauf et al., 2007; Gerdes et al., 2009).

The establishment of LR asymmetries in vertebrates occurs during early stages of embryonic development through a complex process involving epigenetic and genetic mechanisms. This culminates in the activation of a conserved Nodal signalling cascade that starts at the node and is then transferred to the left LPM (Hamada, 2008). Although the timing and mechanism responsible for breaking the initial embryonic symmetry might differ between species, it is clear that a directional fluid flow generated by motile cilia present in the node plays a fundamental role in LR determination, most likely by creating a LR information bias in the node (Levin and Palmer, 2007).

Several lines of evidence support this idea, namely absent cilia in the mouse (Nonaka et al., 1998), shorter cilia in zebrafish mutants and morphants (Kramer-Zucker et al., 2005; Neugebauer et al., 2009) and immotile cilia in mouse, zebrafish and medaka (Essner et al., 2005; Hojo et al., 2007; Supp et al., 1999) resulted in altered fluid flow in the node/KV and ultimately in LR defects. This implies that proper cilia length regulation is crucial for the establishment of LR asymmetries.

Expression of *nodal* and of its antagonist *cerl-2* in the mouse node starts symmetrically (Collignon et al., 1996; Marques et al., 2004). However, the mechanism that turns *nodal* expression asymmetric on the left side and *cerl-2* expression asymmetric on the right side of the node and its potential link to the leftward nodal flow is not fully understood. In zebrafish there is no evidence for asymmetric expression of *spaw* and of its negative regulator *charon* in the KV. Nevertheless, it was suggested that an asymmetric Charon function inhibits the transfer of *spaw* to the right LPM (Hashimoto et al., 2004). To date, the relationship between the fluid flow inside the KV and the asymmetric function of Charon in medaka and its homologue Coco in *Xenopus* was studied (Hojo et al., 2007; Schweickert et al., 2010), but has not been explored in zebrafish.

Notch signalling has been implicated in LR patterning in vertebrates, largely through the activation of *nodal* expression in the murine node (Krebs et al., 2003; Przemeck et al., 2003; Raya et al., 2003; Takeuchi et al., 2007). In zebrafish Notch signalling seems to activate *charon* expression in the KV (Gourronc et al., 2007).

Apart from providing the first genetic evidence in zebrafish for the activation of *charon* expression in the KV, we demonstrate that canonical Notch signalling, through the DeltaD ligand, is a key regulator of ciliary length at the KV. We show that reduction of Notch signalling produces shorter cilia, while hyperactivation of Notch produces longer cilia providing new insights into how cilia length is modulated. We find that proper cilia length regulation has a strong impact on directionality and speed of the fluid flow inside the KV and were able to show that this biomechanical event correlates with asymmetric transcription of *charon*. Altogether,

our results reveal a new and multistep role for the Notch signalling pathway that couples two fundamental processes in left-right determination: transcription of *charon* and ciliary length regulation that then culminates in breaking the symmetry of *charon* expression.

Materials and Methods

Zebrafish lines

AB wild type and mutant (*notch1a*/*des*Tp37, *deltaC*/*bea*tit446, *deltaD*/*aei*tr233) embryos were staged according to Kimmel et al. (1995).

Morpholino antisense oligo (MO) and mRNA microinjections

deltaD-MO as described previously (Holley et al., 2000) was injected from 0.5-1mM into 512-cell stage wt embryos. The MO that blocks translation of *Su(H)1and 2* was used as previously described (Echeverri and Oates, 2007). Notch-intracellular and full-length *deltaD* constructs (Takke and Campos-Ortega, 1999; Takke et al., 1999) were injected at the 1-cell stage at a concentration of 100 pg and 350 pg, respectively. *Foxj1a* and GFP full-length cDNAs were independently cloned into pCS2+ and *in vitro* transcribed using mMESSAGE mMACHINE kit (Ambion). The *foxj1a* and GFP mRNAs were injected at a concentration of 100 pg. Embryos were left to develop at 28oC until the desired stage and then fixed in 4% PFA at 4oC overnight.

in situ hybridization

Whole-mount in situ hybridization was performed as in Thisse and Thisse (2008). Digoxigenin RNA probes were synthesized from DNA templates of *spaw* (Hashimoto et al., 2004), *pitx2* (Essner et al., 2005), *lefty2* (Bisgrove et al., 2005), *foxA3* (Monteiro et al., 2008), *ntl* (Amack and Yost, 2004), *shh* (Essner et al., 2005), *charon* (Hashimoto et al., 2004), *deltaD* (Takke and Campos-Ortega, 1999), *sox17* (Amack and Yost, 2004) and *foxj1a* (Neugebauer et al., 2009; Yu et al., 2008).

Antibody staining and immunofluorescence

We followed the methods described by (Neugebauer et al., 2009). In some cases we also used TOPRO-3 (1:1000; Invitrogen) diluted in blocking solution.

Confocal microscopy

Flat mounted embryos were examined with a Zeiss LSM 510 Meta confocal microscope. Three-colour confocal Z-series images were acquired using sequential laser excitation, converted into a single plane projection and analyzed using ImageJ software (LSM Reader). The length of all cilia in each KV was measured with ImageJ Segmented Line Tool.

High-speed video microscopy

We used the confocal microscope Leica SP5 under the resonance mode, which allows imaging at 8000 lines per second, to acquire images of ciliary beating and debry movements inside the KV of live embryos mounted in 1% low-melting agarose (Sigma). High-speed films of the debris were analyzed using ImageJ and the velocity was measured by tracing the debris frame by frame. The orientation and speed of the debris were calculated using Excel VBA and vectors were drawn using the Gnuplot software and Gimp.

Determination of KV cilia distribution

The total number of cilia and their distribution within the KV were determined from confocal Z-stacks as previously described (Kreiling et al.2007).

Results

V.1. DeltaD is the Notch ligand defining laterality in zebrafish

In order to study the impact of Notch signalling pathway on crucial steps for LR patterning, we used several mutants and reagents. We started by evaluating the asymmetric information in the LPM using the left-identity molecular markers *spaw* and *pitx2*. The nodal-related gene *spaw* is the earliest molecule to be

asymmetrically detected in the left LPM and is known to induce the expression of the transcription factor *pitx2* (Hamada et al., 2002; Long et al., 2003).

We show that mutants in the Notch transmembrane receptor, *des/notch1a-/-* lose their laterality identity by becoming largely bilateral (Fig. 5.1A,B). Upon binding to its ligand, the intracellular domain of Notch (NICD) is cleaved and translocates into the nucleus. In the nucleus, NICD binds to Su(H) thereby changing its repressor status to an activator (Fior and Henrique, 2008). In zebrafish, the two *Su(H)* paralog genes that can be knocked down using a single antisense MO that blocks the translation of both (*Su(H)1+2-MO*) (Echeverri and Oates, 2007). Consistent with our results, *Su(H)1+2* morphants also showed lack of laterality identity (Fig. 5.1A,B). To directly induce the Notch pathway, we injected the mRNA encoding NICD and similarly to what has been described (Raya et al., 2003), we again found a loss in laterality (Fig. 5.1A,B). These results indicate that canonical Notch signalling is required to define laterality in the LPM.

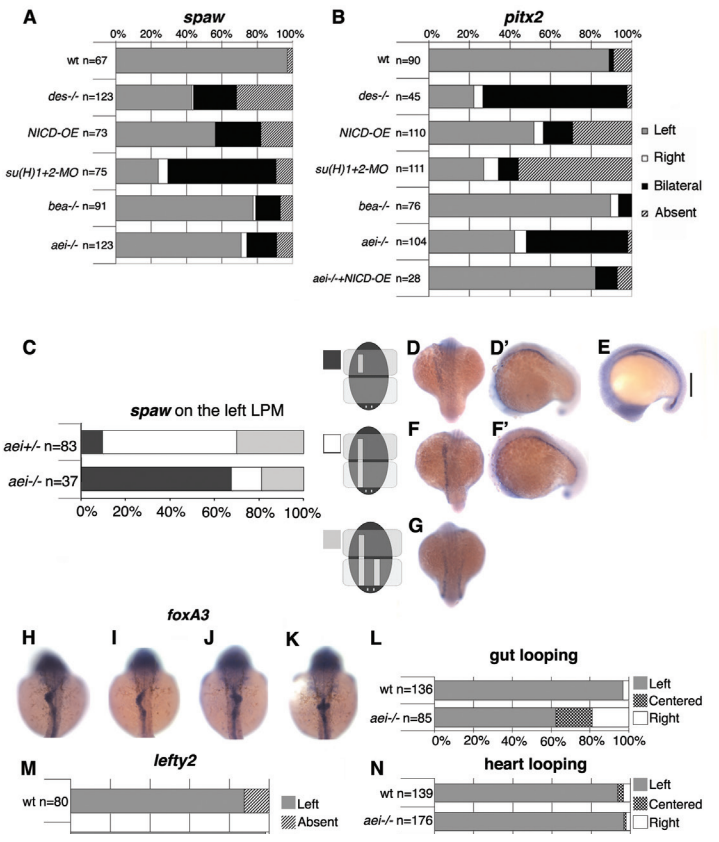

Figure 5.1. Canonical Notch signalling through the DeltaD ligand controls leftright patterning. (**A, B**) Percentages of normal (left), reversed (right), bilateral and absent expression of *spaw* (**A**) and *pitx2* (**B**) in the lateral plate mesoderm when Notch signalling was challenged. Embryos were analysed between 14 to 18-somite stage for *spaw* expression and 18 to 20-somite stage for *pitx2*. (**C**) Percentages of different domains of left-sided expression of *spaw* in the lateral plate mesoderm. In *aei-/-* embryos *spaw* may be expressed in an anterior domain only (**D, D'**), and in an anterior and posterior domain (**F, F'**) and in an anterior and posterior domain with competition on the right side (**G**). (**E**) A double *spaw* and *lefty1 in situ* hybridization showing the posterior gap (vertical line) of these two markers in a *aei-/-* embryo. (**HK**) Expression of *foxA3* in the gut in 50-53 hpf embryos in a dorsal view. In wt embryos the gut loops to the left (**H**). In *aei-/-* embryos, the gut may loop to the left (**I**), to the right (**J**) or show no lopping (**K**). (**L**) Percentages of normal (left), reversed (right) or no looping (centered) of the gut at 50-53 hpf. (**M**) Percentages of normal (left), reversed (right) or absent *lefty2* in the lateral plate mesoderm at the 26-somite stage. (**N**) Percentages of normal (left), reversed (right) or no jogging (centered) of the heart at 30-32 hpf.

In order to assess which Notch ligand was the most relevant in LR establishment, the expression of the left-sided markers was analysed in the null mutants, *aei/deltaD-/-* and *bea/deltaC-/-*. In clear contrast to *bea-/-*, *aei-/-* mutants have a strong *pitx2* laterality phenotype that can be rescued by *NICD* (Fig. 5.1B). Thus, we identify DeltaD as the key Notch ligand for LR asymmetry in zebrafish and we will focus our analysis on this null mutant. We find that the bilateral expression of *pitx2* does not always follow the expression of *spaw* (compare Fig. 5.1A with Fig. 5.1B). A lack of a precise correlation between the expression of *nodal* and *pitx2* in the LPM was already described in the context of *dll1* mouse mutants (Krebs et al., 2003; Przemeck et al., 2003; Raya et al., 2003). Altogether, these results show that Notch signalling regulates *pitx2* expression in a Nodal/Spaw independent manner.

The axial midline is required to maintain LR asymmetry acting as a midline barrier (Chin et al., 2000; Hamada et al., 2002). We checked whether the LR defects arising upon Notch signalling perturbation were due to lack of a midline. We found that the expression pattern of both *shh* and *ntl* markers was normal in all the experimental conditions (Fig. 5.2A-N), with the exception of *ntl* downregulation in *NICD*-injected embryos (Fig. 5.2N), in agreement with what has been described previously (Latimer and Appel, 2006). Therefore, LR defects arising from reduced Notch signalling are not likely due to an absent midline.

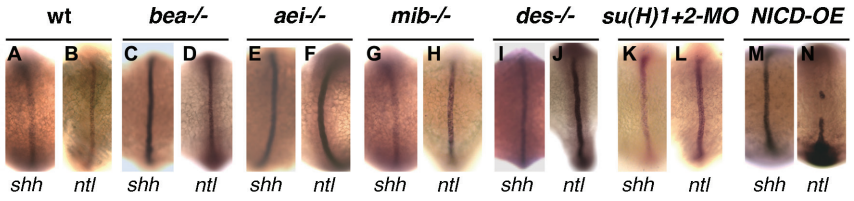

Figure 5.2. Analysis of the midline markers *shh* and *ntl* in wt embryos (A, B) Notch signalling compromised mutant and morphant embryos (C-L) and embryos where Notch signalling is hyperactivated by overexpressing ***NICD*** (M, N).

V.2. DeltaD maintains *spaw* expression in the posterior left LPM

In *aei-/-* mutants, *spaw* expression is only mildly randomized (Fig. 5.1A) but the expression scored as being left-sided (Fig. 5.1A) in fact shows three distinct patterns that were quantified in detail in Fig.1C. Namely, we could detect *spaw* expression in a left anterior domain (Fig. 5.1C,D,D'), in a left anterior and posterior domain (Fig. 5.1C,F,F') and in a left anterior and posterior domain with competition (Fig. 5.1C,G). Although, a posterior downregulation of *spaw* occurs at the 23-somite stage as part of its normal AP expression pattern (Long et al., 2003), our analysis using an *aei* heterozygous cross, clearly shows that this *spaw* downregulation occurs prematurely at 16-somite stage in 67% of the homozygous embryos (Fig. 5.1C,D,D'). In agreement with this posterior downregulation of *spaw*, we observe that *lefty1*, known to be induced by Spaw (Long et al., 2003; Wang and Yost, 2008), has also an abnormal expression gap in the corresponding midline domain (Fig. 5.1E). These results suggest that the maintenance of *spaw* expression in the posterior left LPM and possibly *lefty1* in the midline domain require DeltaD function.

V.3. DeltaD controls gut laterality

Next, we evaluated the impact that the abnormal expression of *spaw* and *pitx2* seen in *aei-/-* mutants has on heart and gut positioning. We scored *aei-/-* mutants for heart asymmetry *in vivo* and made use of the prospective heart marker, *lefty2,* and the gut marker, *foxA3* in fixed embryos. We show that in *aei-/-* mutants, gut looping is randomized (62.3 % loops to the left, 18.8% does not loop and 18.8% loops to the right; n=85) (Fig. 5.1H-L). In contrast, heart jogging is not significantly affected neither when evaluated by *lefty2* expression at 26-somite stage (99% on the left; n=112) nor when judged by direct observation at 30 hpf (90.7% on the left; n=65) (Fig. 5.1M,N). These results indicate uncoupling of laterality of an anterior organ, such as the heart, and more posterior organs, like the liver and pancreas. The heart is the first organ to be asymmetrically positioned in zebrafish, and it seems that its asymmetry may arise by a mechanism different from that

governing other viscera as suggested by others (Chin et al., 2000; Lin and Xu, 2009).

Our data indicate that the prospective heart domain is unaffected in the *aei-/-* mutants and thus provide an explanation why heart laterality is not disturbed. Namely, the anterior left-sided LPM expression of *spaw* is unaffected and *pitx2* does not reach the anterior-most domain when expressed on the right LPM. We propose that the premature absence of *spaw* expression in the posterior LPM coupled with a bilateral *pitx2* expression in this region could underlie the gut laterality phenotype observed in 40% of *aei-/-* mutants.

V.4. DeltaD regulates cilia length in the KV

Increasing evidence shows that a properly formed node/KV with a directional strong fluid flow driven by the beating of motile cilia is essential for LR determination (Amack et al., 2007; Hamada, 2008). We therefore investigated if the laterality problems observed in *aei-/-* mutants were due to KV morphogenesis and/or ciliogenesis defects.

To test KV integrity we performed immunostainings with ZO-1, a tight junction marker and aPKC an apical epithelial marker (Neugebauer et al., 2009) and observed live embryos with high resolution DIC microscopy. The three approaches revealed that KV structure is normal both in *aei-/-* mutants and in *deltaD* overexpressing embryos (Fig. 5.3A-I). We thus conclude that KV morphogenesis and polarity are not affected by downregulation or upregulation of Notch signalling.

To investigate the role of DeltaD in cilia formation, we labelled the KV cilia with an anti-acetylated α-tubulin antibody. We found that cilia length is significantly reduced in *aei-/-* mutants (Fig. 5.3J,K,M; 2.25 µm± 0.62 s.d.m; n=20 embryos; P<4.3x10-9) when compared with cilia length in wt embryos (Fig. 5.3J,K,L; 3.73 µm± 0.76 s.d.m; n=27 embryos). Strikingly, we also found that hyperactivation of Notch signalling significantly increased the length of cilia in the KV either by injection of *NICD* (Fig. 5.3J; 5.28 µm±1.23 s.d.m; n=19 embryos; P<3.5x10-4) or *deltaD* (Fig. 5.3J,K,N; 6.78 µm ±1.18 s.d.m; n=11 em-

bryos; P<1.5x10-4). Additionally, we asked whether cilia motility was also affected in *aei-/-* mutants. We filmed the KV cilia in live *aei-/-* embryos and showed that despite being shorter, cilia are still motile (Supplementary Video 2). These results strongly suggest that Notch signalling, through DeltaD, controls ciliary length in the KV.

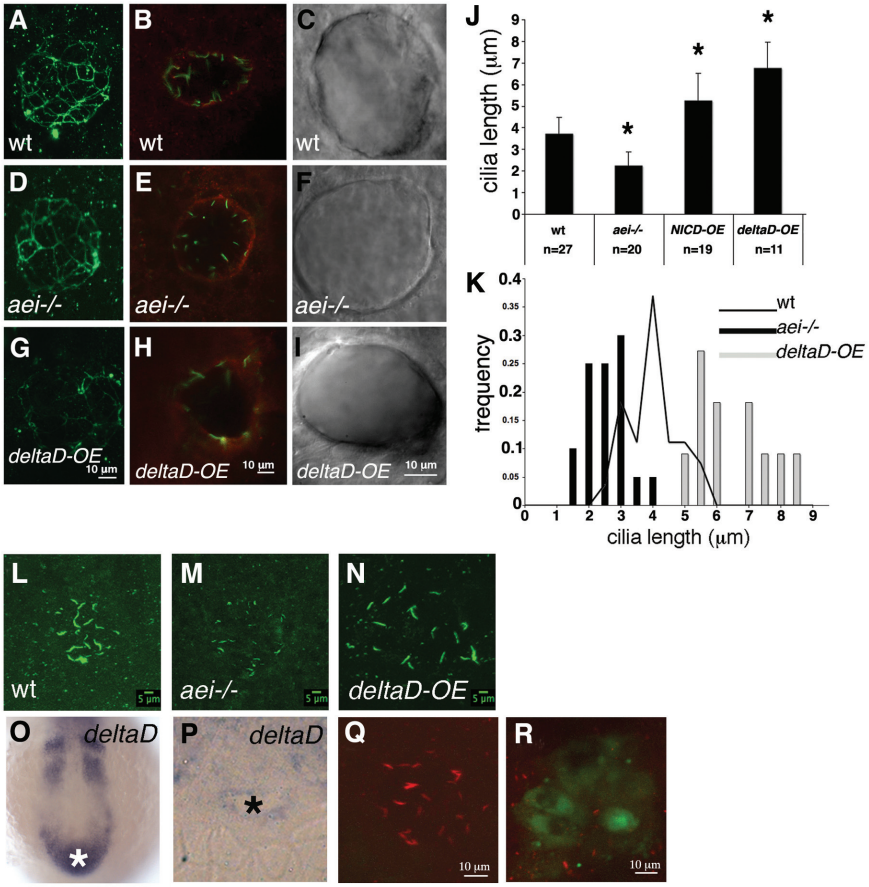

Figure 5.3. DeltaD regulates cilia length in the Kupffer´s vesicle. (**A, D, G**) ZO-1 immunostaining of a representative wt embryo (**A**) an ***aei-/-*** mutant embryo (**D**) and a ***deltaD***-overexpressing embryo (**G**). (**B, E, H**) aPKC immunostaining of a representative wt embryo (**B**), an ***aei-/-*** mutant embryo (**E**) and a ***deltaD***overexpressing embryo (**H**). (**C, F, I)** DIC images of live embryos showing a wt KV (**C**), a KV from an ***aei-/-*** embryo (**F**) and a KV from a ***deltaD***-overexpressing embryo (**I**). (**J**) Quantification of ciliary length at 10-somite

stages in wt, in ***aei-/-*** mutants and in embryos where Notch signalling was hyperactivated by overexpressing ***NICD*** (***NICD-OE***) or ***deltaD*** (***deltaD-OE***). (**K**) Histogram showing the distribution of Kupffer´s vesicle ciliary length at 10-somite stages in ***aei-/-*** mutant (black bars), wt (black line) and embryos subjected to ***deltaD-OE*** (grey bars). (**L-N**) Confocal images of all z-sections spaced 1 µm apart through the entire ciliated Kupffer´s vesicle. Cilia are labelled with anti-acetylated alpha-tubulin in a wt (**L**), ***aei-/-*** mutant (**M**) and in an embryo subjected to ***deltaD-OE*** at 10-somite stage (**N**). (**O, P**) ***deltaD*** expression pattern in a wt at the 10-somite stage in whole-mount (**O**) and in resin section (**P**). The white and the black asterisks label the position and the lumen of the Kupffer´s vesicle, respectively. (**Q, R**) ***deltaD***-MO co-injected with fluorescein lineage tracer in the DFCs. (**Q**) Injected embryo with non-targeted Kupffer´s vesicle cells showing normal length cilia. (**R**) Fluorescein-positive Kupffer´s vesicle cells with shorter cilia. Error bars, s.d.m. Asterisks in the charts indicate experimental conditions significantly different from wt (P<0.001, t-Student, two tail for two samples assuming unequal variances).

deltaD is expressed in the KV (Fig. 5.3O,P) and also in its precursors at the bud stage (10 hpf), in the somites, PSM and tail bud throughout segmentation stages (Hsiao et al. 2007). Therefore, we decided to test if the short cilia phenotype observed in *aei-/-* mutants is caused by the lack of DeltaD function specifically in the KV precursors or in KV cells. We targeted the DFC'c, which are the KV precursors (Essner et al., 2005), by co-injecting the lineage tracer fluorescein and a *deltaD*-MO at the midblastula stage. In KV cells where fluorescein and therefore *deltaD*-MO was successfully detected, we observed a reduction in cilia length comparable to the one quantified in *aei-/-* mutants (Fig. 5.3R; 2.25 µm± 0.6 s.d.m; n=29 cells; P=0.3) and different from the one quantified in KV cells that were not successfully targeted (Fig. 5.3Q; 3.6 µm± 0.6 s.d.m; n=21 cells; P<1.6x10-7). This experiment indicates that DeltaD autonomously regulates cilia length at the level of the KV precursors or the KV cells and not in the somites, PSM and tail bud. In agreement, we found that in embryos where KV precursors were successfully targeted with *deltaD*-MO the trend in *spaw* (84% on the left; 7% on the right; 8% bilateral; n=57) and *pitx2* (33% on the left; 41% bilateral; 25% absent; n=12) expression is similar to the one observed in *aei-/-* mutants. Moreover embryos injected with *deltaD*-MO at the midblastula stage, showed gut looping defects

(74 % loops to the left, 18% does not loop and 8% loops to the right; n=123) and no heart laterality problems similar to what we described for the *aei-/-* mutants.

V.5. DeltaD maintains proper cilia length through modulation of *foxj1a*

In order to investigate why the *aei-/-* mutant cilia are shorter, we analysed the expression pattern of *foxj1a*, a marker of KV motile cilia (Amack and Yost, 2004; Stubbs et al., 2008; Yu et al., 2008). At the bud stage, the DFC marker *sox17* was detected in both *aei-/-* and wt embryos (Fig. 5.4A,B), confirming presence of DFCs. In contrast, *foxj1a* expression was downregulated in *aei-/-* mutants at the same stage compared to wt embryos (Fig. 5.4C,D). We further confirmed that *foxj1a* expression was downregulated at bud stages in 25% of the embryos that resulted from an *aei* heterozygous cross (n=157). In addition, overexpression of both *deltaD* and *NICD* mRNA resulted in ectopic expression of *foxj1a* in the DFCs region at the bud stage (Fig. 5.4E,F). We thus propose that DeltaD controls KV cilia length via the regulation of *foxj1a.* Consistently, *foxj1a* morphants also show shorter or absent cilia in the KV (Stubbs et al., 2008; Yu et al., 2008).

In order to test whether Notch signalling is working via Foxj1a, we performed an epistatic test by co-injecting *foxj1a* mRNA together with GFP mRNA, as a lineage tracer, into one-cell stage *aei-/-* mutant embryos. We found that cilia length was rescued in the KV cells that expressed GFP (Fig. 5.4H). While in the *aei-/-* mutant KV cells the average cilia length was 2.25 μm, in the rescued *aei-/-* mutant cells the average was 4 μm± 0.37 s.d.m (n=53 cilia/5 embryos; P<1.0x10-5). This experiment confirmed that *foxj1a* functions downstream of DeltaD.

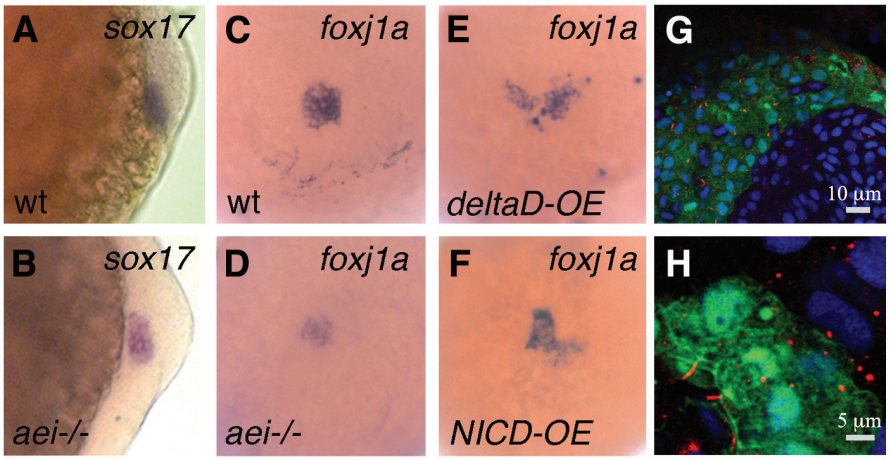

Figure 5.4. DeltaD modulates *foxj1a* expression. (**A, B**) Expression pattern of *sox17* in Kupffer´s vesicle precursor cells at bud stage in wt (**A**) and in an *aei-/-* mutant embryo (**B**). (**C-F**) Expression pattern of *foxj1a* in Kupffer´s vesicle precursor cells at bud stage in a wt (**C**) and in an *aei-/-* mutant embryo (**D**). Wt embryo overexpressing *deltaD* (**E**) and overexpressing *NICD* (**F**). (**G**, **H**) Foxj1a mRNA injection increases ciliary length. (**G**) Tail region of an *aei-/-* mutant embryo showing GFP-positive cells that were co-injected with *foxj1a* and GFP mRNA. In these injected cells cilia are much larger than in adjacent non-targeted cells. (**H**) Cells from the Kupffer's vesicle of an *aei-/-* mutant embryo that was co-injected with *foxj1a* and GFP mRNA showing rescued motile cilia judged by the increased ciliary length. Alfa-acetylated tubulin labels cilia in red, DAPI labels DNA in blue and GFP labels injected cells in green.

V.6. Short cilia generate a weak fluid flow inside the KV

To evaluate the impact that the shorter cilia of *aei-/-* mutants might have on the fluid flow inside the KV, we measured the velocity of the flow in these mutants and compared it to wt embryos. For this, we filmed KVs of live embryos and tracked naturally occurring particles that move with the fluid flow. (Fig. 5.5A,A',B,B' and Supplementary Videos 1 and 2). This non-invasive method safeguards the epithelium and natural osmotic pressure inside the KV. We showed that in *aei-/-* mutants, velocity of the fluid flow is less than half than that of its wt siblings (Fig. 5.5C; 6.74 µm/s and 16.46 µm/s, respectively; $P<1.5x10-4$). Importantly, directionality of the flow is only lost in *aei-/-* mutants (Fig. 5.5B-B', Supplementary Video 2). Loss of directional-

ity could be due to a perturbation in the normal distribution of cilia inside the KV. However, a detailed 3D reconstruction of the spatial distribution of cilia in the KV of *aei-/-* mutants revealed no significant differences when compared to wt embryos (Fig. 5.5D). We thus conclude that the reduced cilia length documented here constitute the most probable cause for the slow and chaotic fluid flow observed in *aei-/-* mutants.

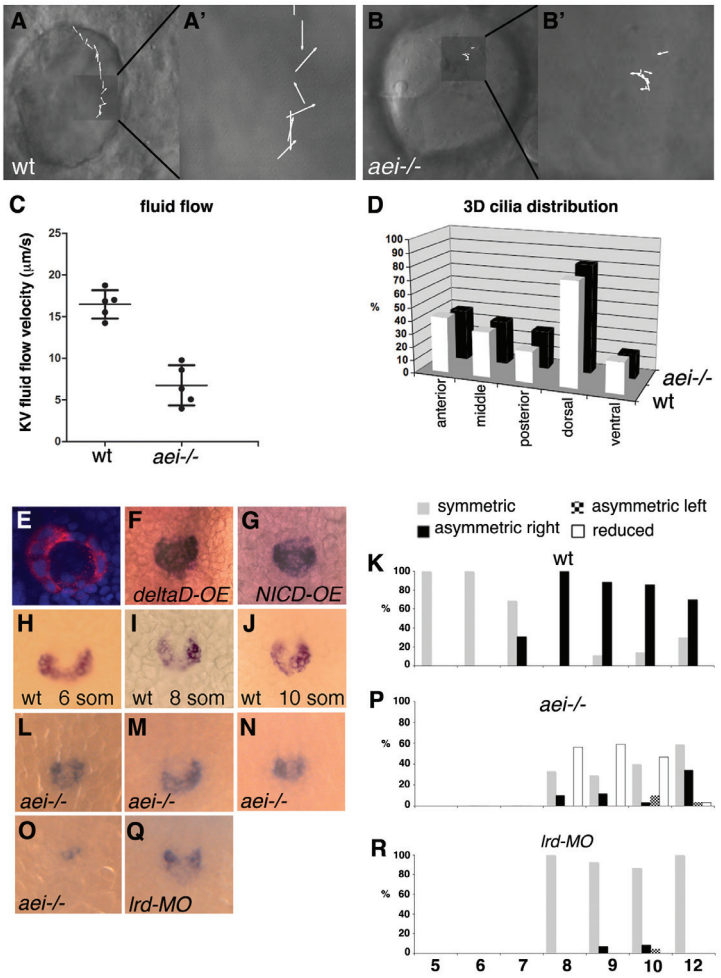

Figure 5.5. Short cilia reduce fluid flow inside the Kupffer´s vesicle and compromise *charon* asymmetric expression. (**A-B**) Still images from wt siblings (**A**) and ***aei-/-*** mutant embryos (**B**) taken from Supplementary Videos 1 and 2,

respectively. Inserts **A'** and **B'** show vectors representing the fluid flow velocity and direction in each experimental situation. (**C**) Quantification of the average fluid flow velocity in wt (n=5, 16.46 ±1.69 μm/s) and in *aei-/-* mutants (n=5, 6.74± 2.41 μm/s). (**D**) Percentage of cilia in different regions of the Kupffer´s vesicle (anterior, middle, posterior, dorsal and ventral) in wt (n=19) and *aei-/-* mutant embryos (n=14). (**E**) A 10-somite stage embryo showing nuclei in blue stained with DAPI and *charon* mRNA cytoplasmic localization in the epithelial cells that surround the Kupffer´s vesicle lumen. (**F, G**) Expression pattern of *charon* in the Kupffer´s vesicle of an embryo overexpressing *deltaD* (**F**) and other overexpressing *NICD* (**G**). (**H-J**) *charon* expression at the Kupffer´s vesicle is symmetric at the 6-somite stage (**H**) and is asymmetric at the 8 and 10-somite stage (**I, J**). (**K**) Percentage of symmetric *versus* asymmetric *charon* expression in the Kupffer´s vesicle in wt embryos from 5 to 12-somite stages (n=18 for each stage). (**L-O**) Range of expression patterns of *charon* in the Kupffer´s vesicle of *aei-/-* mutant embryos; *charon* expression may be symmetric (**L**), asymmetric with stronger expression on the right (**M**), asymmetric with stronger expression on the left (**N**) and reduced (**O**). (**P**) Percentages of the different *charon* expression patterns in the Kupffer´s vesicle in *aei-/-* mutant embryos from 8 to 12-somite stages. (**Q**) *charon* expression pattern in the Kupffer´s vesicle of one representative *lrd1* morphant. (**R**) Percentage of symmetric *versus* asymmetric *charon* expression in the Kupffer´s vesicle of *lrd1* morphants from 8 to 12-somite stages.

V.7. A strong KV fluid flow promotes asymmetric *charon* expression

Charon is a Cerberus/Dan family secreted factor expressed specifically in the cells that line the posterior domain of the KV in a horseshoe shape (Fig. 5.5E). This protein negatively regulates Nodal signalling by blocking the transfer of Spaw from the KV to the right side of the LPM in zebrafish and medaka (Hashimoto et al., 2004; Hojo et al., 2007). In addition, it has been suggested that *charon* might be a potential Notch signalling target in zebrafish (Gourronc et al., 2007). We confirmed this possibility by injecting *deltaD* or *NICD* mRNA into 1 cell stage wt embryos which resulted in clear ectopic expression of *charon* in the KV region (Fig. 5.5F,G). In contrast, the expression of *charon* in *aei-/-* mutants was severely reduced in 35.4% of the embryos from 8-12 somite stage (Fig. 5.5O,P) while in *bea-/-* mutants it was unaffected. Together, these data confirmed that *charon* is a target of the Notch signalling pathway in zebrafish.

In contrast to what has been described (Hashimoto et al., 2004), we found that *charon* expression in a wt zebrafish KV is initially symmetric from 5 to 7-somite stage and then becomes clearly asymmetric on the right side from 8-somite stage onwards (Fig. 5.5H-K). It is still unclear if the switch to higher levels on the right side corresponds to a downregulation of *charon* levels on the left side or to an upregulation on the right side of the KV. Our results identify *charon* as the first asymmetric gene expressed in the zebrafish KV and provide a better explanation for the mechanism underlying the asymmetric inhibition of Spaw transfer to the right LPM.

Since we show that *charon* expression becomes asymmetric after being symmetrically induced (Fig. 5.5H-K), we asked whether fluid flow in the KV could be the mechanism controlling this switch, as suggested in medaka and in *Xenopus* (Hojo et al., 2007). In contrast to wt embryos where there is a clear shift from symmetric to an asymmetric *charon* expression at the 8-somite stage (Fig. 5.5K), in the *aei-/-* mutants this shift does not occur (Fig. 5.5P). In fact, in *aei-/-* mutant embryos where the expression of *charon* was not severely reduced, we could score it as being symmetric in 43.3% and asymmetric in only 21.3% from 8-12 somite stages (Fig. 5.5L-P). This suggests that the slower fluid flow in *aei-/-* mutants characterized above is inefficient to promote the asymmetry switch of *charon* expression in KV cells.

Having shown that DeltaD regulates *charon* transcription (Fig. 5.5L-P), we could hypothesize that the inability to shift to an asymmetric *charon* expression observed in *aei-/-* mutants may be caused by a transcriptional defect and not by the slow flow. To investigate the impact of KV fluid flow on *charon* expression in a transcription competent context, we repeated the experiment in *left-right dynein1* (*lrd1*) morphants. These morphants have a very reduced or absent flow (Essner et al., 2005) and show no problems in *charon* transcription (Gourronc et al., 2007). We injected *lrd1-MO* into wt embryos and scored *charon* expression in 8-12 somite stage embryos. We observed that in *lrd1* morphants the asymmetric shift in *charon* expression does not occur (Fig. 5.5R), strengthening the idea that the fluid flow inside the KV is crucial to originate asymmetric *charon* expression. Our results, together with

those obtained in other species, clearly show that *charon* transcription is sensitive to fluid flow. Therefore, we suggest that *charon* and its homologues may be candidates for flow sensing genes in the KV/GRP/node environment.

Discussion

The involvement of Notch signalling in the establishment of the LR axis is evolutionary conserved among vertebrates. However, there are differences in the mode of action of this molecular signalling pathway between mammals and fish. In the mouse, the analysis of Notch pathway mutants reveals that *nodal* induction in the murine node is impaired (Krebs et al., 2003; Przemeck et al., 2003; Raya et al., 2003; Takeuchi et al., 2007), while the expression of the secreted Nodal antagonist *cerl2* does not seem to be affected (Krebs et al., 2003; Przemeck et al., 2003; Raya et al., 2003; Takeuchi et al., 2007). In contrast, the expression of *spaw* is normal in zebrafish embryos treated with DAPT (a Notch signalling inhibitor) but the expression of the secreted Nodal antagonist *charon* is severely affected in the KV (Gourronc et al., 2007). Using a genetic approach, we were able to confirm and extend these pharmacological results to conclude that the relevant Notch ligand for *charon* transcription in zebrafish is DeltaD. Therefore, Notch signalling in these two organisms targets the transcription of different genes: *nodal* in the mouse and *charon* in the zebrafish.

In the mouse node, the symmetric expression of *nodal,* induced by Notch signalling, and that of *cerl2,* induced by an unknown mechanism, later becomes asymmetric. *nodal* levels become higher on the left side while *cerl2* levels are higher on the right side of the node (Marques et al., 2004). In contrast to what happens in the mouse, there was no evidence for an asymmetric *spaw* or *charon* expression in the zebrafish KV. In our study, we discovered a sharp transition from a symmetric to an asymmetric expression of *charon* at 8-somite stage in the KV, with higher levels of expression on the right side. This finding strengthens the evolutionary conserved feature of *charon* expression since this gene,

and its homologues, are asymmetrically expressed on the right side in medaka KV (Hojo et al., 2007), *Xenopus* GRP (Schweickert et al., 2010) and mouse node (Marques et al., 2004). The mechanism that triggers the left bias of *nodal* expression in the murine node and the right bias of *charon* and *coco* expression on the right side in fish KV and *Xenopus* GRP remains poorly understood.

There is increasing evidence in these organisms that the extracellular fluid flow generated by motile cilia present in the node/KV/GRP is essential to establish the LR asymmetries in the LPM. Therefore, this directional fluid flow is a good candidate to trigger the initial asymmetric expression at the node/KV/GRP (Hamada, 2008). We discovered that in *aei-/-* mutants, the switch in *charon* expression does not occur possibly as a consequence of the slower fluid flow generated by the short motile cilia. In agreement with the possibility that the dynamics of the fluid flow promote a switch in gene expression in the node/KV/GRP are the phenotypes described for the *axonemal dynein* morphants in fish and *Xenopus* and the mouse mutants *iv* and *inv*. In medaka and as shown here in zebrafish embryos, the right bias in *charon* expression is no longer detected when fluid flow is abolished by the knockdown of *lrd1* (Hojo et al., 2007; Fig. 5.5Q,R). In *Xenopus*, *coco* is no longer downregulated on the left side of the GRP in the absence of flow (Schweickert et al., 2010). In the *iv* mouse mutant, where cilia are immotile and no nodal flow is produced, the expression of *nodal* in the node gets randomized. In addition, in the *inv* mouse mutant, where the flow is slow and turbulent, the expression of *nodal* is mostly symmetric in the node (Lowe et al., 1996; Okada et al., 1999; Oki et al., 2009).

Although no asymmetric *charon* expression had been detected before in zebrafish, asymmetric Charon function was suggested to be responsible for inhibiting the transference of Spaw from the KV domain to the right LPM (Hashimoto et al 2004). However, it should be emphasized that in wt embryos *charon* is also expressed on the left side of the KV and still *spaw* can be transferred to the left LPM. This suggests that it is not the absence of *charon* transcripts that allow Spaw transfer to the left LPM but the relative levels of *charon* expression between left and right sides. Thus, we reason

that Spaw is transferred to the left LPM because the levels of *charon* transcripts are lower on the left side of the KV in a wt embryo.

Applying the same reasoning to the *aei-/-* mutants, we propose that the severely reduced *charon* expression observed in 35.4% of the embryos (Fig. 5.5O,P) could correspond to: 1) no differences in the relative levels of *charon* and therefore *spaw* is bilateraly transferred to the LPM as observed in 20% of *aei-/-* embryos (Fig. 5.1A); or 2) undetected small differences in *charon* expression that lead to a weak bilateral situation described as left-sided expression of *spaw* with competition on the right side as observed in 15% of *aei-/-* embryos (Fig. 5.1A). In 43.3% of *aei-/-* mutants, *charon* expression is largely symmetric as visualized by *in situ* hybridization (Fig. 5.5L,P). In this situation, we cannot rule out that a biased difference between the left and the right side of *charon* transcripts in *aei-/-* mutants is still present since most embryos express left-sided *spaw* in the LPM (Fig. 5.1A). A clear asymmetric *charon* expression pattern on the right side of the KV (Fig. 5.5M) was observed in 18.3% of *aei-/-* embryos resulting on left *spaw* expression in the LPM (Fig. 5.1A). A few embryos (3%) expressed stronger *charon* on the left side of the KV (Fig. 5.5N), matching the equivalent percentage of right-sided *spaw* in the LPM (Fig. 5.1A).

In summary, we showed that shorter cilia present in *aei-/-* mutants produce a slower fluid flow that leads to abnormal LR *charon* levels at the KV compromising the maintenance of *spaw* expression in the posterior domain of the left LPM. We show that in the same embryos where we observed a premature downregulation of *spaw*, we also see a reduced *lefty1* expression in the posterior midline domain. We thus propose that this gap in *lefty1* expression contributes, together with abnormal posterior *pitx2* expression, to the gut laterality defects without affecting heart laterality. This phenotype is clinically relevant since there are reports on human patients with Primary Ciliary Dyskinesia that develop *situs inversus abdominalis* with no heart laterality defects (Fliegauf et al., 2007).

To our knowledge, Notch signalling is the first pathway that can both increase or decrease ciliary length, upon upregulation or downregulation,

respectively. In contrast, FGF signalling has only been involved in shortening cilia length, (Hong and Dawid, 2009; Yamauchi et al., 2009). Our experiments identify *foxj1a*, the master motile ciliogenic transcription factor (Yu et al., 2008) as being downstream of DeltaD because it successfully rescued cilia length in *aei-/-* mutants in a cell autonomous manner. These observations are perhaps indicating that the motile cilia programme controlled by *foxj1a*, involves not only the transcription of motility genes such as *dnah9* and *wdr78* (Yu et al., 2008) but may also transcribe genes important for cilia growth yet to be discovered.

A systematic analysis of the experimental conditions where short and long cilia are generated by modulating the Notch activity will provide a framework to determine relevant ciliary length control genes. This will certainly bring new insights into how cilia/flagella length is regulated and may provide ways to increase ciliary length that could ultimately be used to treat ciliopathies often characterized by short cilia (Wemmer and Marshall, 2007).

CHAPTER VI

Discussion

VI.1. Left and Right sides combine symmetry with asymmetry

Vertebrate development shows an overall external symmetric anatomy associated with the formation of bilaterally symmetric bones and muscles, which derive from the somites. At the same time, there is a lack of an internal plane of symmetry with internal organs acquiring an asymmetric disposition. This complex internal arrangement is specified from an initial symmetry breaking event that induces a signaling cascade of left side specific gene expression responsible for ensuring the correct asymmetric organ packing, extremely important for their correct connections and therefore function. Despite presenting a conserved organization within a population, some individuals may have a partial or complete mirror image reversion of the internal organs position that result from congenital anomalies (Brend and Holley, 2009 B).

VI.1.1. Protection of somite formation from asymmetric signals to assure symmetry

Embryonic development is very dynamic with several pathways being established at the same time to regulate different processes. To acquire a symmetric body structure, somites need to be bilaterally symmetric between the left and right sides of the axis, with one pair of somites being formed from the anterior region of the PSM at the same time. In fact, while somites are being formed, the LR asymmetry pathway is also being establishment in nearby tissues. We could expect that it would be enough for somites to be formed in a symmetric way, and not be influence by asymmetric signals, if the PSM did not express the receptors required to interpret these asymmetric signals. The problem comes with the fact that pathways that regulate bilaterally symmetric somite patterning and the ones that instruct LR asymmetry share some molecular players, such as members of the Notch, Fgf and RA pathways. Thus, it is extremely important to block the effect of asymmetric signals on somite formation so that symmetric body features may be correctly established (Brend and Holley, 2009 B).

VI.1.1.1. Conserved role of Retinoic Acid

RA signalling is required to pattern the AP axis but it is also necessary to synchronize bilateral symmetric somite formation. While normally arising as paired structures, in the absence of RA they are asymmetrically formed due to a delayed PSM segmentation on one side of the axis. Despite conserved in several vertebrates, this delay is bias to the right side in mouse and zebrafish, and bias to the left side in chick embryos. This perturbed somite formation correlates with a desynchronization of the segmentation clock oscillations and desynchronization of the regression of the determination front (Kawakami et al., 2005; Vermot et al., 2005; Vermot and Pourquié, 2005). Nevertheless, asymmetric somite formation in chick is not coupled with a misposition of the determination front, since *fgf8* expression is not anteriorly shifted in the left side of the PSM (Vermot and Pourquié, 2005). This lateralization phenotype is only seen during a specific developmental time window that correlates with the transfer of asymmetric information to the left side of the axis and is in fact associated with the LR pathway. Reverting the LR situs in *raldh2* mouse mutants, using double mutants for *raldh2* and *iv* (*raldh2*$^{-/-}$ *iv*$^{-/-}$), leads to a situs alteration and additionally to a randomization of the somite defects between both sides of the axis. This indicates that somite formation is influenced by the LR signalling machinery and that RA is probably compensating for its asymmetric influence in the PSM and this way regulates symmetric somitogenesis (Vermot and Pourquie 2005). Given this, symmetry is not a default state and in fact it needs to be tightly regulated.

The implication of RA in the regulation of symmetric somite formation has recently been more carefully analyzed during mouse embryonic development. It was demonstrated, using a (RARE)-LacZ-reporter transgene, that the levels of RA signaling are actually higher on the right anterior PSM and that it is positively regulated by a complex consisting of Nr2f2a and Rere (Vilhais-Neto et al., 2010). Similarly to *raldh2* mutants, mice mutants for *rere* present a lack of LR synchronization of the cyclic genes, which become posteriorly localized in the right PSM. In addition, these mutants lack syn-

chronized regression of the determination front. While *rere* is ubiquitously expressed in the PSM, *nr2f2a* presents an asymmetric expression in the PSM. Consistent with the fact that absence of RA signaling induces somite defects in the right side of the axis in mouse and on the left side in chick, *nr2f2*a expression in mouse is in fact asymmetric on the right side of the PSM while in chick it is asymmetric on the left (Vilhais-Neto et al., 2010). This inversion of expression patterns and defects in mouse and chick may also be linked with the fact that Fgf8 is a left determinant in the mouse, where it is necessary to induce the Nodal signalling in the left side, while in the chick it is a right determinant, repressing Nodal signalling in the right side (Meyers and Martin, 1999). In addition, it has been shown that in mouse RA is necessary to antagonize *fgf8* expression in the node ectoderm where it becomes expressed in the absence of RA. This excess of Fgf8 in the node ectoderm further increases its own levels in the adjacent PSM shifting it more anteriorly in the right side and leading to somite asymmetries (Sirbu and Duester, 2006). These results suggest that in mouse RA regulates Fgf8 expression in two domains, in the node ectoderm where it regulates Fgf8 levels in the right PSM and also directly in the anterior PSM where RA is actually asymmetrically expressed in the right side (Sirbu and Duester, 2006; Vilhais-Neto et al., 2010). In chick, RA does not seem to be necessary to regulate Fgf8 in the PSM but it may be regulating its expression at the level of the Hensen's node, where Fgf8 is asymmetrically expressed in the right side (Meyers and Martin, 1999; Vermot and Pourquié, 2005).

VI.1.1.2. Notch signalling inputs in establishing asymmetry and symmetry

In addition to Fgf8 having opposite roles in chick and mouse, other differences may explain the fact that the asymmetric somite formation phenotype is different from mouse and zebrafish to chick. In chick, an extracellular calcium accumulation in the left side of the Hensen's node is responsible for inducing an asymmetric Notch activation on the left side of the node, where Notch is required to regulate *nodal* asymmetric expression (Raya et

al., 2004). As a consequence of this asymmetric activation, the fifth wave of *lfng* cyclic expression becomes asymmetric on the left side when reaching the node, before the first somite is formed. However, since no phenotype is seen at the level of the somites, some kind of compensatory mechanisms must exist (Raya et al., 2004).

Notch as also been shown to be required to regulate asymmetric *nodal* transcription at the level of the mouse node however, contrary to what happens in mouse and chick, in zebrafish Notch is necessary to regulate the expression of *charon*, a *nodal* inhibitor (Krebs et al., 2003; Raya et al., 2003; Raya et al., 2004; Takeuchi et al., 2007; Gourronc et al., 2007). In Chapter V, we were able to confirm that Notch is necessary for *charon* expression and we show that DeltaD is in fact the key ligand necessary for this regulation. Through DeltaD, Notch signaling regulates the correct cilia length being the first signalling pathway able to either decrease or increase their size when downregulated or upregulated, respectively. Cilia size regulation, through DeltaD, is then necessary to generate a strong leftward flow required to trigger an asymmetric expression of *charon* in the KV, which is stronger on the right side. Despite being present in both side of the KV, and so far described as being symmetrically expressed, we show that it's this difference in *charon* expression levels that allows it to inhibit *spaw* transfer to the right LPM and still allow its transference to the left side (Chapter V). Just like in medaka and *Xenopus*, we have shown that fluid flow dynamics in zebrafish promotes a switch in the *nodal* antagonist gene expression (Hojo et al., 2007; Schweickert et al., 2010). With several ciliopathies being linked with problems regarding cilia length control, finding that Notch signalling is able to modulate this regulation is of great importance. It will not only allow recovering cilia size in conditions where they are shorter but it will also contribute for the search of other genes that regulate cilia length.

Additionally, Notch as also been shown to be required to maintain symmetry during somite formation interacting with the RA signalling. In zebrafish, in the absence of the Notch signalling component *su(h)*, there is an

unbiased asymmetric somite formation and the levels of *cyp26a1* in the tail bud region are no longer maintained. This indicates that Notch is required to regulate RA levels in the tail bud and consequently bilateral symmetric somite formation (Echeverri and Oates, 2007). Nevertheless, this phenotype does not seem to follow an earlier perturbation of Notch in the LR pathway. It has been shown that when blocking Notch during epiboly stages not only the LR pathway is affected but somites also start to be formed in an unbiased bilaterally asymmetric way. Despite this result, when perturbing the transfer of information from the node to the left LPM, only the LR signalling pathway is affected and somite formation is able to proceed in a symmetric way. This indicates that there must be two non-overlapping periods where Notch is required for somite formation and LR asymmetry pathway (Kawakami et al., 2005).

VI.2. Symmetry vs. asymmetry – the role of Dmrt2

The work described in chapter II, III and IV is focused in the characterization of Dmrt2, a transcription factor that belongs to the Dmrt family which is mainly associated with sex differentiation. We had previously described that, during zebrafish development, Dmrt2a/Terra has a completely different role from the rest of the family. It is required for the regulation of two developmental processes, maintaining symmetry and at the same time the proper LR asymmetry pathway (Saúde et al., 2005). After Dmrt2a/Terra knockdown/overexpression the oscillations of the segmentation clock became desynchronized between both sides of the PSM and there is also a misposition of the determination front, *fgf8* becomes more anteriorly displaced and *raldh2* becomes more posteriorly displaced in the PSM region. In either of the cases there is no bias to either the left or right side of the axis. As a consequence, there is a lack of coordination during somite formation and an extra somite is formed either on the left or right side. Despite the fact that both Dmrt2a/Terra and RA are regulating bilateral symmetric somite formation, they do not seem to be acting together. In

the context of Dmrt2a/Terra absence/overexpression the levels of *raldh2*/*cyp26a1* are not affected and in *raldh2* morphants the levels of *dmrt2a*/*terra* expression are not disturbed, suggesting that they are working in different pathways (data not shown, performed in S. Wilson Lab). Also, while RA somite desynchronization phenotype is biased to one of the sides of the axis, Dmrt2a/Terra phenotype leads to an unbiased asymmetric somite formation. In fact, while RA is only necessary to counteract the LR asymmetry pathway, Dmrt2a/Terra is necessary to regulate the pathway itself by ensuring that left side gene expression is restricted to the left LPM and heart and viscera LR normal displacement (Kawakami et al., 2005; Vermot et al., 2005; Vermot and Pourquié, 2005; Saúde et al., 2005). These results seem to indicate that Dmrt2a/Terra is not required for the regulation of the RA metabolism nevertheless, we may think that it may be interacting with other components of the RA signalling pathway. Additionally, it may also be interacting with Su(H) through a pathway that does not involve the regulation of RA and this way coordinate embryo laterality at the level of somite formation.

VI.2.1. How does Dmrt2 regulates two opposite processes?

Dmrt family members present a wide variation not only in the number of genes but also in their expression pattern (Hong et al., 2007). Recently it was described a second *dmrt2* gene in the zebrafish genome acquired due to a fish-specific genome duplication event (Zhou et al., 2008). This gene is called *dmrt2b* and is functionally divergent from *dmrt2a*/*terra* regarding its role during somite formation. Instead of being necessary for symmetric somite formation, it is in fact involved in the regulation of somite differentiation at the level of slow muscle development through the regulation of the Hedgehog pathway (Liu et al., 2009). While the role in regulating the LR asymmetry pathway seems to be conserved, with both being necessary for the correct transfer of *spaw* to the left LPM and correct internal organ disposition, evidences suggest that they are not regulating the pathway in the same way (Saúde et al., 2005; Liu et al., 2009). In fact, despite sharing

an expression pattern in the anterior region of the PSM and somites, we showed that *dmrt2a/terra* is also expressed in the KV from where *dmrtb* is in fact absent (Chapter II). We suspect that Dmrt2a/Terra is acting at the level of the KV to regulate both pathways and that its expression in the anterior PSM region and somites is probably involved in somites differentiation. If this is true, it may help to understand why *dmrt2b* is not necessary for symmetry somite formation and only somite differentiation. To explain the fact that *dmrt2b* is involved in the regulation of the LR asymmetry pathway despite being absent from the KV, we argue that it is regulating the Hedgehog signaling at the level of the midline, whose integrity is necessary for the correct establishment of the LR asymmetry pathway.

Another strong argument to support the idea that Dmrt2a/Terra in zebrafish is regulating symmetric and asymmetric features in the KV comes from studies in mouse. In the mouse, Dmrt2 is involved in somite differentiation being necessary for rib and vertebrae formation (Seo et al., 2006). We have shown that it is not necessary for somite bilateral symmetric formation or LR asymmetry pathway establishment. In fact, *dmrt2*$^{-/-}$ mutants presented no phenotype resembling the one obtained in zebrafish Dmrt2a/Terra morphants (Chapter II). This, and the fact that mouse *dmrt2* is present in the anterior region of the PSM and somites but absent from the node region, favors the idea that Dmrt2 presence at the level of the somites is responsible for somite differentiation. Concomitantly, it suggests that it is the presence of Dmrt2a/Terra in the zebrafish KV that is responsible for regulating symmetry and asymmetry. Nevertheless, a role for zebrafish Dmrt2a/Terra at the level of somite differentiation needs to be addressed and its role at the level of the KV further analyzed. In addition, data from chick may also sustain our hypothesis. It has been shown that Notch is asymmetrically expressed in the left side of the Hensen's node, which implies that prospective PSM cells on the left side of the node activate the segmentation clock earlier than those on the right side (Raya et al., 2004). The segmentation clock is a Notch based mechanism that starts

even before the formation of the first somite and, in fact, it has been shown that an asymmetric *lfng* expression is seen at the node prior to somite formation. This would then lead to asymmetric cyclic gene expression on the PSM and desynchronized somite formation, which in fact is not observed (Raya et al., 2004). Soon after Notch asymmetric expression, *dmrt2* also becomes asymmetrically expressed in the left side of the chick Hensen's node (Saúde et al., 2005). These results suggest that *dmrt2* in the chick Hensen's node may ensure that somites form in a symmetric way, by compensating this initial Notch asymmetric expression. At the same time, resembling what may be happening in zebrafish, it could also be promoting the correct transfer of asymmetric information to the left side of the LPM. Nevertheless these are only hypothesis and further studies should be conducted in chick embryos.

Analyzes of Dmrt genes in other species, such as *Drosophila*, *C. elegans* and mouse, have shown that they can act has activators, repressors or can even be bifunctional (Coschigano and Wensink 1993; Murphy et al., 2010). Since it is not known how Dmrt2a/Terra is regulating symmetric somite formation and the LR asymmetry pathway, a ChIP-on-chip assay would definitely shade light on this question allowing us to discover its direct target genes. Nevertheless, to perform this assay it is fundamental to have a Dmrt2a/Terra specific antibody, which we were not able to get (Chapter III). As an alternative approach we aimed to perform a microarray and thus compare gene expression levels in the context of absence of Dmrt2a/Terra (by MO injection) and also in the context of its overexpression. To be able to induce Dmrt2a/Terra expression in a time controlled manner, we constructed a zebrafish inducible transgenic line where the gene is under the control of a heat-shock promoter (Chapter IV). The ability to induce gene expression in a specific developmental time window, only when Dmrt2a/Terra starts to be expressed, will allow the search for its direct target genes and this way improve our knowledge on how Dmrt2a/Terra regulates zebrafish embryonic development.

VI.3. Evolutionary origins of asymmetry

Evolutionary LR patterning mechanisms seem to predate vertebrate's origin, being already present in the latest common ancestor of all Bilaterians, which includes Protostomes (the first opening becomes the mouth) and Deuterostomes (the first opening becomes the anus and the second the mouth). In fact, animals belonging to diverse phylum, such as Chordata (vertebrates and closely related invertebrates with a notochord and a neural tube), Arthropod (invertebrates with an exoskeleton, segmented body and jointed appendages) and Mollusca (large phylum of invertebrates that have a mantle that covers the visceral mass and in some cases creates a shell), despite being bilaterally symmetric they also exhibit LR asymmetries at the level of specific structures and organs (Swalla and Smith 2008; Okumura et al., 2008). The role of asymmetric Nodal signaling in patterning the LR axis is well described in Deuterostomes, with most information coming from the studies of vertebrates (Raya and Belmonte, 2008). Nevertheless, studies of non-vertebrate deuterostomes such as the amphioxus, ascidians and sea-urchins have also shed some light on the conservation of Nodal signalling in the LR specification (Yu et al., 2002; Morokuma et al., 2002; Duboc et al., 2005). Despite the fact that its role remains less explored in the non-deuterostomes phylum, it was recently suggested that it did not evolved in a Deuterostome lineage ancestor since Nodal orthologues were found to be asymmetrical expressed in snails, molluscs that belong to a Protostome lineage. In snails, Nodal pathway is required to regulate shell coiling chirality, being asymmetrically expressed in the left side in species presenting a sinistral shell coiling and on the right side in dextral species (Grande and Patel, 2009). The conservation of Nodal signalling in maintaining LR asymmetry in these different phyla, from invertebrates to vertebrates, indicates that part of the genetics involved in LR asymmetry is conserved throughout the Bilaterians and suggests that the Nodal signalling is ancestral to Bilateria.

VI.3.1. Initial breaking of symmetry

Independently of the fact that Nodal signalling is conserved in several species, it does not seem to be the initial mechanism responsible for breaking bilateral symmetry and lateralizing animal bodies. Given this, it is necessary to ask what first determines asymmetry. In some species laterality seems to be set up during the first embryonic cleavage stages. In *Drosophila* and *Xenopus* an organized biased actin cytoskeletal in the cortex of the egg has been shown to be required for the correct LR development (Danilchik et al., 2006; Taniguchi et al., 2007). This suggests that extracellular matrix participates in the correct egg rotation during the first cleavages and is consequently responsible for the LR polarization of an otherwise symmetric embryo. Additionally, it also suggests a common mechanism of polarity establishment between invertebrates and vertebrates. In other species, such as snails, it has also been shown that during the first cells cleavages the blastomere orientation dictates the body and shell chirality (Kuroda et al., 2009). Nevertheless, in zebrafish the earliest mechanism that seems to be required to establish asymmetry consists in ion-channel driven gradients that have been detected at stages preceding gastrulation (Adams et al., 2006). In chick, asymmetry seems to be generated by an asymmetric cells rearrangement that induces a leftward movement of cells around the node (Gros et al., 2009; Cui et al., 2009). Despite these findings in all these species, the first trait of asymmetry during mouse development seems to be imposed much later in development when cilia present in the node create a unidirectional fluid flow that is responsible for inducing asymmetric gene expression (Nonaka et al., 1998; Okada et al., 1999). In other vertebrates, cilia within the organizers seem to be necessary only to amplify an already established asymmetry. The idea that maternal genes involved in cellular cytoskeletal dynamics constitute the mechanism responsible for setting up asymmetry still needs to be addressed in several species so, until then, the question if it is a conserved mechanism in all Bilateria still remains an open question.

VI.4. Evolutionary origins of segmentation

Perturbation of both symmetric somite formation and LR asymmetric patterning during development, gives rise to severe skeletal and laterality disorders. Thus, a tightly regulation of symmetry and asymmetry must be established early in development and must occur to ensure the correct body patterning. Curiously, somites first arise in Cephalochordates, suggesting that their appearance took place in a body plan that already presented LR asymmetric cues. Also of notice is the way that somite formation precedes in the amphioxus, considered to be the ancestor of vertebrates. In fact, it has no unsegmented PSM vertebrate-like zone and somites arise directly from the tail bud, giving rise only to the axial muscle (Schubert et al., 2001). In addition, while the first somites arise as bilateral pairs, the ones from the left side gradually shift anteriorly. In a late phase of somitogenesis they display an asymmetric formation since somites alternately bud off from the left and right sides of the tail bud, with left side somites being the first to be formed (Schubert et al., 2001). Interestingly, the amphioxus *nodal* gene is initially symmetrically expressed in the paraxial mesoderm at gastrula stages and later, at neurula stages, when the left side somites begin to shift anteriorly it becomes asymmetrically expressed in the left side at the LPM (formed as extensions from the paraxial mesoderm). These results seem to indicate that the LR patterning may be involved in the regulation of an asymmetric somite formation (Yu et al., 2002). Despite the fact that amphioxus do not require a buffering mechanism to prevent an asymmetric somite formation, vertebrates on the other hand, require a buffering mechanism to counteract asymmetric signals that may affect symmetric somite formation. This may be due to the fact that in vertebrates, somites give rise not only to the axial muscles but also to the axial skeleton.

References

Adams, D. S., Robinson, K. R., Fukumoto, T., Yuan, S., Albertson, R. C., Yelick, P., Kuo, L., McSweeney, M. and Levin, M. (2006). Early, H+-V-ATPase-dependent proton flux is necessary for consistent left-right patterning of non-mammalian vertebrates. *Development* **133(9)**, 1657-71.

Afzelius, B. A. (1976). A human syndrome caused by immotile cilia. *Science* **193(4250)**, 317-9.

Afzelius, B. A. (1985). The immotile-cilia syndrome: a microtubule-associated defect. *CRC Crit. Rev. Biochem.* **19(1)**, 63-87.

Albertson, R. C. and Yelick, P. C. (2005). Roles for fgf8 signaling in left-right patterning of the visceral organs and craniofacial skeleton. *Dev. Biol.* **283(2)**, 310-21.

Amack, J. D., Wang, X. and Yost, H. J. (2007). Two T-box genes play independent and cooperative roles to regulate morphogenesis of ciliated Kupffer's vesicle in zebrafish. *Developmental Biology* **310,** 196-210.

Amack, J. D. and Yost, H. J. (2004). The T box transcription factor no tail in ciliated cells controls zebrafish left-right asymmetry. *Curr. Biol*. **14(8)**, 685-90.

Amsterdam, A. and Becker, T. S. (2005). Transgenes as screening tools to probe and manipulate the zebrafish genome. *Dev. Dyn*. **234(2)**, 255-68.

Andrade R.P., Palmeirim, I. and Bajanca, F. (2007). Molecular clocks underlying vertebrate embryo segmentation: a 10-year-old hairy-go-round. *Birth Defects Res. C Embryo Today* **81(2)**, 65-83.

Antic, D., Stubbs, J. L., Suyama, K., Kintner, C., Scott, M. P. and Axelrod, J. D. (2010). Planar cell polarity enables posterior localization of nodal cilia and left-right axis determination during mouse and Xenopus embryogenesis. *PLoS One* **5(2)**, e8999.

Aulehla, A. and Pourquié, O. (2008). Oscillating signaling pathways during embryonic development. *Curr. Opin. Cell Biol.* **20(6)**, 632-7.

Aulehla, A., Wehrle, C., Brand-Saberi, B., Kemler, R., Gossler, A., Kanzler, B. and Herrmann, B. G. (2003). Wnt3a plays a major role in the segmentation clock controlling somitogenesis. *Dev. Cell* **4(3)**, 395-406.

Aulehla, A., Wiegraebe, W., Baubet, V., Wahl, M. B., Deng, C., Taketo, M., Lewandoski, M. and Pourquié, O. (2008). A beta-catenin gradient links the clock and wavefront systems in mouse embryo segmentation. *Nat. Cell Biol.* **10(2)**, 186-93.

Barth, K. A., Miklosi, A., Watkins, J., Bianco, I. H., Wilson, S. W. and Andrew, R. J. (2005). fsi zebrafish show concordant reversal of laterality of viscera, neuroanatomy, and a subset of behavioral responses. *Curr. Biol.* **15(9)**, 844-50.

Basu, B. and Brueckner, M. (2008). Cilia multifunctional organelles at the center of vertebrate left-right asymmetry. *Curr. Top. Dev. Biol.* **85**, 151-74.

Bessho, Y., Hirata, H., Masamizu, Y. and Kageyama, R. (2003). Periodic repression by the bHLH factor Hes7 is an essential mechanism for the somite segmentation clock. *Genes. Dev.* **17(12)**, 1451-6.

Bessho, Y., Sakata, R., Komatsu, S., Shiota, K., Yamada, S. and Kageyama R. (2001). Dynamic expression and essential functions of Hes7 in somite segmentation. *Genes Dev.* **15(20)**, 2642-7.

Bisgrove, B., Snarr, B., Emrazian, A. and Yost, H. (2005). Polaris and Polycystin-2 in dorsal forerunner cells and Kupffer's vesicle are required for specification of the zebrafish left–right axis. *Developmental Biology* **15**, 274-88.

Blais, A. and Dynlacht, B. D. (2005). Constructing transcriptional regulatory networks. *Genes Dev*. **19(13)**, 1499-511.

Boettger, T., Wittler, L. and Kessel, M. (1999). FGF8 functions in the specification of the right body side of the chick. *Curr. Biol.* **9(5)**, 277-80.

Borovina, A., Superina, S., Voskas, D. and Ciruna, B. (2010). Vangl2 directs the posterior tilting and asymmetric localization of motile primary cilia. *Nat. Cell Biol.* **12(4)**, 407-12.

Bowers, P. N., Brueckner, M. and Yost, H. J. (1996). The genetics of left-right development and heterotaxia. *Semin. Perinatol.* **20(6)**, 577-88.

Brend, T. and Holley, S. A. (2009). Expression of the oscillating gene her1 is directly regulated by Hairy/Enhancer of Split, T-box, and Suppressor of Hairless proteins in the zebrafish segmentation clock. *Dev. Dyn.* **238(11)**, 2745-59. **A**

Brend, T. and Holley, S. A. (2009). Balancing segmentation and laterality during vertebrate development. *Semin. Cell Dev. Biol.* **20**, 472–478. **B**

Brent, A. E. and Tabin, C. J. (2002). Developmental regulation of somite derivatives: muscle, cartilage and tendon. *Curr. Opin. Genet. Dev.* **12(5)**, 548-57.

Buchberger, A., Seidl, K., Klein, C., Eberhardt, H. and Arnold, H. H. (1998). cMeso-1, a novel bHLH transcription factor, is involved in somite formation in chicken embryos. *Dev. Biol.* **199(2)**, 201-15.

Bulman, M. P., Kusumi, K., Frayling, T. M., McKeown, C., Garrett, C., Lander, E. S., Krumlauf, R., Hattersley, A. T., Ellard, S. and Turnpenny, P. D. (2000). Mutations in the human delta homologue, DLL3, cause axial skeletal defects in spondylocostal dysostosis. *Nat. Genet.* **24(4)**, 438-41.

Burtis, K. C. and Baker, B. S. (1989). Drosophila doublesex gene controls somatic sexual differentiation by producing alternatively spliced mRNAs encoding related sex-specific polypeptides. *Cell* **56(6)**, 997-1010.

Chin, A. J., Tsang, M. and Weinberg, E. S. (2000). Heart and gut chiralities are controlled independently from initial heart position in the developing zebrafish. *Dev. Biol.* **227,** 403-21.

Collignon, J., Varlet, I. and Robertson, E. J. (1996). Relationship between asymmetric nodal expression and the direction of embryonic turning. *Nature* **381(6578)**, 155-8.

Concha, M. L., Burdine, R. D., Russell, C., Schier, A. F. and Wilson, S. W. (2000). A nodal signaling pathway regulates the laterality of neuroanatomical asymmetries in the zebrafish forebrain. *Neuron.* **28(2)**, 399-409.

Concha, M. L., Russell, C., Regan, J. C.,Tawk, M., Sidi, S., Gilmour, D. T., Kapsimali, M., Sumoy, L., Goldstone, K., Amaya, E., Kimelman, D., Nicolson, T., Gründer, S., Gomperts, M., Clarke, J. D. and Wilson, S. W. (2003). Local tissue interactions across the dorsal midline of the forebrain establish CNS laterality. *Neuron* **39(3)**, 423-38.

Concha, M. L. and Wilson, S. W. (2001). Asymmetry in the epithalamus of vertebrates. *J. Anat.* **199**, 63-84.

Conlon, R. A., Reaume, A. G. and Rossant, J. (1995). Notch1 is required for the coordinate segmentation of somites. *Development* **121(5)**, 1533-45.

Cooke, J. and Zeeman, E. C. (1976). A clock and wavefront model for control of the number of repeated structures during animal morphogenesis. *J. Theor. Biol.* **58(2)**, 455-76.

Coschigano, K. T. and Wensink, P. C. (1993). Sex-specific transcriptional regulation by the male and female doublesex proteins of Drosophila. *Genes Dev*. **7(1)**, 42-54.

Cui, C., Little, C. D. and Rongish, B. J. (2009). Rotation of organizer tissue contributes to left-right asymmetry. *Anat. Rec.* **292(4)**, 557-61.

Dale, J. K., Maroto, M., Dequeant, M. L., Malapert, P., McGrew, M. and Pourquie, O. (2003). Periodic notch inhibition by lunatic fringe underlies the chick segmentation clock. *Nature* **421(6920)**, 275-8.

Danilchik, M. V., Brown, E. E. and Riegert, K. (2006). Intrinsic chiral properties of the Xenopus egg cortex: an early indicator of left-right asymmetry? *Development* **133(22)**, 4517-26.

Davidson, E. H., McClay, D. R. and Hood, L. (2003). Regulatory gene networks and the properties of the developmental process. *Proc Natl Acad Sci USA* **100(4)**, 1475-80.

Debrus, S., Sauer, U., Gilgenkrantz, S., Jost, W., Jesberger, H. J. and Bouvagnet, P. (1997). Autosomal recessive lateralization and midline defects: blastogenesis recessive 1. *Am. J. Med. Genet.* **68(4)**, 401-4.

Delfini, M. C., Dubrulle, J., Malapert, P., Chal, J. and Pourquié, O. (2005). Control of the segmentation process by graded MAPK/ERK activation in the chick embryo. *Proc. Natl. Acad. Sci. USA* **102(32)**, 11343-8.

Dequéant, M. L., Glynn, E., Gaudenz, K., Wahl, M., Chen, J., Mushegian, A. and Pourquié, O. (2006). A complex oscillating network of signaling genes underlies the mouse segmentation clock. *Science* **314(5805)**, 1595-8.

Dequéant, M. L. and Pourquié, O. (2008). Segmental patterning of the vertebrate embryonic axis. *Nat. Rev. Genet.* **9**, 370-382.

Diez del Corral, R., Olivera-Martinez, I., Goriely, A., Gale, E., Maden, M. and Storey, K. (2003). Opposing FGF and retinoid pathways

control ventral neural pattern, neuronal differentiation, and segmentation during body axis extension. *Neuron*. **40(1)**, 65-79.

Dobbs-McAuliffe, B., Zhao, Q. and Linney, E. (2004). Feedback mechanisms regulate retinoic acid production and degradation in the zebrafish embryo. *Mech. Dev*. **121(4)**, 339-50.

Duboc, V., Röttinger, E., Lapraz, F., Besnardeau, L. and Lepage, T. (2005). Left-right asymmetry in the sea urchin embryo is regulated by nodal signaling on the right side. *Dev. Cell* **9(1)**, 147-58.

Dubrulle, J., McGrew, M. J. and Pourquié, O. (2001). FGF signaling controls somite boundary position and regulates segmentation clock control of spatiotemporal Hox gene activation. *Cell* **106(2)**, 219-32.

Dubrulle, J. and Pourquié, O. (2004). fgf8 mRNA decay establishes a gradient that couples axial elongation to patterning in the vertebrate embryo. *Nature* **427(6973)**, 419-22.

Durai, S., Mani, M., Kandavelou, K., Wu, J., Porteus, M. H. and Chandrasegaran, S. (2005). Zinc finger nucleases: custom-designed molecular scissors for genome engineering of plant and mammalian cells. *Nucleic Acids Res*. **33(18)**, 5978-90.

Durbin, L., Sordino, P., Barrios, A., Gering, M., Thisse, C., Thisse, B., Brennan, C., Green, A., Wilson, S. and Holder, N. (2000). Anteroposterior patterning is required within segments for somite boundary formation in developing zebrafish. *Development* **127(8)**, 1703-13.

Echeverri, K. and Oates, A. C. (2007). Coordination of symmetric cyclic gene expression during somitogenesis by Suppressor of Hairless involves regulation of retinoic acid catabolism. *Dev. Biol.* **301(2)**, 388-403.

Essner, J. J., Amack, J. D., Nyholm, M. K., Harris, E. B. and Yost, H. J. (2005). Kupffer's vesicle is a ciliated organ of asymmetry in the zebrafish embryo that initiates left-right development of the brain, heart and gut. *Development* **132(6)**, 1247-60.

Feller, J., Schneider, A., Schuster-Gossler, K. and Gossler, A. (2008). Noncyclic Notch activity in the presomitic mesoderm demonstrates uncoupling of somite compartmentalization and boundary formation. *Genes Dev.* **15;22(16)**, 2166-71.

Ferjentsik, Z., Hayashi, S., Dale, J. K., Bessho, Y., Herreman, A., De Strooper, B., del Monte, G., de la Pompa, J. L. and Maroto, M. (2009). Notch is a critical component of the mouse somitogenesis oscillator and is essential for the formation of the somites. *PLoS Genet.* **5(9)**, e1000662.

Fior, R. and Henrique, D. (2009). "Notch-Off": a perspective on the termination of Notch signalling. *Int. J. Dev. Biol.* **53(8-10)**, 1379-84.

Fliegauf, M., Benzing, T. and Omran, H. (2007). When cilia go bad: cilia defects and ciliopathies. *Nat. Rev. Mol. Cell Biol.* **8(11)**, 880-93.

Force, A., Lynch, M., Pickett, F. B., Amores, A., Yan, Y. L. and Postlethwait J. (1999). Preservation of duplicate genes by complementary, degenerative mutations. *Genetics* **151(4)**, 1531-45.

Forsberg, H., Crozet, F. and Brown, N. A. (1998). Waves of mouse Lunatic fringe expression, in four-hour cycles at two-hour intervals, precede somite boundary formation. *Curr. Biol.* **8(18)**, 1027-30.

Fukumoto, T., Blakely, R. and Levin, M. (2005). Serotonin transporter function is an early step in left-right patterning in chick and frog embryos. *Dev. Neurosci.* **27(6)**, 349-63.

Fukumoto, T., Kema, I. P. and Levin, M. (2005). Serotonin signaling is a very early step in patterning of the left–right axis in chick and frog embryos. *Curr. Biol.* **15**, 794–803.

Gaio, U., Schweickert, A., Fischer, A., Garratt, A. N., Müller, T., Ozcelik, C., Lankes, W., Strehle, M., Britsch, S., Blum, M. and Birchmeier, C. (1999). A role of the cryptic gene in the correct establishment of the left-right axis. *Curr. Biol.* **9(22)**, 1339-42.

Gardner, R. L. (2010). Normal bias in the direction of fetal rotation depends on blastomere composition during early cleavage in the mouse. *PLoS One* **5(3)**, e9610.

Georges-Labouesse, E. N., George, E. L., Rayburn, H. and Hynes, R. O. (1996). Mesodermal development in mouse embryos mutant for fibronectin. *Dev. Dyn.* **207(2)**, 145-56.

Gerdes, J. M., Davis, E. E. and Katsanis, N. (2009). The vertebrate primary cilium in development, homeostasis, and disease. *Cell* **137**, 32-45.

Giudicelli, F., Ozbudak, E. M., Wright, G. J. and Lewis, J. (2007). Setting the tempo in development: an investigation of the zebrafish somite clock mechanism. *PLoS Biol.* **5(6)**, e150.

Goldbeter, A. and Pourquié, O. (2008). Modeling the segmentation clock as a network of coupled oscillations in the Notch, Wnt and FGF signaling pathways. *J. Theor. Biol.* **252(3)**, 574-85.

Gourronc, F., Ahmad, N., Nedza, N., Eggleston, T. and Rebagliati, M. (2007). Nodal activity around Kupffer's vesicle depends on the T-box transcription factors Notail and Spadetail and on Notch signaling. *Dev. Dyn.* **236(8)**, 2131-46.

Grande, C. and Patel, N. H. (2009). Nodal signalling is involved in left-right asymmetry in snails. *Nature* **457(7232)**, 1007-11.

Gritsman, K., Zhang, J., Cheng, S., Heckscher, E., Talbot, W. S. and Schier, A. F. (1999). The EGF-CFC protein one-eyed pinhead is essential for nodal signaling. *Cell* **97(1)**, 121-32.

Gros, J., Feistel, K., Viebahn, C., Blum, M. and Tabin, C. J. (2009). Cell movements at Hensen's node establish left/right asymmetric gene expression in the chick. *Science* **324(5929)**, 941-4.

Gruneberg, H. (1961). Genetical studies on the skeleton of the mouse: XXIX. PUDGY. *Genet. Res.* **2**, 384–393.

Grunwald, D. J. and Eisen, J. S. (2002). Headwaters of the zebrafish -- emergence of a new model vertebrate. *Nat. Rev. Genet.* **3(9)**, 717-24.

Hamada, H. (2008). Breakthroughs and future challenges in left-right patterning. *Dev. Growth Differ.* **Suppl 1**, S71-8.

Hamada, H., Meno, C., Watanabe, D. and Saijoh, Y. (2002). Establishment of vertebrate left-right asymmetry. *Nat. Rev. Genet.* **3**, 103-13.

Hashimoto, M. and Hamada, H. (2010). Translation of anterior-posterior polarity into left-right polarity in the mouse embryo. *Curr. Opin. Genet. Dev.* **20(4)**, 433-7.

Hashimoto, H., Rebagliati, M., Ahmad, N., Muraoka, O., Kurokawa, T., Hibi, M. and Suzuki, T. (2004). The Cerberus/Dan-family protein Charon is a negative regulator of Nodal signaling during left-right patterning in zebrafish. *Development* **131**, 1741-53.

Hatler, J. M., Essner, J. J. and Johnson, R. G. (2009). A gap junction connexin is required in the vertebrate left-right organizer. *Dev. Biol.* **336(2)**, 183-91.

Havis, E., Anselme, I. and Schneider-Maunoury, S. (2006). Whole embryo chromatin immunoprecipitation protocol for the in vivo study of zebrafish development. *Biotechniques* **40(1)**, 34, 36, 38.

Heasman, J. (2002). Morpholino oligos: making sense of antisense? *Dev. Biol*. **243(2)**, 209-14.

Herpin, A., Braasch, I., Kraeussling, M., Schmidt, C., Thoma, E. C., Nakamura, S., Tanaka, M. and Schartl, M. (2010). Transcriptional rewiring of the sex determining dmrt1 gene duplicate by transposable elements. *PLoS Genet*. **6(2)**, e1000844.

Hirata, H., Bessho, Y., Kokubu, H., Masamizu, Y., Yamada, S., Lewis, J. and Kageyama, R. (2004). Instability of Hes7 protein is crucial for the somite segmentation clock. *Nat. Genet.* **36(7)**, 750-4.

Hirata, H., Yoshiura, S., Ohtsuka, T., Bessho, Y., Harada, T., Yoshikawa, K. and Kageyama, R. (2002). Oscillatory expression of the bHLH factor Hes1 regulated by a negative feedback loop. *Science* **298(5594)**, 840-3.

Hojo, M., Takashima, S., Kobayashi, D., Sumeragi, A., Shimada, A., Tsukahara, T., Yokoi, H., Narita, T., Jindo, T., Kage, T., Kitagawa, T., Kimura, T., Sekimizu, K., Miyake, A., Setiamarga, D., Murakami, R., Tsuda, S., Ooki, S., Kakihara, K., Naruse, K. and Takeda, H. (2007). Right-elevated expression of charon is regulated by fluid flow in medaka Kupffer's vesicle. *Dev. Growth Differ.* **49(5)**, 395-405.

Holley, S. A., Geisler, R. and Nüsslein-Volhard, C. (2000). Control of her1 expression during zebrafish somitogenesis by a delta-dependent oscillator and an independent wave-front activity. *Genes Dev*. **14(13)**, 1678-90.

Holley, S. A., Jülich, D., Rauch, G.J., Geisler, R. and Nüsslein-Volhard, C. (2002). her1 and the notch pathway function within the oscillator mechanism that regulates zebrafish somitogenesis. *Development* **129(5)**, 1175-83.

Hong, S. K. and Dawid, I. B. (2009). FGF-dependent left-right asymmetry patterning in zebrafish is mediated by Ier2 and Fibp1. *Proc. Natl. Acad. Sci. USA* **106**, 2230-5.

Hong, C. S., Park, B. Y. and Saint-Jeannet, J. P. (2007) The function of Dmrt genes in

vertebrate development: it is not just about sex. *Dev. Biol.* **310(1)**, 1-9.

Horikawa, K., Ishimatsu, K., Yoshimoto, E., Kondo, S. and Takeda, H. (2006). Noise-resistant and synchronized oscillation of the segmentation clock. *Nature* **441(7094)**,719-23.

Hsiao, C. D., You, M. S., Guh, Y. J., Ma, M., Jiang, Y. J. and Hwang, P. P. (2007). A positive regulatory loop between foxi3a and foxi3b is essential for specification and differentiation of zebrafish epidermal ionocytes. *PLoS One* **2**, e302.

Huang, R., Zhi, Q., Patel, K., Wilting, J. and Christ, B. (2000). Contribution of single somites to the skeleton and muscles of the occipital and cervical regions in avian embryos. *Anat. Embryol.* **202(5)**, 375-83.

Huppert, S. S., Ilagan, M. X., De Strooper, B. and Kopan, R. (2005). Analysis of Notch function in presomitic mesoderm suggests a gamma-secretase-independent role for presenilins in somite differentiation. *Dev.Cell.* **8(5)**, 677-88.

Isaac, A., Sargent, M. G. and Cooke, J. (1997). Control of vertebrate left-right asymmetry by a snail-related zinc finger gene. *Science* **275(5304)**, 1301-4.

Jiang, Y. J., Aerne, B. L., Smithers, L., Haddon, C., Ish-Horowicz, D. and Lewis, J. (2000). Notch signalling and the synchronization of the somite segmentation clock. *Nature* **408(6811)**, 475-9.

Johnson, J., Rhee, J., Parsons, S. M., Brown, D., Olson, E. N. and Rawls, A. (2001). The anterior/posterior polarity of somites is disrupted in paraxis-deficient mice. *Dev. Biol.* **229(1)**, 176-87.

Jülich, D., Hwee Lim, C., Round, J., Nicolaije, C., Schroeder, J., Davies, A., Geisler, R., Lewis, J., Jiang, Y. J. and Holley, S. A. (2005). beamter/deltaC and the role of Notch ligands in the zebrafish somite segmentation, hindbrain neurogenesis and hypochord differentiation. *Dev. Biol.* **286(2)**, 391-404.

Kageyama, R., Ohtsuka, T. and Kobayashi, T. (2007). The Hes gene family: repressors and oscillators that orchestrate embryogenesis. *Development* **134(7)**, 1243-51.

Kalcheim, C. and Ben-Yair, R. (2005). Cell rearrangements during development of the somite and its derivatives. *Curr. Opin. Genet. Dev.* **15(4)**, 371-80.

Kanzler, B., Kuschert, S.J., Liu, Y. H. and Mallo, M. (1998) Hoxa-2 restricts the chondrogenic domain and inhibits bone formation during development of the branchial area. *Development* **125**, 2587–2597.

Kartagener, M. and Stucki, P. (1962). Bronchiectasis with situs inversus. *Arch. Pediatr.* **79**, 193-207.

Kawakami, Y., Raya, A., Raya, R. M., Rodríguez-Esteban, C. and Belmonte, J. C. (2005). Retinoic acid signalling links left-right asymmetric patterning and bilaterally symmetric somitogenesis in the zebrafish embryo. *Nature* **435(7039)**, 165-71.

Kawakami, K., Shima, A. and Kawakami, N. (2000). Identification of a functional

transposase of the Tol2 element, an Ac-like element from the Japanese medaka fish, and its transposition in the zebrafish germ lineage. *Proc. Natl. Acad. Sci. USA* **97(21)**, 11403-8.

Kennedy, D. N., O'Craven, K. M., Ticho, B. S., Goldstein, A. M., Makris, N. and Henson, J. W. (1999). Structural and functional brain asymmetries in human situs inversus totalis. *Neurology*. **53(6)**, 1260-5.

Kim, S. H., Jen, W. C., De Robertis, E. M. and Kintner, C. (2000). The protocadherin PAPC establishes segmental boundaries during somitogenesis in xenopus embryos. *Curr. Biol.* **10(14)**, 821-30.

Kim, S., Kettlewell, J. R., Anderson, R. C., Bardwell, V. J. and Zarkower, D. (2003) Sexually dimorphic expression of multiple doublesex-related genes in the embryonic mouse gonad. *Gene Expr. Patterns* **3(1)**, 77-82.

Kimmel, C. B. (1989). Genetics and early development of zebrafish. *Trends Genet*. **5(8)**, 283-8.

Kimmel, C. B., Ballard, W. W., Kimmel, S. R., Ullmann, B. and Schilling, T. F. (1995) Stages of embryonic development of the zebrafish. *Dev. Dyn.* **203**, 253-310.

Kramer-Zucker, A., Olale, F., Haycraft, C., Yoder, B., Schier, A. and Drummond, I. (2005). Cilia-driven fluid flow in the zebrafish pronephros, brain and Kupffer's vesicle is required for normal organogenesis. *Development* **132**, 1907-1921.

Krebs, L. T., Iwai, N., Nonaka, S., Welsh, I. C., Lan, Y., Jiang, R., Saijoh, Y., O'Brien, T. P., Hamada, H. and Gridley, T. (2003). Notch signaling regulates left-right asymmetry determination by inducing Nodal expression. *Genes Dev.* **17(10)**, 1207-12.

Kreiborg, S., Barr, M. Jr. and Cohen, M. M. Jr. (1992). Cervical spine in the Apert syndrome. *Am. J. Med. Genet.* **43(4)**, 704-8.

Kreiling, J. A., Prabhat, Williams, G. and Creton, R. (2007). Analysis of Kupffer's vesicle in zebrafish embryos using a cave automated virtual environment. *Dev. Dyn*. **236(7)**, 1963-9.

Kuroda, R., Endo, B., Abe, M. and Shimizu, M. (2009). Chiral blastomere arrangement dictates zygotic left-right asymmetry pathway in snails. *Nature* **462(7274)**, 790-4.

Kwan, K. M., Fujimoto, E., Grabher, C., Mangum, B. D., Hardy, M. E., Campbell, D. S., Parant, J. M., Yost, H. J., Kanki, J. P. and Chien, C. B. (2007). The Tol2kit: a multisite gateway-based construction kit for Tol2 transposon transgenesis constructs. *Dev. Dyn*. **236(11)**, 3088-99.

Latimer, A. J. and Appel, B. (2006). Notch signaling regulates midline cell specification and proliferation in zebrafish. *Dev. Biol.* **298**, 392-402.

Levin, M. and Mercola, M. (1998). Gap junctions are involved in the early generation of left-right asymmetry. *Dev. Biol.* **203(1)**, 90-105.

Levin, M. and Palmer, A. R. (2007). Left-right patterning from the inside out: widespread evidence for intracellular control. *Bioessays* **29**, 271-87.

Levin, M., Thorlin, T., Robinson, K. R., Nogi, T. and Mercola, M. (2002). Asymmetries in H+/K+-ATPase and cell membrane potentials comprise a very early step in left-right patterning. *Cell* **111(1)**, 77-89.

Lewis, J. (2003). Autoinhibition with transcriptional delay: a simple mechanism for the zebrafish somitogenesis oscillator. *Curr. Biol.* **13(16)**, 1398-408.

Liang, J. O., Etheridge, A., Hantsoo, L., Rubinstein, A. L., Nowak, S. J., Izpisúa Belmonte, J. C. and Halpern, M. E. (2000). Asymmetric nodal signaling in the zebrafish diencephalon positions the pineal organ. *Development* **127(23)**, 5101-12.

Lin, X. and Xu, X. (2009). Distinct functions of Wnt/beta-catenin signaling in KV development and cardiac asymmetry. *Development* **136**, 207-17.

Liu S, Li Z and Gui JF (2009). Fish-specific duplicated dmrt2b contributes to a divergent function through Hedgehog pathway and maintains left-right asymmetry establishment function. *PLoS One* **4(9)**, e7261.

Long, S., Ahmad, N. and Rebagliati, M. (2003). The zebrafish nodal-related gene southpaw is required for visceral and diencephalic left-right asymmetry. *Development* **130(11)**, 2303-16.

Lopes, S. S., Lourenço, R., Pacheco, L., Moreno, N., Kreiling, J. and Saúde, L. (2010). Notch signalling regulates left-right asymmetry through ciliary length control. *Development* **137(21)**, 3625-32.

Lourenço, R., Lopes, S. S. and Saúde, L. (2010). Left-Right Function of dmrt2 Genes Is Not Conserved between Zebrafish and Mouse. *PLoS One* **5(12)**, e14438.

Lourenço, R. and Saúde, L. (2010). Symmetry OUT, Asymmetry IN. *Symmetry* **2**, 1033-1054.

Lowe, L. A., Supp, D. M., Sampath, K., Yokoyama, T., Wright, C. V., Potter, S. S., Overbeek, P. and Kuehn, M. R. (1996). Conserved left-right asymmetry of nodal expression and alterations in murine situs inversus. *Nature* **381(6578)**,158-61.

Lurie, I. W., Kappetein, A. P., Loffredo, C. A. and Ferencz, C. (1995). Non-cardiac malformations in individuals with outflow tract defects of the heart: the Baltimore-Washington Infant Study (1981-1989). *Am. J. Med. Genet.* **59(1)**, 76-84.

Magnani, E., Bartling, L. and Hake, S. (2006). From Gateway to MultiSite Gateway in one recombination event. *BMC Mol. Biol*. **7**, 46.

Männer, J. (2001). Does an equivalent of the "ventral node" exist in chick embryos? A scanning electron microscopic study. *Anat. Embryol.* **203(6)**, 481-90.

Mara, A., Schroeder, J., Chalouni, C. and Holley, S. A. (2007). Priming, initiation and synchronization of the segmentation clock by deltaD and deltaC. *Nat. Cell Biol.* **9(5)**, 523-30.

Maroto, M., Dale, J. K., Dequéant, M. L., Petit, A. C. and Pourquié, O. (2005). Synchronised cycling gene oscillations in presomitic mesoderm cells require cell-cell contact. *Int. J. Dev. Biol.* **49(2-3)**, 309-15.

Marques, S., Borges, A. C., Silva, A. C., Freitas, S., Cordenonsi, M. and Belo, J. A. (2004). The activity of the Nodal antagonist Cerl-2 in the mouse node is required for correct L/R body axis. *Genes Dev.* **18**, 2342-7.

Masamizu, Y., Ohtsuka, T., Takashima, Y., Nagahara, H., Takenaka, Y., Yoshikawa, K., Okamura, H. and Kageyama, R. (2006). Real-time imaging of the somite segmentation clock: revelation of unstable oscillators in the individual presomitic mesoderm cells. *Proc. Natl. Acad. Sci. USA* **103(5)**, 1313-8.

McDaniell, R., Warthen, D. M., Sanchez-Lara, P. A., Pai, A., Krantz, I. D., Piccoli, D. A. and Spinner, N. B. (2006). NOTCH2 mutations cause Alagille syndrome, a heterogeneous disorder of the notch signaling pathway. *Am. J. Hum. Genet.* **79(1)**, 169-73.

McGrath, J. and Brueckner, M. (2003). Cilia are at the heart of vertebrate left-right asymmetry. *Curr. Opin. Genet. Dev.* **13(4)**, 385-92.

McGrath, J., Somlo, S., Makova, S., Tian, X. and Brueckner, M. (2003). Two populations of node monocilia initiate left-right asymmetry in the mouse. *Cell* **114(1)**, 61-73.

McManus, I. C., Martin, N., Stubbings, G. F., Chung, E. M. and Mitchison, H. M. (2004). Handedness and situs inversus in primary ciliary dyskinesia. *Proc. Biol. Sci.* **271(1557)**, 2579-82.

Meng, A., Moore, B., Tang, H., Yuan, B. and Lin, S. (1999) A Drosophila doublesex-related gene, terra, is involved in somitogenesis in vertebrates. *Development* **126(6)**, 1259-68.

Meyers, E. N. and Martin, G. R. (1999). Differences in left-right axis pathways in mouse and chick: functions of FGF8 and SHH. *Science* **285(5426)**, 403-6.

Minowada, G., Jarvis, L. A., Chi, C. L., Neubüser, A., Sun, X. et al. (1999) Vertebrate Sprouty genes are induced by FGF signaling and can cause chondrodysplasia when overexpressed. *Development* **126(20)**, 4465-75

Mockler, T. C., Chan, S., Sundaresan, A., Chen, H., Jacobsen, S. E. and Ecker, J. R. (2005). Applications of DNA tiling arrays for whole-genome analysis. *Genomics* **85(1)**, 1-15.

Monteiro, R., van Dinther, M., Bakkers, J., Wilkinson, R., Patient, R., ten Dijke, P. and Mummery, C. (2008). Two novel type II receptors mediate BMP signalling and are required to establish left-right asymmetry in zebrafish. *Dev. Biol.* **315**, 55-71.

Morales, A. V., Acloque, H., Ocaña, O. H., de Frutos, C. A., Gold, V. and Nieto, M. A. (2007). Snail genes at the crossroads of symmetric and asymmetric processes in the developing mesoderm. *EMBO Rep.* **8(1)**, 104-9.

Moreno, T. A. and Kintner, C. (2004). Regulation of segmental patterning by retinoic acid signaling during Xenopus somitogenesis. *Dev. Cell* **6(2)**, 205-18.

Morokuma, J., Ueno, M., Kawanishi, H., Saiga, H. and Nishida, H. (2002). HrNodal, the ascidian nodal-related gene, is expressed in the left side of the epidermis, and lies upstream of HrPitx. *Dev. Genes Evol.* **212(9)**, 439-46.

Murphy, M. W., Sarver, A. L., Rice, D., Hatzi, K., Ye, K., Melnick, A., Heckert, L. L., Zarkower, D. and Bardwell, V. J. (2010). Genome-wide analysis of DNA binding and transcriptional regulation by the mammalian Doublesex homolog DMRT1 in the juvenile testis. *Proc. Natl. Acad. Sci. USA* **107(30)**, 13360-5.

Murphy, M. W., Zarkower, D. and Bardwell, V. J. (2007). Vertebrate DM domain proteins bind similar DNA sequences and can heterodimerize on DNA. *BMC Mol. Biol*. **8**, 58.

Nakaya, M. A., Biris, K., Tsukiyama, T., Jaime, S., Rawls, J. A. and Yamaguchi, T. P. (2005). Wnt3a links left-right determination with segmentation and anteroposterior axis elongation. *Development* **132(24)**, 5425-36.

Neugebauer, J. M., Amack, J. D., Peterson, A. G., Bisgrove, B. W. and Yost, H. J. (2009). FGF signalling during embryo development regulates cilia length in diverse epithelia. *Nature* **458**, 651-4.

Niederreither, K. and Dollé, P. (2008). Retinoic acid in development: towards an integrated view. *Nat. Rev. Genet.* **9(7)**, 541-53.

Nonaka, S., Shiratori, H., Saijoh, Y. and Hamada, H. (2002). Determination of left-right patterning of the mouse embryo by artificial nodal flow. *Nature* **418(6893)**, 96-9.

Nonaka, S., Tanaka, Y., Okada, Y., Takeda, S., Harada, A., Kanai, Y., Kido, M. and Hirokawa, N. (1998). Randomization of left-right asymmetry due to loss of nodal cilia generating leftward flow of extraembryonic fluid in mice lacking KIF3B motor protein. *Cell* **95(6)**, 829-37.

Nonaka, S., Yoshiba, S., Watanabe, D., Ikeuchi, S., Goto, T., Marshall, W. F. and Hamada, H. (2005). De novo formation of left-right asymmetry by posterior tilt of nodal cilia. *PLoS Biol.* **3(8)**, e268.

Norris, D. P., Brennan, J., Bikoff, E. K. and Robertson, E. J. (2002). The Foxh1-dependent autoregulatory enhancer controls the level of Nodal signals in the mouse embryo. *Development* **129(14),** 3455-68.

Nugent, E. W., Plauth, W. H. and Edwards, J. E. (1994). The pathology, pathophysiology, recognition and treatment of congenital heart disease. McGraw-Hill, New York

Oates, A. C and Ho, R. K. (2002). Hairy/E(spl)-related (Her) genes are central components of the segmentation oscillator and display redundancy with the Delta/Notch signaling pathway in the formation of anterior segmental boundaries in the zebrafish. *Development* **129(12)**, 2929-46.

Okada, Y., Nonaka, S., Tanaka, Y., Saijoh, Y., Hamada, H. and Hirokawa, N. (1999). Abnormal nodal flow precedes situs inversus in iv and inv mice. *Mol. Cell* **4(4)**, 459-68.

Okada, Y., Takeda, S., Tanaka, Y., Belmonte, J. C. and Hirokawa, N. (2005). Mechanism of nodal flow: a conserved symmetry breaking event in left-right axis determination. *Cell* **121(4)**, 633-44.

Oki, S., Hashimoto, R., Okui, Y., Shen, M. M., Mekada, E., Otani, H., Saijoh, Y. and Hamada, H. (2007). Sulfated glycosaminoglycans are necessary for Nodal signal transmission from the node to the

left lateral plate in the mouse embryo. *Development* **134(21)**, 3893-904.

Oki, S., Kitajima, K., Marques, S., Belo, J. A., Yokoyama, T., Hamada, H. and Meno, C. (2009). Reversal of left-right asymmetry induced by aberrant Nodal signaling in the node of mouse embryos. *Development* **136**, 3917-25.

Okumura, T., Utsuno, H., Kuroda, J., Gittenberger, E., Asami, T. and Matsuno, K. (2008). The development and evolution of left-right asymmetry in invertebrates: lessons from Drosophila and snails. *Dev. Dyn*. **237(12)**, 3497-515.

Ottolenghi, C., Veitia, R., Barbieri, M., Fellous, M. and McElreavey K. (2000). The human doublesex-related gene, DMRT2, is homologous to a gene involved in somitogenesis and encodes a potential bicistronic transcript. *Genomics* **64(2)**, 179-86.

Ozbudak, E. M. and Lewis, J. (2008). Notch signalling synchronizes the zebrafish segmentation clock but is not needed to create somite boundaries. *PLoS Genet.* **4(2)**, e15.

Pagán-Westphal, S. M. and Tabin, C. J. (1998). The transfer of left-right positional information during chick embryogenesis. *Cell* **93(1)**, 25-35.

Palmeirim, I., Henrique, D., Ish-Horowicz, D. and Pourquie, O. (1997). Avian *hairy* gene expression identifies a molecular clock linked to vertebrate segmentation and somitogenesis. *Cell* **91**, 639–648.

Peeters, H. and Devriendt, K. (2006). Human laterality disorders. *Eur. J. Med. Genet*. **49(5)**, 349-62.

Przemeck, G. K., Heinzmann, U., Beckers, J. and Hrabé de Angelis, M. (2003). Node and midline defects are associated with left-right development in Delta1 mutant embryos. *Development* **130**, 3-13.

Ramsdell, A. F. (2005). Left-right asymmetry and congenital cardiac defects: getting to the heart of the matter in vertebrate left-right axis determination. *Dev. Biol.* **288(1)**, 1-20.

Raya, A. and Izpisúa Belmonte, J. C. (2008). Insights into the establishment of left-right asymmetries in vertebrates. *Birth Defects Res. C. Embryo Today* **84(2)**, 81-94.

Raya, A., Kawakami, Y., Rodriguez-Esteban, C., Buscher, D., Koth, C. M., Itoh, T., Morita, M., Raya, R. M., Dubova, I., Bessa, J. G., de la Pompa, J. L. and Izpisua Belmonte, J. C. (2003). Notch activity induces Nodal expression and mediates the establishment of left-right asymmetry in vertebrate embryos. *Genes Dev.* **17(10)**, 1213-8.

Raya, A., Kawakami, Y., Rodríguez-Esteban, C., Ibañes, M., Rasskin-Gutman, D., Rodríguez-León, J., Büscher, D., Feijó, J. A. and Izpisúa Belmonte, J. C. (2004). Notch activity acts as a sensor for extracellular calcium during vertebrate left-right determination. *Nature* **427(6970)**, 121-8.

Raymond, C. S., Shamu, C. E., Shen, M. M., Seifert, K. J., Hirsch, B., Hodgkin, J. and Zarkower D. (1998). Evidence for evolutionary conservation of sex-determining genes. *Nature* **391(6668)**, 691-5.

Reifers, F., Böhli, H., Walsh, E. C., Crossley, P. H., Stainier, D. Y. and Brand, M. (1998).

Fgf8 is mutated in zebrafish acerebellar (ace) mutants and is required for maintenance of midbrain-hindbrain boundary development and somitogenesis. *Development* **125(13)**, 2381-95.

Riedel-Kruse, I. H., Müller, C. and Oates, A. C. (2007). Synchrony dynamics during initiation, failure, and rescue of the segmentation clock. *Science* **317(5846)**, 1911-5.

Rifes, P., Carvalho, L., Lopes, C., Andrade, R. P., Rodrigues, G., Palmeirim, I. and Thorsteinsdóttir, S. (2007). Redefining the role of ectoderm in somitogenesis: a player in the formation of the fibronectin matrix of presomitic mesoderm. *Development* **134(17),** 3155-65.

Rodríguez-Esteban, C., Capdevila, J., Kawakami, Y. and Izpisúa Belmonte, J. C. (2001). Wnt signaling and PKA control Nodal expression and left-right determination in the chick embryo. *Development* **128(16)**, 3189-95.

Ross, J. M., Kalis, A. K., Murphy, M. W. and Zarkower, D. (2005). The DM domain protein MAB-3 promotes sex-specific neurogenesis in C. elegans by regulating bHLH proteins. *Dev. Cell* **8(6)**, 881-92.

Roussigné, M., Bianco, I. H., Wilson, S. W. and Blader, P. (2009). Nodal signalling imposes left-right asymmetry upon neurogenesis in the habenular nuclei. *Development* **136(9)**, 1549-57.

Saga, Y., Hata, N., Koseki, H. and Taketo, M. M. (1997). Mesp2: a novel mouse gene expressed in the presegmented mesoderm and essential for segmentation initiation. *Genes Dev.* **11(14)**, 1827-39.

Saijoh, Y., Adachi, H., Sakuma, R., Yeo, C. Y., Yashiro, K., Watanabe, M., Hashiguchi, H., Mochida, K., Ohishi, S., Kawabata, M., Miyazono, K., Whitman, M. and Hamada, H. (2000). Left-right asymmetric expression of lefty2 and nodal is induced by a signaling pathway that includes the transcription factor FAST2. *Mol. Cell* **5(1)**, 35-47.

Sarmah, B., Latimer, A. J., Appel, B. and Wente, S. R. (2005). Inositol polyphosphates regulate zebrafish left-right asymmetry. *Dev. Cell* **9(1)**, 133-45.

Saúde, L., Lourenço, R., Gonçalves, A. and Palmeirim, I. (2005). terra is a left-right asymmetry gene required for left-right synchronization of the segmentation clock. *Nat. Cell Biol.* **7(9)**, 918-20.

Sawada, A., Fritz, A., Jiang, Y. J., Yamamoto, A., Yamasu, K., Kuroiwa, A., Saga, Y.and Takeda, H. (2000). Zebrafish Mesp family genes, mesp-a and mesp-b are segmentally expressed in the presomitic mesoderm, and Mesp-b confers the anterior identity to the developing somites. *Development* **127(8)**, 1691-702.

Sawada, A., Shinya, M., Jiang, Y. J., Kawakami, A., Kuroiwa, A. and Takeda, H. (2001). Fgf/MAPK signalling is a crucial positional cue in somite boundary formation. *Development* **128(23)**, 4873-80.

Schena, M., Heller, R. A., Theriault, T. P., Konrad, K., Lachenmeier, E. and Davis, R. W. (1998). Microarrays: biotechnology's discovery platform for functional genomics. *Trends Biotechnol.* **16(7)**, 301-6.

Schilling, T. F., Concordet, J. P. and Ingham, P. W. (1999) Regulation of left-right asymmetries in the zebrafish by Shh and BMP4. *Dev. Biol.* **210(2)**, 277-87.

Schreiner, C. M., Scott, W. J. Jr., Supp, D. M. and Potter, S. S. (1993). Correlation of forelimb malformation asymmetries with visceral organ situs in the transgenic mouse insertional mutation, legless. *Dev. Biol.* **158(2)**, 560-2.

Schubert, M., Holland, L. Z., Stokes, M. D. and Holland, N. D. (2001). Three amphioxus Wnt genes (AmphiWnt3, AmphiWnt5, and AmphiWnt6) associated with the tail bud: the evolution of somitogenesis in chordates. *Dev. Biol*. **240(1)**, 262-73.

Schweickert, A., Vick, P., Getwan, M., Weber, T., Schneider, I., Eberhardt, M., Beyer, T., Pachur, A. and Blum, M. (2010). The Nodal Inhibitor Coco Is a Critical Target of Leftward Flow in Xenopus. *Curr Biol*.

Schweickert, A., Weber, T., Beyer, T., Vick, P., Bogusch, S., Feistel, K. and Blum, M. (2007). Cilia-driven leftward flow determines laterality in Xenopus. *Curr. Biol.* **17(1)**, 60-6.

Sefton, M., Sánchez, S. and Nieto, M. A. (1998). Conserved and divergent roles for members of the Snail family of transcription factors in the chick and mouse embryo. *Development* **125(16)**, 3111-21.

Seo, K. W., Wang, Y., Kokubo, H., Kettlewell, J. R., Zarkower, D. A. and Johnson, R. L. (2006). Targeted disruption of the DM domain containing transcription factor Dmrt2 reveals an essential role in somite patterning. *Dev. Biol.* **290(1)**, 200-10.

Shen, M. M. and Hodgkin, J. (1988). mab-3, a gene required for sex-specific yolk protein expression and a male-specific lineage in C. elegans. *Cell* **54(7)**, 1019-31.

Shen, M. M., Wang, H. and Leder, P. (1997). A differential display strategy identifies Cryptic, a novel EGF-related gene expressed in the axial and lateral mesoderm during mouse gastrulation. *Development* **124(2)**, 429-42.

Shu, X., Huang, J., Dong, Y., Choi, J., Langenbacher, A. and Chen, J. N. (2007). Na,K-ATPase alpha2 and Ncx4a regulate zebrafish left-right patterning. *Development* **134(10)**, 1921-30.

Sieger, D., Tautz, D. and Gajewski, M. (2003). The role of Suppressor of Hairless in Notch mediated signalling during zebrafish somitogenesis. *Mech. Dev.* **120(9)**,1083-94.

Singh, G., Supp, D. M., Schreiner, C., McNeish, J., Merker, H. J., Copeland, N. G., Jenkins, N. A., Potter, S. S. and Scott, W. (1991). legless insertional mutation: morphological, molecular, and genetic characterization. *Genes Dev.* **5(12A)**, 2245-55.

Sirbu, I. O. and Duester, G. (2006). Retinoic-acid signalling in node ectoderm and posterior neural plate directs left-right patterning of somitic mesoderm. *Nat. Cell Biol.* **8(3)**, 271-7.

Song, H., Hu, J., Chen, W., Elliott, G., Andre, P., Gao, B. and Yang, Y. (2010). Planar cell polarity breaks bilateral symmetry by controlling ciliary positioning. *Nature* **466(7304)**, 378-82.

Sternick, E. B., Márcio Gerken, L., Max, R. and Osvaldo Vrandecic, M. (2004). Radiofrequency catheter ablation of an accessory pathway in a patient with Wolff-Parkinson-White and Kartagener's syndrome. *Pacing Clin. Electrophysiol.* **27(3)**, 401-4.

Stubbs, J. L., Oishi, I., Izpisúa Belmonte, J. C. and Kintner, C. (2008). The forkhead protein Foxj1 specifies node-like cilia in Xenopus and zebrafish embryos. *Nat. Genet.* **40**, 1454-60.

Sulik, K., Dehart, D. B., Iangaki, T., Carson, J. L., Vrablic, T., Gesteland, K. and Schoenwolf, G. C. (1994). Morphogenesis of the murine node and notochordal plate. *Dev. Dyn.* **201(3)**, 260-78.

Supp, D. M., Brueckner, M., Kuehn, M. R., Witte, D. P., Lowe, L. A., McGrath, J., Corrales, J. and Potter, S. S. (1999). Targeted deletion of the ATP binding domain of left-right dynein confirms its role in specifying development of left-right asymmetries. *Development* **126**, 5495-504.

Supp, D. M., Witte, D. P., Potter, S. S. and Brueckner, M. (1997). Mutation of an axonemal dynein affects left-right asymmetry in inversus viscerum mice. *Nature* **389(6654)**, 963-6.

Swalla, B. J. and Smith, A. B. (2008). Deciphering deuterostome phylogeny: molecular, morphological and palaeontological perspectives. *Philos Trans. R. Soc. Lond. Biol. Sci*. **363(1496)**, 1557-68.

Swindell, E. C., Thaller, C., Sockanathan, S., Petkovich, M., Jessell, T. M. and Eichele, G. (1999). Complementary domains of retinoic acid production and degradation in the early chick embryo. *Dev. Biol.* **216(1)**, 282-96.

Tabin, C. J. (2006) The key to left-right asymmetry. *Cell* **127(1)**, 27-32.

Tabin, C. J. and Vogan, K. J. (2003). A two-cilia model for vertebrate left-right axis specification. *Genes Dev.* **17(1)**, 1-6.

Takeda, S., Yonekawa, Y., Tanaka, Y., Okada, Y., Nonaka, S. and Hirokawa, N. (1999). Left-right asymmetry and kinesin superfamily protein KIF3A: new insights in determination of laterality and mesoderm induction by kif3A-/- mice analysis. *J. Cell Biol.* **145(4)**, 825-36.

Takeuchi, J. K., Lickert, H., Bisgrove, B. W., Sun, X., Yamamoto, M., Chawengsaksophak, K., Hamada, H., Yost, H. J., Rossant, J. and Bruneau, B. G. (2007). Baf60c is a nuclear Notch signaling component required for the establishment of left-right asymmetry. *Proc. Natl. Acad. Sci. USA* **104(3)**, 846-51.

Takke, C. and Campos-Ortega, J. A. (1999). her1, a zebrafish pair-rule like gene, acts downstream of notch signalling to control somite development. *Development* **126**, 3005-14.

Takke, C., Dornseifer, P., v Weizsäcker, E. and Campos-Ortega, J. A. (1999). her4, a zebrafish homologue of the Drosophila neurogenic gene E(spl), is a target of NOTCH signalling. *Development* **126**, 1811-21.

Tanaka, S., Kanzaki, R., Yoshibayashi, M., Kamiya, T. and Sugishita, M. (1999). Dichotic listening in patients with situs

inversus: brain asymmetry and situs asymmetry. *Neuropsychologia* **37(7)**, 869-74.

Tanaka, Y., Okada, Y. and Hirokawa, N. (2005). FGF-induced vesicular release of Sonic hedgehog and retinoic acid in leftward nodal flow is critical for left-right determination. *Nature* **435(7039)**, 172-7.

Taniguchi, K., Hozumi, S., Maeda, R., Okumura, T. and Matsuno, K. (2007). Roles of type I myosins in Drosophila handedness. *Fly (Austin)* **1(5)**, 287-90.

Taylor, B. J. and Truman, J. W. (1992). Commitment of abdominal neuroblasts in Drosophila to a male or female fate is dependent on genes of the sex-determining hierarchy. *Development* **114(3)**, 625-42.

Terpe K. (2003). Overview of tag protein fusions: from molecular and biochemical fundamentals to commercial systems. *Appl. Microbiol. Biotechnol.* **60(5)**, 523-33

Thisse, C. and Thisse, B. (2008) High-resolution in situ hybridization to whole-mount zebrafish embryos. *Nat. Protoc.* **3**, 59-69.

Toga, A. W. and Thompson, P. M. (2003). Mapping brain asymmetry. *Nat. Rev. Neurosci.* **4(1)**, 37-48.

Ton, C., Stamatiou, D., Dzau, V. J. and Liew, C. C. (2002). Construction of a zebrafish cDNA microarray: gene expression profiling of the zebrafish during development. *Biochem. Biophys. Res. Commun*. **296(5)**, 1134-42.

Turnpenny, P. D., Kusumi, K., Sillence, D. and Dunwoodie, S. L. (2006). Mutation of the LUNATIC FRINGE gene in humans causes spondylocostal dysostosis with a severe vertebral phenotype. *Am. J. Hum. Genet.* **78(1)**, 28-37.

van Eeden, F. J., Granato, M., Schach, U., Brand, M., Furutani-Seiki, M., Haffter, P., Hammerschmidt, M., Heisenberg, C. P. et al. (1996). Mutations affecting somite formation and patterning in the zebrafish, Danio rerio. *Development* **123**, 153-64

Vermot, J., Gallego Llamas, J., Fraulob, V., Niederreither, K., Chambon, P.and Dollé, P. (2005). Retinoic acid controls the bilateral symmetry of somite formation in the mouse embryo. *Science* **308(5721)**, 563-6.

Vermot, J. and Pourquié, O. (2005). Retinoic acid coordinates somitogenesis and left-right patterning in vertebrate embryos. *Nature* **435(7039)**, 215-20.

Vilhais-Neto, G. C., Maruhashi, M., Smith, K. T., Vasseur-Cognet, M., Peterson, A. S., Workman, J. L. and Pourquié, O. (2010). Rere controls retinoic acid signalling and somite bilateral symmetry. *Nature* **463(7283)**, 953-7.

Volff, J. N., Zarkower, D., Bardwell, V. J. and Schartl, M. (2003) Evolutionary dynamics of the DM domain gene family in metazoans. *J. Mol. Evol.* **57**, S241-9.

Walhout, A. J. (2006). Unraveling transcription regulatory networks by protein-DNA and protein-protein interaction mapping. *Genome Res.* **16(12)**, 1445-54.

Wang, X. and Yost, H. J. (2008). Initiation and propagation of posterior to anterior (PA) waves

in zebrafish left-right development. *Dev. Dyn.* **237**, 3640-7.

Wardle, F. C., Odom, D. T., Bell, G. W., Yuan, B., Danford, T. W., Wiellette, E. L., Herbolsheimer, E., Sive, H. L., Young, R. A and Smith, J. C. (2006). Zebrafish promoter microarrays identify actively transcribed embryonic genes. *Genome Biol*. **7(8)**, R71.

Waugh, D. S. (2005). Making the most of affinity tags. *Trends Biotechnol.* **23(6)**, 316-20.

Weinberg, E. S., Allende, M. L., Kelly, C. S., Abdelhamid, A., Murakami, T., Andermann, P., Doerre, O. G., Grunwald, D. J. and Riggleman, B. (1996). Developmental regulation of zebrafish MyoD in wild-type, no tail and spadetail embryos. *Development* **122(1)**, 271-80.

Wemmer, K. A. and Marshall, W. F. (2007). Flagellar length control in chlamydomonas--paradigm for organelle size regulation. *Int. Rev. Cytol.* **260**, 175-212.

Whittock, N. V., Sparrow, D. B., Wouters, M. A., Sillence, D., Ellard, S., Dunwoodie, S. L. and Turnpenny, P. D. (2004). Mutated MESP2 causes spondylocostal dysostosis in humans. *Am. J. Hum. Genet.* **74(6)**, 1249-54.

Wienholds, E., van Eeden, F., Kosters, M., Mudde, J., Plasterk, R. H. and Cuppen, E. (2003). Efficient target-selected mutagenesis in zebrafish. *Genome Res*. **13(12)**, 2700-7.

Yamamoto, A., Amacher, S. L., Kim, S. H., Geissert, D., Kimmel, C. B. and De Robertis, E. M. (1998). Zebrafish paraxial protocadherin is a downstream target of spadetail involved in morphogenesis of gastrula mesoderm. *Development* **125(17)**, 3389-97.

Yamamoto, M., Mine, N., Mochida, K., Sakai, Y., Saijoh, Y., Meno, C. and Hamada, H. (2003). Nodal signaling induces the midline barrier by activating Nodal expression in the lateral plate. *Development* **130(9)**, 1795-804.

Yamauchi, H., Miyakawa, N., Miyake, A. and Itoh, N. (2009). Fgf4 is required for left-right patterning of visceral organs in zebrafish. *Dev. Biol*. **332(1)**, 177-85.

Yan, Y. T., Gritsman, K., Ding, J., Burdine, R. D., Corrales, J. D., Price, S. M., Talbot, W. S., Schier, A. F. and Shen, M. M. (1999). Conserved requirement for EGF-CFC genes in vertebrate left-right axis formation. *Genes Dev.* **13(19)**, 2527-37.

Yelon, D., Horne, S. A. and Stainier, D. Y. (1999). Restricted expression of cardiac myosin genes reveals regulated aspects of heart tube assembly in zebrafish. *Dev. Biol*. **214(1)**, 23-37.

Yi, W. and Zarkower, D. (1999). Similarity of DNA binding and transcriptional regulation by Caenorhabditis elegans MAB-3 and Drosophila melanogaster DSX suggests conservation of sex determining mechanisms. *Development* **126(5)**, 873-81.

Yoshioka H, Meno C, Koshiba K, Sugihara M, Itoh H et al. (1998) Pitx2, a bicoid-type homeobox gene, is involved in a lefty-signaling pathway in determination of left-right asymmetry. *Cell* **94(3)**, 299-305.

Yu, J. K., Holland, L. Z. and Holland, N. D. (2002). An amphioxus nodal gene

(AmphiNodal) with early symmetrical expression in the organizer and mesoderm and later asymmetrical expression associated with left-right axis formation. *Evol. Dev*. **4(6)**, 418-25.

Yu, X., Ng, C. P., Habacher, H. and Roy, S. (2008). Foxj1 transcription factors are master regulators of the motile ciliogenic program. *Nat. Genet.* **40**, 1445-53.

Zhang, J., Talbot, W. S. and Schier, A. F. (1998). Positional cloning identifies zebrafish one-eyed pinhead as a permissive EGF-related ligand required during gastrulation. *Cell* **92(2)**, 241-51.

Zhang, N. and Gridley, T. (1998). Defects in somite formation in lunatic fringe-deficient mice. *Nature* **394(6691)**, 374-7.

Zhou, X., Li, Q., Lu, H., Chen, H., Guo, Y. et al. (2008) Fish specific duplication of Dmrt2: characterization of zebrafish Dmrt2b. *Biochimie.* **90(6)**, 878-87.

Zhu, L., Wilken, J., Phillips, N. B., Narendra, U., Chan, G., Stratton, S. M., Kent, S. B. and Weiss, M. A. (2000). Sexual dimorphism in diverse metazoans is regulated by a novel class of intertwined zinc fingers. *Genes Dev.* **14(14)**, 1750-64.

APPENDIX I

Lourenço and Saúde, 2010

Symmetry **2010**, *2*, 1-x (manuscript): doi:10.3390/symx0x000x

OPEN ACCESS

symmetry

ISSN 2073-8994

www.mdpi.com/journal/symmetry

Article, Review, Communication (Type of Paper)

Symmetry OUT, Asymmetry IN

Raquel Lourenço[1,2] and Leonor Saúde[1,2,*]

1-Instituto de Medicina Molecular e Instituto de Histologia e Biologia do Desenvolvimento, Faculdade de Medicina da Universidade de Lisboa, Portugal

2- Instituto Gulbenkian de Ciência, Oeiras, Portugal

E-mail: (ralourenco@fm.ul.pt). E-mail: (msaude@fm.ul.pt)

* Author to whom correspondence should be addressed.

Received: / Accepted: / Published:

Abstract: The formation of a perfect vertebrate body plan poses many questions that thrill developmental biologists. Special attention has been given to the symmetric segmental patterning that allows the formation of the vertebrae and skeletal muscles. These segmented structures derive from bilaterally symmetric units called somites, which are formed under the control of a segmentation clock. At the same time that these symmetric units are being formed, asymmetric signals are establishing laterality in nearby embryonic tissues, allowing the asymmetric placement of the internal organs. More recently, a "shield" that protects symmetric segmentation from the influence of laterality cues was uncovered. Here we review the mechanisms that control symmetric *versus* asymmetric development along the left-right axis among vertebrates. We also discuss the impact that these studies might have in the understanding of human congenital disorders characterized by congenital vertebral malformations and abnormal laterality phenotypes.

Keywords: segmentation clock, bilateral synchronization, left-right asymmetry, organ laterality

---

1. How to produce a symmetric body plan

1.1. The bilateral symmetry of somite formation

The bilateral symmetric appearance of the vertebrate body plan is largely due to the symmetric organization of the skeleton and its associated muscles. The origin of this symmetry can be traced back to early developmental stages when the somites, embryonic structures that will differentiate into the axial skeleton (vertebrae, intervertebral discs and ribs) and skeletal muscles, are being formed. Each new pair of somites is progressively laid down from the rostral region of the presomitic mesoderm (PSM) in a bilateral symmetric way on both sides of the axial structures *i.e*. neural tube and notochord. Somite formation is coupled with the constant supply of new somite precursors cells that are added into the caudal region of the PSM coming from a progenitor zone located in the tailbud. The long lasting interest in the somites comes from the observation that these embryonic structures are produced in species-specific regular intervals in space and time. Every 4-5 hours a new pair of somites is formed in the human embryo, every 120 minutes in the mouse, every 90 minutes in the chick and every 30 minutes in the zebrafish [1].

1.2. The segmentation clock sets the periodicity of somite formation

The "clock and wavefront" model proposed by Cooke and Zeeman in 1976 provides an explanation for the precise temporal and spatial segmental pattern established in the vertebrate body plan [2]. It postulates the existence of an internal clock that sets the time when PSM cells are competent to form a somite and a wavefront of differentiation that moves posteriorly along the PSM and positions the next pair of somites, *i.e.* the determination front. With these two components, both temporal and spatial patterns can be established in the PSM. Only when PSM cells are located anterior to the determination front, a transition from an immature to a mature state can occur and a new somite will form in response to the clock cycle.

The molecular evidence for the existence of a segmentation clock came with the discovery of the first cyclic gene, the avian basic-helix-loop-helix (bHLH) transcription factor *hairy1*. The chick *hairy1* gene shows a dynamic and reiterated expression pattern in the PSM with the exact same periodicity of somite formation [3]. These *hairy1* mRNA oscillations occur autonomously in PSM cells and because they are synchronized with adjacent cells, describe a wave of expression starting at the posterior PSM and moving towards the anterior PSM, where it slows down and eventually stops, concomitant with somite formation (Figure 1). Therefore, PSM cells undergo several periodic oscillations of *hairy1* gene expression before they incorporate into the next somite [3].

Figure 1. The formation of a new pair of somites is under the control of a molecular clock and a wavefront of differentiation. mRNA oscillations of cyclic genes are detected in PSM cells (blue dots) and since they are synchronized with neighboring cells, describe a wave of expression that starts at the

posterior region of the PSM and moves towards the anterior region of the PSM. Here, the wave of expression slows down and stabilizes in the formed somite (S-I). Somite formation is also under the control of a wavefront of differentiation defined by a Fgf/Wnt signalling gradient in the posterior region of the PSM, which is counteracted by a RA gradient in the anterior region of the PSM. Anterior (A) is up, posterior is down (P). S-0 is the new forming somite.

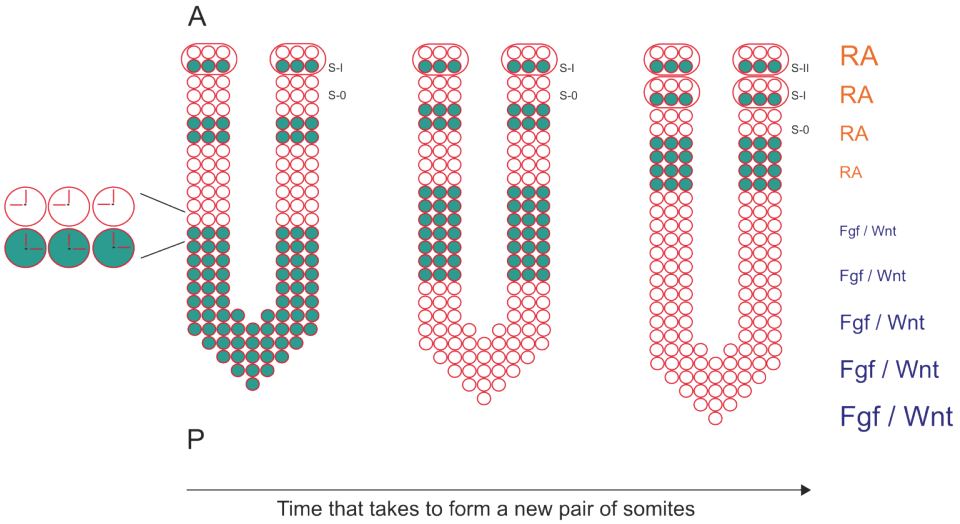

Soon after this discovery, several of *Hairy-Enhancer of Split*-related genes, named *hes* in mice and *her* in zebrafish, were identified and shown to produce the same type of oscillating behavior at the level of the PSM [1]. These genes are primary targets of the Notch signaling pathway and encode transcriptional regulators of the bHLH class that mainly work as repressors [4]. This suggested that the oscillatory behavior of the cyclic genes could be due to feedback inhibition. Indeed the first indication that this was the case came from a pioneering study performed in cell culture. It was shown that not only the mRNA but also the Hes1 protein levels oscillate with the same periodicity as somite formation. These oscillations are generated by a mechanism of negative feedback, where the Hes1 protein periodically represses its own transcription [5]. It has been shown that negative feedback loops also underlie the oscillatory expression of a number of cyclic genes in the mouse, zebrafish and chick PSM [6, 7, 8, 9, 10, 11, 12]. A mathematical model based essentially on experimental data of zebrafish

her genes clearly shows that sustained oscillations can indeed be generated by a negative feedback loop, if transcriptional and translational time delays are taken into account and if the half-life of cyclic mRNAs and proteins are short [13]. Data obtained in the mouse is also in agreement with this model, since a disorganized oscillatory gene expression and a perturbation in somite formation are observed when the half-life of Hes7 protein is increased [10].

The fact that the *Hairy-Enhancer of Split*-related genes are targets of Notch signaling suggested that this pathway is a fundamental component of the segmentation clock. Indeed, the analysis of mouse and zebrafish mutants for several components of the Notch pathway revealed that cyclic gene expression and somite boundary formation were disrupted to varying degrees. Nevertheless, the anterior somites developed normally and only the posterior ones were affected in the Notch mutants [14, 15, 16]. These findings showed that Notch signaling is not entirely necessary for somite formation but instead suggested that its failure leads to a gradual perturbation in somite segmentation.

Furthermore, a closer look at the expression of the Notch ligand *deltaC*, one of the oscillatory genes in zebrafish, in Notch signaling mutants revealed that individual PSM cells still expressed *deltaC* in a cyclic manner but the levels varied quite a lot between neighboring cells. This led to the idea that the main function of Notch signaling is to coordinate oscillations between individual cells and to keep them synchronized and not so much to drive the oscillations (Figure 2). Therefore, it was proposed that in zebrafish Notch mutants, PSM cells begin oscillations in synchrony forming normal anterior somites but after a few cycles gradually loose their synchrony forming abnormal somite boundaries [17].

A model put forward by Lewis (2003) proposed a way by which DeltaC synchronizes oscillations between neighboring cells (Figure 2). It postulates that the intracellular negative feedback oscillations of *her1*/*her7* genes are coupled to an intercellular oscillator involving Delta ligands. In fact, Her1/Her7 negatively regulate *deltaC,* influencing Notch activity in the neighboring cells and finally their own intracellular oscillations. This Delta/Notch mediated coupling mechanism results in synchronization between adjacent cells [13, 18, 19, 20, 21].

Several studies performed in zebrafish clearly demonstrated that DeltaC maintains synchronized oscillations in PSM cells. Mosaic embryos were generated by transplantation of prospective PSM cells taken from an embryo with impaired expression of the oscillatory *her* genes into the prospective PSM region of a wild-type embryo. In these mosaics, the transplanted cells caused an abnormal segmentation behavior in their neighbors but failed to cause segmentation defects if in addition they did not express *deltaC* [22]. The same type of conclusion was reached from a high-resolution in situ hybridization analysis that allowed the visualization of the distinct sub-cellular localizations of the cyclic mRNAs corresponding to their different phases of oscillations in PSM cells. In contrast to a wild-type PSM, in the absence of DeltaC*,* completely different mRNA localizations could be observed

in PSM cells located next to each other [23]. Further support that Notch signaling serves to maintain synchrony in the PSM but is not necessary for oscillations of individual cells comes from studies where the γ-secretase inhibitor DAPT was used to block Notch signaling in a time controlled manner [21, 24]. In these reports, it was shown that there is a delay between the time of DAPT treatment and the disruption of somite boundaries and a delay between DAPT wash and the recovery of normal somite boundaries. Altogether, these results argue, at least in zebrafish, against the idea that Notch signaling is the oscillation generator and favors the idea that its main function is to synchronize oscillations within the PSM cells. Recently, a detailed sub-cellular mRNA localization study, revealed that besides its role in the synchronization of oscillations in posterior PSM, Notch signaling through DeltaD is necessary to initiate non-oscillating expression of the cyclic genes and to start the oscillations in PSM progenitors located in the tail bud [23].

In contrast to what happens in zebrafish, it was recently shown that elimination of all Notch activity abolishes cyclic gene expression and somite formation in mouse PSM [25]. This finding is not incompatible with the possibility presented by others of Notch being a clock synchronizer during mouse somitogenesis [26, 27] since it could integrate both functions. Although a clear demonstration that this pathway synchronizes the oscillations of PSM cells in amniotes is still missing, this could still be a possibility since perturbation of cell-cell interactions upon PSM cell dissociation in chick and mouse leads to irregular desynchronized oscillations [28, 29].

The different roles that Notch signaling seems to play during mouse and zebrafish somitogenesis could be due to different degrees of complexity of the segmentation clock mechanism in these two species. A mouse transcriptome study has shown that a large number of genes are in fact oscillating in the mouse PSM. Many of these genes belong not only to the Notch pathway as expected but also to the Wnt and FGF pathways. In addition, this study also revealed that while the Notch and FGF pathway genes oscillate in synchrony, they are in anti-phase with the oscillations of the Wnt pathway genes. This points to a possible cross-talk between them in a way that Wnt pathway may be coupled to Notch and FGF through mutual inhibition, so that all are integrated in one molecular clock [30]. In zebrafish there is no evidence for the existence of Wnt or FGF-based cyclic genes [1].

Figure 2. Synchronized oscillations between adjacent cells in zebrafish presomitic mesoderm. Activation of Notch, upon interaction with DeltaC, activates the expression *her* genes. *her* genes encode transcriptional repressors that have the ability to inhibit their own expression generating negative feedback loops that are then responsible for the PSM intracellular oscillations. Importantly, the period of these oscillations are dependent on both transcriptional (Tm) and translational delays

(Tp). Her proteins will not only inhibit their own expression, but also inhibit the expression of *deltaC* that for this reason is also expressed in an oscillatory manner. DeltaC in one cell will then activate Notch signalling in the neighbouring cell and as a consequence generates intracellular oscillations. Thus, oscillations between adjacent cells are synchronized with one another since they are coupled via Notch signalling.

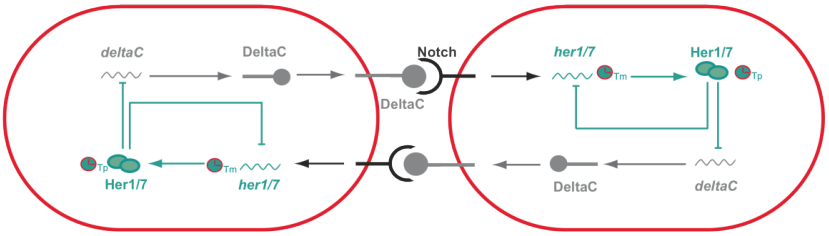

1.3. The wavefront sets the position of somite formation

According to the original clock and wavefront model, the regular spacing of somites is also under the control of a wavefront that sets the position where the next somite boundary is going to be formed. Indeed there are several lines of evidence that show that this position is defined by a threshold of FGF and Wnt signaling along the PSM [31, 32] (Figure 1). While under the influence of FGF/Wnt signaling, the PSM cells are maintained in an immature state and are prevented from starting the genetic program of somite formation.

The posterior-to-anterior gradient of *fgf8* mRNA in the PSM was the first one to be described in several vertebrate embryos (mouse, zebrafish and chick) [31, 33, 34]. This gradient is generated via a decay mechanism from a pool of transcripts produced by progenitor PSM cells [34]. According to the clock and wavefront model [2], displacing the position of the determination front by altering the extent

of the *fgf8* gradient results in the shift of the somite boundary position [31]. It is thought that this gradient is translated into a protein gradient, which is then converted into a MAPK/ERK activity gradient along the PSM [33, 34, 35].

Parallel to the *fgf* gradient there is also a posterior-to-anterior gradient of Wnt signaling along the PSM. The expression of *wnt3a* in the posterior PSM [32] could be responsible for the nuclear *β-catenin* gradient reaching from the tailbud to the determination front [36] and for the graded expression of the Wnt target *axin2* [32].

It has been proposed that the determination front established by the *fgf* and *wnt* gradients is opposed by an anterior-to-posterior gradient of retinoic acid (RA) [37, 38] (Figure 1). RA is the oxidized version of vitamin A. It is synthesized in the anterior PSM and somite region by the enzyme retinaldehyde dehydrogenase 2 (Raldh2), and degraded in the posterior PSM by the enzyme Cyp26a1 [39]. RA in the anterior PSM has been shown to control somite boundary positioning by attenuating Fgf8 in that region. These mutually inhibitory gradients and control somite differentiation by defining the determination front in a growing tissue [37].

2. Is the body plan all about symmetry?

When looking at the exterior of a vertebrate body, one could say that it is fully bilaterally symmetric. Nonetheless, this external symmetry encloses unexpected surprises, since the internal organs acquire a consistently asymmetric disposition with respect to the left-right (LR) axis. On the left side of the vertebrate body we can find the heart, stomach, spleen and the part of the lung with fewer lobes, while on the right side we have the liver, gall bladder and the part of the lung with more lobes. This normal distribution of the internal organs is referred to as *situs solitus* and is largely conserved among a population of a given species. Nevertheless, deviations from the norm can arise in single individuals and will result in laterality defects: *situs inversus* corresponds to a situation where the position of the internal organs is completely reverted as a mirror-image; left or right isomerism is a situation where bilateral symmetry is not broken and two left or two right sides will form; *situs ambiguus* or heterotaxia that corresponds to some organs being properly oriented and others reversed [40, 41].

Well before visible morphological asymmetries can be observed in the vertebrate embryo, a conserved cascade of asymmetrically expressed genes, called the Nodal cascade is activated at the onset of gastrulation. Genes belonging to this cascade are the TGF-β family members, *nodal*, *lefty1*, *lefty2* and the homeobox transcription factor, *pitx2*. It is thought that an excess of Nodal activity on the left-hand side of the node will be transferred to the left lateral plate mesoderm (LPM) and in this

location Nodal exerts a positive feedback on itself. Consequently, the expression of *nodal* is amplified in the left LPM. At the same time, nodal activates its negative regulators, the *lefty* genes. *Lefty1* in the midline prevents *nodal* activation on the right LPM, while *lefty2* restricts the domain of *nodal* expression on the left LPM. Here, Nodal induces *pitx2* expression. Pitx2 will promote LR asymmetry of the internal organs, through a mechanism not yet fully understood [42] (Figure 3C).

Although the Nodal cascade is conserved among vertebrates, the mechanism that induces *nodal* in the node in the first place shows differences between vertebrates. In mouse and chick, Notch signaling activates *nodal* in the node region [43, 44]. In zebrafish Notch signaling activates the Nodal negative regulator *charon* [45] around the Kupffer's vesicle (KV), the structure analogous to the mammalian node. In addition to Notch signaling, Fgf8 also regulates *nodal* asymmetric expression in the mouse and chick node. In the mouse, Fgf8 acts as a positive *nodal* regulator and therefore is a left determinant. In the chick, *fgf8* is asymmetrically expressed on the right side of the node where it represses *nodal,* thereby acting as a right determinant [46]. The role of Fgf8 in controlling expression at the KV has not been determined, although *fgf8* mutants show LR defects [47]. Also Wnt signaling, namely Wnt3a, indirectly regulates *nodal* expression in the mouse node indirectly through Delta-like1 [48]. In the chick, *wnt8c* is asymmetrically expressed on the right side of the node but functions as a left determinant controlling the expression of *nodal* [49].

Figure 3. Set of events that might culminate with the establishment of the left-right patterning in different vertebrates. A) Prior to gastrulation in *Xenopus*, zebrafish and chick, ion transporters asymmetrically distributed in the embryo generate differences in membrane voltage potential between the left and right side. It is thought that this asymmetric membrane polarization promotes the accumulation of LR determinants through directional transport involving gap-junction channels. B) In mouse, it is though that mechanosensory cilia present in the node epithelia sense the leftward fluid flow created by motile cilia and as a consequence trigger an asymmetric Ca^{2+} release which will induce an asymmetric *nodal* expression around the node. This Ca^{2+} accumulation on the left side has also been described in zebrafish and chick although its relation with cilia-driven flow has not been established. C) A conserved Nodal cascade is activated at the onset of gastrulation in *Xenopus*, zebrafish, chick and mouse. *nodal* is asymmetrically transferred from the node to the left LPM. There, it induces its own expression through a positive feedback loop and also the expression of its own inhibitors, *lefty1* and *lefty2*. *Lefty1* is expressed in the midline and prevents *nodal* spreading to the right LPM, while *lefty2* is expressed in the left LPM restricting Nodal expression on the left side.

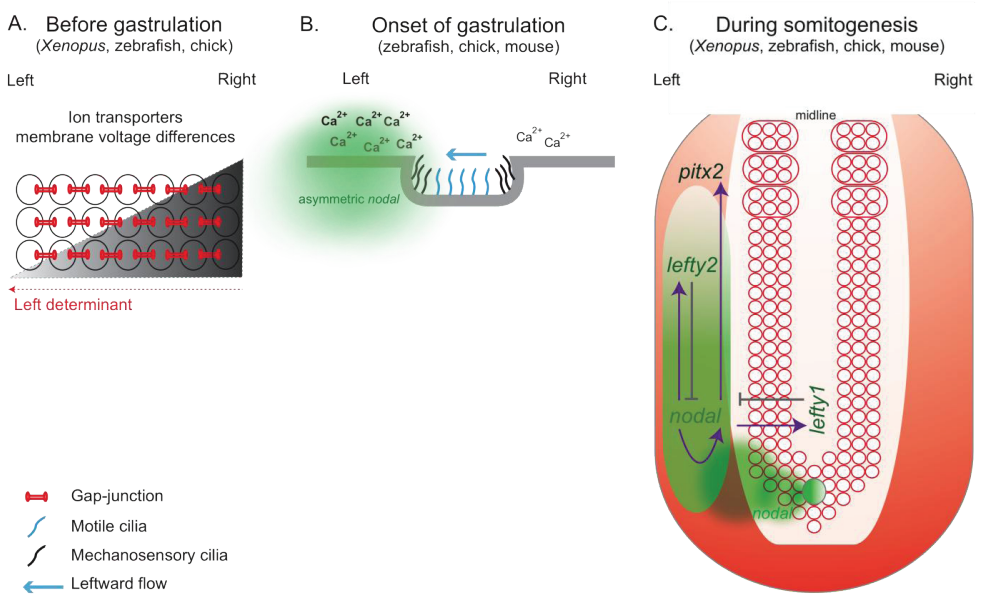

2.1. How can cilia break symmetry?

Apart from of the signaling pathways that might activate *nodal* in the node region and the subsequent signaling cascade, it is important to understand the event that turns *nodal* expression asymmetric on the left side of the node. In other words, how is the initial embryonic symmetry broken in the node region? A clue to start to solve this question came from the observation that Kartagener's syndrome patients have ultrastructural defects in Dynein, a component of the ciliary motion motor [50, 51]. This particular defect was readily associated with the chronic respiratory infections and male infertility observed in these patients as a result of lack of cilia/flagella motility within the respiratory epithelium and sperm. However, the connection with *situs inversus* was only established later. It turned out that *left-right dynein* (*lrd*) is expressed in the mouse node [52], that node cells possess monocilia [53] and that the *inversus viscerum* (*iv*) mutant mouse that shows a clear randomized laterality phenotype has a mutation in *lrd* [54, 55, 56]. Most importantly it was shown that these node cilia rotate in a clockwise manner and due to their posteriorly tilted position on each cell create a leftward extracellular fluid flow that induces left-side specific gene expression [57, 58] (Figure 3B). The reversed laterality obtained when an artificial rightward flow is imposed on the mouse node is consistent with the idea that a directional fluid flow provides the asymmetry cue that determines

laterality [59]. Moreover, using the same experimental setup, it was possible to rescue the laterality phenotype of the *iv* mouse mutant, in which no flow is observed by simply exposing their nodes to a strong leftward fluid flow [59, 60].

How the flow is interpreted and then converted into LR asymmetric gene expression is still unknown. Nevertheless, two models have been proposed to date. One model states that a morphogen might be transported as a consequence of the leftward fluid flow created by motile *lrd*-containing cilia. The resulting asymmetric morphogen distribution would initiate downstream molecular events that then establish left-right asymmetries in the LPM [57]. More recently, vesicular particles containing Sonic hedgehog (Shh) and retinoic acid (RA) were shown to form in the node stimulated by FGF and are transported to the left edge of the node where they fragment and release their contents [61]. An alternative model mentions the existence of two different subpopulations of cilia in the node. In addition to the motile *lrd*-containing cilia, there are also immotile mechanosensory cilia containing the polycystin-2 calcium activated channel [62, 63]. It has been proposed that immotile mechanosensory cilia sense the fluid flow pressure on the left side of the node and trigger an asymmetric intracellular Ca^{2+} flux that then breaks LR symmetry by inducing asymmetric *nodal* expression [62] (Figure 3B). These two models are not mutually exclusive and it is possible that both mechanosensors and morphogens are involved in setting up the asymmetric pathway.

2.2. More than cilia: other players in the scene

Although, first described in mouse, the directional flow produced by motile cilia in the node is not exclusive to murine embryos. In fact a directional type of flow is generated in node-equivalent structures in a wide range of vertebrates. In zebrafish and medaka, the motile cilia inside the KV produce a counterclockwise fluid flow. Moreover, when cilia motility is impaired, fluid flow is abolished and LR development is perturbed [64, 65, 66, 67]. The rabbit posterior notochord (PNC) and *Xenopus* gastrocoel roof plate (GRP) also have motile cilia, which have been shown to create a leftward fluid flow [68, 69, 70]. As for the chick, it is clear that ciliated cells are present in the Hensen's node. However no directional flow has been described in the chick node possibly because the distance between single monocilia is too long to create a directional flow thus compromising their role in LR determination [71, 72]. Instead, it seems that asymmetry in the node is promoted by outside tissues [73]**,** most likely through asymmetric cell rearrangements that generate a leftward movement of cells around the node [74, 75].

Although it is clear that monocilia play a fundamental role in LR patterning, several lines of evidence suggest that earlier LR asymmetries already exist prior to the directional fluid flow generated by ciliary motion, at least in amphibians, chick and fish.

In *Xenopus*, an asymmetrically localized ion flux is set up through an H^+/K^+ ATPase transporter (pumps H^+ out of the cell in exchange for K^+). In fact, *H^+/K^+ ATPase* maternal mRNA is already asymmetrically localized on the right-hand side of the embryo during the first two cell divisions. In addition, it was shown that inhibition of this pump results in randomization of left side specific genes and organ heterotaxia [76]. It has been suggested that asymmetric ion flux might be responsible for directing the positioning of a LR determinant to the left side through gap junction communication channels (GJC) since inhibition of these channels induces heterotaxia in *Xenopus* [76, 77]. Generation of LR voltage differences that control laterality also seem to be important in the chicken embryo. In fact, a differential H^+/K^+ ATPase activity across Hensen's node results in left side asymmetric ion flux, which creates a differential membrane potential between the left and right sides of the primitive streak. Asymmetric ion flux has also been suggested to direct LR determinants through GJC in chick, since GJC inhibition also leads to LR patterning problems [76, 78]. H^+/K^+ ATPase activity results in extracellular Ca^{2+} accumulation on the left side of Hensen´s node, a possible candidate for being a LR determinant molecule that passes through the GJC. In fact, Ca^{2+} accumulation was shown to induce an asymmetric activation of Notch on the left side of the node that then translates this differential activity into asymmetric *nodal* expression. Perturbing this early asymmetric ion flux, will lead to randomized gene expression and organ heterotaxia [44]. In zebrafish it has been shown that the early activity of the H^+/K^+ ATPase pump determines the LR axis without affecting cilia or KV fluid flow [79]. More recently, the function of another proton pump, the H^+-V-ATPase, was shown to be important to establish LR asymmetries in *Xenopus*, fish and chick and in the case of zebrafish clearly impacts on cilia size/number within the KV [80]. In zebrafish another pump, the Na,K-ATPase alpha2, modulates the levels of intracellular Ca^{2+} already in the cells that are going to give rise to the KV, the dorsal forerunner cells (DFC's). In turn, these Ca^{2+} levels regulate cilia motility in the KV and consequently the cilia-driven leftward fluid flow [81]. Propagation of the intracellular asymmetric Ca^{2+} flux is regulated by inositol polyphosphates, which in turn are candidates for the LR determinant that passes through GJC and influence LR determination [82]. Consistent with this idea, Connexin43.4 (Cx43.4), a protein of the GJC channel, is required for the LR patterning through the development of a functional KV with normal cilia [83].

Another possible candidate for the LR determinant is the neurotransmitter serotonin, which has been demonstrated to regulate LR patterning in *Xenopus* and chick before the appearance of cilia. Maternal serotonin has a rightward gradient localization during cleavage stages and its localization

requires the set up of an asymmetric voltage gradient created by the H^+/K^+ ATPase coupled with GJC channels [84, 85].

Although the fluid flow generated by cilia seems to be the first symmetry-breaking event in mouse, it may not be the initial event in other organisms where it is more likely to serve as an amplification mechanism of the LR decision made earlier in development. In zebrafish, Xenopus and chick, different mechanisms seem to act prior to the leftward flow initiation, such as asymmetric localization of ion channels and asymmetric function of gap junctions (Figure 3A). So far, no ion transporters or gap junctions have been described to be involved in LR establishment in mammals, however there is still the possibility that an unidentified symmetry breaking event may occur earlier in mouse development. Interestingly, a recent report states that manipulation of initial cleavages in the mouse embryo leads to a reverted direction of fetal axial rotation, although the heart and gut laterality was not affected [86]. This finding sets the ground for the possibility that in mammals LR embryonic patterning may be set during the cleavage stages similarly to what has been described in snails, where manipulation of the first cleavages resulted in reverted shell coiling and visceral situs inversus [87].

3. How are symmetric tissues protected from LR asymmetric signals?

The formation of a perfect vertebrate body plan involves the establishment of LR asymmetries in the LPM to position the internal organs. In addition, it is also crucial that bilateral symmetry is maintained in the PSM ensuring the symmetric formation of the somites and consequently of the axial skeleton and skeletal muscles. Besides sharing the same signaling pathways as discussed above, somitogenesis and LR patterning take place at around the same time during development in nearby embryonic regions. Therefore, the asymmetric signals that originate in the node have to be able to influence the LPM without affecting the bilateral symmetry of somite formation in the juxtaposed PSM. In fact, several lines of evidence show that bilateral symmetry is not a default state but instead has to be actively maintained through a mechanism that protects this territory from the LR asymmetric signals [88].

3.1. Retinoic acid buffers the PSM from the influence of LR signals

RA binds to heterodimers of retinoic acid receptor (RAR) and retinoid X receptor (RXR) and activates transcription of RA-responsive genes upon binding to specific DNA sequences known as retinoic acid response elements (RAREs) [89]. RA has been implicated in the control of bilateral symmetry in vertebrates, acting as a buffer that prevents LR signals to reach the PSM and influence somitogenesis (Figure 4A).

When the function of the RA producing enzyme *raldh2* is abolished either by a null mutation in the mouse or by morpholino-knockdown in zebrafish embryos, somite formation is delayed with a bias on the right side as assayed by the expression of *uncx4.1*, a marker of the posterior half of the mature somite [79, 90] (Figure 4B). In the *neckless* mutant, that carry a missense mutation in *raldh2*, the same phenotype is observed [79]. Interestingly, the somitogenesis delay on the right side observed in the *raldh2* mutants and morphants only happens in a specific time window, between 8-15 somite stage in mouse and 6-13 somite stage in zebrafish. The reason for this particular time window lies on the fact that these somites derive from progenitor PSM cells that were near the node/KV when the LR information was being transferred earlier from the node/KV to the LPM [91, 92]. The delay in somite formation in not caused by a defect in LR patterning in general, since no laterality defects are observed in the absence of *raldh2* in mouse and zebrafish [79, 90, 93]. In addition, epistatic experiments by crossing the *raldh2* with *lrd* mouse mutants lead to randomized somite defects instead of the right biased defects seen in *raldh2* single mutants [94]. This particular experiment shows that RA acts to counteract LR signals.

The right biased somite defects seen in the absence of *raldh2* can be explained by the LR desynchronization of the segmentation clock [79, 90] (Figure 4B). In these embryos, the expression of the cyclic genes *hes7* and *lfng* (in mouse), *deltaC*, *her1* and *her7* (in zebrafish) are out of phase between the left and right sides. Also consistent with the somite phenotype is the anterior displacement of the wavefront seen by the anterior expansion of *fgf8* on the right side of the PSM. These LR desynchronization defects are only detected within a small time window that correlates with asymmetric somite formation [79, 90].

When *raldh2* was inhibited with disulphiram in chick embryos, again a delay in somite formation was observed and this effect was restricted to a specific time window. But in contrast to mouse and zebrafish fewer somites are formed on the left side of the axis [94]. The segmentation clock is in different phases between the left and the right side of PSM, as seen by the asymmetric expression of *lfng*. However in contrast to mouse and zebrafish, *fgf8* does not show a clear expansion anteriorly in an asymmetric manner in disulphiram-treated chick embryos, suggesting that wavefront may not be responsible for asymmetric somite formation [94].

Thus, RA has a conserved function which is vital for symmetric somite formation, by protecting the PSM form the LR cues that are being transferred from the node into the LPM during a specific period of time (Figure 4A). After this discovery the next question that arises is what are the LR cues that RA is counteracting and where and when is this action being performed? Due to the fact that *radlh2* is expressed in the PSM it is reasonable to predict that RA is performing its function in this mesodermal

tissue. However, using a retinoic-acid response element (RARE)-LacZ-reporter transgene it was shown that RA signaling in mouse embryos is present not only in somites and anterior PSM, but it also extends to the adjacent neural plate and the node ectoderm [93]. In the node ectoderm, RA antagonizes *fgf8* that is expressed nearby in the epiblast (primitive ectoderm). In *raldh2* mutants already at early somite stages there is an expansion of *fgf8* expression from the epiblast into the neural plate and node ectoderm. At later stages, these embryos show a right shift of *fgf8* expression in the anterior PSM, suggesting that the expansion of *fgf8* into the node ectoderm may be increasing its own levels in the adjacent PSM shifting it more anteriorly [93]. These authors suggest that RA is ensuring bilateral somite formation not at the level of the PSM but at the level of the node ectoderm, where it controls the limits of *fgf8*.

Recently, an independent study using the same (RARE)-LacZ-reporter transgene showed however that the levels of RA signaling in the mouse PSM are higher on the right side [95]. In addition, these authors show that this asymmetric RA signaling results from the function of a complex consisting of Nr2f2a and a novel RA signaling component called Rere. While *rere* is ubiquitously expressed, *nr2f2a* is asymmetrically expressed on the right PSM. In mice mutant for *Rere*, there is a lack of LR synchronization of the cyclic genes and of the *fgf8* anterior limit in the PSM, leading to a somitogenesis defect similar to the one described for *raldh2* mutants. This asymmetric RA signaling seems to be important to control the LR determination function of Fgf8 in the PSM. Interestingly, *nr2f2*a expression in the mouse is asymmetric on the right, while in the chick it is asymmetric on the left side of the PSM. This provides an explanation for the different bias in the somite formation defects observed in the absence of RA signaling in these two vertebrates [94, 95] and might be linked with the fact that Fgf8 is a left determinant in the mouse while in the chick it is a right determinant [46, 96].

Fgf8 does not seem to be the only LR cue corrected by RA signaling. In both chick and mouse embryos, *snail1* is transiently asymmetrically expressed in the right LPM and plays a role in organ lateralization [97, 98]. Furthermore, it was shown that the period of asymmetric *snail1* expression in the LPM coincides with the time window during which RA is necessary to protect the PSM from asymmetric signals [99]. Indeed, in the chick it was shown that in the absence of RA signaling, *snail1* expression is not affected in the LPM but starts to be asymmetrically expressed in the right anterior PSM. This asymmetric PSM expression of *snail1* results in asymmetric expression of the cyclic genes *snail2* and *lfng* and later leads to asynchronous somitogenesis [99]. In mouse, asymmetric somite formation seen in the absence of RA signaling [94] may be due to a misregulation of *snail1* expression in the PSM, since it has been shown that in mice mutants for *Rere* there is an asymmetric *snail1* expression in the PSM [95].

RA perturbation does not result in LR defects in the LPM since the expression of *spaw* and *pitx2* in the LPM is normal. However, the somite laterality defects are linked to the LR pathway. In fact, the bias in somite defects is lost in *raldh2/lrd* double mutants where RA signaling is perturbed together with randomization of the LR asymmetric cues [79, 94, 95].

Perturbations of RA function lead to a biased somitogenesis defect in a specific time window that correlates with the timing of LR cues establishment [79, 94, 95]. Therefore, RA signaling has emerged as a conserved keeper of bilateral somite formation.

Figure 4. Protection of PSM segmentation from LR asymmetric patterning cues. A) PSM is protected from LR signals that come from the node and are implicated in left-right patterning (red arrows). This protection consists of a "shield" (white) which so far has been shown to be composed by RA, Snail, Su(H) and Terra. In its presence, cyclic gene expression (blue) and somite formation are symmetric between the left and right sides. B) In the absence of this protection, cyclic gene expression becomes desynchronised between both sides. Consequently, somite formation proceeds in an asymmetric way, with the left side exhibiting more somites than the right (this biased asymmetry towards the right side is seen in mouse and fish embryos, while in chick asymmetries are biased to the left side).

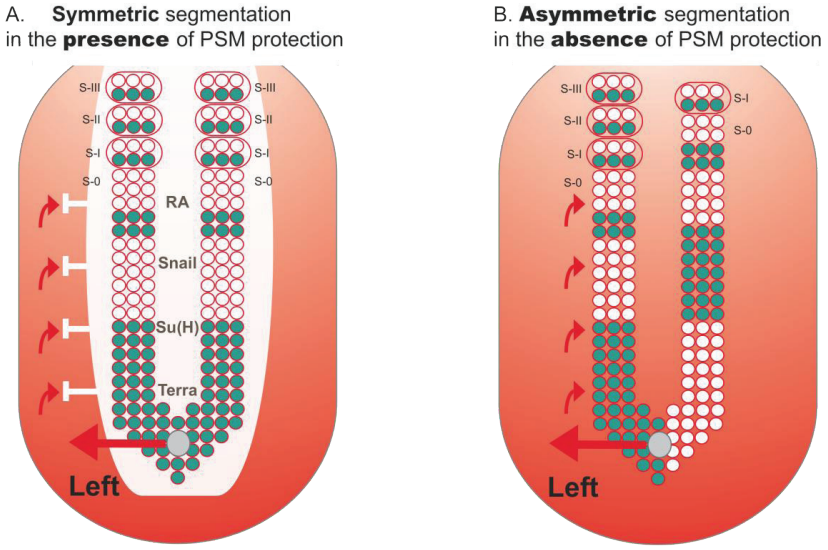

3.2. Bridge between LR patterning and somitogenesis

Direct links between LR patterning and somitogenesis were revealed in studies in zebrafish. The transcription factor Suppressor of Hairless (Su(H)), belongs to a complex that mediates Notch signaling [100]. The downregulation of any of the two Su(H) paralog genes in zebrafish leads to randomization of LR markers in the LPM and to an unbiased asymmetric somite formation. In the *su(H)* morphants, the RA degrading enzyme *cyp26a1* is misregulated in the tailbud. Since *cyp26a1* knockdown can also lead to asymmetric cycling gene expression, this suggests that Su(H) is required to regulate RA in the tailbud that will in turn regulate symmetric cycling gene expression in the PSM [101] (Figure 4A,B).

We have shown that Dmrt2a/Terra, a zinc finger-like transcription factor belonging to the DMRT (DM Related Transcription Factor) family, regulates the body plan along the LR axis in zebrafish. In Dmrt2a/Terra morphants, the LR asymmetry pathway is also affected, with the expression of left side LPM markers being randomized and consequently affecting the positioning of the heart. On the other hand, dynamic cyclic expression of *deltaC*, *her1* and *her7* becomes desynchronized between the left and right sides of the PSM in a specific time window, leading to an unbiased somite number. Therefore, Dmrt2a/Terra has a dual role, it ensures the correct flow of LR asymmetry information to the LPM and in combination with RA signaling ensures the maintenance of symmetry in the PSM [102] (Figure 4A,B). In the mouse, the knockout of *dmrt2* strongly affected somite differentiation leading to severe rib and vertebral malformations [103]. It would be interesting to know whether it also regulates synchronization of the clock genes and if it has an impact on heart laterality.

Even more striking is the observation that the simple disruption of the LR determination pathway results in asymmetric somite formation in zebrafish. Downregulation of the H^+/K^+-ATPase activity, with omeoprazole from 1-cell to bud stages only, results in randomization of LR markers in the LPM and in an unbiased asymmetric somite formation between the left and right sides of the PSM [79]. Also when Notch signaling is perturbed, with the γ-secretase inhibitor DAPT from bud to early somitogenesis stages, there is a randomization of LR markers in the LPM and an unbiased asymmetric somite formation. Once again the somitic defects are only detected in a specific time window from 6 to 13-somite stage, corresponding to the moment when LR information is being transferred from the KV to the LPM cascade [79].

At this moment, there is no evidence for the existence of a LR desynchronization phenotype in somite formation upon perturbation of early LR asymmetric information in mouse laterality mutants. Since the bilateral somite phenotype can only be detected in a specific time window, there is still the possibility that it was not noticed over the extensive organ laterality analysis.

4. Human developmental disorders related to the LR axis

The set up of the axial skeleton is dependent on somite formation and differentiation. After epithelialization from the anterior region of the PSM, each somite undergoes a dorsal-ventral compartmentalization so that the ventral region, enclosing the sclerotome, is different from the dorsal region, the dermomyotome. This subdivision is important for later patterning events, with the sclerotome differentiating into the axial skeleton and ribs, and the dermomyotome giving rise to the dermis of the back and skeletal muscles [104]. A diverse number of human conditions associated with vertebral malformations arise as a consequence of mutations in important somitogenesis-related genes. Mutations in Notch ligand *delta-like 3* (*dll3*) [105], *mesp2* [106] and *lfng* [107] are associated with the spondylocostal dysostosis syndrome. This condition exhibits vertebral column malformations from rib fusions to kypho-scoliosis (abnormal curvature of the spine). This phenotype is reminiscent of what happens in mouse mutants, highlighting the importance of mouse models in the search for the genes associated with human disorders [108, 109, 110]. Mutations in other genes of the Notch pathway can also lead to vertebral malformations. Mutations in two Notch pathway ligands, *jag1* and *notch2*, are associated with the Alagille syndrome which has been shown to present, among other symptoms, abnormal vertebrae formation which are "butterfly shaped" [111]. Fgf signalling has also been implicated in disorders associated with skeletal development. A mutation in *fgfr2* results in fused cervical vertebrae, known as the Apert syndrome [112]. A minor perturbation in segmentation can lead to severe clinical consequences. Thus the identification of molecules that can reduce vertebral patterning disorders will subsequently help in their prevention.

LR asymmetric cues are important to position the internal organs in a normal configuration termed *situs solitus*. When LR patterning is disturbed by a series of events, as previously discussed, abnormal laterality phenotypes appear namely *situs inversus* and *situs ambiguus*. The morbidity and mortality associated with laterality defects is mainly due to congenital heart disease (CHD) [113]. Human patients with *situs inversus* have 3% incidence of CHD compared with normal *situs solitus* humans that show a 0.08% incidence [114, 115, 116]. In *situs ambiguus* patients the incidence of CHD is greater than 90% [115]. The cardiac defects in these patients include atrial and ventricular septal defects, transposition of great arteries, double outlet right ventricle, anomalous venous return and aortic arch anomalies [117]. The clinical observations together with a number of molecular evidence from animal models are helping to understand the ethiology of CHD. It is becoming clear that heart diseases may result from abnormal looping and remodeling of the primitive heart tube into a multi-chambered organ as a consequence of LR patterning defects.

In addition, human laterality defects are associated with primary cilia dyskinesia (PCD), which is characterized by deficiencies in ciliary motility. In PCD patients, 47.7% display *situs inversus*, 6.3% display *situs ambiguus* or heterotaxy, most of them also presenting cardiovascular abnormalities, while the remaining 46% show normal organ *situs* [50, 118, 119]. Once again, clinical data together with experimental results from animal models provided a biological explanation for this association, revealing that cilia are indeed early players in LR patterning.

It should be noticed that laterality defects in humans are often associated with abnormal vertebrae and scoliosis [120]. The genetic etiology of these conditions is unknown, however we speculate that they may relate to the recently uncovered molecular link between LR patterning and bilateral synchronization of the segmentation clock.

5. Conclusions

To design the vertebrate body plan it is fundamental to create asymmetry between the left and the right side of the lateral plate mesoderm, in order to correctly position the internal organs. Also, it is crucial to maintain symmetry between the left and the right side of the presomitic mesoderm to ensure the perfect allocation of symmetric body structures such as the axial skeleton, skeletal muscles and peripheral nerves. Although different strategies were shown to initiate the left-right asymmetry in the vertebrate embryo [121], only recently the existence of mechanisms that promote symmetry have been described in several organisms [90, 94, 79, 102]. Therefore, symmetry is no longer perceived as a default embryonic state but rather as a developmental process involving an active molecular mechanism. Although the mechanism that bridges LR patterning and bilateral synchronization of the segmentation clock is not understood, the new studies here reviewed point to the idea that a correct flow of LR signals is necessary for bilateral somite formation.

Acknowledgements

We are grateful to A. Hanisch, R. Andrade, A.T. Tavares, S.S. Lopes, R. Fior, S. Pascoal and N. Afonso for comments on the manuscript. R.L. was supported by a FCT fellowship (SFRH/BPD/6755/2001). R.L. and L.S. were supported by two FCT grants (PTDC/SAU-OBD/71596/2006 and PTDC/SAU-OBD/64628/2006).

References and Notes

1. Dequéant, M. L.; Pourquié, O. Segmental patterning of the vertebrate embryonic axis. *Nat. Rev. Genet.* **2008**, 9, 370-382.
2. Cooke, J.; Zeeman, E. C. A clock and wavefront model for control of the number of repeated structures during animal morphogenesis. *J. Theor. Biol.* **1976**, 58(2), 455-76.
3. Palmeirim, I.; Henrique, D.; Ish-Horowicz, D.; Pourquie, O. Avian hairy gene expression identifies a molecular clock linked to vertebrate segmentation and somitogenesis. Cell **1997**, 91, 639–648.
4. Kageyama, R.; Ohtsuka, T.; Kobayashi, T. The Hes gene family: repressors and oscillators that orchestrate embryogenesis. *Development* **2007**, 134(7), 1243-51.
5. Hirata, H.; Yoshiura, S.; Ohtsuka, T.; Bessho, Y.; Harada, T.; Yoshikawa, K.; Kageyama, R. Oscillatory expression of the bHLH factor Hes1 regulated by a negative feedback loop. *Science* **2002**, 298(5594), 840-3.
6. Oates, A. C.; Ho, R. K. Hairy/E(spl)-related (Her) genes are central components of the segmentation oscillator and display redundancy with the Delta/Notch signaling pathway in the formation of anterior segmental boundaries in the zebrafish. *Development* **2002**, 129(12), 2929-46.
7. Holley, S. A.; Jülich, D.; Rauch, G.J.; Geisler, R.; Nüsslein-Volhard, C. her1 and the notch pathway function within the oscillator mechanism that regulates zebrafish somitogenesis. *Development* **2002**, 129(5), 1175-83.
8. Dale, J. K.; Maroto, M.; Dequeant, M. L.; Malapert, P.; McGrew, M.; Pourquie, O. Periodic notch inhibition by lunatic fringe underlies the chick segmentation clock. *Nature* **2003**, 421(6920), 275-8.
9. Bessho, Y.; Hirata, H.; Masamizu, Y.; Kageyama, R. Periodic repression by the bHLH factor Hes7 is an essential mechanism for the somite segmentation clock. *Genes. Dev.* **2003**, 17(12), 1451-6.
10. Hirata, H.; Bessho, Y.; Kokubu, H.; Masamizu, Y.; Yamada, S.; Lewis, J.; Kageyama, R. Instability of Hes7 protein is crucial for the somite segmentation clock. *Nat. Genet*. **2004**, 36(7), 750-4.
11. Sieger, D.; Tautz, D.; Gajewski, M. The role of Suppressor of Hairless in Notch mediated signalling during zebrafish somitogenesis. *Mech. Dev.* **2003**, 120(9),1083-94.
12. Brend, T.; Holley, S. A. Expression of the oscillating gene her1 is directly regulated by Hairy/Enhancer of Split, T-box, and Suppressor of Hairless proteins in the zebrafish segmentation clock. *Dev. Dyn.* **2009**, 238(11), 2745-59.
13. Lewis, J. Autoinhibition with transcriptional delay: a simple mechanism for the zebrafish somitogenesis oscillator. *Curr. Biol.* **2003**, 13(16), 1398-408.
14. Conlon, R. A.; Reaume, A. G.; Rossant, J. Notch1 is required for the coordinate segmentation of somites. *Development* **1995**, 121(5), 1533-45.
15. Huppert, S. S.; Ilagan, M. X.; De Strooper, B.; Kopan, R. Analysis of Notch function in presomitic mesoderm suggests a gamma-secretase-independent role for presenilins in somite differentiation. *Dev.Cell.* **2005**, 8(5), 677-88.
16. van Eeden, F. J.; Granato, M.; Schach, U.; Brand, M.; Furutani-Seiki, M.; Haffter, P.; Hammerschmidt, M.; Heisenberg, C. P.; Jiang, Y. J.; Kane, D. A.; Kelsh, R. N.; Mullins, M. C.; Odenthal, J.; Warga, R. M.; Allende, M. L.; Weinberg, E. S.; Nüsslein-Volhard, C. Mutations

affecting somite formation and patterning in the zebrafish, Danio rerio. Development **1996**, 123:153-64.

17. Jiang, Y. J.; Aerne, B. L.; Smithers, L.; Haddon, C.; Ish-Horowicz, D.; Lewis, J. Notch signalling and the synchronization of the somite segmentation clock. *Nature* **2000**, 408(6811), 475-9.
18. Oates, A. C.; Ho, R. K. Hairy/E(spl)-related (Her) genes are central components of the segmentation oscillator and display redundancy with the Delta/Notch signaling pathway in the formation of anterior segmental boundaries in the zebrafish. *Development* **2002**, 129(12), 2929-46.
19. Giudicelli, F.; Ozbudak, E. M.; Wright, G. J.; Lewis, J. Setting the tempo in development: an investigation of the zebrafish somite clock mechanism. PLoS Biol. **2007**, 5(6), e150.
20. Jülich, D.; Hwee Lim, C.; Round, J.; Nicolaije, C.; Schroeder, J.; Davies, A.; Geisler, R.; Lewis, J.; Jiang, Y. J.; Holley, S. A. beamter/deltaC and the role of Notch ligands in the zebrafish somite segmentation, hindbrain neurogenesis and hypochord differentiation. *Dev. Biol.* **2005**, 286(2), 391-404.
21. Ozbudak, E. M.; Lewis, J. Notch signalling synchronizes the zebrafish segmentation clock but is not needed to create somite boundaries. *PLoS Genet.* **2008**, 4(2), e15.
22. Horikawa, K.; Ishimatsu, K.; Yoshimoto, E.; Kondo, S.; Takeda, H. Noise-resistant and synchronized oscillation of the segmentation clock. *Nature* **2006**, 441(7094),719-23.
23. Mara, A.; Schroeder, J.; Chalouni, C.; Holley, S. A. Priming, initiation and synchronization of the segmentation clock by deltaD and deltaC. *Nat. Cell Biol.* **2007**, 9(5), 523-30.
24. Riedel-Kruse, I. H.; Müller, C.; Oates, A. C. Synchrony dynamics during initiation, failure, and rescue of the segmentation clock. *Science* **2007**, 317(5846), 1911-5.
25. Ferjentsik, Z.; Hayashi, S.; Dale, J. K.; Bessho, Y.; Herreman, A.; De Strooper, B.; del Monte, G.; de la Pompa, J. L.; Maroto, M. Notch is a critical component of the mouse somitogenesis oscillator and is essential for the formation of the somites. *PLoS Genet.* **2009**, 5(9), e1000662.
26. Aulehla, A.; Pourquié, O. Oscillating signaling pathways during embryonic development. *Curr. Opin. Cell Biol.* **2008**, 20(6), 632-7.
27. Feller, J.; Schneider, A.; Schuster-Gossler, K.; Gossler, A. Noncyclic Notch activity in the presomitic mesoderm demonstrates uncoupling of somite compartmentalization and boundary formation. *Genes Dev*. **2008**, 15;22(16), 2166-71.
28. Maroto, M.; Dale, J. K.; Dequéant, M. L.; Petit, A. C.; Pourquié, O. Synchronised cycling gene oscillations in presomitic mesoderm cells require cell-cell contact. *Int. J. Dev. Biol.* **2005**, 49(2-3), 309-15.
29. Masamizu, Y.; Ohtsuka, T.; Takashima, Y.; Nagahara, H.; Takenaka, Y.; Yoshikawa, K.; Okamura, H.; Kageyama, R. Real-time imaging of the somite segmentation clock: revelation of unstable oscillators in the individual presomitic mesoderm cells. Proc. Natl. Acad. Sci. USA **2006**, 103(5), 1313-8.
30. Dequéant, M. L.; Glynn, E.; Gaudenz, K.; Wahl, M.; Chen, J.; Mushegian, A.; Pourquié, O. A complex oscillating network of signaling genes underlies the mouse segmentation clock. *Science* **2006**, 314(5805), 1595-8.

31. Dubrulle, J.; McGrew, M. J.; Pourquié, O. FGF signaling controls somite boundary position and regulates segmentation clock control of spatiotemporal Hox gene activation. *Cell* **2001**, 106(2), 219-32.
32. Aulehla, A.; Wehrle, C.; Brand-Saberi, B.; Kemler, R.; Gossler, A.; Kanzler, B.; Herrmann, B. G. Wnt3a plays a major role in the segmentation clock controlling somitogenesis. *Dev. Cell* **2003**, 4(3), 395-406.
33. Sawada, A.; Shinya, M.; Jiang, Y. J.; Kawakami, A.; Kuroiwa, A.; Takeda, H. Fgf/MAPK signalling is a crucial positional cue in somite boundary formation. *Development* **2001**, 128(23), 4873-80.
34. Dubrulle, J.; Pourquié, O. fgf8 mRNA decay establishes a gradient that couples axial elongation to patterning in the vertebrate embryo. *Nature* **2004**, 427(6973), 419-22.
35. Delfini, M. C.; Dubrulle, J.; Malapert, P.; Chal, J.; Pourquié, O. Control of the segmentation process by graded MAPK/ERK activation in the chick embryo. *Proc. Natl. Acad.* Sci. USA **2005,** 102(32), 11343-8.
36. Aulehla, A.; Wiegraebe, W.; Baubet, V.; Wahl, M. B.; Deng, C.; Taketo, M.; Lewandoski, M.; Pourquié, O. A beta-catenin gradient links the clock and wavefront systems in mouse embryo segmentation. *Nat. Cell Biol.* **2008**, 10(2), 186-93.
37. Diez del Corral, R.; Olivera-Martinez, I.; Goriely, A.; Gale, E.; Maden, M.; Storey, K. Opposing FGF and retinoid pathways control ventral neural pattern, neuronal differentiation, and segmentation during body axis extension. *Neuron* **2003**, 40(1), 65-79.
38. Moreno, T. A.; Kintner, C. Regulation of segmental patterning by retinoic acid signaling during Xenopus somitogenesis. *Dev. Cell* **2004**, 6(2), 205-18.
39. Swindell, E. C.; Thaller, C.; Sockanathan, S.; Petkovich, M.; Jessell, T. M.; Eichele, G. Complementary domains of retinoic acid production and degradation in the early chick embryo. *Dev. Biol*. **1999**, 216(1), 282-96.
40. Fliegauf, M.; Benzing, T.; Omran, H. When cilia go bad: cilia defects and ciliopathies. *Nat. Rev. Mol. Cell Biol*. **2007**, 8(11), 880-93.
41. Gerdes, J. M.; Davis, E. E.; Katsanis, N. The vertebrate primary cilium in development, homeostasis, and disease. *Cell* **2009**, 137(1), 32-45.
42. Hamada, H. (2008). Breakthroughs and future challenges in left-right patterning. *Dev. Growth Differ.* **2008**, Suppl 1, S71-8.
43. Collignon, J.; Varlet, I.; Robertson, E. J. Relationship between asymmetric nodal expression and the direction of embryonic turning. *Nature* **1996**, 381(6578), 155-8.
44. Raya, A.; Kawakami, Y.; Rodríguez-Esteban, C.; Ibañes, M.; Rasskin-Gutman, D.; Rodríguez-León, J.; Büscher, D.; Feijó, J. A.; Izpisúa Belmonte, J. C. Notch activity acts as a sensor for extracellular calcium during vertebrate left-right determination. *Nature* **2004**, 427(6970), 121-8.
45. Gourronc, F.; Ahmad, N.; Nedza, N.; Eggleston, T.; Rebagliati, M. Nodal activity around Kupffer's vesicle depends on the T-box transcription factors Notail and Spadetail and on Notch signaling. *Dev. Dyn*. **2007**, 236(8), 2131-46.
46. Meyers, E. N.; Martin, G. R. Differences in left-right axis pathways in mouse and chick: functions of FGF8 and SHH. Science **1999**, 285(5426), 403-6.

47. Albertson, R. C.; Yelick, P. C. Roles for fgf8 signaling in left-right patterning of the visceral organs and craniofacial skeleton. *Dev. Biol*. **2005**, 283(2), 310-21.
48. Nakaya, M. A.; Biris, K.; Tsukiyama, T.; Jaime, S.; Rawls, J. A.; Yamaguchi, T. P. Wnt3a links left-right determination with segmentation and anteroposterior axis elongation. *Development* **2005**, 132(24), 5425-36.
49. Rodríguez-Esteban, C.; Capdevila, J.; Kawakami, Y.; Izpisúa Belmonte, J. C. Wnt signaling and PKA control Nodal expression and left-right determination in the chick embryo. *Development* **2001**, 128(16), 3189-95.
50. Afzelius, B. A. A human syndrome caused by immotile cilia. *Science* **1976**, 193(4250), 317-9.
51. Afzelius, B. A. The immotile-cilia syndrome: a microtubule-associated defect. *CRC Crit. Rev. Biochem*. **1985**, 19(1), 63-87.
52. Supp, D. M.; Witte, D. P.; Potter, S. S.; Brueckner, M. Mutation of an axonemal dynein affects left-right asymmetry in inversus viscerum mice. *Nature* **1997**, 389(6654), 963-6.
53. Sulik, K.; Dehart, D. B.; Iangaki, T.; Carson, J. L.; Vrablic, T.; Gesteland, K.; Schoenwolf, G. C. Morphogenesis of the murine node and notochordal plate. *Dev. Dyn*. **1994**, 201(3), 260-78.
54. Singh, G.; Supp, D. M.; Schreiner, C.; McNeish, J.; Merker, H. J.; Copeland, N. G.; Jenkins, N. A.; Potter, S. S.; Scott, W. legless insertional mutation: morphological, molecular, and genetic characterization. *Genes Dev*. **1991**, 5(12A), 2245-55.
55. Schreiner, C. M.; Scott WJ Jr,; Supp, D. M.; Potter, S. S. Correlation of forelimb malformation asymmetries with visceral organ situs in the transgenic mouse insertional mutation, legless. *Dev. Biol*. **1993**, 158(2), 560-2.
56. Lowe, L. A.; Supp, D. M.; Sampath, K.; Yokoyama, T.; Wright, C. V.; Potter, S. S.; Overbeek, P.; Kuehn, M. R. Conserved left-right asymmetry of nodal expression and alterations in murine situs inversus. *Nature* **1996**, 381(6578),158-61.
57. Nonaka, S.; Tanaka, Y.; Okada, Y.; Takeda, S.; Harada, A.; Kanai, Y.; Kido, M.; Hirokawa, N. Randomization of left-right asymmetry due to loss of nodal cilia generating leftward flow of extraembryonic fluid in mice lacking KIF3B motor protein. *Cell* **1998**, 95(6), 829-37.
58. Nonaka, S.; Yoshiba, S.; Watanabe, D.; Ikeuchi, S.; Goto, T.; Marshall, W. F.; Hamada, H. De novo formation of left-right asymmetry by posterior tilt of nodal cilia. *PLoS Biol*. **2005**, 3(8), e268.
59. Nonaka, S.; Shiratori, H.; Saijoh, Y.; Hamada, H. Determination of left-right patterning of the mouse embryo by artificial nodal flow. *Nature* **2002**, 418(6893), 96-9.
60. Okada, Y.; Nonaka, S.; Tanaka, Y.; Saijoh, Y.; Hamada, H.; Hirokawa, N. Abnormal nodal flow precedes situs inversus in iv and inv mice. *Mol. Cell* **1999**, 4(4), 459-68.
61. Tanaka, Y.; Okada, Y.; Hirokawa, N. FGF-induced vesicular release of Sonic hedgehog and retinoic acid in leftward nodal flow is critical for left-right determination. *Nature* **2005**, 435(7039), 172-7.
62. McGrath, J.; Somlo, S.; Makova, S.; Tian, X.; Brueckner, M. Two populations of node monocilia initiate left-right asymmetry in the mouse. *Cell* **2003**, 114(1), 61-73.
63. Tabin, C. J.; Vogan, K. J. A two-cilia model for vertebrate left-right axis specification. *Genes Dev*. **2003**, 17(1), 1-6.

64. Essner, J. J.; Amack, J. D.; Nyholm, M. K.; Harris, E. B.; Yost, H. J. Kupffer's vesicle is a ciliated organ of asymmetry in the zebrafish embryo that initiates left-right development of the brain, heart and gut. *Development* **2005**, 132(6), 1247-60.
65. Kramer-Zucker, A. G.; Olale, F.; Haycraft, C. J.; Yoder, B. K.; Schier, A. F.; Drummond, I. A. Cilia-driven fluid flow in the zebrafish pronephros, brain and Kupffer's vesicle is required for normal organogenesis. *Development* **2005**, 132(8), 1907-21.
66. Hojo, M.; Takashima, S.; Kobayashi, D.; Sumeragi, A.; Shimada, A.; Tsukahara, T.; Yokoi, H.; Narita, T.; Jindo, T.; Kage, T.; Kitagawa, T.; Kimura, T.; Sekimizu, K.; Miyake, A.; Setiamarga, D.; Murakami, R.; Tsuda, S.; Ooki, S.; Kakihara, K.; Naruse, K.; Takeda, H. Right-elevated expression of charon is regulated by fluid flow in medaka Kupffer's vesicle. Dev. Growth Differ. **2007**, 49(5), 395-405.
67. Neugebauer, J. M.; Amack, J. D.; Peterson, A. G.; Bisgrove, B. W.; Yost, H. J. FGF signalling during embryo development regulates cilia length in diverse epithelia. *Nature* **2009**, 458(7238), 651-4.
68. Okada, Y.; Takeda, S.; Tanaka, Y.; Belmonte, J. C.; Hirokawa, N. Mechanism of nodal flow: a conserved symmetry breaking event in left-right axis determination. *Cell* **2005**, 121(4), 633-44.
69. Schweickert, A.; Weber, T.; Beyer, T.; Vick, P.; Bogusch, S.; Feistel, K.; Blum, M. Cilia-driven leftward flow determines laterality in Xenopus. *Curr. Biol*. **2007**, 17(1), 60-6.
70. Vick, P.; Schweickert, A.; Weber, T.; Eberhardt, M.; Mencl, S.; Shcherbakov, D.; Beyer, T.; Blum, M. Flow on the right side of the gastrocoel roof plate is dispensable for symmetry breakage in the frog Xenopus laevis. *Dev. Biol*. **2009**, 331(2), 281-91.
71. Essner, J. J.; Vogan, K. J.; Wagner, M. K.; Tabin, C. J.; Yost, H. J.; Brueckner, M. Conserved function for embryonic nodal cilia. *Nature* **2002**, 418(6893), 37-8.
72. Männer, J. Does an equivalent of the "ventral node" exist in chick embryos? A scanning electron microscopic study. *Anat. Embryol. (Berl)* **2001**, 203(6), 481-90.
73. Pagán-Westphal, S. M. and Tabin, C. J. The transfer of left-right positional information during chick embryogenesis. *Cell* **1998**. 93(1), 25-35.
74. Gros, J.; Feistel, K.; Viebahn, C.; Blum, M. and Tabin, C. J. Cell movements at Hensen's node establish left/right asymmetric gene expression in the chick. *Science* **2009**. 324(5929): 941-4.
75. Cui, C.; Little, C. D. and Rongish, B. J. Rotation of organizer tissue contributes to left-right asymmetry. *Anat. Rec. (Hoboken)* **2009**. 292(4):557-61.
76. Levin, M.; Thorlin, T.; Robinson, K. R.; Nogi, T.; Mercola, M. Asymmetries in H+/K+-ATPase and cell membrane potentials comprise a very early step in left-right patterning. *Cell* **2002**, 111(1), 77-89.
77. Levin, M.; Mercola, M. Gap junctions are involved in the early generation of left-right asymmetry. *Dev. Biol*. **1998**, 203(1), 90-105.
78. Levin, M.; Mercola, M. Gap junction-mediated transfer of left-right patterning signals in the early chick blastoderm is upstream of Shh asymmetry in the node. *Development* **1999**, 126(21), 4703-14.
79. Kawakami, Y.; Raya, A.; Raya, R. M.; Rodríguez-Esteban, C.; Belmonte, J. C. Retinoic acid signalling links left-right asymmetric patterning and bilaterally symmetric somitogenesis in the zebrafish embryo. *Nature* **2005**, 435(7039), 165-71.

80. Adams, D. S.; Robinson, K. R.; Fukumoto, T.; Yuan, S.; Albertson, R. C.; Yelick, P.; Kuo, L.; McSweeney, M.; Levin, M. Early, H+-V-ATPase-dependent proton flux is necessary for consistent left-right patterning of non-mammalian vertebrates. *Development* **2006**, 133(9), 1657-71.
81. Shu, X.; Huang, J.; Dong, Y.; Choi, J.; Langenbacher, A.; Chen, J. N. Na,K-ATPase alpha2 and Ncx4a regulate zebrafish left-right patterning. *Development* **2007**, 134(10), 1921-30.
82. Sarmah, B.; Latimer, A. J.; Appel, B.; Wente, S. R. Inositol polyphosphates regulate zebrafish left-right asymmetry. *Dev. Cell* **2005**, 9(1), 133-45.
83. Hatler, J. M.; Essner, J. J.; Johnson, R. G. A gap junction connexin is required in the vertebrate left-right organizer. *Dev. Biol*. **2009**, 336(2), 183-91.
84. Fukumoto, T.; Kema, I. P.; Levin, M. Serotonin signaling is a very early step in patterning of the left–right axis in chick and frog embryos. Curr. Biol. **2005**, 15, 794–803.
85. Fukumoto, T.; Blakely, R.; Levin, M. Serotonin transporter function is an early step in left-right patterning in chick and frog embryos. Dev. Neurosci. **2005**, 27(6), 349-63.
86. Gardner, R. L. Normal bias in the direction of fetal rotation depends on blastomere composition during early cleavage in the mouse. *PLoS One* **2010**. 5(3):e9610.
87. Kuroda, R.; Endo, B.; Abe, M. and Shimizu, M. Chiral blastomere arrangement dictates zygotic left-right asymmetry pathway in snails. *Nature* **2009**. 462(7274):790-4.
88. Brend, T. and Holley, S. A. Balancing segmentation and laterality during vertebrate development. *Semin. Cell Dev. Biol.* **2009**. 20(4):472-8.
89. Niederreither, K.; Dollé, P. Retinoic acid in development: towards an integrated view. *Nat. Rev. Genet*. **2008**, 9(7), 541-53.
90. Vermot, J.; Gallego Llamas, J.; Fraulob, V.; Niederreither, K.; Chambon, P.; Dollé, P. Retinoic acid controls the bilateral symmetry of somite formation in the mouse embryo. *Science* **2005**, 308(5721), 563-6.
91. Lowe, L. A.; Supp, D. M.; Sampath, K.; Yokoyama, T.; Wright, C. V.; Potter, S. S.; Overbeek, P. and Kuehn, M. R. Conserved left-right asymmetry of nodal expression and alterations in murine situs inversus. *Nature* **1996**. 381(6578):158-61.
92. Long, S.; Ahmad, N. and Rebagliati, M. The zebrafish nodal-related gene southpaw is required for visceral and diencephalic left-right asymmetry. *Development* **2003**. 130(11):2303-16.
93. Sirbu, I. O.; Duester, G. Retinoic-acid signalling in node ectoderm and posterior neural plate directs left-right patterning of somitic mesoderm. *Nat. Cell Biol*. **2006**, 8(3), 271-7.
94. Vermot, J.; Pourquié, O. Retinoic acid coordinates somitogenesis and left-right patterning in vertebrate embryos. *Nature* **2005**, 435(7039), 215-20.
95. Vilhais-Neto, G. C.; Maruhashi, M.; Smith, K. T.; Vasseur-Cognet, M.; Peterson, A. S.; Workman, J. L.; Pourquié, O. Rere controls retinoic acid signalling and somite bilateral symmetry. *Nature* **2010**, 463(7283), 953-7.
96. Boettger, T.; Wittler, L.; Kessel, M. FGF8 functions in the specification of the right body side of the chick. *Curr. Biol*. **1999**, 9(5), 277-80.
97. Isaac, A.; Sargent, M. G.; Cooke, J. Control of vertebrate left-right asymmetry by a snail-related zinc finger gene. *Science* **1997**, 275(5304), 1301-4.

98. Sefton, M.; Sánchez, S.; Nieto, M. A. Conserved and divergent roles for members of the Snail family of transcription factors in the chick and mouse embryo. *Development* **1998**, 125(16), 3111-21.
99. Morales, A. V.; Acloque, H.; Ocaña, O. H.; de Frutos, C. A.; Gold, V.; Nieto, M. A. Snail genes at the crossroads of symmetric and asymmetric processes in the developing mesoderm. *EMBO Rep*. **2007**, 8(1), 104-9.
100. Fior, R.; Henrique, D. "Notch-Off": a perspective on the termination of Notch signalling. *Int. J. Dev. Biol*. **2009**, 53(8-10), 1379-84.
101. Echeverri, K.; Oates, A. C. Coordination of symmetric cyclic gene expression during somitogenesis by Suppressor of Hairless involves regulation of retinoic acid catabolism. *Dev. Biol*. **2007**, 301(2), 388-403.
102. Saúde, L.; Lourenço, R.; Gonçalves, A.; Palmeirim, I. terra is a left-right asymmetry gene required for left-right synchronization of the segmentation clock. *Nat. Cell Biol*. **2005**, 7(9), 918-20.
103. Seo, K. W.; Wang, Y.; Kokubo, H.; Kettlewell, J. R.; Zarkower, D. A.; Johnson, R. L. Targeted disruption of the DM domain containing transcription factor Dmrt2 reveals an essential role in somite patterning. *Dev. Biol*. **2006**, 290(1), 200-10.
104. Andrade R.P.; Palmeirim, I; Bajanca, F. Molecular clocks underlying vertebrate embryo segmentation: a 10-year-old hairy-go-round. *Birth Defects Res. C Embryo Today* **2007**, 81(2), 65-83.
105. Bulman, M. P.; Kusumi, K.; Frayling, T. M.; McKeown, C.; Garrett, C.; Lander, E. S.; Krumlauf, R.; Hattersley, A. T.; Ellard, S.; Turnpenny, P. D. Mutations in the human delta homologue, DLL3, cause axial skeletal defects in spondylocostal dysostosis. *Nat. Genet*. **2000**, 24(4), 438-41.
106. Whittock, N. V.; Sparrow, D. B.; Wouters, M. A.; Sillence, D.; Ellard, S.; Dunwoodie, S. L.; Turnpenny, P. D. Mutated MESP2 causes spondylocostal dysostosis in humans. *Am. J. Hum. Genet*. **2004**, 74(6), 1249-54.
107. Sparrow, D. B.; Chapman, G.; Wouters, M. A.; Whittock, N. V.; Ellard, S.; Fatkin, D.; Turnpenny, P. D.; Kusumi, K.; Sillence, D.; Dunwoodie, S. L. Mutation of the LUNATIC FRINGE gene in humans causes spondylocostal dysostosis with a severe vertebral phenotype. *Am. J. Hum. Genet*. **2006**, 78(1), 28-37.
108. Gruneberg, H. Genetical studies on the skeleton of the mouse: XXIX. PUDGY. Genet. Res. **1961**, 2, 384–393.
109. Saga, Y.; Hata, N.; Koseki, H.; Taketo, M. M. Mesp2: a novel mouse gene expressed in the presegmented mesoderm and essential for segmentation initiation. *Genes Dev*. **1997**, 11(14), 1827-39.
110. Zhang, N.; Gridley, T. Defects in somite formation in lunatic fringe-deficient mice. *Nature* **1998**, 394(6691), 374-7.
111. McDaniell, R.; Warthen, D. M.; Sanchez-Lara, P. A.; Pai, A.; Krantz, I. D.; Piccoli, D. A.; Spinner, N. B. NOTCH2 mutations cause Alagille syndrome, a heterogeneous disorder of the notch signaling pathway. *Am. J. Hum. Genet*. **2006**, 79(1), 169-73.
112. Kreiborg, S.; Barr, M. Jr.; Cohen, M. M. Jr. Cervical spine in the Apert syndrome. *Am. J. Med. Genet*. **1992**, 43(4), 704-8.

113. Ramsdell, A. F. Left-right asymmetry and congenital cardiac defects: getting to the heart of the matter in vertebrate left-right axis determination. *Dev. Biol*. **2005**, 288(1), 1-20.
114. Lurie, I. W.; Kappetein, A. P.; Loffredo, C. A.; Ferencz, C. Non-cardiac malformations in individuals with outflow tract defects of the heart: the Baltimore-Washington Infant Study (1981-1989). *Am. J. Med. Genet*. **1995**, 59(1), 76-84.
115. Nugent, E.W.; Plauth, W. H.; Edwards, J. E. The pathology, pathophysiology, recognition and treatment of congenital heart disease. McGraw-Hill, New York **1994**
116. Sternick, E. B.; Márcio Gerken, L.; Max, R.; Osvaldo Vrandecic, M. Radiofrequency catheter ablation of an accessory pathway in a patient with Wolff-Parkinson-White and Kartagener's syndrome. *Pacing Clin. Electrophysiol*. **2004**, 27(3), 401-4.
117. Bowers, P. N.; Brueckner, M.; Yost, H. J. The genetics of left-right development and heterotaxia. *Semin. Perinatol*. **1996**, 20(6), 577-88.
118. Kartagener, M.; Stucki, P. Bronchiectasis with situs inversus. *Arch. Pediatr*. **1962**, 79, 193-207.
119. Kennedy, M. P.; Omran, H.; Leigh, M. W.; Dell, S.; Morgan, L.; Molina, P. L.; Robinson, B. V.; Minnix, S. L.; Olbrich, H.; Severin, T.; Ahrens, P.; Lange, L.; Morillas, H. N.; Noone, P. G.; Zariwala, M. A. and Knowles, M. R. Congenital heart disease and other heterotaxic defects in a large cohort of patients with primary ciliary dyskinesia. *Circulation* **2007**. 115(22):2814-21.
120. Debrus, S.; Sauer, U.; Gilgenkrantz, S.; Jost, W.; Jesberger, H. J.; Bouvagnet, P. Autosomal recessive lateralization and midline defects: blastogenesis recessive 1. *Am. J. Med. Genet.* **1997**, 68(4), 401-4.
121. Levin, M. Left-right asymmetry in embryonic development: a comprehensive review. *Mech. Dev.* **2005**. 122(1):3-25

APPENDIX II

Lopes *et al.*, 2010

Development ePress online publication date 28 September 2010

Development 137, 3625-3632 (2010) doi:10.1242/dev.054452

Notch signalling regulates left-right asymmetry through ciliary length control

Susana S. Lopes[1,2], Raquel Lourenço[1,2], Luís Pacheco[2], Nuno Moreno[2], Jill Kreiling[3] and Leonor Saúde[1,2,*]

SUMMARY

The importance of cilia in embryonic development and adult physiology is emphasized by human ciliopathies. Despite its relevance, molecular signalling pathways behind cilia formation are poorly understood. We show that Notch signalling is a key pathway for cilia length control. In *deltaD* zebrafish mutants, cilia length is reduced in Kupffer´s vesicle and can be rescued by the ciliogenic factor *foxj1a*. Conversely, cilia length increases when Notch signalling is hyperactivated. Short cilia found in *deltaD* mutants reduce the fluid flow velocity inside Kupffer´s vesicle, thus compromising the asymmetric expression of the flow sensor *charon*. Notch signalling brings together ciliary length control and fluid flow hydrodynamics with transcriptional activation of laterality genes. In addition, our *deltaD* mutant analysis discloses an uncoupling between gut and heart laterality.

KEY WORDS: Notch, Cilia, Left-right, Zebrafish

INTRODUCTION

Internal body left-right (LR) asymmetry is a common trait among vertebrates. In contrast to the symmetric external body plan, the heart, digestive organs and parts of the brain display highly conserved asymmetric orientations that are essential for their correct functions. When the normal asymmetric distribution of the internal organs is compromised, human laterality disorders arise such as heterotaxy and situs inversus (Fliegauf et al., 2007; Gerdes et al., 2009).

The establishment of LR asymmetries in vertebrates occurs during early stages of embryonic development through a complex process involving epigenetic and genetic mechanisms. This culminates in the activation of a conserved Nodal signalling cascade that starts at the node and is then transferred to the left lateral plate mesoderm (LPM) (Hamada, 2008). Although the timing and mechanism responsible for breaking the initial embryonic symmetry might differ between species, it is clear that a directional fluid flow generated by motile cilia present in the node plays a fundamental role in LR determination, most likely by creating a LR information bias in the node (Levin and Palmer, 2007). Several lines of evidence support this idea, namely absent cilia in the mouse (Nonaka et al., 1998), shorter cilia in zebrafish mutants and morphants (Kramer-Zucker et al., 2005; Neugebauer et al., 2009), and immotile cilia in mouse, zebrafish and medaka (Essner et al., 2005; Hojo et al., 2007; Supp et al., 1999). All these cilia defects result in altered fluid flow in the node/Kupffer's vesicle (KV) and ultimately in LR defects. This implies that proper cilia length regulation is crucial for the establishment of LR asymmetries.

Expression of *Nodal* and of its antagonist *Cerl2* (*Dand5* – Mouse Genome Informatics) in the mouse node starts symmetrically (Collignon et al., 1996; Marques et al., 2004). However, the mechanism that produces asymmetrical expression of *Nodal* and *Cerl2* on the left and right sides of the node, and its potential link to the leftward nodal flow, is not fully understood. In zebrafish, there is no evidence for asymmetric expression of *spaw* and of its negative regulator *charon* in KV. Nevertheless, it has been suggested that an asymmetric Charon function inhibits the transfer of *spaw* to the right LPM (Hashimoto et al., 2004). To date, the relationship between the fluid flow inside KV and the asymmetric function of Charon in medaka and its homologue Coco in *Xenopus* have been studied (Hojo et al., 2007; Schweickert et al., 2010), but this relationship has not been explored in zebrafish.

Notch signalling has been implicated in LR patterning in vertebrates, largely through the activation of *Nodal* expression in the murine node (Krebs et al., 2003; Przemeck et al., 2003; Raya et al., 2003; Takeuchi et al., 2007). In zebrafish, Notch signalling seems to activate *charon* expression in KV (Gourronc et al., 2007).

Apart from providing the first genetic evidence in zebrafish for the activation of *charon* expression in KV, we demonstrate that canonical Notch signalling, through the DeltaD ligand, is a key regulator of ciliary length at the KV. We show that reduction of Notch signalling produces shorter cilia, whereas hyperactivation of Notch produces longer cilia; thus, providing new insights into how cilia length is modulated. We find that the correct regulation of cilia length has a strong impact on the directionality and speed of fluid flow inside KV, and we were able to show that this biomechanical event correlates with asymmetric transcription of *charon*. Altogether, our results reveal a new and multistep role for the Notch signalling pathway that couples two fundamental processes in left-right determination: transcription of *charon* and ciliary length regulation that then culminates in breaking the symmetry of *charon* expression.

MATERIALS AND METHODS

Zebrafish line

AB wild type and mutant (*notch1a*/*des*^{Tp37}, *deltaC*/*bea*^{tit446}, *deltaD*/*aei*^{tr233}) embryos were staged according to Kimmel et al. (Kimmel et al., 1995).

[1]Instituto de Medicina Molecular e Instituto de Histologia e Biologia do Desenvolvimento, Faculdade de Medicina da Universidade de Lisboa, 1649-028 Lisboa, Portugal. [2]Instituto Gulbenkian de Ciência, P-2780-156 Oeiras, Portugal. [3]Department of Molecular Biology, Cell Biology, and Biochemistry, Brown University, Providence, RI 02912, USA.

*Author for correspondence (msaude@fm.ul.pt)

Accepted 25 August 2010

Morpholino antisense oligo (MO) and mRNA microinjections

deltaD-MO as described previously (Holley et al., 2000) was injected from 0.5-1.0 mM into 512-cell stage wild-type embryos. The MO that blocks translation of *Su(H)1* and *Su(H)2* was used as previously described (Echeverri and Oates, 2007). Notch-intracellular and full-length *deltaD* constructs (Takke and Campos-Ortega, 1999; Takke et al., 1999) were injected at the one-cell stage at a concentration of 100 pg and 350 pg, respectively. *foxj1a* and GFP full-length cDNAs were independently cloned into pCS2^{+} and in vitro transcribed using mMESSAGE mMACHINE kit (Ambion). The *foxj1a* and GFP mRNAs were injected at a concentration of 100 pg. Embryos were left to develop at 28°C until the desired stage and then fixed in 4% PFA at 4°C overnight.

In situ hybridization

Whole-mount in situ hybridization was performed as described previously (Thisse and Thisse, 2008). Digoxigenin RNA probes were synthesized from DNA templates of *spaw* (Hashimoto et al., 2004), *pitx2* (Essner et al., 2005), *lefty2* (Bisgrove et al., 2005), *foxa3* (Monteiro et al., 2008), *ntl* (Amack and Yost, 2004), *shh* (Essner et al., 2005), *charon* (Hashimoto et al., 2004), *deltaD* (Takke and Campos-Ortega, 1999), *sox17* (Amack and Yost, 2004) and *foxj1a* (Neugebauer et al., 2009; Yu et al., 2008).

Antibody staining and immunofluorescence

We followed the methods described previously (Neugebauer et al., 2009) for immunostaining. In some cases, we also used TOPRO-3 (1:1000; Invitrogen) diluted in blocking solution.

Confocal microscopy

Flat-mounted embryos were examined with a Zeiss LSM 510 Meta confocal microscope. Three-colour confocal *z*-series images were acquired using sequential laser excitation, converted into a single plane projection and analyzed using ImageJ software (LSM Reader). The length of all cilia in each KV was measured using ImageJ Segmented Line Tool.

High-speed video microscopy

We used the confocal microscope Leica SP5 under the resonance mode, which allows imaging at 8000 lines per second, to acquire images of ciliary beating and debris movements inside KV of live embryos mounted in 1% low-melting agarose (Sigma). High-speed films of the debris were analyzed using ImageJ and the velocity was measured by tracing the debris frame by frame. The orientation and speed of the debris were calculated using Excel VBA, and vectors were drawn using the Gnuplot software and Gimp.

Determination of KV cilia distribution

The total number of cilia and their distribution within KV were determined from confocal *z*-stacks as previously described (Kreiling et al. 2007).

RESULTS

DeltaD is the Notch ligand that defines laterality in zebrafish

In order to study the impact of Notch signalling pathway on crucial steps for LR patterning, we used several mutants and reagents. We started by evaluating the asymmetric information in the LPM using the left-identity molecular markers *spaw* and *pitx2*. The *nodal*-related gene *spaw* is the earliest molecule to be asymmetrically detected in the left LPM and is known to induce the expression of the transcription factor *pitx2* (Hamada et al., 2002; Long et al., 2003).

We show that mutants in the Notch transmembrane receptor, *des/notch1a*$^{-/-}$, lose their laterality identity by becoming largely bilateral (Fig. 1A,B). Upon binding to its ligand, the intracellular domain of Notch (NICD) is cleaved and translocates into the nucleus. In the nucleus, NICD binds to Suppressor-of-Hairless [Su(H)] thereby changing its repressor status to an activator (Fior and Henrique, 2009). In zebrafish, two *Su(H)* gene paralogs (*rbpja* and *rbpjb* – Zebrafish Information Network) can be knocked down using a single antisense morpholino that blocks the translation of both [*Su(H)1+2-MO*] (Echeverri and Oates, 2007). Consistent with our results, *Su(H)1+2* morphants also showed lack of laterality identity (Fig. 1A,B). To directly induce the Notch pathway, we injected the mRNA encoding NICD and, similar to what has been described previously (Raya et al., 2003), we again found a loss in laterality (Fig. 1A,B). These results indicate that canonical Notch signalling is required to define laterality in the LPM.

In order to assess which Notch ligand was the most relevant in LR establishment, the expression of the left-sided markers was analysed in the null mutants *aei/deltaD*$^{-/-}$ and *bea/deltaC*$^{-/-}$. In clear contrast to *bea*$^{-/-}$, *aei*$^{-/-}$ mutants have a strong *pitx2* laterality phenotype that can be rescued by NICD (Fig. 1B). Thus, we identified DeltaD as the key Notch ligand for LR asymmetry in zebrafish and we focus our analysis on this null mutant. We find that the bilateral expression of *pitx2* does not always follow the expression of *spaw* (compare Fig. 1A with 1B). A lack of a precise correlation between the expression of *nodal* and *pitx2* in the LPM was already described in the context of delta-like 1 (*Dll1*) mouse mutants (Krebs et al., 2003; Przemeck et al., 2003; Raya et al., 2003). Altogether, these results show that Notch signalling regulates *pitx2* expression in a Nodal/Spaw independent manner.

The axial midline is required to maintain LR asymmetry by acting as a midline barrier (Chin et al., 2000; Hamada et al., 2002). We checked whether the LR defects that arise upon Notch signalling perturbation were due to lack of a midline. We found that the expression pattern of both *shh* and *ntl* markers was normal in all the experimental conditions (see Fig. S1A-N in the supplementary material), with the exception of *ntl* downregulation in NICD-injected embryos (see Fig. S1N in the supplementary material), in agreement with what has been described previously (Latimer and Appel, 2006). Therefore, LR defects arising from reduced Notch signalling are not likely to be due to an absent midline.

DeltaD maintains *spaw* expression in the posterior left LPM

In *aei*$^{-/-}$ mutants, *spaw* expression is only mildly randomized (Fig. 1A), but the expression scored as being left-sided (Fig. 1A) shows three distinct patterns that have been quantified in detail in Fig. 1C. Namely, we could detect *spaw* expression in a left anterior domain (Fig. 1C,D,D′), in a left anterior and posterior domains (Fig. 1C,F,F′), and in a left anterior domain with bilateral posterior domains with competition (Fig. 1C,G). Although, a posterior downregulation of *spaw* occurs at the 23-somite stage as part of its normal anteroposterior (AP) expression pattern (Long et al., 2003), our analysis using an *aei* heterozygous cross, clearly shows that this *spaw* downregulation occurs prematurely at the 16-somite stage in 67% of the homozygous embryos (Fig. 1C,D,D′). In agreement with this posterior downregulation of *spaw*, we observe that *lefty1*, which is known to be induced by Spaw (Long et al., 2003; Wang and Yost, 2008), has also an abnormal expression gap in the corresponding midline domain (Fig. 1E). These results suggest that the maintenance of *spaw* expression in the posterior left LPM and possibly *lefty1* in the midline domain require DeltaD function.

DeltaD controls gut laterality

Next, we evaluated the impact that the abnormal expression of *spaw* and *pitx2* seen in *aei*$^{-/-}$ mutants has on heart and gut positioning. We scored *aei*$^{-/-}$ mutants for heart asymmetry in vivo and made use of the prospective heart marker *lefty2* and of the gut marker *foxa3* in fixed embryos. We show that in *aei*$^{-/-}$ mutants, gut

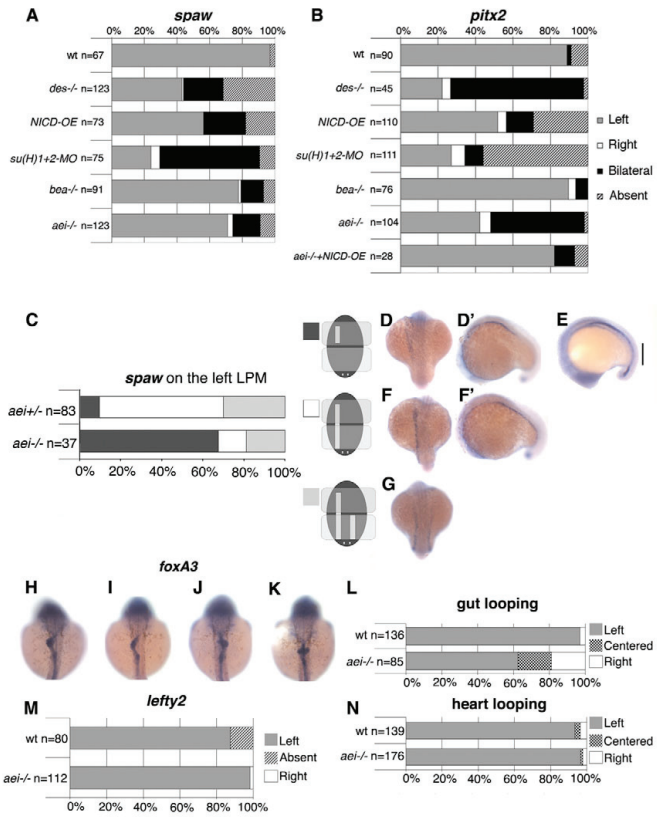

Fig. 1. Canonical Notch signalling through the DeltaD ligand controls left-right patterning. (**A**,**B**) Percentages of normal (Left, grey), reversed (Right, white), bilateral (black) and absent (stripes) expression of *spaw* (A) and *pitx2* (B) in the lateral plate mesoderm when Notch signalling was challenged. Embryos were analysed between the 14- and 18-somite stages for *spaw* expression and between the 18- and 20-somite stages for *pitx2*. (**C**) Percentages of different domains of left-sided expression of *spaw* in the lateral plate mesoderm. (**D**,**D′**,**F**,**F′**,**G**) In *aei*$^{-/-}$ embryos, *spaw* may be expressed in an anterior domain only (D,D′), in an anterior with bilateral posterior domains (F,F′), and in anterior and posterior domains with competition on the right side (G). (**E**) A double *spaw* and *lefty1* in situ hybridization showing the posterior gap (vertical line) of these two markers in an *aei*$^{-/-}$ embryo. (**H-K**) Expression of *foxa3* in the gut in 50-53 hpf embryos (dorsal views). In wild-type embryos, the gut loops to the left (H). In *aei*$^{-/-}$ embryos, the gut may loop to the left (I), or to the right (J), or show no looping (K). (**L**) Percentages of normal (Left), reversed (Right) or no looping of the gut at 50-53 hpf. (**M**) Percentages of normal (Left), reversed (Right) or absent *lefty2* in the lateral plate mesoderm at the 26-somite stage. (**N**) Percentages of normal (Left), reversed (Right) or no jogging (Centered) of the heart at 30-32 hpf.

looping is randomized (62.3% loops to the left, 18.8% failed loops and 18.8% loops to the right; n=85) (Fig. 1H-L). By contrast, heart jogging is not significantly affected when evaluated by *lefty2* expression at 26-somite stage (99% on the left; n=112) or when judged by direct observation at 30 hpf (90.7% on the left; n=65) (Fig. 1M,N). These results indicate the uncoupling of laterality of an anterior organ, such as the heart, and of more posterior organs, such as the liver and pancreas. The heart is the first organ to be asymmetrically positioned in zebrafish, and it seems that its asymmetry may arise by a mechanism different from that governing other viscera, as suggested by others (Chin et al., 2000; Lin and Xu, 2009).

Our data indicate that the prospective heart domain is unaffected in the *aei*$^{-/-}$ mutants and thus provide an explanation for why heart laterality is not disturbed. Namely, the anterior left-sided LPM expression of *spaw* is unaffected and *pitx2* does not reach the anterior-most domain when expressed on the right LPM. We propose that the premature absence of *spaw* expression in the posterior LPM, coupled with a bilateral *pitx2* expression in this region could underlie the gut laterality phenotype observed in 40% of *aei*$^{-/-}$ mutants.

DeltaD regulates cilia length in KV

Increasing evidence shows that a properly formed node/KV with a directional strong fluid flow driven by the beating of motile cilia is essential for LR determination (Amack et al., 2007; Hamada, 2008). We therefore investigated whether the laterality problems observed in *aei*$^{-/-}$ mutants were due to KV morphogenesis and/or ciliogenesis defects.

To test KV integrity, we performed immunostaining with ZO-1, a tight junction marker and aPKC an apical epithelial marker (Neugebauer et al., 2009) and observed live embryos with high resolution DIC microscopy. The three approaches revealed that KV structure is normal both in *aei*$^{-/-}$ mutants and in *deltaD* overexpressing embryos (Fig. 2A-I). We thus conclude that KV morphogenesis and polarity are not affected by downregulation or upregulation of Notch signalling.

To investigate the role of DeltaD in cilia formation, we labelled the KV cilia with an anti-acetylated α-tubulin antibody. We found that cilia length is significantly reduced in *aei*$^{-/-}$ mutants [Fig. 2J,K,M; 2.25±0.62 μm (s.d.m.); n=20 embryos; $P<4.3\times10^{-9}$) when compared with cilia length in wild-type embryos (Fig. 2J,K,L; 3.73±0.76 μm (s.d.m.); n=27 embryos). Strikingly, we also found that hyperactivation of Notch signalling significantly increased the length of cilia in KV either by injection of NICD [Fig. 2J; 5.28±1.23 μm (s.d.m.); n=19 embryos; $P<3.5\times10^{4}$] or *deltaD* [Fig. 2J,K,N; 6.78±1.18 μm (s.d.m.); n=11 embryos; $P<1.5\times10^{-4}$]. Additionally, we asked whether cilia motility was also affected in *aei*$^{-/-}$ mutants. We filmed the KV cilia in live *aei*$^{-/-}$ embryos and showed that, despite being shorter, cilia are still motile (see Movie 2 in the supplementary material). These results strongly suggest that Notch signalling, through DeltaD, controls ciliary length in KV.

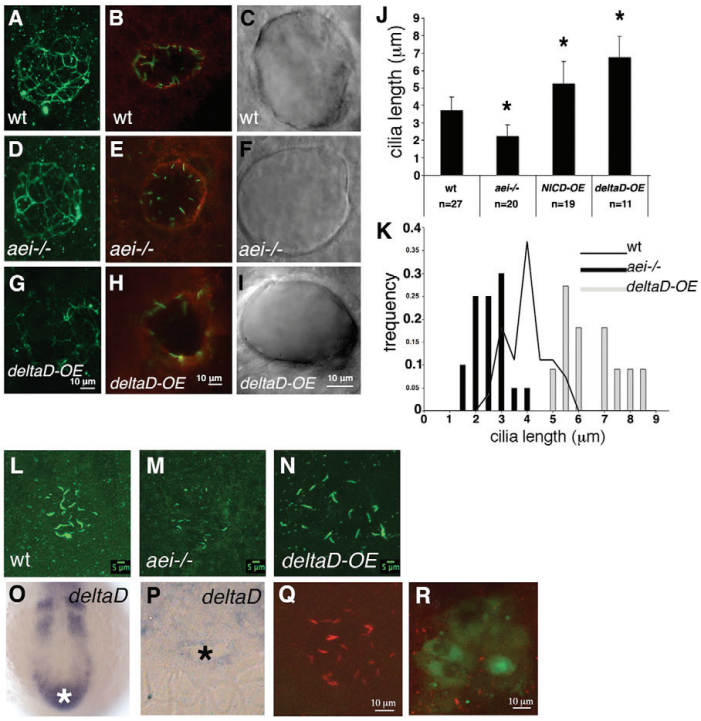

Fig. 2. DeltaD regulates cilia length in the Kupffer's vesicle. (**A**,**D**,**G**) ZO-1 immunostaining of a representative wild-type embryo (A), an *aei*$^{-/-}$ mutant embryo (D) and a *deltaD*-overexpressing embryo (G). (**B**,**E**,**H**) aPKC immunostaining of a representative wild-type embryo (B), an *aei*$^{-/-}$ mutant embryo (E) and a *deltaD*-overexpressing embryo (H). (**C**,**F**,**I**) DIC images of live embryos showing a wild-type KV (C), a KV from an *aei*$^{-/-}$ embryo (F) and a KV from a *deltaD*-overexpressing embryo (I). (**J**) Quantification of ciliary length at 10-somite stages in wild type, in *aei*$^{-/-}$ mutants and in embryos where Notch signalling was hyperactivated by overexpressing NICD (*NICD-OE*) or *deltaD* (*deltaD-OE*). Asterisks indicate experimental conditions that produce changes that are significantly different from wild type ($P<0.001$, Student's *t*-test, two tail for two samples assuming unequal variances). (**K**) Histogram showing the distribution of Kupffer's vesicle ciliary length at 10-somite stages in *aei*$^{-/-}$ mutant embryos (black bars), wild-type embryos (black line) and embryos subjected to *deltaD-OE* (grey bars). (**L-N**) Confocal images of all *z*-sections spaced 1 μm apart through the entire ciliated Kupffer's vesicle at the 10-somite stage. Cilia are labelled with anti-acetylated α-tubulin in a wild-type embryo (L), an *aei*$^{-/-}$ mutant (M) and an embryo subjected to *deltaD-OE* (N). (**O**,**P**) Wild-type *deltaD* expression at the 10-somite stage in whole mount (O) and in resin section (P). The white and the black asterisks label the position and the lumen of the Kupffer's vesicle, respectively. (**Q**,**R**) *deltaD*-MO co-injected with fluorescein lineage tracer in the dorsal forerunner cells (DFCs). (Q) Injected embryo with non-targeted Kupffer's vesicle cells showing normal length cilia. (R) Fluorescein-positive Kupffer's vesicle cells with shorter cilia. Error bars indicate s.d.m.

deltaD is expressed in the KV (Fig. 2O,P) and also in its precursors at the bud stage (10 hpf), in the somites, presomitic mesoderm and tail bud throughout segmentation stages (Hsiao et al., 2007). Therefore, we decided to test whether the short cilia phenotype observed in *aei*$^{-/-}$ mutants is caused by the lack of DeltaD function specifically in the KV precursors or in KV cells. We targeted the dorsal forerunner cells (DFC), which are the KV precursors (Essner et al., 2005), by co-injecting the lineage tracer fluorescein and a *deltaD*-MO at the midblastula stage. In KV cells where fluorescein (and therefore *deltaD*-MO) was successfully detected, we observed a reduction in cilia length comparable with the one quantified in *aei*$^{-/-}$ mutants [Fig. 2R; 2.25 ±0.6 μm (s.d.m.); $n=29$ cells; $P=0.3$) and different from the one quantified in KV cells that were not successfully targeted [Fig. 2Q; 3.6±0.6 μm (s.d.m.); $n=21$ cells; $P<1.6\times10^{-7}$]. This experiment indicates that DeltaD autonomously regulates cilia length at the level of the KV precursors or the KV cells and not in the somites, presomitic mesoderm and tail bud. In agreement, we found that in embryos where KV precursors were successfully targeted with *deltaD*-MO the trend in *spaw* (84% on the left; 7% on the right; 8% bilateral; $n=57$) and *pitx2* (33% on the left; 41% bilateral; 25% absent; $n=12$) expression is similar to the one observed in *aei*$^{-/-}$ mutants. Moreover, embryos injected with *deltaD*-MO at the midblastula stage, showed gut looping defects (74% loops to the left, 18% does not loop and 8% loops to the right; $n=123$) and had no heart laterality problems similar to what we described for the *aei*$^{-/-}$ mutants.

DeltaD maintains proper cilia length through modulation of *foxj1a*

In order to investigate why the *aei*$^{-/-}$ mutant cilia are shorter, we analysed the expression pattern of *foxj1a*, a marker of KV motile cilia (Amack and Yost, 2004; Stubbs et al., 2008; Yu et al., 2008). At the bud stage, the DFC marker *sox17* was detected in both *aei*$^{-/-}$

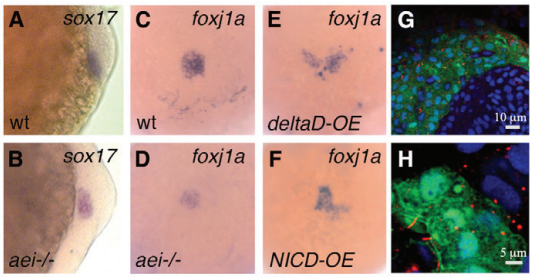

Fig. 3. DeltaD modulates *foxj1a* expression. (**A**,**B**) Expression pattern of *sox17* in Kupffer's vesicle precursor cells at bud stage in wild-type (A) and *aei*$^{-/-}$ mutant (B) embryos. (**C-F**) Expression pattern of *foxj1a* in Kupffer's vesicle precursor cells at bud stage in a wild-type (C), an *aei*$^{-/-}$ mutant (D), a wild type overexpressing *deltaD* and a wild type overexpressing NICD (F). (**G**,**H**) Foxj1a mRNA injection increases ciliary length. (G) Tail region of an *aei*$^{-/-}$ mutant embryo showing GFP-positive cells that were co-targeted with *foxj1a* and GFP mRNA. In these cells, cilia are much larger than in adjacent non-targeted cells. (H) Cells from the Kupffer's vesicle in an *aei*$^{-/-}$ mutant embryo that was co-injected with *foxj1a* and GFP mRNA showing rescued motile cilia judged by the increased ciliary length. α-Acetylated tubulin labels cilia in red, DAPI labels DNA in blue and GFP labels targeted cells in green.

and wild-type embryos (Fig. 3A,B), confirming presence of DFCs. By contrast, *foxj1a* expression was downregulated in *aei*$^{-/-}$ mutants at the same stage compared with wild-type embryos (Fig. 3C,D). We further confirmed that *foxj1a* expression was downregulated at bud stages in 25% of the embryos that resulted from an *aei* heterozygous cross (n=157). In addition, overexpression of both *deltaD* and *NICD* mRNA resulted in ectopic expression of *foxj1a* in the DFCs region at the bud stage (Fig. 3E,F). We thus propose that DeltaD controls KV cilia length via the regulation of *foxj1a.* Consistently, *foxj1a* morphants also show shorter or absent cilia in the KV (Stubbs et al., 2008; Yu et al., 2008).

In order to test whether Notch signalling is working via Foxj1a, we performed an epistatic test by co-injecting *foxj1a* mRNA together with GFP mRNA, as a lineage tracer, into one-cell stage *aei*$^{-/-}$ mutant embryos. We found that cilia length was rescued in the KV cells that expressed GFP (Fig. 3H). Although in the *aei*$^{-/-}$ mutant KV cells the average cilia length was 2.25 μm, in the rescued *aei*$^{-/-}$ mutant cells, the average was 4±0.37 μm (s.d.m.) (n=53 cilia/5 embryos; $P<1.0\times10^{-5}$). This experiment confirmed that *foxj1a* functions downstream of DeltaD.

Short cilia generate a weak fluid flow inside the KV

To evaluate the impact that the shorter cilia of *aei*$^{-/-}$ mutants might have on the fluid flow inside the KV, we measured the velocity of the flow in these mutants and compared it with wild-type embryos. For this, we filmed KVs of live embryos and tracked naturally occurring particles that move with the fluid flow (Fig. 4A,A′,B,B′; see Movies 1 and 2 in the supplementary material). This non-invasive method safeguards the epithelium and natural osmotic pressure inside the KV. We showed that in *aei*$^{-/-}$ mutants, velocity of the fluid flow is less than half than that of its wild-type siblings (Fig. 4C; 6.74 μm/s and 16.46 μm/s, respectively; $P<1.5\times10^{-4}$). Importantly, directionality of the flow is only lost in *aei*$^{-/-}$ mutants (Fig. 4B-B′, see Movie 2 in the supplementary material). Loss of directionality could be due to a perturbation in the normal distribution of cilia inside the KV. However, a detailed 3D reconstruction of the spatial distribution of cilia in the KV of *aei*$^{-/-}$ mutants revealed no significant differences when compared with wild-type embryos (Fig. 4D). We thus conclude that the reduced cilia length documented here constitute the most probable cause for the slow and chaotic fluid flow observed in *aei*$^{-/-}$ mutants.

A strong KV fluid flow promotes asymmetric *charon* expression

Charon is a Cerberus/Dan family secreted factor expressed specifically in the cells that line the posterior domain of the KV in a horseshoe shape (Fig. 4H). This protein negatively regulates Nodal signalling by blocking the transfer of Spaw from the KV to the right side of the LPM in zebrafish and medaka (Hashimoto et al., 2004; Hojo et al., 2007). In addition, it has been suggested that *charon* might be a potential Notch signalling target in zebrafish (Gourronc et al., 2007). We confirmed this possibility by injecting *deltaD* or *NICD* mRNA into one-cell stage wild-type embryos, which resulted in clear ectopic expression of *charon* in the KV region (Fig. 4F,G). By contrast, the expression of *charon* in *aei*$^{-/-}$ mutants was severely reduced in 35.4% of the embryos from eight- to 12-somite stage (Fig. 4O,P), whereas in *bea*$^{-/-}$ mutants it was unaffected. Together, these data confirmed that *charon* is a target of the Notch signalling pathway in zebrafish.

In contrast to what has been described (Hashimoto et al., 2004), we found that *charon* expression in a wild-type zebrafish KV is initially symmetric from the five- to seven-somite stage and then becomes clearly asymmetric on the right side from eight-somite stage onwards (Fig. 4H-K). It is still unclear whether the switch to higher levels on the right side corresponds to a downregulation of *charon* levels on the left side or to an upregulation on the right side of the KV. Our results identify *charon* as the first asymmetric gene expressed in the zebrafish KV and provide a better explanation for the mechanism underlying the asymmetric inhibition of Spaw transfer to the right LPM.

As we show that *charon* expression becomes asymmetric after being symmetrically induced (Fig. 4H-K), we asked whether fluid flow in the KV could be the mechanism controlling this switch, as suggested in medaka and in *Xenopus* (Hojo et al., 2007; Schweickert et al., 2010). In contrast to wild-type embryos where there is a clear shift from symmetric to an asymmetric *charon* expression at the eight-somite stage (Fig. 4K), in the *aei*$^{-/-}$ mutants, this shift does not occur (Fig. 4P). In fact, in *aei*$^{-/-}$ mutant embryos where the expression of *charon* was not severely reduced, we could score it as being symmetric in 43.3% and asymmetric in only 21.3% from 8-12 somite stages (Fig. 4L-P). This suggests that the slower fluid flow in *aei*$^{-/-}$ mutants characterized above is inefficient to promote the asymmetry switch of *charon* expression in KV cells.

Having shown that DeltaD regulates *charon* transcription (Fig. 4L-P), we could hypothesize that the inability to shift to the asymmetric *charon* expression observed in *aei*$^{-/-}$ mutants may be caused by a transcriptional defect and not by the slow flow. To investigate the impact of KV fluid flow on *charon* expression in a transcription competent context, we repeated the experiment in *left-right dynein1* (*lrd1*) morphants. These morphants have a very reduced or absent flow (Essner et al., 2005) and show no problems in *charon* transcription (Gourronc et al., 2007). We injected *lrd1-MO* into wild-type embryos and scored *charon* expression in eight- to 12-somite stage embryos. We observed that in *lrd1* morphants the asymmetric shift in *charon* expression does not occur (Fig. 4R), strengthening the idea that the fluid

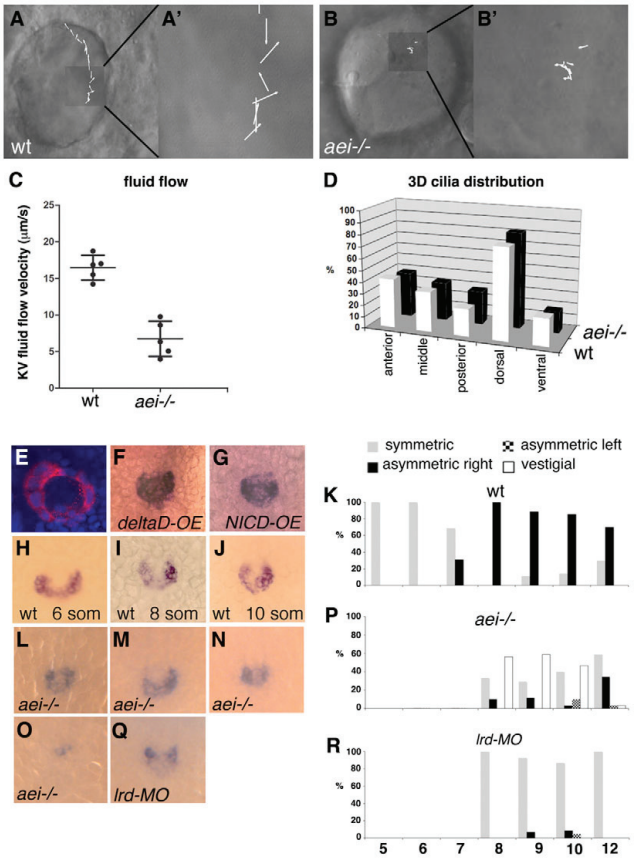

Fig. 4. Short cilia reduce fluid flow inside Kupffer´s vesicle and compromise *charon* asymmetric expression. (**A-B'**) Still images from wild-type siblings (A) and *aei*$^{-/-}$ mutant embryos (B) taken from Movies 1 and 2, respectively, in the supplementary material. Inserts A′ and B′ show vectors representing the fluid flow velocity and direction in each experimental situation. (**C**) Quantification of the average fluid flow velocity in wild type (n=5, 16.46±1.69 μm/s) and in *aei*$^{-/-}$ mutants (n=5, 6.74±2.41 μm/s). (**D**) Percentage of cilia in different regions of Kupffer´s vesicle (anterior, middle, posterior, dorsal and ventral) in wild-type (n=19) and *aei*$^{-/-}$ mutant embryos (n=14). (**E**) A 10-somite stage embryo showing nuclei stained with DAPI in blue and *charon* mRNA cytoplasmic localization in the epithelial cells that surround the lumen of Kupffer´s vesicle. (**F**,**G**) Expression pattern of *charon* in Kupffer´s vesicle of embryos overexpressing *deltaD* (F) and NICD (G). (**H-J**) *charon* expression at Kupffer´s vesicle is symmetric at the six-somite stage (H) and is asymmetric at the eight- and ten-somite stages (I,J). (**K**) Percentage of symmetric versus asymmetric *charon* expression in Kupffer´s vesicle in wild-type embryos from five- to 12-somite stages (n=18 for each stage). (**L-O**) Range of expression patterns of *charon* in Kupffer´s vesicle of *aei*$^{-/-}$ mutant embryos; *charon* expression may be symmetric (L), asymmetric with stronger expression on the right (M), asymmetric with stronger expression on the left (N) or reduced (O). (**P**) Percentages of the different *charon* expression patterns in Kupffer´s vesicle in *aei*$^{-/-}$ mutant embryos from the eight- to 12-somite stages (n=34 on average for each stage). (**Q**) *charon* expression pattern in Kupffer´s vesicle of one representative *lrd1* morphant. (**R**) Percentage of symmetric versus asymmetric *charon* expression in Kupffer´s vesicle of *lrd1* morphants from the eight- to 12-somite stages (n=27 on average for each stage).

flow inside the KV is crucial for inducing asymmetric *charon* expression. Our results, together with those obtained in other species, clearly show that *charon* transcription is sensitive to fluid flow. Therefore, we suggest that *charon* and its homologues may be candidates for flow-sensing genes in the KV/GRP/node environment.

DISCUSSION

The involvement of Notch signalling in the establishment of the left-right axis is evolutionary conserved among vertebrates. However, there are differences in the mode of action of this molecular signalling pathway between mammals and fish. In the mouse, the analysis of Notch pathway mutants reveals that *nodal* induction in the murine node is impaired (Krebs et al., 2003; Przemeck et al., 2003; Raya et al., 2003; Takeuchi et al., 2007), whereas the expression of the secreted Nodal antagonist *cerl2* does not seem to be affected (Krebs et al., 2003; Przemeck et al., 2003; Raya et al., 2003; Takeuchi et al., 2007). By contrast, the expression of *spaw* is normal in zebrafish embryos treated with DAPT (a Notch signalling inhibitor) but the expression of the secreted Nodal antagonist *charon* is severely affected in the KV (Gourronc et al., 2007). Using a genetic approach, we were able to confirm and extend these pharmacological results to conclude that the relevant Notch ligand for *charon* transcription in zebrafish is DeltaD. Therefore, Notch signalling in these two organisms targets the transcription of different genes: *nodal* in the mouse and *charon* in the zebrafish.

In the mouse node, the symmetric expression of *nodal*, induced by Notch signalling, and that of *cerl2*, induced by an unknown mechanism, later becomes asymmetric. *nodal* levels become higher on the left side, whereas *cerl2* levels are higher on the right side of the node (Marques et al., 2004). In contrast to what happens in the mouse, there was no evidence for an asymmetric *spaw* or *charon* expression in the zebrafish KV. In our study, we discovered a sharp transition from a symmetric to an asymmetric expression of *charon* at the eight-somite stage in the KV, with higher levels of expression on the right side. This finding strengthens the evolutionary conserved feature of *charon* expression because this gene, and its homologues, are asymmetrically expressed on the right side in medaka KV (Hojo et al., 2007), *Xenopus* gastrocoel roof plate (GRP) (Schweickert et al., 2010) and mouse node (Marques et al., 2004). The mechanism that triggers the left bias of *nodal* expression in the murine node and the right bias of *charon* and *coco* expression on the right side in fish KV and *Xenopus* GRP remains poorly understood.

There is increasing evidence in these organisms that the extracellular fluid flow generated by motile cilia present in the node/KV/GRP is essential to establish the LR asymmetries in the

LPM. Therefore, this directional fluid flow is a good candidate to trigger the initial asymmetric expression at the node/KV/GRP (Hamada, 2008). We discovered that in *aei*$^{-/-}$ mutants, the switch in *charon* expression does not occur, possibly as a consequence of the slower fluid flow generated by the short motile cilia. In agreement with the possibility that the dynamics of the fluid flow promote a switch in gene expression in the node/KV/GRP are the phenotypes described for the *axonemal dynein* morphants in fish and *Xenopus* and the mouse mutants *iv* and *inv*. In medaka and as shown here in zebrafish embryos, the right bias in *charon* expression is no longer detected when fluid flow is abolished by the knockdown of *lrd1* (Hojo et al., 2007) (Fig. 4Q,R). In *Xenopus*, *coco* is no longer downregulated on the left side of the GRP in the absence of flow (Schweickert et al., 2010). In the *iv* mouse mutant, where cilia are immotile and no nodal flow is produced, the expression of *nodal* in the node becomes randomized (Okada et al., 1999). In addition, in the *inv* mouse mutant, where the flow is slow and turbulent, the expression of *nodal* is mostly symmetric in the node (Lowe et al., 1996; Okada et al., 1999; Oki et al., 2009).

Although no asymmetric *charon* expression had been detected before in zebrafish, asymmetric Charon function was suggested to be responsible for inhibiting the transference of Spaw from the KV domain to the right LPM (Hashimoto et al., 2004). However, it should be emphasized that in wild-type embryos, *charon* is also expressed on the left side of the KV and *spaw* can still be transferred to the left LPM. This suggests that it is not the absence of *charon* transcripts that allow Spaw transfer to the left LPM but the relative levels of *charon* expression between left and right sides. Thus, we reason that Spaw is transferred to the left LPM because the levels of *charon* transcripts are lower on the left side of the KV in a wild-type embryo.

Applying the same reasoning to the *aei*$^{-/-}$ mutants, we propose that the severely reduced *charon* expression observed in 35.4% of the embryos (Fig. 4O,P) could correspond to: (1) no differences in the relative levels of *charon* [and therefore *spaw* is bilateraly transferred to the LPM as observed in 20% of *aei*$^{-/-}$ embryos (Fig. 1A)]; or (2) undetected small differences in *charon* expression that lead to a weak bilateral situation described as a *spaw* left anterior domain with bilateral posterior domains as observed in 15% of *aei*$^{-/-}$ embryos (Fig. 1A). In 43.3% of *aei*$^{-/-}$ mutants, *charon* expression is largely symmetric as visualized by in situ hybridization (Fig. 4L,P). In this situation, we cannot rule out that a biased difference between the left and the right side of *charon* transcripts in *aei*$^{-/-}$ mutants is still present as most embryos express left-sided *spaw* in the LPM (Fig. 1A). A clear asymmetric *charon* expression pattern on the right side of the KV (Fig. 4M) was observed in 18.3% of *aei*$^{-/-}$ embryos, resulting in left-sided *spaw* expression in the LPM (Fig. 1A). A few embryos (3%) expressed *charon* more strongly on the left side of the KV (Fig. 4N), matching the equivalent percentage of right-sided *spaw* in the LPM (Fig. 1A).

In summary, we showed that shorter cilia present in *aei*$^{-/-}$ mutants produce a slower fluid flow that leads to abnormal LR *charon* levels at the KV, which compromises the maintenance of *spaw* expression in the posterior domain of the left LPM. We show that in the same embryos where we observed a premature downregulation of *spaw*, we also see a reduced *lefty1* expression in the posterior midline domain. We thus propose that this gap in *lefty1* expression contributes, together with abnormal posterior *pitx2* expression, to the gut laterality defects without affecting heart laterality. This phenotype is clinically relevant as there are reports on individuals with primary ciliary dyskinesia that develop situs inversus abdominalis with no heart laterality defects (Fliegauf et al., 2007).

To our knowledge, Notch signalling is the first pathway that can both increase or decrease ciliary length, upon upregulation or downregulation, respectively. By contrast, FGF signalling has only been involved in shortening cilia length, (Hong and Dawid, 2009; Yamauchi et al., 2009). Our experiments identify *foxj1a*, the master motile ciliogenic transcription factor (Yu et al., 2008) as being downstream of DeltaD because it successfully rescued cilia length in *aei*$^{-/-}$ mutants in a cell-autonomous manner. These observations perhaps indicate that the motile cilia programme controlled by *foxj1a*, involves not only the transcription of motility genes such as *dnah9* and *wdr78* (Yu et al., 2008) but may also transcribe genes important for cilia growth yet to be discovered.

A systematic analysis of the experimental conditions where short and long cilia are generated by modulating the Notch activity will provide a framework to determine relevant ciliary length control genes. This will certainly bring new insights into how cilia/flagella length is regulated and may provide ways to increase ciliary length that could ultimately be used to treat ciliopathies often characterized by short cilia (Wemmer and Marshall, 2007).

Acknowledgements

We thank J. Lewis and S. Holley for fixed *aei*^{tr233} and *bea*^{tit446} mutant embryos, respectively; A. Oates for *Su(H)1+2-MO*; and S. Roy, W. Norton, S. Wilson, J. Yost, C.-P. Heisenberg, M. Hibi and J. Lewis for in situ probes. We are grateful to A. T. Tavares, J. Regan, D. Henrique, A. Jacinto, M. Godinho Ferreira, M. Bettencourt-Dias, J. Lewis, R. Monteiro, S. Marques and the Saúde labaoratory for comments on the manuscript; and to Lara Carvalho and the zebrafish facility team for excellent fish husbandry. S.S.L. and R.L. were supported by FCT fellowships (SFRH/BPD/34822/2007 and SFRH/BD/24861/2005). L.S. was supported by two FCT grants (PTDC/SAU-OBD/71596/2006 and PTDC/SAU-OBD/64628/2006).

Competing interests statement

The authors declare no competing financial interests.

Supplementary material

Supplementary material for this article is available at
http://dev.biologists.org/lookup/suppl/doi:10.1242/dev.054452/-/DC1

References

Amack, J. and Yost, H. (2004). The T box transcription factor No Tail in ciliated cells controls zebrafish left-right asymmetry. *Curr. Biol.* **14**, 685-690.

Amack, J., Wang, X. and Yost, H. (2007). Two T-box genes play independent and cooperative roles to regulate morphogenesis of ciliated Kupffer's vesicle in zebrafish. In *Dev. Biol.* **310**, 196-210.

Bisgrove, B., Snarr, B., Emrazian, A. and Yost, H. (2005). Polaris and Polycystin-2 in dorsal forerunner cells and Kupffer's vesicle are required for specification of the zebrafish left-right axis. *Dev. Biol.* **15**, 274-288.

Chin, A. J., Tsang, M. and Weinberg, E. S. (2000). Heart and gut chiralities are controlled independently from initial heart position in the developing zebrafish. *Dev. Biol.* **227**, 403-421.

Collignon, J., Varlet, I. and Robertson, E. J. (1996). Relationship between asymmetric nodal expression and the direction of embryonic turning. *Nature* **381**, 155-158.

Echeverri, K. and Oates, A. (2007). Coordination of symmetric cyclic gene expression during somitogenesis by Suppressor of Hairless involves regulation of retinoic acid catabolism. *Dev. Biol.* **301**, 388-403.

Essner, J. J., Amack, J. D., Nyholm, M. K., Harris, E. B. and Yost, H. J. (2005). Kupffer's vesicle is a ciliated organ of asymmetry in the zebrafish embryo that initiates left-right development of the brain, heart and gut. *Development* **132**, 1247-1260.

Fior, R. and Henrique, D. (2009). "Notch-Off": a perspective on the termination of Notch signalling. *Int. J. Dev. Biol.* **53**,1379-1384. Review.

Fliegauf, M., Benzing, T. and Omran, H. (2007). When cilia go bad: cilia defects and ciliopathies. *Nat. Rev. Mol. Cell Biol.* **8**, 880-893.

Gerdes, J. M., Davis, E. E. and Katsanis, N. (2009). The vertebrate primary cilium in development, homeostasis, and disease. *Cell* **137**, 32-45.

Gourronc, F., Ahmad, N., Nedza, N., Eggleston, T. and Rebagliati, M. (2007). Nodal activity around Kupffer's vesicle depends on the T-box transcription factors notail and spadetail and on notch signaling. *Dev. Dyn.* **236**, 2131-2146.
Hamada, H. (2008). Breakthroughs and future challenges in left-right patterning. *Dev. Growth Differ.* **5**, S71-S78.
Hamada, H., Meno, C., Watanabe, D. and Saijoh, Y. (2002). Establishment of vertebrate left-right asymmetry. *Nat. Rev. Genet.* **3**, 103-113.
Hashimoto, H., Rebagliati, M., Ahmad, N., Muraoka, O., Kurokawa, T., Hibi, M. and Suzuki, T. (2004). The Cerberus/Dan-family protein Charon is a negative regulator of Nodal signaling during left-right patterning in zebrafish. *Development* **131**, 1741-1753.
Hojo, M., Takashima, S., Kobayashi, D., Sumeragi, A., Shimada, A., Tsukahara, T., Yokoi, H., Narita, T., Jindo, T., Kage, T. et al. (2007). Right-elevated expression of charon is regulated by fluid flow in medaka Kupffer's vesicle. *Dev. Growth Differ.* **49**, 395-405.
Holley, S. A., Geisler, R. and Nüsslein-Volhard, C. (2000). Control of her1 expression during zebrafish somitogenesis by a delta-dependent oscillator and an independent wave-front activity. *Genes Dev.* **14**, 1678-1690.
Hong, S. K. and Dawid, I. B. (2009). FGF-dependent left-right asymmetry patterning in zebrafish is mediated by ler2 and Fibp1. *Proc. Natl. Acad. Sci. USA* **106**, 2230-2235.
Hsiao, C. D., You, M. S., Guh, Y. J., Ma, M., Jiang, Y. J. and Hwang, P. P. (2007). A positive regulatory loop between foxi3a and foxi3b is essential for specification and differentiation of zebrafish epidermal ionocytes. *PLoS ONE* **2**, e302.
Kimmel, C. B., Ballard, W. W., Kimmel, S. R., Ullmann, B. and Schilling, T. F. (1995). Stages of embryonic development of the zebrafish. *Dev. Dyn.* **203**, 253-310.
Kramer-Zucker, A., Olale, F., Haycraft, C., Yoder, B., Schier, A. and Drummond, I. (2005). Cilia-driven fluid flow in the zebrafish pronephros, brain and Kupffer's vesicle is required for normal organogenesis. *Development* **132**, 1907-1921.
Krebs, L. T., Iwai, N., Nonaka, S., Welsh, I. C., Lan, Y., Jiang, R., Saijoh, Y., O'Brien, T. P., Hamada, H. and Gridley, T. (2003). Notch signaling regulates left-right asymmetry determination by inducing Nodal expression. *Genes Dev.* **17**, 1207-1212.
Latimer, A. J. and Appel, B. (2006). Notch signaling regulates midline cell specification and proliferation in zebrafish. *Dev. Biol.* **298**, 392-402.
Levin, M. and Palmer, A. R. (2007). Left-right patterning from the inside out: widespread evidence for intracellular control. *BioEssays* **29**, 271-287.
Lin, X. and Xu, X. (2009). Distinct functions of Wnt/beta-catenin signaling in KV development and cardiac asymmetry. *Development* **136**, 207-217.
Long, S., Ahmad, N. and Rebagliati, M. (2003). The zebrafish nodal-related gene southpaw is required for visceral and diencephalic left-right asymmetry. *Development* **130**, 2303-2316.
Lowe, L. A., Supp, D. M., Sampath, K., Yokoyama, T., Wright, C. V., Potter, S. S., Overbeek, P. and Kuehn, M. R. (1996). Conserved left-right asymmetry of nodal expression and alterations in murine situs inversus. *Nature* **381**, 158-161.
Marques, S., Borges, A. C., Silva, A. C., Freitas, S., Cordenonsi, M. and Belo, J. A. (2004). The activity of the Nodal antagonist Cerl-2 in the mouse node is required for correct L/R body axis. *Genes Dev.* **18**, 2342-2347.
Monteiro, R., van Dinther, M., Bakkers, J., Wilkinson, R., Patient, R., ten Dijke, P. and Mummery, C. (2008). Two novel type II receptors mediate BMP signalling and are required to establish left-right asymmetry in zebrafish. *Dev. Biol.* **315**, 55-71.
Neugebauer, J. M., Amack, J. D., Peterson, A. G., Bisgrove, B. W. and Yost, H. J. (2009). FGF signalling during embryo development regulates cilia length in diverse epithelia. *Nature* **458**, 651-654.
Nonaka, S., Tanaka, Y., Okada, Y., Takeda, S., Harada, A., Kanai, Y., Kido, M. and Hirokawa, N. (1998). Randomization of left-right asymmetry due to loss of nodal cilia generating leftward flow of extraembryonic fluid in mice lacking KIF3B motor protein. *Cell* **95**, 829-837.
Okada, Y., Nonaka, S., Tanaka, Y., Saijoh, Y., Hamada, H. and Hirokawa, N. (1999). Abnormal nodal flow precedes situs inversus in iv and inv mice. *Mol. Cell* **4**, 459-468.
Oki, S., Kitajima, K., Marques, S., Belo, J. A., Yokoyama, T., Hamada, H. and Meno, C. (2009). Reversal of left-right asymmetry induced by aberrant Nodal signaling in the node of mouse embryos. *Development* **136**, 3917-3925.
Przemeck, G. K., Heinzmann, U., Beckers, J. and Hrabé de Angelis, M. (2003). Node and midline defects are associated with left-right development in Delta1 mutant embryos. *Development* **130**, 3-13.
Raya, A., Kawakami, Y., Rodriguez-Esteban, C., Buscher, D., Koth, C. M., Itoh, T., Morita, M., Raya, R. M., Dubova, I., Bessa, J. G. et al. (2003). Notch activity induces Nodal expression and mediates the establishment of left-right asymmetry in vertebrate embryos. *Genes Dev.* **17**, 1213-1218.
Schweickert, A., Vick, P., Getwan, M., Weber, T., Schneider, I., Eberhardt, M., Beyer, T., Pachur, A. and Blum, M. (2010). The nodal inhibitor Coco is a critical target of leftward flow in Xenopus. *Curr. Biol.* Epub ahead of print.
Stubbs, J. L., Oishi, I., Izpisúa Belmonte, J. C. and Kintner, C. (2008). The forkhead protein Foxj1 specifies node-like cilia in Xenopus and zebrafish embryos. *Nat. Genet.* **40**, 1454-1460.
Supp, D. M., Brueckner, M., Kuehn, M. R., Witte, D. P., Lowe, L. A., McGrath, J., Corrales, J. and Potter, S. S. (1999). Targeted deletion of the ATP binding domain of left-right dynein confirms its role in specifying development of left-right asymmetries. *Development* **126**, 5495-5504.
Takeuchi, J., Lickert, H., Bisgrove, B., Sun, X., Yamamoto, M., Chawengsaksophak, K., Hamada, H., Yost, H., Rossant, J. and Bruneau, B. (2007). Baf60c is a nuclear Notch signaling component required for the establishment of left-right asymmetry. *Proc. Natl. Acad. Sci. USA* **104**, 846-851.
Takke, C. and Campos-Ortega, J. A. (1999). her1, a zebrafish pair-rule like gene, acts downstream of notch signalling to control somite development. *Development* **126**, 3005-3014.
Takke, C., Dornseifer, P., van Weizsäcker, E. and Campos-Ortega, J. A. (1999). her4, a zebrafish homologue of the Drosophila neurogenic gene E(spl), is a target of NOTCH signalling. *Development* **126**, 1811-1821.
Thisse, C. and Thisse, B. (2008). High-resolution in situ hybridization to whole-mount zebrafish embryos. *Nat. Protoc.* **3**, 59-69.
Wang, X. and Yost, H. J. (2008). Initiation and propagation of posterior to anterior (PA) waves in zebrafish left-right development. *Dev. Dyn.* **237**, 3640-3647.
Wemmer, K. A. and Marshall, W. F. (2007). Flagellar length control in chlamydomonas-paradigm for organelle size regulation. *Int. Rev. Cytol.* **260**, 175-212.
Yamauchi, H., Miyakawa, N., Miyake, A. and Itoh, N. (2009). Fgf4 is required for left-right patterning of visceral organs in zebrafish. *Dev. Biol.* **332**, 177-185.
Yu, X., Ng, C. P., Habacher, H. and Roy, S. (2008). Foxj1 transcription factors are master regulators of the motile ciliogenic program. *Nat. Genet.* **40**, 1445-1453.

APPENDIX III

Lourenço *et al.*, 2010

OPEN ACCESS Freely available online

PLoS one

Left-Right Function of *dmrt2* Genes Is Not Conserved between Zebrafish and Mouse

Raquel Lourenço[1,2], Susana S. Lopes[1,2], Leonor Saúde[1,2]*

1 Instituto de Medicina Molecular e Instituto de Histologia e Biologia do Desenvolvimento, Faculdade de Medicina da Universidade de Lisboa, Lisboa, Portugal, **2** Instituto Gulbenkian de Ciência, Oeiras, Portugal

Abstract

Background: Members of the Dmrt family, generally associated with sex determination, were shown to be involved in several other functions during embryonic development. Dmrt2 has been studied in the context of zebrafish development where, due to a duplication event, two paralog genes *dmrt2a* and *dmrt2b* are present. Both zebrafish *dmrt2a/terra* and *dmrt2b* are important to regulate left-right patterning in the lateral plate mesoderm. In addition, *dmrt2a/terra* is necessary for symmetric somite formation while *dmrt2b* regulates somite differentiation impacting on slow muscle development. One *dmrt2* gene is also expressed in the mouse embryo, where it is necessary for somite differentiation but with an impact on axial skeleton development. However, nothing was known about its role during left-right patterning in the lateral plate mesoderm or in the symmetric synchronization of somite formation.

Methodology/Principal Findings: Using a *dmrt2* mutant mouse line, we show that this gene is not involved in symmetric somite formation and does not regulate the laterality pathway that controls left-right asymmetric organ positioning. We reveal that *dmrt2a/terra* is present in the zebrafish laterality organ, the Kupffer's vesicle, while its homologue is excluded from the mouse equivalent structure, the node. On the basis of evolutionary sub-functionalization and neo-functionalization theories we discuss this absence of functional conservation.

Conclusions/Significance: Our results show that the role of *dmrt2* gene is not conserved during zebrafish and mouse embryonic development.

Citation: Lourenço R, Lopes SS, Saúde L (2010) Left-Right Function of *dmrt2* Genes Is Not Conserved between Zebrafish and Mouse. PLoS ONE 5(12): e14438. doi:10.1371/journal.pone.0014438

Editor: Immo A. Hansen, New Mexico State University, United States of America

Received June 22, 2010; **Accepted** December 7, 2010; **Published** December 28, 2010

Funding: Two Fundacao para a Ciencia e a Technologia (FCT) (http://alfa.fct.mctes.pt) grants PTDC/SAU-OBD/71596/2006 and PTDC/SAU-OBD/64628/2006 supported this work. The funders had no role in study design, data collection and analysis, decision to publish, or preparation of the manuscript.

Competing Interests: The authors have declared that no competing interests exist.

* E-mail: msaude@fm.ul.pt

Introduction

The organization of the axial skeleton and skeletal muscles is bilaterally symmetric. In contrast, vertebrates are also characterized by stereotypic LR asymmetries in the distribution of the internal organs such as the heart and stomach on the left, and the liver on the right [1].

The axial skeleton and skeletal muscles are derived from embryonic structures called the somites. The epithelialization of a new pair of somites occurs in a bilateral symmetric manner from the anterior-most region of the mesenchymal presomitic mesoderm (PSM) [2]. This process is tightly regulated in space and time, with a new pair of somites of approximately the same size being formed with a regular species-specific time period [2].

The "clock and wavefront" model [3] postulates the existence of two independent phenomena accounting for periodic somite formation. The clock is evident in the PSM as periodic oscillations in gene expression of the so-called cyclic genes. These genes show a dynamic and reiterated expression in PSM cells with the same periodicity of somite formation [2]. Although the list of cycling genes is increasing, the conserved ones across species include mainly Notch targets, namely the bHLH (basic-helix-loop-helix) transcription repressors, the *hes* genes in the mouse and the *her* genes in zebrafish. More recently, a large scale transcriptome analysis revealed that the segmentation clock mechanism shows different degrees of complexity between mouse and zebrafish. In the mouse, many of the cyclic genes belong not only to the Notch pathway but also to the Wnt and FGF pathways [4]. In zebrafish there is no evidence for the existence of cyclic genes of the Wnt or FGF pathways [2]. In addition to the presence of a molecular clock, the PSM cells are under the influence of a wavefront of differentitaion. This wavefront is determined by gradients of Fgf and Wnt signalling coming from the posterior region of the embryo and fading towards the anterior portion of the PSM. While under the influence of Fgf/Wnt signalling, the PSM cells are maintained in an immature state and are prevented from starting the genetic program of somite formation [5,6]. Soon after being formed the somites differentiate into the dermomyotome, which segregates into the dermal layer of the skin and skeletal muscles, and into the sclerotome that forms the vertebral column [7].

At the same time somites are being formed, left-right asymmetric information is establishing laterality in the nearby lateral plate mesoderm (LPM), culminating with the asymmetric positioning of internal organs. Before there are any signs of asymmetric organ localization in the vertebrate embryo, a conserved cascade of asymmetrically expressed genes is activated around the node in the

mouse and around the Kupffer's vesicle (KV), the functionally equivalent fish organ. An excess of Nodal activity on the left side of the node/KV is transferred to the left LPM and in this location Nodal exerts a positive feedback on itself. As a consequence, the expression of nodal is amplified in the left LPM. Nodal also activates its negative regulators, the lefty genes. Lefty1 in the midline prevents *nodal* activation on the right LPM, while Lefty2 restricts the domain of *nodal* expression on the left LPM. The strong *nodal* expression on the left LPM induces *pitx2* expression that in turn activates morphogenetic proteins required for LR asymmetry of the internal organs [8]. Even though this Nodal cascade is conserved, the mechanism that induces nodal in the node/KV is different between vertebrates. Notch signaling activates *nodal* in the murine node region, while in zebrafish it activates the Nodal negative regulator *charon* around the KV [9,10–12]. In addition to Notch signaling, Fgf8 and Wnt3a regulate *nodal* expression in the mouse node [13,14]. The role of Fgf and Wnt signaling in controlling *nodal* expression at the KV has not been determined.

Somitogenesis and LR patterning share the same signalling pathways that occur at overlapping developmental time windows and in nearby embryonic tissues. For this reason, the asymmetric signals from the node have to be able to reach the LPM without affecting the bilateral symmetry of somite formation in the adjacent PSM. In fact, several lines of evidence show that bilateral symmetry is not a default state but instead has to be actively maintained through a mechanism that protects this territory from the LR asymmetric signals [15].

Retinoic acid (RA) has emerged as a conserved keeper of bilateral somite formation by buffering the PSM from the influence of LR cues [16–19]. Several lines of evidence show that Fgf8 and Snail1 are the LR cues that are being antagonized by RA signaling in the PSM [17,19–22]. In zebrafish, another key player regulating development along the LR axis is the zinc-finger like transcription factor Dmrt2a/Terra, that belongs to the Dmrt (Doublesex (dsx) and Mab-3 Related Transcription Factor) family. We have previously shown that in zebrafish when Dmrt2a/Terra function is blocked, the expression of the cycling genes becomes desynchronized between the left and right sides and as a consequence somite formation is no longer symmetric. In addition, the positioning of the internal organs is compromised as a result of a randomization of left side LPM markers [23].

On the other hand, the mouse *dmrt2* null mutants have severe somite differentiation defects but nothing was known regarding a possible role of Dmrt2 in regulating symmetric somite formation and establishing the LR asymmetry pathway [24].

Here we report that *dmrt2* homozygous mouse mutants do not show LR desynchronization of somite formation and do not have LR defects regarding internal organs positioning. We show that *dmrt2a/terra* is expressed in the zebrafish KV in agreement with its function in LR development. In contrast, we did not detect *dmrt2* expression in the mouse node, consistent with its non-conserved function during the process of LR axis determination in this vertebrate.

Results

The murine Dmrt2 is not required for bilateral synchronization of somite formation

The process of somite formation is under the control of a molecular clock, revealed by the dynamic expression of the cyclic genes. This expression pattern is subdivided into three consecutive phases that are reiterated with the formation of each somite pair [2]. Importantly, the expression pattern of the cyclic genes on the left side of the PSM is always in phase with the one present on the right side.

In zebrafish, the expression of the cyclic genes *deltaC*, *her1* and *her7* becomes out of phase between the left and right sides of the PSM when *dmrt2a/terra* is knocked-down [23]. This eventually leads to the formation of an extra somite on either the left or the right side of the embryonic axis. Hence, it was proposed that Dmrt2a/Terra maintains the symmetry of somite formation possibly by protecting the PSM from the influence of LR asymmetric cues. This protection is only needed in a specific developmental time window that corresponds to the timing of transfer of LR information to the LPM [23]. In the mouse, it was shown that Dmrt2 is required for somite differentiation with severe implications on axial skeleton development [24]. However, its potential role in synchronizing the molecular clock that underlies somite formation was not evaluated in murine embryos.

In order to investigate the effect of abolishing Dmrt2 function in the mouse molecular clock, we analyzed the expression of cyclic genes of the Notch, Wnt and Fgf pathways in the context of *dmrt2* null mutants [24]. Embryos from *dmrt2* heterozygous crosses were collected between 8 to 15-somite stages, the developmental window that corresponds to the time when the PSM needs to be protected from LR signals [17]. These embryos were genotyped by PCR and analyzed by whole-mount *in situ* hybridization to reveal the expression of the Notch pathway cyclic genes *hes7* and *lfng*, the Wnt pathway cyclic gene *axin2* and the Fgf pathway cyclic gene *sprouty2* [6,25,26,27]. Similarly to their wild-type and heterozygous siblings, in *dmrt2* homozygous mutants the dynamic expression of *hes7* (n = 8) (fig. 1A–E) and *lnfg* (n = 14) (fig. 1F–J) was not affected and normal phases of cyclic gene expression were observed. In addition, in all embryos analyzed, cyclic gene expression was in the same phase and therefore bilaterally symmetric on the left and right PSM's (fig. 1A–J). When analyzing the expression of *axin2* and *sprouty2*, the same results were observed (fig. 1K–P). The expression of *axin2* (n = 3) (fig. 1K–M) and *sprouty2* (n = 3) (fig. 1N–P) in wild-type, heterozygous and *dmrt2* homozygous mutant embryos was not affected and normal phases of cyclic gene expression were bilaterally symmetric in the PSM. In clear contrast to its role in zebrafish, Dmrt2 is not necessary to maintain bilateral symmetry of cyclic gene expression and therefore is dispensable for symmetric somite formation in the mouse embryo.

Mouse left-right LPM patterning is independent of Dmrt2 function

The distribution of the internal organs is controlled by a conserved LR patterning cascade of information that starts early in development in the node/KV region and is then transferred asymmetrically to the LPM.

In zebrafish, Dmrt2a/Terra is necessary for the establishment of LR asymmetries. In the absence of Dmrt2a/Terra, the transfer of the *nodal*-related gene *spaw*, from the KV region to the left LPM, is randomized instead of being consistently transferred to the left LPM. In addition, the expression of the *spaw* downstream target, *pitx2*, is also randomized in the LPM. Concomitant with this randomization of left-side specific genes, heart positioning is also misplaced [23].

To further evaluate the putative role of Dmrt2 in LR asymmetry patterning in mouse development, we studied the expression of left-sided specific markers in *dmrt2* null mutants [24]. Embryos from *dmrt2* heterozygous crosses were collected between E8.0 and E8.5, genotyped and processed by whole-mount *in situ* hybridization to reveal the expression of the left LPM genes *nodal* and *pitx2* [28,29]. At embryonic day E8.0, *nodal* expression was stronger on the left side of the node and restricted to the left LPM in both $dmrt2^{-/-}$ mutants (n = 8) and their siblings (fig. 2A–C). At embryonic day E8.5, in both *dmrt2* mutants (n = 9) and their sibling embryos, *pitx2* was expressed on the left side of the LPM (fig. 2D–

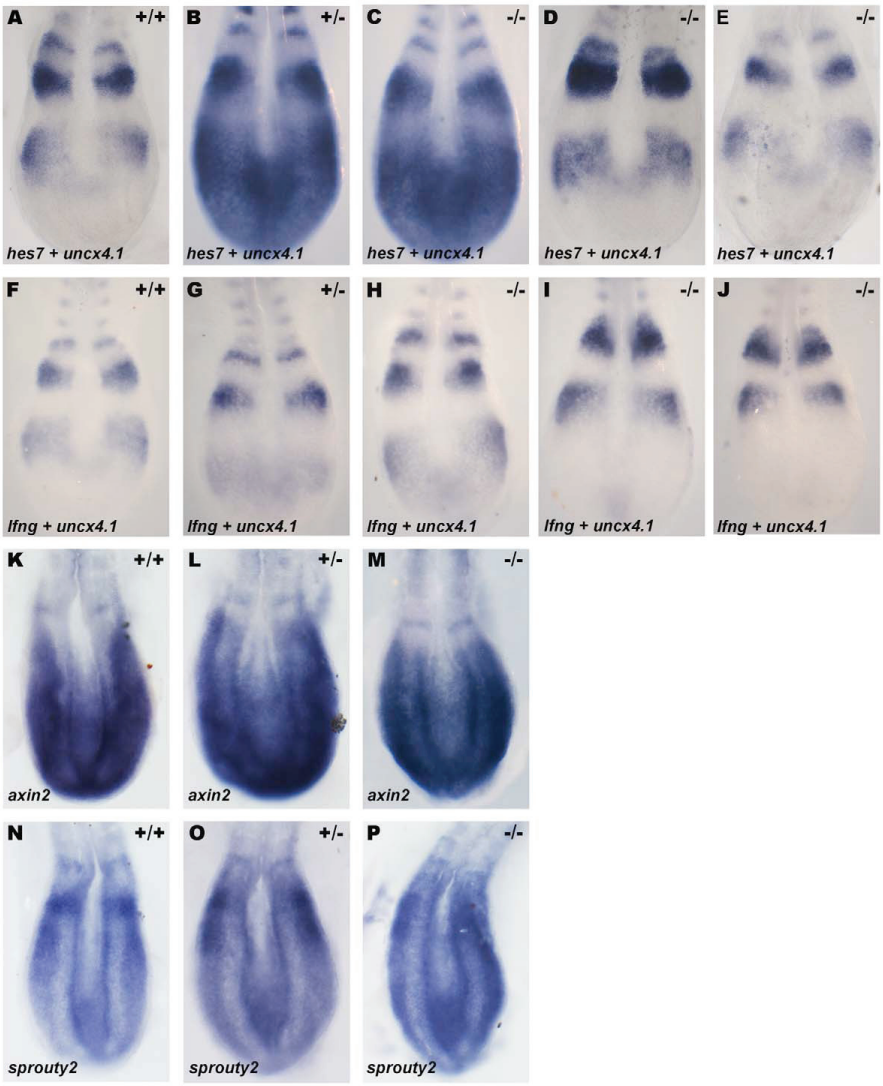

Figure 1. Dmrt2 is not required for symmetric somite formation in the mouse embryo. (A–P) Expression pattern of the cyclic genes *hes7* (A–E), *lfng* (F–J), *axin2* (K–M) and *sprouty2* (N–P) in E8.5 mouse embryos. (A–J) Embryos were also hybridized with the somite marker *uncx4.1*. (A, F, K, N) WT, (B, G, L, O) heterozygous and (C–E, H–J, M, P) *dmrt2* homozygous mutant embryos show the same phase of *hes1*, *hes7*, *axin2* and *sprouty2* cyclic expression in the PSM. All views are dorsal with anterior to the top.
doi:10.1371/journal.pone.0014438.g001

F). This analysis reveals that Dmrt2 is not important to establish LPM laterality in the mouse embryo.

We next examined the laterality of the internal organs in newborn *dmrt2* mutants. Similarly to their siblings, *dmrt2* mutant mice (n = 16) showed normal internal organ organization (fig. 2G–L). The left lung had only one lobule, the right lung four lobules and the stomach and heart were always on the left side of the body cavities (fig. 2I, L). This data on organ localization is in agreement with the normal expression pattern of early LR markers and indicates that the role of Dmrt2 in establishing LR asymmetries is not conserved between zebrafish and mouse.

dmrt2a/terra is expressed in the zebrafish Kupffer's vesicle but its homologous gene is absent from the mouse node

Our data clearly shows that the role of Dmrt2a/Terra in synchronizing somite formation and establishing LR asymmetries in

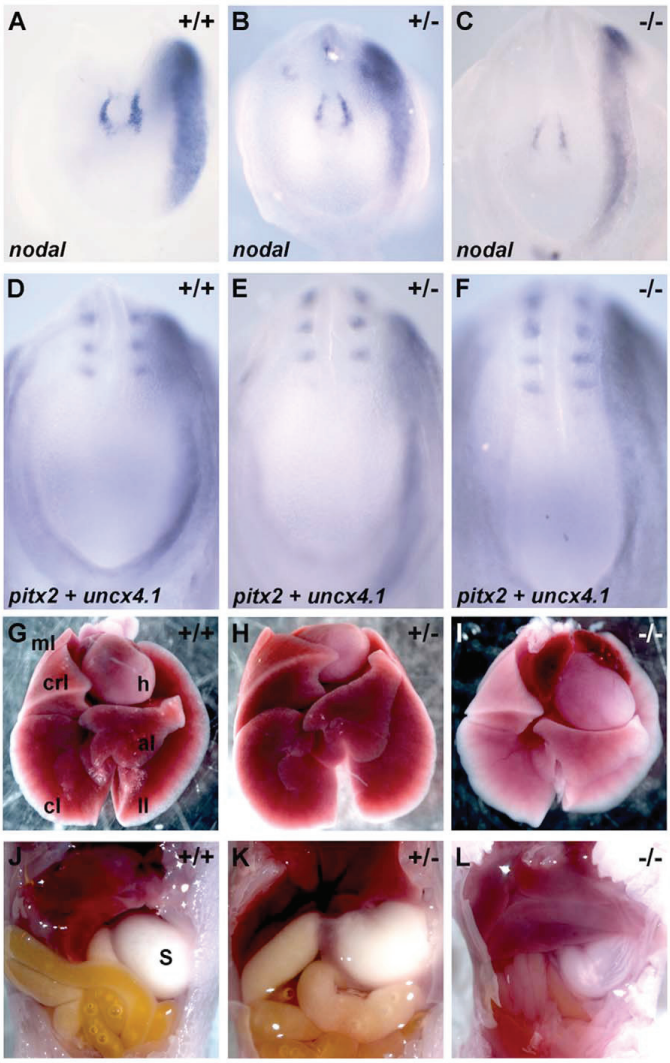

Figure 2. Dmrt2 is not required for the left-right LPM patterning in the mouse embryo. (A–F) Embryos between E8.0 and E8.5 processed by whole mount *in situ* hybridization with *nodal* (A–C) and *pitx2* (D–F) probes, respectively. (A–C) *nodal* expression is restricted to the left side of the node and left LPM in (A) WT, (B) heterozygous and (C) *dmrt2* homozygous mutant embryos. (D–F) *pitx2* expression is also restricted to the left LPM in (D) WT, (E) heterozygous and (F) *dmrt2* homozygous mutant embryos. (G–L) Localization of the internal organs in newborn mice. (G) In WT, (H) heterozygous and (I) *dmrt2* homozygous mutants the heart always bend to the left, the left lung always has one lobe (ll) and the right lung has four lobes (ml, crl, cl, al). (J–L) Concomitant with the normal situs of the heart and lungs, the stomach is also always placed on the correct left side of the axis. ml (middle lobe); crl (cranial lobe); cl (caudal lobe); al (accessory lobe); ll (left lobe); h (heart); s (stomach). All views are ventral with anterior to the top.
doi:10.1371/journal.pone.0014438.g002

the LPM, previously described in zebrafish [23], is not conserved in the mouse. We reasoned that this non-conserved role could be due to a differential pattern of expression in these two vertebrates.

We confirmed that zebrafish *dmrt2a/terra* and its mouse homologue are expressed in the anterior region of the PSM and somites in both vertebrates (fig. 3A–F) [24,30]. In addition, we could detect *dmrt2a/terra* transcripts in the zebrafish KV from the 3-somite stage until the 10-somite stage (fig. 3D–F). However, we could not find any expression of *dmrt2* in the mouse node from 1-somite stage to 7-somite stage, which is the equivalent laterality organ of zebrafish KV (fig. 3A–C). The differential expression in the laterality organs of zebrafish and mouse may explain the

different role that this transcription factor plays in controlling LR laterality and symmetric somite formation in these two vertebrates.

Discussion

The *dmrt* genes belong to a large family of transcription factors. These genes are present in several metazoan phyla (arthropods, nematodes and vertebrates) and show low sequence conservation outside the common DM domain, even within species [31]. The number of *dmrt* orthologue genes varies in different phyla, suggesting multiple instances of independent gene duplication and/or loss throughout evolution. In the vertebrate lineage alone the number of dmrt genes varies widely: eight genes (*dmrt1-8*) in human and mouse, five genes (*dmrt1-5*) in fish, two genes (*dmrt1* and *dmrt4*) in Xenopus and three genes (*dmrt1-3*) in chick [31,32].

Despite being mainly expressed in developing gonads and associated with sex differentiation, not all the vertebrate *dmrt* genes are associated exclusively with this function. So far, from the eight known *dmrt* genes, five of them have already been implicated in other developmental processes other than sex differentiation. *dmrt* genes have been detected in the central nervous system (*dmrt3* in mouse, chick and medaka; *dmrt4* in mouse, *Xenopus*, medaka and platyfish; *dmrt5* in mouse, platyfish and zebrafish; *dmrt6* in mouse), nasal placodes (*dmrt3* in mouse and chick; *dmrt4* in *Xenopus* and platyfish; *dmrt5* in platyfish) and in the somites (*dmrt2* in mouse, chick and fish; *dmrt3* in chick) [32]. It is clear that Dmrt family members present a wide variation in gene number and their expression pattern suggests distinct functions. The possible variation at the level of gene function implies that during evolution paralog genes may have been subjected to either a sub-functionalization, with the functions of the ancestral gene being segregated into a set of paralog genes, or a neo-functionalization, with one of the paralog genes acquiring a new function. A careful functional analysis should be done to fully understand the extension of the role of these genes. Additional studies on Dmrt genes from ancestor organisms would give insight on the origin and evolution of these genes.

The first *dmrt* gene suggested to have a role unrelated to sexual development was *dmrt2*. It was detected in zebrafish and mouse PSM and somites and was reported to be absent from gonadal tissues [24,30,33]. Indeed, male and female homozygous mouse mutant embryos are obtained with the same frequency [24]. Functional studies in zebrafish showed that Dmrt2a/Terra protects the bilateral symmetric somite formation from the influence of LR cues. Without Dmrt2a/Terra the expression of the cycling genes in the PSM becomes desynchronized and consequently somite formation is no longer synchronized between the left and right sides of the zebrafish axis [23]. In addition, Dmrt2a/Terra was shown to establish asymmetry in the LPM, being necessary to restrict left-specific genes in the left LPM and having an impact in the localization of the heart on the left side [23]. In the mouse, these early Dmrt2 roles were not analyzed and only a later function in somite differentiation was reported [24].

To investigate the degree of functional conservation of *dmrt2* in mice, we started by characterizing the expression of the PSM Notch-related cycling genes *her7* and *lfgn*. This analysis was

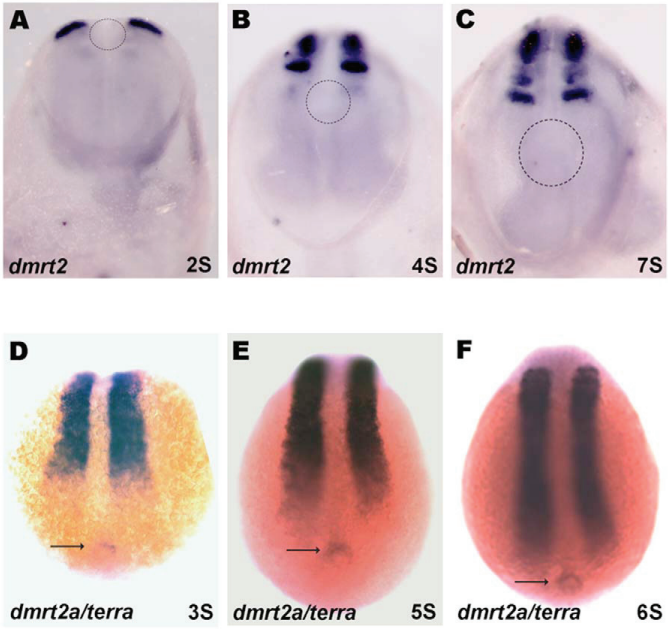

Figure 3. *dmrt2/terra* is expressed in the zebrafish kupfer's vesicle. (A–F) Whole mount *in situ* hybridization confirming the *dmrt2* conserved expression pattern in the anterior PSM and somites in mice (A–C) and zebrafish (D–F) embryos. Despite not being expressed in the mouse node (dashed circle) (A–C), *dmrt2a/terra* is present in the zebrafish equivalent structure, the kupffer's vesicle (arrow) (D–F). (A–C) Ventral views of mice embryos with anterior to the top. (D–F) Dorsal views of zebrafish embryos with anterior to the top. S, somite stage.
doi:10.1371/journal.pone.0014438.g003

restricted to a specific developmental time window, 6–13 somites, which corresponds to the period when LR information is being transferred from the node to the left LPM - the time when PSM must be protected from the influence of these signals. The cyclic expression pattern of *her7* and *lfgn* in *dmrt2* null mutants showed no differences between the left and right sides of the PSM and consequently somite formation proceeded in a bilateral symmetric way. In contrast to the zebrafish, where all the cyclic genes identified so far belong to the Notch pathway, in the mouse several PSM cyclic genes are Wnt and Fgf pathway components. Among those are *axin2* and *sprouty2*, which are negative feedback inhibitors of the Wnt and Fgf pathway, respectively [34]. Similarly to what happens with the Notch cyclic genes, no desynchronization of *axin2* and *sprouty2* expression was observed between the left and the right PSM in *dmrt2* null mutants. This is in agreement with the idea supported by experimental data and computational modeling that suggest that oscillations in the Notch, Wnt and Fgf pathways are coupled and integrated in one molecular clock [34;35]. These results reflect a lack of conservation of the role of Dmrt2 during mouse development in what concerns LR synchronization of somite formation. Regarding a possible conservation of Dmrt2 function in establishing the LR asymmetry pathway, we looked at the expression of left-specific genes. In mice embryos mutant for *dmrt2* the expression of *spaw* and *pitx2* was restricted to the left LPM and consistently we observed a correct LR disposition of all the internal organs. Once again, these results indicate that mouse Dmrt2 does not play a role in the establishment of the LR asymmetric cascade.

During evolution the process of gene duplication is one key driving force for gene functional innovation. The evolutionary significance of gene duplication is explained by the duplication-degeneration-complementation (DDC) model, which states that the probability of a duplicate gene to be preserved increases with the occurrence of degenerative mutations in its regulatory region [36]. Since genes may have several functions that are controlled by different regulatory regions, when a specific subset of the gene function is subjected to a degenerative mutation, it may lose this given function and gain a new one. This leads to the emergence of different gene family members that become expressed in different tissues and/or developmental stages, thus allowing gene preservation during evolution [36].

Teleost fish underwent a genome duplication that occurred during the evolution of ray-finned fish. Recently, it was reported that, due to this genome duplication event, zebrafish *dmrt2a/terra* has a paralog gene named *dmrt2b* [37]. Contrary to *dmrt2a/terra*, that is present in all vertebrates, *dmrt2b* duplication only exists in the fish genome (zebrafish, tilapia, takifugu, tetraodon, medaka and stickleback), probably due to the fish lineage specific genome duplication [38]. In clear contrast to *dmrt2a/terra*, the fish-specific duplicated *dmrt2b* contributes to Hedgehog pathway [37]. Due to this new function of *dmrt2b*, these two genes are not redundant and therefore one does not compensate for the loss of the other [37]. The fact that *dmrt2b* allows an effective response to Hedgehog signaling explains the impact on somite differentiation in particular on slow muscle development [37]. Since Shh regulates the establishment of LR asymmetries in zebrafish [39] through its role in the midline, it is most likely that the LPM LR phenotype seen in *dmrt2b* morphants results from an impaired Hedgehog signaling at this level. This possibility is reinforced by the fact that we could not detect any *dmrt2b* expression in the zebrafish KV (data not shown). In addition, the fact that *dmrt2b* morphants lack desynchronizations of cyclic gene expression in the PSM [37] also suggests that the LR phenotype in these embryos arises from a different source when compared to *dmrt2a* LR phenotype.

We show here that *dmrt2a/terra* is expressed in the zebrafish KV, which is consistent with its role in LPM LR asymmetry establishment. In addition, we have previously shown that *dmrt2/terra* is asymmetrically expressed on the left side of Hensen's node in chick embryos [23]. Although no functional studies were performed, this expression pattern is highly suggestive of a LR patterning function of *dmrt2/terra* during chick development. In contrast to the fish and chick, we show here that *dmrt2* is not expressed in the mouse node, which is in agreement with the absence of a LR phenotype in *dmrt2* mutant mice.

Given the fact that zebrafish *dmrt2a/terra* is expressed in the KV and its homologue in chick Hensen's node, we propose that its expression and consequently its function in LR patterning was lost in the mouse lineage. This difference in function observed in mouse could arise: 1) from mutations occurring in the dmrt2 enhancer responsible for the node expression. To test this hypothesis, it would be interesting to combine bioinformatics and transgenics production to identify the zebrafish KV dmrt2 enhancer and show that it is indeed absent from the mouse genomic sequence; 2) from the loss in the mouse of a protein(s) necessary to activate specifically the node enhancer. In this situation, a bioinformatics analysis would reveal that the node enhancer will be present in the mouse genomic sequence and a new search for putative binding sites for known regulators could then be performed.

In contrast to the differential *dmrt2* expression in the KV/node reported in fish, chick and mouse, the expression at the level of the PSM and somites is conserved across all vertebrates studied so far [23,24,37]. In mouse, Dmrt2 is required for somite differentiation, in particular for patterning the axial skeleton [24]. In the absence of *dmrt2*, extracellular matrix components levels in the dermomyotome are downregulated leading to disrupted differentiation of the myotome. Furthermore, signaling between myotome and the sclerotome is compromised culminating with rib and vertebral malformations and postnatal death due to respiratory problems [24]. Therefore, the expression of *dmrt2* in the anterior PSM and somites correlates with its function in somite differentiation, a role already well described in mouse but still to be addressed in chick and zebrafish [24]. In zebrafish, *dmrt2a/terra* is necessary for bilateral somite formation due to its ability to synchronize the segmentation clock between the left and right PSM [23]. Since LR synchronized cycling gene expression starts already in the posterior PSM, the desynchronization observed in the absence of *dmrt2a/terra* is not easily explained by its expression in the anterior PSM and somites. We propose that *dmrt2a/terra* is synchronizing the clock in the posterior most part of the PSM, through its function in the KV. In the developing zebrafish embryo, the KV is placed in close contact with the most posterior part of the PSM and therefore makes it an ideal location to protect the PSM from the asymmetric signals that emerge from this organ. Again, since *dmrt2* expression in the mouse is absent from the node, no desynchronizations of cyclic gene expression are observed in the *dmrt2* mutants.

While some *dmrt* ortholog genes show a conservation of their function in different vertebrates, some may have divergent functions. Here we report one of such cases illustrated by the mouse ortholog of the zebrafish *dmrt2*.

Materials and Methods

Ethics Statement

All experiments involving animals were approved by the Animal User and Ethical Committees at the Instituto Gulbenkian de

Ciência and Instituto de Medicina Molecular, according with directives from Direcção Geral Veterinária (PORT 1005/92).

Zebrafish line

AB wild-type zebrafish were crossed and embryos collected and kept at 28°C until the appropriate stage [40].

Mice breeding and genotyping

Mice carrying the *dmrt2* null mutation where previously described [24] and obtained from David Zarkower's laboratory. Dmrt2 heterozygous mice were maintained on a C57BL/6 genetic background. DNA was extracted from the tail tip of adult mice and genotyped by PCR using Dmrt2 specific primers. Dmrt2 WT forward primer 5′-CTGGACCCGAGTACAGTTCC-3′, Dmrt2 WT reverse primer 5′-AATGGTGCGTTCAACTCAGG-3′, Dmrt2 mutant forward primer 5′- TGCGGAGGGCTGGATCT-TAAGGAG-3′ and Dmrt2 mutant reverse primer 5′-AGGGGGTGGGGATTTGACACCATC-3′, which resulted in a 830 bp band and a 270 bp band for the WT and mutant alleles, respectively. Dmrt2 heterozygous mice were crossed and embryos collected at specific stages (8.0–9.0 dpc). Mutant embryos were identified by PCR on DNA isolated from the yolk sacs using the same primers as for the adult mice genotyping.

Cloning of mouse and zebrafish *dmrt2a/terra* and *dmrt2b* genes

Mouse *dmrt2* cDNA (IMAGE: 1248080) was used to synthesize an antisense RNA probe, linearized with EcoRI and transcribed with T3. Total RNA was extracted from appropriate staged zebrafish embryos using TRIzol (Invitrogen) and cDNA was synthesized with MMLV-Reverse Transcriptase kit (Promega). *dmrt2a/terra* full length sequence was amplified by PCR with the following primer set: *dmrt2a/terra* forward primer 5′-ATGACG-GATCTGTCCGGCACG-3′ and *dmrt2a/terra* reverse primer 5′-AGCAAGAAGCCTTACTGAGATTTCCG-3′. dmrt2b *was amplified by PCR with the following primer set:* dmrt2b *forward primer 5′-TTTCTTCCCGCTGTCAGACC-3′ and* dmrt2b *reverse primer 5′-TTATCTCATGAGCAGTGCCTCG-3′. The* dmrt2a/terra *amplified DNA fragment was cloned in the pCS2+ vector and* dmrt2b *in the pGEM-T easy vector. To synthesize the antisense* dmrt2a/terra *and* dmrt2b *RNA probes, plasmids were linearized with ApaI and SpeI and transcribed with SP6 and T7, respectively.*

Whole-mount *in situ* hybridization

Mouse embryos were analyzed by whole-mount in situ hybridization (WISH) as previously described [41] using the digoxigenin (DIG) labeled antisense RNA probes for *dmrt2*, *hes7*, *lfng*, *axin2*, *sprouty2*, *nodal* and *pitx2*. Zebrafish embryos were analyzed by WISH as previously described [42] using the digoxigenin (DIG) labeled antisense RNA probes for dmrt2a/*terra* and *dmrt2b*. Embryos were photographed with a LEICA Z6 APO stereoscope coupled to a LEICA DFC490 camera.

Acknowledgments

We thank D. Zarkower for the mice carrying the *dmrt2* null mutation, M. Mallo for the *hes7* and *lfng* probes, J. Belo for the *nodal* and *pitx2* probes, O. Pourquié for the *axin2* and *sprouty2* probes, L. Gonçalves and A. M. Salgueiro for teaching how to dissect mouse embryos, and S. Marques for teaching how to collect mouse internal organs. We thank R. Fior for comments on the manuscript and are most grateful to É. Sucena for critical suggestions on the manuscript.

Author Contributions

Conceived and designed the experiments: RAL LS. Performed the experiments: RAL SSL. Analyzed the data: RAL SSL LS. Wrote the paper: RAL SSL LS.

References

1. Lourenço R, Saúde L (2010) Symmetry OUT, Asymmetry IN. Symmetry 2: 1033–1054.
2. Dequéant ML, Pourquié O (2008) Segmental patterning of the vertebrate embryonic axis. Nat Rev Genet 9: 370–382.
3. Cooke J, Zeeman EC (1976) A clock and wavefront model for control of the number of repeated structures during animal morphogenesis. J Theor Biol 58: 455–476.
4. Dequéant ML, Glynn E, Gaudenz K, Wahl M, Chen J, et al. (2006) A complex oscillating network of signaling genes underlies the mouse segmentation clock. Science 314: 1595–1598.
5. Dubrulle J, McGrew MJ, Pourquié O (2001) FGF signaling controls somite boundary position and regulates segmentation clock control of spatiotemporal Hox gene activation. Cell 106: 219–232.
6. Aulehla A, Wehrle C, Brand-Saberi B, Kemler R, Gossler A, et al. (2003) Wnt3a plays a major role in the segmentation clock controlling somitogenesis. Dev Cell 4: 395–406.
7. Andrade RP, Palmeirim I, Bajanca F (2007) Molecular clocks underlying vertebrate embryo segmentation: A 10-year-old hairy-go-round. Birth Defects Res C Embryo Today 81: 65–83.
8. Tabin CJ (2006) The key to left-right asymmetry. Cell 127(1): 27–32.
9. Raya A, Kawakami Y, Rodriguez-Esteban C, Buscher D, Koth CM, et al. (2003) Notch activity induces Nodal expression and mediates the establishment of left-right asymmetry in vertebrate embryos. Genes Dev 17: 1213–8.
10. Krebs L T, Iwai N, Nonaka S, Welsh IC, Lan Y, et al. (2003) Notch signaling regulates left-right asymmetry determination by inducing Nodal expression. Genes Dev 17: 1207–12.
11. Takeuchi J, Lickert H, Bisgrove B, Sun X, Yamamoto M, et al. (2007) Baf60c is a nuclear Notch signaling component required for the establishment of left-right asymmetry. Proceedings of the National Academy of Sciences 104: 846–851.
12. Gourronc F, Ahmad N, Nedza N, Eggleston T, Rebagliati M (2007) Nodal activity around Kupffer's vesicle depends on the T-box transcription factors notail and spadetail and on notch signaling. Dev Dyn 236(8): 2131–2146.
13. Meyers EN, Martin GR (1999) Differences in left-right axis pathways in mouse and chick: Functions of FGF8 and SHH. Science 285: 403–406.
14. Nakaya MA, Biris K, Tsukiyama T, Jaime S, Rawls JA, et al. (2005) Wnt3a links left-right determination with segmentation and anteroposterior axis elongation. Development 132: 5425–5436.
15. Brend T, Holley SA (2009) Balancing segmentation and laterality during vertebrate development. Semin Cell Dev Biol 20: 472–478.
16. Kawakami Y, Raya A, Raya RM, Rodriguez-Esteban C, Belmonte JC (2005) Retinoic acid signalling links left-right asymmetric patterning and bilaterally symmetric somitogenesis in the zebrafish embryo. Nature 435: 165–171.
17. Vermot J, Gallego Llamas J, Fraulob V, Niederreither K, Chambon P, et al. (2005) Retinoic acid controls the bilateral symmetry of somite formation in the mouse embryo. Science 308: 563–566.
18. Vermot J, Pourquié O (2005) Retinoic acid coordinates somitogenesis and left-right patterning in vertebrate embryos. Nature 435: 215–220.
19. Vilhais-Neto GC, Maruhashi M, Smith KT, Vasseur-Cognet M, Peterson AS, et al. (2010) Rere controls retinoic acid signalling and somite bilateral symmetry. Nature 463: 953–957.
20. Sirbu IO, Duester G (2006) Retinoic-acid signalling in node ectoderm and posterior neural plate directs left-right patterning of somitic mesoderm. Nat Cell Biol 8: 271–277.
21. Isaac A, Sargent MG, Cooke J (1997) Control of vertebrate left-right asymmetry by a snail-related zinc finger gene. Science 275: 1301–1304.
22. Morales AV, Acloque H, Ocaña OH, de Frutos CA, Gold V, et al. (2007) Snail genes at the crossroads of symmetric and asymmetric processes in the developing mesoderm. EMBO Rep 8: 104–109.
23. Saúde L, Lourenço R, Gonçalves A, Palmeirim I (2005) Terra is a left-right asymmetry gene required for left-right synchronization of the segmentation clock. Nat Cell Biol 7: 918–920.
24. Seo KW, Wang Y, Kokubo H, Kettlewell JR, Zarkower DA, et al. (2006) Targeted disruption of the DM domain containing transcription factor Dmrt2 reveals an essential role in somite patterning. Dev Biol 290: 200–210.
25. Bessho Y, Sakata R, Komatsu S, Shiota K, Yamada S, et al. (2001) Dynamic expression and essential functions of Hes7 in somite segmentation. Genes Dev 15(20): 2642–7.

26. Forsberg H, Crozet F, Brown NA (1998) Waves of mouse Lunatic fringe expression, in four-hour cycles at two-hour intervals, precede somite boundary formation. Curr Biol 8(18): 1027–30.
27. Minowada G, Jarvis LA, Chi CL, Neubüser A, Sun X, et al. (1999) Vertebrate Sprouty genes are induced by FGF signaling and can cause chondrodysplasia when overexpressed. Development 126(20): 4465–75.
28. Collignon J, Varlet I, Robertson EJ (1996) Relationship between asymmetric nodal expression and the direction of embryonic turning. Nature 381(6578): 155–8.
29. Yoshioka H, Meno C, Koshiba K, Sugihara M, Itoh H, et al. (1998) Pitx2, a bicoid-type homeobox gene, is involved in a lefty-signaling pathway in determination of left-right asymmetry. Cell 94(3): 299–305.
30. Meng A, Moore B, Tang H, Yuan B, Lin S (1999) A Drosophila doublesex-related gene, terra, is involved in somitogenesis in vertebrates. Development 126(6): 1259–68.
31. Volff JN, Zarkower D, Bardwell VJ, Schartl M (2003) Evolutionary dynamics of the DM domain gene family in metazoans. J Mol Evol 57: Suppl 1, S241–9.
32. Hong CS, Park BY, Saint-Jeannet JP (2007) The function of Dmrt genes in vertebrate development: it is not just about sex. Dev Biol 310(1): 1–9.
33. Kim S, Kettlewell JR, Anderson RC, Bardwell VJ, Zarkower D (2003) Sexually dimorphic expression of multiple doublesex-related genes in the embryonic mouse gonad. Gene Expr Patterns 3(1): 77–82.
34. Dequéant ML, Glynn E, Gaudenz K, Wahl M, Chen J, et al. (2006) A complex oscillating network of signaling genes underlies the mouse segmentation clock. Science 314(5805): 1595–8.
35. Goldbeter A, Pourquié O (2008) Modeling the segmentation clock as a network of coupled oscillations in the Notch, Wnt and FGF signaling pathways. J Theor Biol 252(3): 574–85.
36. Force A, Lynch M, Pickett FB, Amores A, Yan YL, et al. (1999) Preservation of duplicate genes by complementary, degenerative mutations. Genetics 151(4): 1531–45.
37. Liu S, Li Z, Gui JF (2009) Fish-specific duplicated dmrt2b contributes to a divergent function through Hedgehog pathway and maintains left-right asymmetry establishment function. PLoS One 4(9): e7261.
38. Zhou X, Li Q, Lu H, Chen H, Guo Y, et al. (2008) Fish specific duplication of Dmrt2: characterization of zebrafish Dmrt2b. Biochimie 90(6): 878–87.
39. Schilling TF, Concordet JP, Ingham PW (1999) Regulation of left-right asymmetries in the zebrafish by Shh and BMP4. Dev Biol 210(2): 277–87.
40. Kimmel CB, Ballard WW, Kimmel SR, Ullmann B, Schilling TF (1995) Stages of embryonic development of the zebrafish. Dev Dyn 203: 253–310.
41. Kanzler B, Kuschert SJ, Liu YH, Mallo M (1998) Hoxa-2 restricts the chondrogenic domain and inhibits bone formation during development of the branchial area. Development 125: 2587–2597.
42. Thisse C, Thisse B (2008) High-resolution in situ hybridization to whole-mount zebrafish embryos. Nat Protoc 3: 59–69.